A Remote Sensing Investigation into the evolution of Folgefonna Glacier over the last 150 years

Benjamin Aubrey Robson

Master's thesis in Earth Science

Department of Earth Science

University of Bergen

Nansen Environmental and Remote Sensing Centre

2012

Front cover picture: The eastern side of Sørfonna (Southern Folgefonna) in September 2010

Abstract

The evolution of Folgefonna, three large maritime ice masses in Hardanger, Western Norway has been assessed over the last 150 years using a variety of remote sensing datasets (optical and microwave satellite images, aerial photography, digital elevation models (DEMs) and old maps). Changes in glacier area, volume and elevation of the transient snowline (TSL), a commonly used glacier mass balance proxy are determined. All three parameters show a similar trend, although the scarcity of glacier volume data points means that changes cannot be resolved in as much detail as the measurements of glacier area or the TSL elevation. Since the Little Ice Age (LIA) maxima at the end of the nineteenth century Folgefonna has been retreating and losing mass with noticeable glacier advances in the 1960s/70s and the 1990s. Since the turn of the millennium Folgefonna has retreated rapidly interrupted only by a short lived advance between 2005 and 2008. In 2011 Nordfonna, Midtfonna and Sørfonna had respective areas of 24.8 km^2, 9.1 km^2 and 156.7 km^2, reductions of 47%, 68% and 20% compared with their LIA maxima sizes in 1860. The TSL mirrors this trend albeit with less magnitude compared with the other observations, it is therefore assumed that in actual fact it the firn line being measured and not the TSL. Absolute ice volume calculations are only possible for Nordfonna where the subglacial topography is known; Nordfonna measured 1.84 km^3 in 2010, a reduction of 43% of its 1937 volume. If planar bedrock surfaces beneath 95% of the ice surfaces are assumed then rudimentary percentage losses can be calculated. Over the same time span Midtfonna lost 1441 million kg (50%) of mass, while Sørfonna lost 8268 million kg (18%) between 1987 and 2010, the portion of Sørfonna visible on the 1937 topographic map lost 5658 million kg (21%) between then and 2010. The changes observed remotely in Folgefonna relate well to the *in-situ* data as well as the climatic data, it is evident that winter precipitation has traditionally been the principle driver of Folgefonna, however recent increases in summer temperature have been responsible for the acceleration in glacier shrinkage. Folgefonna is found to have advanced and retreated roughly in synchronisation with ice masses in Scandinavia, Europe and further afield suggesting that a global force is partly responsible for driving the glacier.

Sammendrag

Utviklingen av Folgefonna, som består av tre store maritime platåbreer i Hardanger i Vest-Norge er rekonstruert de siste 150 år ved bruk av flere data fra fjernmåling (optiske og radar satellittbilder, flybilder, digitale høydemodeller (DEMs) og historiske kart) og endringer i breareal, volum og høyde på firngrensen, som vanligvis er brukt til å rekonstruere massebalanse for breer. Alle tre parametrene viser en lik trend, men på grunn av manglende målinger av brevolum betyr det at endringene ikke kan vises i like stor detaljrikdom som målingene av breareal eller høyden på firngrensen. Siden Lille istids maksimum på slutten av 1900-tallet har Folgefonna trukket seg tilbake og mistet mye masse, selv med et betydelig brefremstøt på 60-, 70- og 90-tallet, men etter tusenårsskiftet har Folgefonna raskt trukket seg tilbake bare avbrutt av et kort fremstøt mellom 2005 og 2008. I 2011 hadde Midtfonna og Sørfonna de respektive arealene på 24.8 km^2, 9.1 km^2 and 156.7 km^2 med en reduksjon på 47%, 68% og 20% sammenlignet med deres Lille Istids maksimumsposisjoner i 1860. Absolutt isvolum er det bare mulig å kalkulere for Nordfonna og gav et volum på 1.84 km^3 i 2010, en reduksjon på 43% av dens volum i 1937. Med forutsetningen at topografi under 95% av isen er flatt kan en regne ut at Midtfonna ble 1441 million kg (50%) mindre, mens Sørfonna mistet 8268 million kg (18%) mellom 1987 og 2010, og med delen av Sørfonna som er synlig på topografiske kart viser et tapt på 5658 million kg (21%) mellom 1937 og 2010. De endringene som er observert med fjernmåling på Folgefonna korrelerer godt med klimatiske data fra området, det er tydelig at vinternedbør tradisjonelt har vært hovedmekanismen for endringer av breens størrelse, men økning i sommertemperatur er nylig blitt hovedgrunnen til breens tilbakesmeltning på 2000-tallet. Folgefonna har hatt bremfremstøt og tilbaketrekninger i samsvar med andre breer i Skandinavia, Europa og videre omkretser, som tyder på at globale prosesser delvis styrer endringene sett i Folgefonnas fluktuasjoner.

Table of Contents

Acknowledgements

There are numerous people that have contributed to this master thesis that I would like to thank. Firstly I thank my supervisor Dr. Jostein Bakke, for answering my bombardment of emails, always providing sound advice and assistance when every necessary and sharing his passion about Folgefonna.

I would especially like to thank everyone at the Nansen Centre, who without their financial support these two fantastic years in Bergen would not have been remotely possible, I am especially grateful to Dr. Mohamed Babiker who provided all sorts of help ranging from GIS and remote sensing problems to thesis structure. Also thank you to Stein Sandven, the leader of my department at Nansen Centre, who has been supportive of all my work and aided me in any way he can. I also received a great deal of GIS help from Håvard Juliussen of the Department of Geography who has been enthusiastic and interested in my work, and certainly some areas of my work would not have been possible without his assistance. Also thanks to the people that have read drafts of part of this thesis – Stephen Fischer, Andrea Boyco Orams, Monika Dragosics and Linda Salvesson. Thanks also to Sunniva Vatle for proof reading the half page of Norwegian.

Lastly a big thank you to my friends, to those I have met during my time in Bergen and have travelled Norway with and had all sorts of fun with, to those back in the UK too that have supplied me with delicacies when visiting me and to those in the department who had to have entire courses taught in English solely because of my presence.

Bergen, May 2012

Benjamin Robson

List of Figures

List of Tables

List of Abbreviations

°C	Degrees centigrade
µm/mm/m/km	Micrometre/millimetre/metre/kilometre
ASAR	Advanced Synthetic Aperture Radar
ASTER	Advanced Spaceborne Thermal Emission and Reflection
DEM	Digital Elevation Model
DJFM (NAO)	North Atlantic Oscillation Index mean values for December, January, February and March
dpi	Dots per inch
ELA	Equilibrium Line Altitude
ERS	European Remote Sensing (name of two satellites)
ETM	Enhanced Thematic Mapper
FL	Firn line
GCP	Ground Control Point
GIS	Geographic Information System
GLIMS	Global Land Ice Measurements from Space
GPR	Ground Penetrating Radar
HEP	Hydro-electric plant
InSAR	Interferometric Synthetic Aperture Radar
IPCC	Intergovernmental Panel on Climate Change
Kg	Kilogram
LIA	Little Ice Age
LiDAR	Light Detection And Ranging
m.a.s.l	Metres above Sea Level
MSS	Multispectral sensor
NAO	North Atlantic Oscillation
NERSC	Nansen Environmental and Remote Sensing Centre
NRK	Norsk rikskringkasting (Norwegian Broadcasting Corporation)
NVE	Norges vassdrags- og energidirektorat (Norwegian Water Resources and Energy Directorate)
PDO	Pacific Decadal Oscillation
SAR	Synethetic Aperature Radar
SKL	Sunnhordaland Kraftag
SPOT	System Pour l'Observation de la Terre (System for Earth Observation)
SRTM	Shuttle Radar Topography Mission
TIN	Triangular Irregular Networks
TM	Thermal Mapper, also used to denote a band of a Landsat image
TSL	Transient Snowline
Yr	Year

1.0 Introduction

This chapter shall give a broad background to the importance of studying changes in the planet's glaciers during a time of changing climate, and how remote sensing as a methodology can be utilised in such studies. The purposes set out for this investigation are also given.

1.1 Glaciers in the context of climate change

Changes observed in glaciers are amongst the clearest and most pronounced signals that exist in nature of a dynamic climate (Kääb et al., 2002, Barry, 2006). Their high thermal sensitivity mean that even small changes in climate can result in length changes of several hundred metres (Paul and Andreassen, 2009). It is for this reason that high mountain glaciers have been referred to as "*the canary in the coal mine"* of climate change (Bishop et al., 2004) and are recognised by The Intergovernmental Panel on Climate Change (IPCC) as an important parameter to measure climate over decadal to centurial timescales (Andreassen et al., 2005b). The dramatic downwasting and recession of glaciers worldwide since the Little Ice Age (LIA) maxima, has seen European glaciers lose approximately 50% of their volume and is one of the most documented glacier responses to a shift in climate (Knoll et al., 2009, Hall et al., 2003). The cryosphere is an important component of the climate system which is responsible for forcings and feedbacks related to the atmosphere, the ocean and sea level, surface hydrology, erosion and topographic evolution. In addition to this interannual variabilities such as El Niño and the North Atlantic Oscillation (NAO) can be seen in glacier mass balance records (Bishop et al., 2004). For these reasons it is therefore imperative to maintain up-to-date and frequent glacier inventories to assess current change and place it in context of paleoglacier conditions (Kääb et al., 2002).

1.2 The importance of glaciated catchments and mountainous environments

Mountainous environments are critical to our planet. They directly support 10% and indirectly support over half of Earth's population through water supply or other resources (Beniston et al., 1997). Approximately 54,000 km^2 of Europe (excluding Greenland) is ice-covered, and while the majority of this is found in Svalbard (68%) and Iceland (21%) there are still significant ice-masses found in Scandinavia (6%) and the Alps (5%) (Nesje, 2005). These being smaller than the great ice-caps found elsewhere and possessing temperatures closer to the melting point, make them more in-tune and sensitive to climate perturbations (Nesje and Matthews, 2012). Glaciers cover 1% of mainland Norway and their presence plays an important role for the Norwegian economy, no more so than in hydro-electric power production (HEP) (Andreassen et al., 2005b). 98% of electricity in Norway is generated from HEP, and 15% of this comes from glaciated catchments, therefore the health of Norwegian mountain glaciers such as Folgefonna is indispensable to power production in Norway (Andreassen et al., 2005b).

1.3 Climate change globally and in Western Norway

Climate change is causing what were formally constants to become variables (Paskal, 2010). During the twentieth century the mean global surface temperature rose by ~0.6°C with a stronger warming nearer the poles, there are indications that some areas may be at their warmest for the last 1500 years (Ruddiman, 2007). Depending on which CO_2 emission scenario is considered, temperatures may continue to rise globally by between 1.8 – 4.5°C by the end of the twenty-first century (Imhof et al., 2011). It has been suggested that even a few degrees of warming could halve the snowpack volume of glaciers in many areas (Surazakov and Aizen, 2006).

South-western Norway has also seen changes in climate. The annual winter and summer precipitation between 1900 and 2000 in Bergen increased by 19% and 7% respectively, while the mean annual temperature and mean winter temperature increased by 0.71°C and 0.93°C per 100 years (Nesje et al., 2000). Summer ablation temperatures since the late 1990s have been 2°C above the normal for the period 1961 – 1990 (Winkler and Nesje, 2009).

There is now more of an urgency than ever before to map the planet's cryosphere. Many small glaciers that existed a few decades ago have now completely ablated away, and it seems probable that many of today's smaller ice masses will be completely gone within the next years or decades (Raup et al., 2007). In addition to this over a quarter of the projected 39 cm rise in sea level estimated by the end of the century is postulated to be sourced from the melting of small, temperature mountain glaciers (Raper and Braithwaite, 2006), although this contribution could potentially be even greater (Rahmstorf, 2010). Such an ice shrinkage would have a substantial impact on the economy of such regions, for example Western Norway would be affected by a long-term reduction in HEP which relies upon predictable runoff patterns (Agrawala et al., 2003), tourism centred around the glaciers such as glacier hiking and summer skiing, as well as problems of a less predictable water supply (Barry, 2006). In comparison it has been estimated by Schaefli et al. (2007) that HEP production in the Swiss Alps could decrease by up to 36% by the end of the century due to a decreased ice volume and a greater rate of evapotranspiration. Given the importance of glaciers to Norway's electricity production it is not surprising that Norway has one of the world's most extensive and oldest glacier measurement system (Andreassen et al., 2005b).

By detecting the changes within a catchment, steps can be taken to minimise the possible impacts from varying water flow or high-mountain hazards such as ice-avalanches, rockslides and glacial lake outburst floods (Salzmann et al., 2004). In most cases prevention before the full change takes places is favourable to reparations afterwards (Paskal, 2010).

1.4 The role of remote sensing in glaciology

When compared with traditional glaciology methods, remote sensing is still very much in its infancy, however the ability to incorporate historical aerial photography and cartography plus the comprehensive spatial and temporal coverage of satellite data makes remote sensing a very

attractive option for glaciologists for all manners of investigations (Bamber and Rivera, 2007). A number of glacial features can be extracted from remotely sensed data within a few hours as opposed to lengthy and expensive fieldwork campaigns (Gao and Liu, 2001). As of 2006 only 44% of the planet's ~160,000 glaciers have been mapped and documented, remotely sensed imagery coupled with Geographic Information Technology are one practical solution to update the world glacier inventory (Imhof et al., 2011).

1.5 Purpose of this investigation

This investigation set out to investigate the potential of the application of remote sensing as a tool for glaciology on a plateau glacier such as Folgefonna. *In-situ* data is scarce from Folgefonna; some sparse and sporadic mass balance exist for four catchments of Sørfonna for several years in the 1960s, 1970s and post-2003 (*5.4.2.1),* along with non-continuous glacier terminus positions from 7 outlet glaciers (6 on Sørfonna and 1 on Nordfonna) that in some cases date back to the start of the twentieth century (NVE, 2011a). This provides an interesting stimulus for the use of remote sensing – the remotely sensed data can be compared with the available ground data to assess the quality of the data, while also extending the knowledge of Folgefonna's glacial history.

The investigation centred on the following main research question:

Can modern satellite imagery be combined with aerial photography and historical maps to provide a detailed history of Folgefonna glacier, and used to visualise the recent evolution of the ice mass?

This was further divided into the following sub-research questions:

1. To what extent has the areal extent of Folgefonna changed over the last two centuries?
2. To what extent has the ice volume of Folgefonna changed over the last 80 years?
3. How has the prevailing climate conditions of the time correlated to the changes of ice area and volume?
4. How has the altitude of the transient snowline (TSL) on Sørfonna changed over the last three decades, and to what extent does this correlate with the mass balance of glaciers from the region?
5. By how long does the glacier area, volume and TSL lag behind the climatic forcing for Folgefonna?
6. How do remote sensing methods compare with *in-situ* and historical data available and what can be said about the suitability for remotely sensed investigations for future glaciological work?

In the following section the setting, theory and history of Folgefonna shall be discussed, following this a sum-up of the advantages and disadvantages associated with remote sensing along with a review of past significant work. The methods that were used in this investigation shall then be described before the results are presented, the findings are then discussed and compared with climatic and *in-situ* data along with the results found by others. Finally this investigation's results are put in a local, regional Scandinavian and global context.

2.0 Study area

In this chapter an overview of Folgefonna is given. A background to maritime glaciers is also offered along with the particularly significant relationship between Scandinavian ice masses and the North Atlantic Oscillation. Finally the history of how Folgefonna has varied and evolved from ~5000 BC to present day is described.

2.1 Study Setting

Folgefonna is located in Hardanger in South-Western Norway, on a peninsular between Hardangerfjorden, Sørfjorden and Maurangerfjorden, as shown in Figure 1. Folgefonna is comprised of three separate ice-masses, Nordfonna, Midtfonna and Sørfonna. Sørfonna; the largest of the three ice-masses is the third largest ice mass in mainland Norway at 168 km^2 of ice, Midtfonna covers 11 km^2, while Nordfonna is 26 km^2 in size (NVE, 2009).

Some of the catchments around Folgefonna are exploited by the hydro-electric industry, and have their meltwater discharges utilised for hydro-electric power generation, operated both by *Statkraft* and *Sunnhordaland Kraftlag (SKL)* (Bakke, 2010). Mauranger, a catchment to the west of Folgefonna that *Statkraft* generates electricity within. 62 km^2 or 38% of the entire catchment area were glacier-covered in 1975 (Østrem, 1975), making the health and mass balance of Folgefonna of vital importance.

Being situated on the western coast of Norway; Folgefonna is a maritime glacier with a high amount of snow accumulation during the winter from mild and humid winds off the North Atlantic (Imhof et al., 2011), but also high rates of ablation in summer (Nesje et al., 2000). The local topography, aspect and elevation all influence the accumulation through avalanche-prone terrain and valleys that funnel snowfall, as well as the ablation through wind deflation, calving and evaporation (Imhof et al., 2011).

The annual mass balance of maritime glaciers in Norway has been shown to be controlled more by the winter balance than the summer balance, that is that the amount of winter precipitation is more influential than the summer temperature (Nesje, 2005, Winkler and Nesje, 2009, Andreassen et al., 2005b). Reichert et al. (2001) found that for Nigardsbreen, another Norwegian maritime glacier, precipitation has 1.6 times more impact on glacier mass balance than temperature does. Maritime glaciers have a high annual mass turnover and therefore are more sensitive than continental glaciers to climate perturbations (Winkler et al., 2009, Hooker and Fitzharris, 1999). Folgefonna is therefore a well suited glacier to study the influence of climate change on the glacier size and the height of the equilibrium line altitude (ELA).

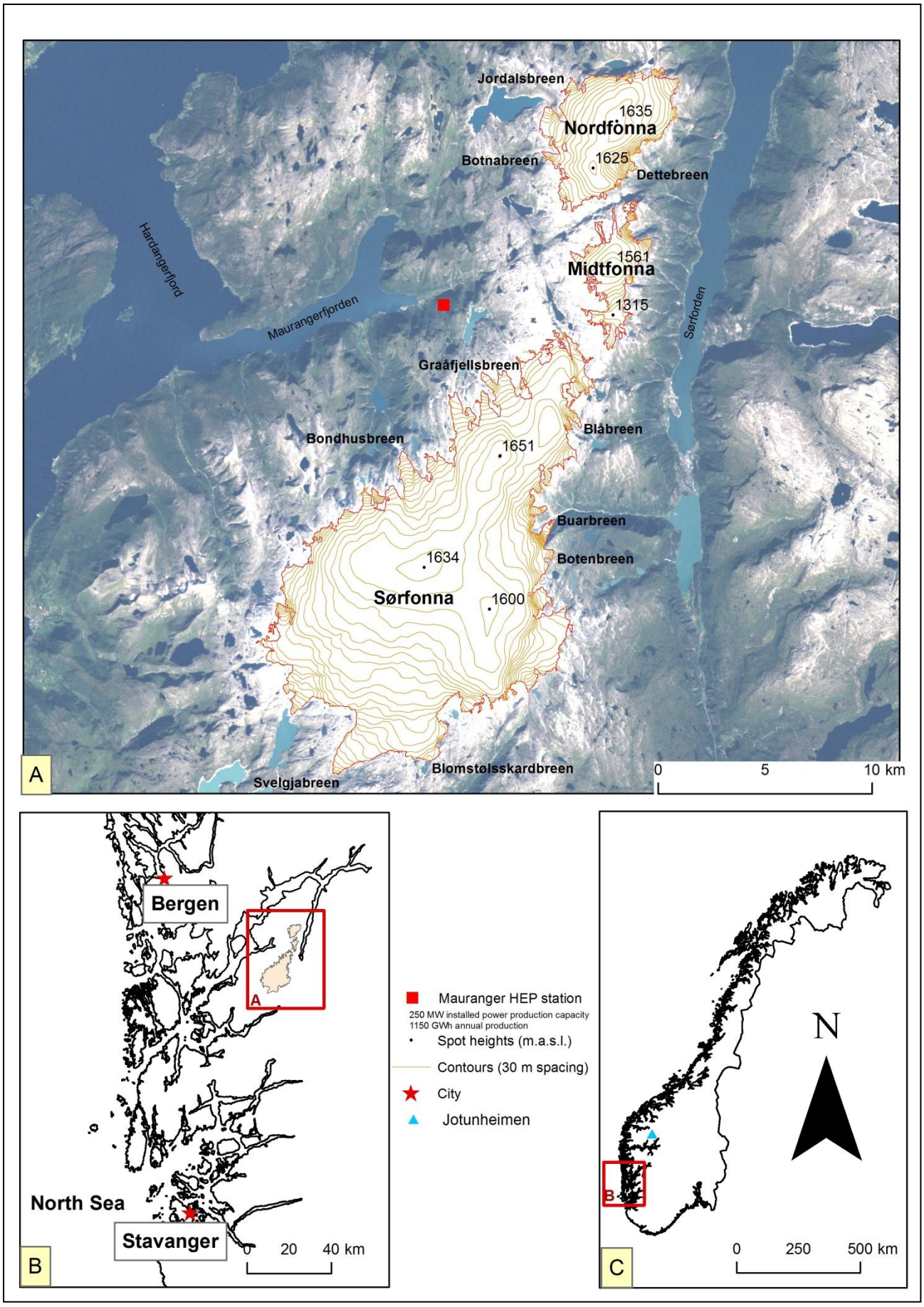

Figure 1: The location of Folgefonna glacier within South-West Norway(B), and Norway (C). The relative topography of the glacier is shown (A) along with the location of Mauranger Hydro-electric power plant. Partially modified from Statkraft.no (2008), Glacier outlet information from Furdal (2010). The location Jotunheimen national park, another large source of Norwegian glaciers, and one that is referred to frequently in this investigation, is also shown. Note than although Mauranger HEP station is shown on this map, SKL operate approximately 15 km south of Sørfonna (Bakke, 2012a).

2.2 The North Atlantic Oscillation (NAO)

Given that winter precipitation is traditionally the main driver of Norwegian maritime glacier mass balances, and that this in turn is driven mainly by the humid and mild winds off of the North Atlantic, it is not that surprising that the mass balance of Norwegian glaciers correlated well with the North Atlantic Oscillation (NAO). The NAO is a decadal scale coupled ocean and atmosphere climate oscillation between alternative high and low pressures over the Arctic and the subtropical Atlantic Ocean (Nesje et al., 2000). Changes in the NAO phase control the amount of heat and moisture transported alternatively between the mid-latitudes and the Mediterranean. During a *positive* NAO phase, low pressure over Iceland and the Arctic combined with high pressures over the sub-tropical Atlantic (such as the Azores) increase the strength of the westerlies over the mid-latitudes causing warmer and wetter conditions over Northern Europe and the Eastern United States (Visbeck et al., 2001). Nesje et al. (2000) finds a strong, positive correlation ($r^2 = 0.77$) between the amount of winter precipitation in western Norway and the NAO index. The NAO index is also reflected in the mass balance of Norwegian glaciers, Nigardsbreen's mass balance for example has a positive correlation ($r^2 = 0.55$) with the NAO index (Reichert et al., 2001), while Ålfotbreen has a correlation of $r^2 = 0.51$ (Nesje et al., 2000).

2.3 Folgefonna and western Norwegian glacier History

The NAO is supposed by many to have been a principle driver in the historical waxes and wanes of Folgefonna and Norwegian maritime glaciers in general. There is evidence that ice was present at Folgefonna from around about 5200 cal. yr BP, but it wasn't until about 2200 cal. yr BP that the glacier expanded to a size larger than it is now. Since then Folgefonna has fluctuated with decadal to centurial scale timescales over the last 2000 years, growing through the latest part of the *medieval warm period* and then later in the LIA (Bakke et al., 2005). Many written documents and works of art exist from the 1800s (Figure 2) especially about two of Folgefonna's outlet glaciers – Bondhusbreen and Buerbreen (Nussbaumer et al., 2011). Written accounts suggest that Folgefonna was expanding from the late 1700s into the early 1800s, it was once even remarked that Bondhusbreen covered a whole parish (Pontoppidan (1752) in Nussbaumer et al., 2011). Both outlet glaciers peaked in size during the 1870s, having both undergone slight retreats and advances since the turn of the century (Nussbaumer et al., 2011). Folgefonna is thought to have reached its LIA maximum in the late 1870s (Nussbaumer et al., 2011), while moraines from around Nordfonna suggest smaller LIA peaks around 1750, and 1930 (Bakke et al., 2005). Tree rings from Northern Norway show that conditions in Norway during the LIA were not especially cool, Nesje et al. (2008b) interpret this to say that the early eighteenth century glacial expansion was caused by humid and mild winters rather than cool summers. A widespread 20% reduction in winter precipitation is thought to have initiated glacier shrinkage towards the termination of the LIA in approximately the 1920s (Imhof et al., 2011).

After a period of relative stability many Norwegian maritime glaciers retreated strongly in the 1930s and 1940s, this was then followed by a slow advance that began on some glaciers as early as mid 1950s and was punctuated by many years of stability (Winkler et al., 2009). A shift to more positive NAO values during the late 1980s and 1990s is supposed by many to be the driver for the well-documented accelerated advances of Norwegian glaciers during the 1990s often referred to as *The Briksdalsbre Event* (Nesje and Matthews, 2012). Periods of abundant rates of winter accumulation during the winter of 1988/89, 1989/90, 1992/93, 1994/95, 1997/98 and 1999/2000 caused glaciers to rapidly advance, in the case of Briksdalsbreen, an outlet glacier of Jostedalsbreen, an advance of 285 m occurred in less than a decade (Nesje and Matthews, 2012).

1

2

Name of glacier								
Briksdalsbreen				1872		1910	1929	1996
Bøyabreen				1872	1888	1909	1931	
Store Supphellebreen						1912	1929	1996
Bergsetbreen	**1743**	(1844)	(1857)	(1876)		1910	1938	2000
Nigardsbreen	**1748**	1839		1873		1909	1930	2003
Lodalsbreen	**(1750)**			(1870)				
Bondhusbrea		1807	1855	**1875**	1889/1890	1911	1930	(1996)
Buerbreen		(1822)	1852	**1878/1879**	1892/1893	1911	1933	1998

3

Figure 2. 1. Bondjusbrea in 1851, painted by James David Forbes ('Glacier of Bondhuus'; lithograph; 13.5 cm × 20.7 cm; Forbes, 1853) (Nussbaumer et al., 2011)

Figure 2.2: Photos of Buerbreen, Folgefonna in 1864, 1869 just before the LIA maximum and then in 1897 towards the end of the LIA. Photos: Universitetsbiblioteket i Bergen Taken from Nussbaumer et al. (2011)

Figure 2.3: Glacier advances of different outlet glaciers of Jostedalsbreen and Folgefonna. Dates in bold are the LIA maximums while dates in brackets are poorly documented (Nussbaumer et al., 2011).

This era of glacier advance came to an end at the turn of the millennium and was subsequently followed by a few years of stationary glacier fronts. All of the glaciers monitored by *NVE* have had negative mass balances since 2001 (Andreassen et al., 2005b), and since 2002 most Norwegian maritime glaciers have been considerably retreating (Winkler et al., 2009).

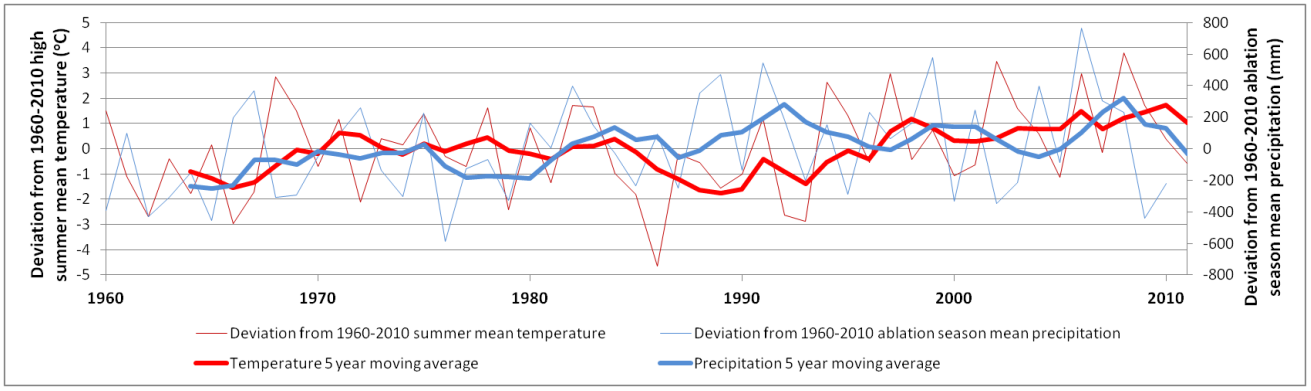

Figure 3: The deviation of both the high summer (July, August and September) mean temperature measured at Florida, Bergen and the ablation season (November to April) mean precipitation measured at Rosendal between 1960 and 2010. Climate data downloaded from met.no. It can be seen that generally the ablation season temperatures over the last 40 years, while the precipitation has varied. Lower temperatures were the cause of the 1960s Folgefonna advance, while the 1990s and mid-2000s advances were due more to abundances of winter precipitation.

Most of the glacier fluctuations before the mid-1990s have been related more to the increase in winter precipitation (19% per 100 years (Nesje et al.,2000)) than the increase in summer temperature (0.43°C per 100 years (Nesje et al.,2000)). However towards the end of the 1990s August and September temperatures have been rising strongly, for example 1997 saw a mean temperature of 16.4°C for June and July, considerably higher than the 1962 – 2005 mean of 13.9°C as shown in Figure 3 (Winkler et al., 2009).

As well as summer temperatures rising, winter accumulation has also decreased in some years. The balance year of 2002/03, which was western Norway's warmest year since 1734 (Imhof et al., 2011), saw eight Norwegian glaciers receive 66% of their normal (1962 – 2003) accumulation, yet 156% of their normal ablation(Nesje, 2005), this is visible in Figure 3. Many Norwegian glaciers experienced a short-lived glacier advance between 2005 and 2008 due to a 20% increase in winter precipitation (NRK, 2008). However despite considerabe winter balances; high summer ablation rates caused all measured glaciers in Norway to lose mass as of 2010 (Kjøllmoen, 2011), while all measured Folgefonna outlet glaciers have been losing mass the last two years (Kjøllmoen et al., 2012)

3. Literature Review

In this chapter a review of the advantages and disadvantages associated with the use of remote sensing in glaciological investigations is given. Following this significant work for each remote sensing method is summarised, with some thoughts also given to relevant methods that were not used in this investigation but could be useful in the future.

3.1. Advantages of remote sensing methods over the traditional glaciological methods

In recent years remote sensing methodologies have become more commonly used in glaciological work. Both remote sensing and traditional glaciological methods have advantages and disadvantages, and depending on the *in-situ* conditions a particular setting can favour one set of methods over the other. Ideally both methods should be used to an extent in tandem to enable ground-truthing and verification (Gao and Liu, 2001).

3.1.1 Deployment in remote areas

Much of the planet's land ice lies in remote, rugged and inhospitable areas (Racoviteanu et al., 2008, Gudmundsson et al., 2011) while some glaciated mountain chains are politically hard to reach (Kääb et al., 2005a). Fieldwork in such areas can be extremely costly and logistically complicated (Bamber and Rivera, 2007), and must be focused in the short ablation-season (Bindschadler et al., 2001). Therefore only a relatively small sample of the world's glaciers can be studied in depth and over a suitably long timescale using the traditional glaciological methods (Bindschadler et al., 2001). This means that for many areas no ground data exists, however by purely using remote sensed sources useful conclusions can still be obtained (Quincey et al., 2005).

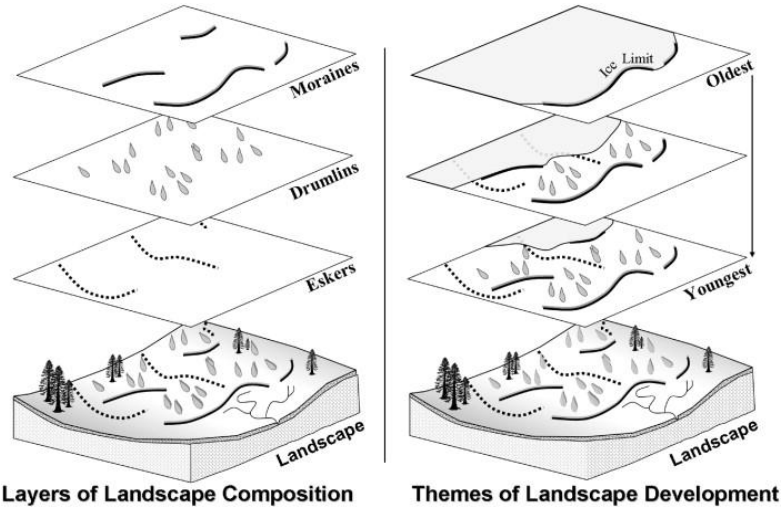

Figure 4: Using a paper map, it is often difficult to distinguish spatial or temporal landform patterns. GIS permits landform assemblages to be "stripped" away into separate layers, which can then be arranged into various themes (Napieralski et al., 2007).

3.1.2. Working at new perspectives

Remotely sensed data allows scientists to work at a regional scale, and for the first time permits a sustainable and global-scale monitoring of the cryosphere (Kääb, 2007). While before it was possible only to measure the terminus position of a glacier; a variable that is indirectly linked to the state of the climate, using satellite images it is now feasible and efficient to map the entire glacier area, or volume (Gudmundsson et al., 2011, Barry, 2006).

By conducting glaciological investigations with a Geographic Information System (GIS), previously unrecognised temporal and spatial patterns in landform development can be discovered, thanks to easy data incorporation and integration of numerical modelling over various scales, as shown in Figure 4 (Napieralski et al., 2007). For example some low relief ridges in Illinois were identified as end moraines when examined using DEMs, this data could be then used as the southern extent of the Laurentide Ice Sheet during ice sheet reconstructions (Napieralski et al., 2007). Data incorporated into a GIS can easily be shared digitally between scientists and disciplines, can be queried by location or attributes and can be worked on by several authors; using GIS can also help generate new hypotheses and research questions, as shown in Figure 5.

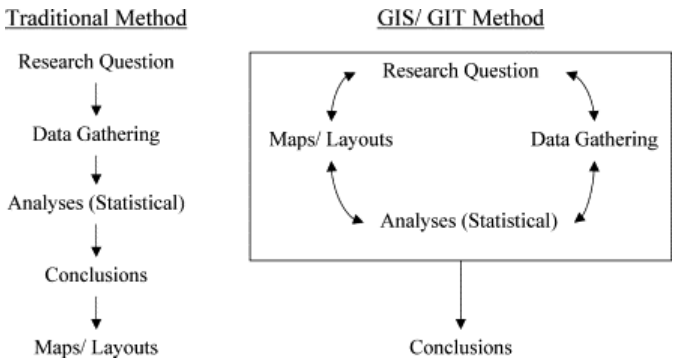

Figure 5: Using GIS in scientific investigations can help stimulate further research and create additional hypotheses (Napieralski et al., 2007).

3.1.3 Temporal resolution and archives

The high frequency of satellite imagery acquisition allows a glacier to be analysed multiple times during the ablation season. ASTER images for example orbit the Earth every 16 days, while some satellites permit the snowline of glaciers to be analysed with weekly observations (Kulkarni et al., 2011). This frequency of data collection would not be practical to collect from fieldwork campaigns (Racoviteanu et al., 2008).

Remote sensing really comes into its element in extending glaciological records backwards in time. While outside of Western Europe and North America lengthy glacier records are sparse, by utilising a variety of remote sensing sources, a glacier record can be extracted for most areas of the world. ASTER images date back to 2002, Landsat to 1972, and declassified American *Corona* images date back to 1959 for certain parts of the world (Bamber and Rivera, 2007). In some cases records can be further extended with aerial photography, back to the 1930s, and beyond this the with the aid of historical maps (Hall et al., 2003). The first photogrammetric map of a glacier dates from 1889 from Vernagtferner, Austria (Braithwaite, 2002), while maps dating to the 1860s exist of western Norway (Imhof et al., 2011). All of this data, no matter of the scale or source can then be incorporated digitally into a GIS, where they can be manipulated and analysed together, as most satellite data comes already geo-referenced; data can usually be loaded into a GIS and is already aligned automatically together, ready for analysis (Gao and Liu, 2001).

The GLIMS (*Global Land Ice Measurements from Space*) initiative aims to compile a global glacier inventory using remotely sensed data and aims to act as a stimulus for further studies (Raup et al., 2007).

3.2. Disadvantages of remote sensing methods compared with traditional glaciological methods

While remote sensing methods possess many advantages, there are also several disadvantages that must be considered.

3.2.1. Measurements of glacier mass balance

Mass balance is the glacier variable that responds most directly to the changing health of the glacier, and is most useful in assessing responses to a changing climate (Williams et al., 1997, Winkler et al., 2009). While semi-automated techniques exist (Bøggild et al., 2004) there is no way to measure glacier mass balance remotely. Either the traditional methods must be used, or remote sensing can be used if certain assumptions or proxies are deployed.

The most common way to directly measure glacier mass balance is with a series of stakes drilled into the glacier ice, the change in the glacier surface at the stakes is then integrated across the entire glacier and converted into a change in mass. Alternately snow-pits and snow probes can be used in winter (Benn and Evans, 2010, Racoviteanu et al., 2008). Given the amount of work and maintenance that goes into measuring glacier mass balance; it is not surprising that glacier mass balance worldwide is significantly under-sampled. For example only 46 km^2 out of Himalayas' 33,000 km^2 of glacier ice has been studied, and between 1977 and 1999 an average of only 6.6 km^2 was studied for glacier mass balance (Berthier et al., 2007).

Different proxies exist for glacier mass balance, the two most common are either the elevation of the transient snowline (TSL), or the change in surface elevation. The change in volume can be calculated by comparing DEMs, and if the bedrock topography is known; absolute ice volumes can be determined.

3.2.1. Dependency on weather conditions

Perhaps the greatest disadvantage associated with remote sensing is the dependency on weather conditions. Optical satellite and aerial imagery can only operate in clear weather conditions. Glaciers and especially maritime glaciers are mainly found in regions prone to high levels of cloud and precipitation (Racoviteanu et al., 2008, Andreassen et al., 2008). The high relief and complicated topography of mountains can also throw a lot of the ice into shadow, especially on northern facing slopes, this can allow seasonal snow to persist longer into the season, or can cause distortion when areas are hidden from the backwards-looking ASTER sensor (Kääb et al., 2005a). Similar problems can arise from haze, image saturation and varying light conditions (Huang et al., 2011, Svoboda and Paul, 2009).

When a satellite orbits above an area once every 18 days (in the case of Landsat), the odds that the image acquired will be cloud free are not always so high. In addition to this recent precipitation can cause a significant problem in the demarcation of the glacier area. Snows persisting from a previous winter or from summer snow events have the potential to mask the glacier margin (Paul

and Andreassen, 2009), while rain which freezes can increase the reflectivity of the surface (Williams et al., 1991). As an example a study mapping glacier areas in the *Isla Riesco*, Chile, over-estimated glacier area by as much as 74% due to seasonal snow (Casassa et al., 2002). As long as the seasonal snow cover isn't excessively deep a DEM can be used to help delineate the margins of a glacier due to the morphological differences, although this works mainly with thick glacier termini (Li et al., 1998).

Microwave satellite images such as *ERS* and *ASAR* offer a solution to this, possessing the ability to pass through clouds and work in the absence of daylight. However their sensitises to water moisture means such images cannot differentiate ice from rock especially well, rendering them impractical for area or volume delineation, with accuracies reported of approximately 40% (Shi and Dozier, 1993). Microwave images can however be used for other glaciological purposed, as shall be discussed in *4.3.3.2* (De Wildt and Oerlemans, 2003).

It should be noted that the *scan line corrector* (SLC), a component on Landsat that aimed to account for the undersampling of the primary scan mirror, malfunctioned on the 31st of June 2003 (USGS, 2010b). This has caused small data gaps on recent imagery, however although this can confuse automatic classification techniques it makes little difference when manually working on the images.

3.2.3. Errors from spectral similarities

Further errors can arise from spectral similarities that can make differentiation between bedrock and debris covered ice, glacier ice and seasonal snow or cloud, and to a lesser extent turbid pro-glacial lakes and glacier ice a formidable operation (Svoboda and Paul, 2009, Andreassen et al., 2008). However digital elevation models (DEMs) and thermal spectral bands found on Landsat TM and ASTER images can to a degree help mitigate this problem (Paul et al., 2004, Bhambri et al., 2011). The effects of spectral errors in this investigation are discussed in *6.1.1*.

3.2.4. Spatial resolution

Currently the main limitation in terms of accuracy and application of remote sensing in glaciology is the spatial resolution (Kääb et al., 2005a). A distinction must be made between spatial resolution and pixel size, the terms are often used interchangeable, yet the spatial resolution (the smallest identifiable feature on an image) is not necessarily the size of the pixel (Canada Centre for Remote Sensing, 2008). Landforms and features must exceed the pixel size in order to be visible on the images (Kääb, 2002), pixels that contain more than one surface type can be assigned erroneously to a particular landform, which over the whole image can create a considerable error (Konig et al., 2001). The current pixel size of 15 m for ASTER and Landsat ETM+ is adequate for medium and large sized glaciers, but struggles with smaller ice masses such as alpine glaciers (Gao and Liu, 2001). Variables such as glacier surface velocities are not always possible to extract with the current resolution. While satellite sensors with higher pixel sizes of up to 1 m and finer exist, such

as Quickbird, SPOT and IKONOS, acquiring data from such sensors can be expensive, and some of the sensors such as Quickbird only covers a small area (Kääb et al., 2005a).

3.3. Remotely sensed glaciological work: Background theory and significant work

Since its emergence, remote sensing has been used increasingly within the field of glaciology. There are numerous sources that are applicable to remote sensing investigations of the cryosphere, and more advanced and sophisticated sources are being developed all the time (Herman et al., 2011). Decadal-scale changes can be visualised by digitising old glacier inventories and maps or aerial photographs in archives and incorporated them into a GIS. In the case of maps this can allow changes back to the mid-1800s to be assessed, while aerial photographs date back to the 1930s in Norway (Fjellanger Widerøe, (date unknown)). Examples of such sources being used include incorporating the digitised 1970s glacier inventories of the Svartisen region of Norway into a GIS (Paul and Andreassen, 2009) and using maps dating from the 1930s of Jotunheimen (Andreassen et al., 2008).

Significant work that has focused on the glacier parameters of area, volume, and mass balance will now be discussed, in addition to parameters not included in this study – glacier velocity and glacier facies.

3.3.1. Glacier Area

The easy acquisition of satellite imagery in digital form combined with the development of GIS technology has greatly augmented the number of studies delineating glacier area remotely. While manually delineating glacier outlines retains the highest overall accuracy (Figure 6) (Albert, 2002), the lengthy analysis time required means many studies instead opt to automatically delineate glacier area..

Ice Area, Threshold Values for Ice,[a] Processing Time, Percent Over- and Under-Classification, and Accuracy of Each Method[b]

Method	Threshold value	Resulting ice area (km^2)	Estimated processing time	Over-classified ice area (%)	Under-classified ice area (%)	Estimated accuracy (%)
The control						
A. Hand Digitized		58.0	12 hours	n/a	n/a	~ 99.8
Supervised techniques						
B. Maximum Likelihood		52.0	18 min	0.4	9.4	90.2
C. Minimum Distance		43.2	15 min	0.0	24.5	75.5
D. Parallelepiped		49.8	15 min	0.0	12.9	87.1
*E. Spectral Angle Mapper (SAM)		57.7	15 min	2.1	1.2	96.7
Unsupervised techniques						
F. ISODATA		56.7	2.25 min	4.4	5.1	90.6
Fuzzy classification techniques						
G. Linear Unmixing	>0.2	58.2	16 min	5.8	4.0	90.2
H. MTMF	>0.0	47.5	16 min	1.0	17.9	81.1
I. SFF - Scatterplot vs. RMS		46.8	20 min	0.1	18.2	81.7
J. SFF	>0.5	49.8	18 min	0.5	13.3	86.2
K. MNF - PPI - MTMF - Scatterplot		47.0	2 hours	4.3	22.0	73.7
L. MNF - PPI - Linear Unmixing		49.6	2 hours	3.2	16.5	80.3
Band math and threshold techniques						
M. 3/5 Ratio	>4.0	52.6	10 sec	0.5	8.5	91.0
*N. 4/5 Ratio	>3.3	53.1	10 sec	0.5	7.5	92.0
*O. NDSI	>0.5	54.6	11 sec	0.9	5.2	93.9
P. MNF Transform	>10	52.2	1 min	0.0	8.7	91.3
Mean:		51.35	69 min	2.0	13.2	84.8

[a]Where applicable.
[b]Asterisks indicate the three methods recommended for future studies (E, N, and O).

Figure 6: Measured accuracy of different methods of mapping glacial extent from Landsat TM data (Albert, 2002). Although manual delineation is the most accurate it is also time-demanding, therefore different automatic methods can be used to map glaciers.

Manual delineation can be aided by using certain spectral band combinations to help augment the contrast between glacier ice and rock. Band combinations 4,5,3 and 5,4,2 are commonly used. One of the most

accurate automatic delineation methods is spectral band ratioing. Band ratios work by the dividing one spectral band by another. For example the *TM4/ TM5* ratio is based on how snow and ice reflect radiation more in the TM band 4 range of the radiation spectrum (0.76 to 0.90μm), while TM 5 (1.55 to 1.76μm) detects more the reflectance of rock and other terrain. Therefore when TM 4 is divided by TM 5 high values are generated over snow and ice and lower values over rock and other terrain. A *threshold value* can be chosen which allows a cut off, allowing the area of glacier ice to be clearly delineated (Paul et al., 2002). Two of the most widely used band ratios are *TM3/ TM5* and *TM4/ TM5* (Andreassen et al., 2008); the *natural difference snow index* (NDSI) is another commonly used ratio, however when this was tested on Folgefonna it gave poor results.

These techniques have been deployed in the European Alps (Paul, 2002), in the tropical Peruvian glaciers with accuracies of 92% (Albert, 2002), the Himalayas (Li et al., 2006, Ye et al., 2006), Canadian ice fields (Sidjak and Wheate, 1999), Alaska and Iceland amongst other areas (Williams et al., 1997). DEMs can be used to aid glacier margin differentiation in situations with high debris cover (Bhambri et al., 2011, Paul et al., 2004, Silverio and Jaquet, 2005).

3.3.3. Glacier Volume

Glacier area gives a delayed response to climate perturbations, in some cases the glacier area can remain almost constant while the glacier downwastes, as has happened to some of the Alps largest glaciers (Barry, 2006). It is therefore advantageous to understand glacier changes in terms of a change in mass in order to assess how the glacier has responded to a changing climate. This is especially the case for plateau glaciers such as Folgefonna, where ice thickness can be considerable (Førre, 2012). Understandings of glacier volume can also be used to determine the changing contribution to sea level from melting glaciers (Barry, 2006).

Calculating glacier volumes has become easier since the availability of stereoscopic images such as ASTER or SPOT 5, which can be used to create relatively high resolution DEMs, as long as the topography is not overly complicated and some sort of base source to provide ground control points is available (Kääb, 2007). ASTER DEMs have been used to assess volumetric glacier change in many studies (Kääb, 2002, Bolch et al., 2008, Bolch et al., 2011).

While such imagery can be used to determine volumetric change over the last 10 years, it is far more interesting to assess the change over longer timescales. In order for this older DEMs from other sources are compared with the more recent satellite-derived DEMs. Commonly used DEM sources are digitised contour lines from topographic maps (Bauder et al., 2007, Vignon et al., 2003, Surazakov and Aizen, 2006), aerial photographs (Rivera et al., 2005, Andreassen et al., 2002, Quincey and Glasser, 2009) and older satellite data such as Corona (Narama et al., 2006). SAR interferometry (InSAR) can also be used to generate highly accurate DEMs, InSAR works by converting the difference in phase of the returning microwave signal from two SAR images into a

distance from the ground, in a similar vein to optical stereoscopy the differences from the two images are used to generate a DEM (Arora and Patel, 2002).

The last decade has also seen a rise in the use of laser altimetry such as LiDAR, as a high resolution elevation data source (Muskett et al., 2009, Foy et al., 2011). By compiling such sources together it has been possible in some cases to assess the change in glacier volume to be determined back to the late-1800s (Bauder et al., 2007).

Geographically speaking there has been a number of volume change studies in the Himalayas, the Andes, the Rockies, Alaska, the European Alps and the high Arctic, however other than work on Svalbard glaciers there has been very little work investigating the changes in glacier volume in Norway. The 2007 Statkraft/NVE investigation compared a 2007 LiDAR DEM of Folgefonna with a 1997 DEM generated from aerial photos. Andreassen et al. (2002) compared DEMs derived from both aerial photos and topographic maps for 7 Norwegian glaciers (although not Folgefonna), the majority of the glaciers were found to have lost volume up until the 1990s. Similarly Kjøllmoen and Østrem (1997) compared two aerial photography DEMs from 1960 and 1993 over Storsteinsfjellbreen in Nordland, while Kennett and Eiken (1997) compared two LiDAR DEMs over Hardagerjøkulen taken 6 months apart and found a mean change of 4.43 m in elevation, consistent with the estimate of -4.2± 1 m from mass-balance measurements. Andreassen (1999) determined the change in glacier mass balance of Storbreen, Jotunheimen based on the volume change between different topographic maps and found a high level of agreement with the annual mass balance record of the glacier.

The vast majority of studies assume *Sorge's Law;* that the density profile is constant across the glacier, and therefore use a density of 900 kg m^{-3} or 917 kg m^{-3} when converting volume to mass (Berthier et al., 2007). This however is problematic - while the density can safely be assumed to be close to 900 kgm^{-3} in the ablation zone, accumulating snow can have a density as low as 50 kgm^{-3} and can take a considerable amount of time to metamorphose to near glacier ice densities (Benn and Evans, 2010). Some studies such as Hagg et al. (2004) slightly improve on this by assuming a lower density of 600 kg m^{-3} in the accumulation zone, while this is a definite improvement it is still a hefty generalisation.

One very recent study that is worth mentioning is Gardelle et al. (2012), who used DEM differencing over the Karakoram mountains, an especially inaccessible area of the Himalayas. By comparing a 2000 SRTM DEM with a 2008 DEM generated from SPOT imagery and assuming Sorge's Law (both with densities of 900 kgm^{-3} for the whole glacier and with 600 kgm^{-3} for the accumulation zone) it was found that glaciers in this region had defied the global trend and gained a modest about of mass, this remote sensing study came to the attention of the media due to this result (Black, 2012).

3.3.4. Mass Balance Proxies

The glacier mass balance cannot be directly measured using remote sensing data and instead must be measured using proxies. Changes in volume can give a good indication of the health of a glacier, but another commonly used proxy for glacier mass balance is that of measuring the *transient snowline* (TSL) or *firnline* (Bamber and Rivera, 2007). Østrem (1975) was amongst the first to suggest a link between the annual specific mass balance and the TSL, defined as *"the lower boundary of last year's snow at the time of imaging"*. This relationship has been successfully used to reconstruct a twenty-five year record of glacier mass balance using Landsat images on Glacier Blanc, in the French Alps, the remotely sensed mass balance had a strong ($r > 0.67$) correlation with *in-situ* data (Rabatel et al., 2008). Other work has been conducted with comparable methodology in Canada (Sidjak and Wheate, 1999), Alaska (Pelto, 2011), Iceland (Williams et al., 1991), Tajikistan (Kamniansky and Pertziger, 1996), New Zealand (Mathieu et al., 2009) and the tropical Andes (McFadden et al., 2011).

The TSL is often mapped with the fourth spectral band of Landsat images (TM band 4), which is the most sensitive to the snow grain size (Figure 7). This band is therefore the best suited at differentiation between dry and wet snow, and therefore the boundary of the TSL.

Microwave images such as ERS and ASAR data are also suitable for mapping the TSL. These images can pass through clouds and work independently of daylight conditions. They can also penetrate dry-snow allowing their use in winter to observe the transient snowline from the end of the ablation season (De Wildt and Oerlemans, 2003, Kelly, 2002). Some glaciers, especially temperate and maritime glaciers can however undergo episodes of surface melting throughout the winter, preventing the microwaves from penetrating the snow, making winter images unusable (Jaenicke et al., 2006). A lot of work on Norwegian maritime glaciers has used summer microwave images due to this fact (König et al., 2000, König et al., 2001, Storvold et al., 2004). Microwave images are then used to identify at what elevation no melt has occurred, and therefore where the TSL lies. As these images have the added benefit that the sensor can work regardless of weather or daylight conditions they can be used from the same date each year, allowing more consistent mass balance estimations.

It has been pointed out by some authors, and indeed appears to be the case in this investigation (*6.5*) that the distinct boundary visible on SAR images is not actually the TSL, but the *firn line*, formed by previous years' layers of snow and slightly influenced by glacier flow (König et al., 2000). The firn line also reflects changes in the climate, albeit over a longer timescale (De Wildt and Oerlemans, 2003). The mapped boundary is therefore sometimes referred as *the transient snow line – firn line* (TSL-FL) (Rott et al., 2007).

3.4 Glacier Parameters not measured in this investigation

Because the imagery over Folgefonna's outlet glaciers did not provide a high enough temporal resolution, and surface features were not sufficiently prominent it was unfortunately not possible to measure glacier surface velocity. Delineating glacier faces on the other hand would have needed ground data in different albedos and reflectances, so was also infeasible (Kulkarni et al., 2011). However as both of these parameters are potentially possible to calculate in the near future, some past work will still be discussed.

3.4.1 Glacier Velocity

The most commonly used method for calculating glacier velocity is that of *feature tracking*, where prominent features on the glacier surface such as crevasses or debris cover are tracked between successive images either automatically or manually, and their displacement is used to calculate velocity (Racoviteanu et al., 2008, Raup et al., 2007). Landsat and ASTER images can be used on glaciers with especially prominent landforms (Quincey and Glasser, 2009, Kääb et al., 2005b) and aerial photos have even been used successfully to measure velocities on Engabreen (Jackson et al., 2005). The higher pixel size of data such as SPOT imagery (up to 2.5 m) lends itself more to velocity calculations over other satellite sensors.

Reported accuracies have ranged from 0.5 m with SPOT data to 30 m with Landsat images (Berthier et al., 2007, Quincey et al., 2005). The time interval between images must be sufficiently large for the feature displacement to be visible, but not so large that features such as crevasses have deformed or melted (Berthier et al., 2005).

Automated velocity calculation techniques exist but are particularly sensitive to the effect of varying illumination of the glacier (Whillans and Tseng, 1995). It is worth mentioning that glacier velocity can also be measured using inSAR (*3.3.3*), when two images are compared an inferogram can be generated which displays relative ground motion (Winther et al., 2005, Goldstein et al., 1993). In the case of Folgefonna however the microwave data available was of a too poor pixel size to be used.

It is important to note that velocity measurements only provide a snapshot of the glacier flow during the ablation season, which is when glaciers would typically be flowing at their fastest (Gao and Liu, 2001, Evans, 2000); however the traditional method of measuring velocity are not completely free from such problems (Benn and Evans, 2010). Glacier velocity measurements make it possible to infer basal processes - the average velocity, as well as the rate of change of velocity can be used to distinguish whether the glacier is flowing due to internal deformation or by basal sliding, and therefore if water is present at the glacier bed (Copland et al., 2009).

3.4.2 Glacier Facies

In addition to being able to detect the TSL remotely, different snow and ice facies can be mapped (Konig et al., 2001). Commonly identified zones are fresh and wet snow, firn, clean ice and dirty ice (Williams et al., 1991, Hall et al., 1988). The different reflectances of each category is shown in Figure 7, it can be seen that TM band 4 detects the greatest differences in reflectance for each zone, and is therefore best suited for differentiating between different glacier faces.

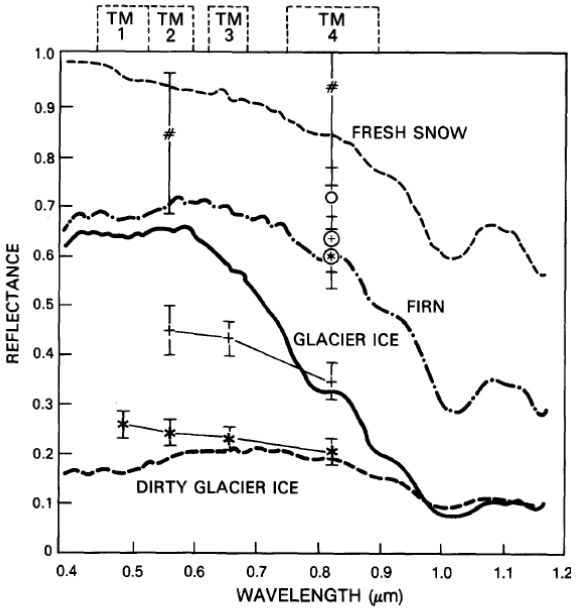

Figure 7: The calculated Landsat at-satellite reflectances in the various spectrally delineated zones of the glaciers (Hall et al., 1988). It can be seen that Landsat TM band 4 is the most sensitive to differentiating between different snow and ice faces.

ERS or ASAR imagery can be used to detect wet snow facies; which as they have no surface manifestations are invisible to optical images (Williams et al., 1991). Wet snow absorbs the majority of the microwave signals, while glacier ice and dry snow shows a higher backscatter (Winther et al., 2005, Jaenicke et al., 2006). However in-situ reflectivity data of each zone must be collected first to aid analysis, failure to do so can lead to spurious results (Williams et al., 1991).

Based on the literature detailed above, the methods for this investigation were selected and shall be discussed in the following chapter.

4.0 Data and Methods

This chapter will introduce the various methods that were deployed in order to extract the desired glaciological parameters. All work was carried out using a combination of *ArcMap 10.0*, *ERDAS Imagine 2010, NEST 4B-1.1* and *PCI Geomatica V10.3.2.* An assessment of errors and uncertainties present in the data used is given later *(6.1*).

4.1 Remote Sensing Data

The two most significant data sources in this investigation were Landsat and ASTER imagery, both optical satellite sensors. In addition to this ENVISAT ASAR microwave images, Digital Elevation Models (DEMs), aerial photographs and old maps were also used in the investigation. The data that was included in this investigation shall now be described.

4.1.1 Landsat Imagery (MSS, ETM+)

Landsat images are one of the most important datasets in remote sensing glaciological studies (Gao and Liu, 2001). Landsat provides near-global optical imagery for the last 40 years, since its initial launch in 1972 the pixel size of Landsat images has increased from 80 m per pixel to the current 15 m. Landsat 4-7 images (post-1982) consist of 7 spectral bands: three visible, three infrared and one thermal band, since 1999 an 8th pan-chromatic band has been included which makes it possible to sharpen images to a 15 m pixel size (Table 1).

In total 26 Landsat images of sufficient cloud and weather conditions were downloaded from the *USGS Earth Explorer* website (earthexplorer.usgs.gov). Each image had the individual spectral bands that would be used in analysis (optical bands 1,2,3,4 and 5 as well as the pan-chromatic band when applicable) *stacked* using *ERDAS IMAGINE;* combining them into one IMG file. Each stacked image could then be configured to use any combination of the spectral bands to display the image (Figure 1). A table of the Landsat images used in this study is shown in Table 2.

Table 1: The different specifications of each of the 5 operational Landsat missions (Lillesand et al., 2004). In the case of Folgefonna Landsat provided coverage from 1976 onwards. By sharpening the TM bands with the 8th band (panchromatic band) using a tool such as ArcMap's *Pan-sharpen tool (Arc GIS Resource Center, 2011a)* it is possible to conduct analysis at a resolution of 15 m per pixel. Five different sensors have been included in various combinations on the Landsat missions – Return Beam Vicicon (RBV), Multispectral Scanner (MSS), Thematic Mapper (TM), Enhanced Thematic Mapper (ETM) and Enhanced Thematic Mapper plus (ETM+). The RBV sensor is not useful to analysis as it was an analogue (non-digital) television like camera.

Satellite	Launched	Decommissioned	RBV Bands	MSS Bands	TM Bands	Pixel size (m)
Landsat 1	23/7/1972	6/1/1978	1-3 (simultaneous images)	4-7	None	80
Landsat 2	22/1/1975	25/2/1982	1-3 (simultaneous images)	4-7	None	80
Landsat 3	5/3/1978	31/3/1983	1-3 (simultaneous images)	4-8	None	80
Landsat 4	16/5/1982	15/6/2001	None	1-4	1-7	30
Landsat 5	1/3/1984	-	None	1-4	1-7	30
Landsat 7	15/4/1999	-	None	None	1-7 plus panchromatic (ETM+)	30 (panchromatic 15 m)

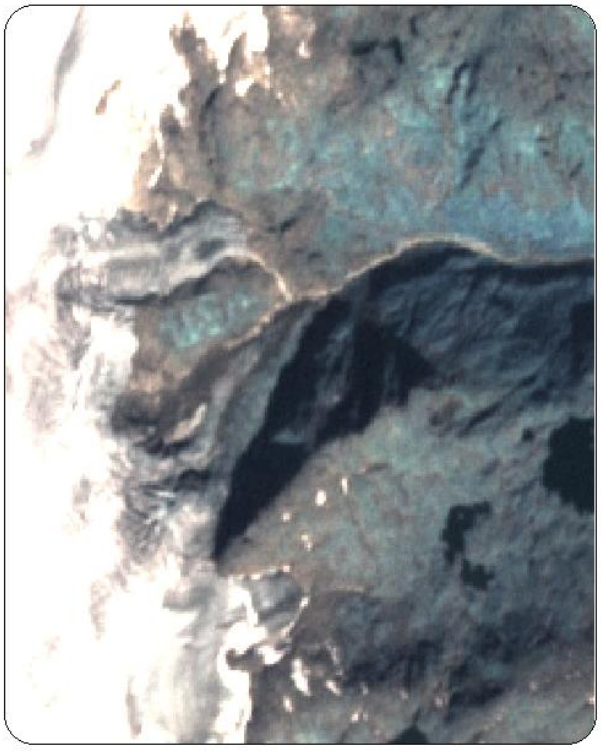

Natural look image - spectral band combination 3,2,1.

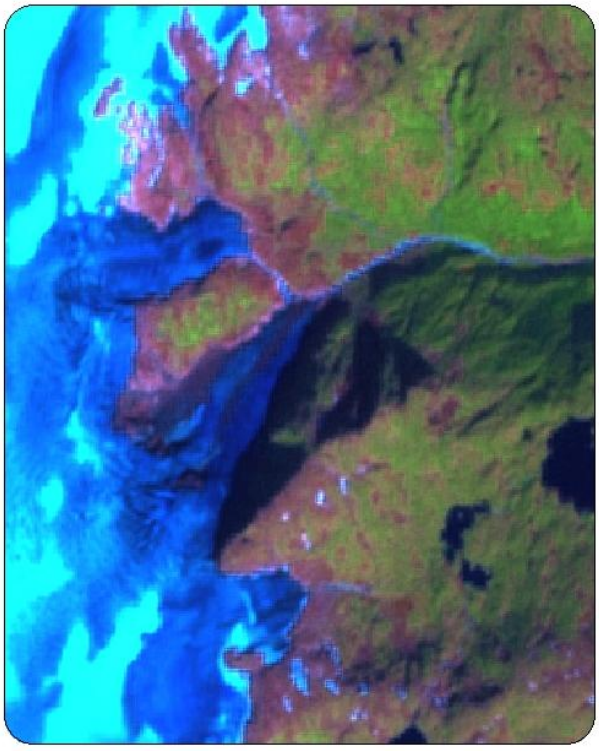

False Colour image - spectral band combination 5,4,2

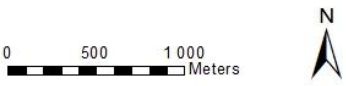

Figure 8: Buerbreen, Sørfonna – shown with two different spectral band combinations. Using a false colour spectral band combination such as either 5,4,2 or 4,5,3 greatly aids the identification and delineation of glacier ice.

4.1.2 ASTER (Advanced Spaceborne Thermal Emission and Reflection Radiometer) Imagery

ASTER images date back to 2002 and consist of three bands in the visible and near-infrared spectrum at a pixel size of 15 m, and six bands in the short-wave infrared spectrum at 30 m. Arguably the most useful aspect of ASTER images is the 15 m pixel size stereo image (bands 3N and 3B, as shown in Figure 9) that can be combined to generate digital elevation models (DEMs) using software such as *ERDAS IMAGINE* or *PCI Geomatica (Kääb et al., 2002, Svoboda and Paul, 2009).*

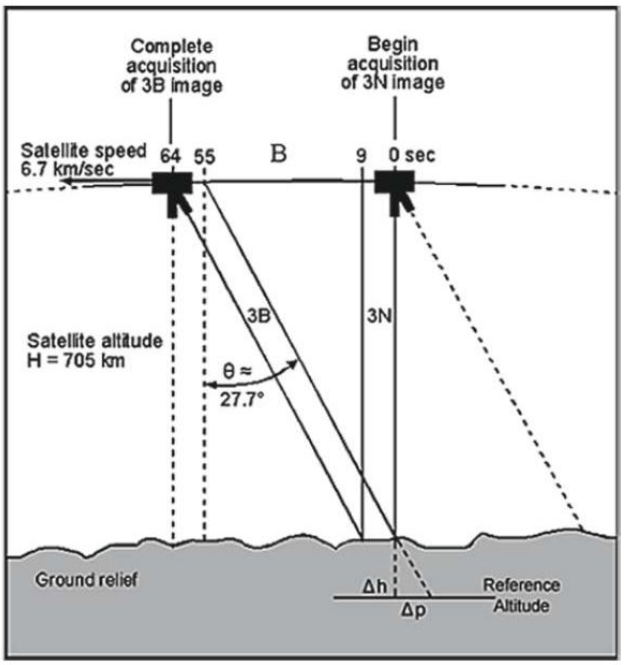

Figure 9: Configuration of ASTER's 3N and 3B stereoscopic bands, which can be combined to create DEMs (Toutin, 2011).

A total of thirteen ASTER scenes were obtained from the *NASA REVERB* website (reverb.echo.nasa.gov), of which ten were unsuitable for DEM generation due to prolific cloud cover. ASTER images are available in *HDF* format, which contains all the spectral bands in one file, therefore no stacking is required. A table of all ASTER imagery used in this investigation is shown in Table 3.

4.1.3 ENVISAT ASAR Imagery

Active Microwave sensors conversely do not rely on the sunlight for illumination and instead use their own microwave source (Heywood et al., 2006). ERS1, ERS2 and ENVISAT ASAR are all microwave S*ynthetic Aperature Radar* (SAR) sensors, that is they exploit the relative motion of the orbiting satellite, the delay in time and the change in phase of the returning radar pulse is converted into an image.

The microwave images used in this investigation were all ENVISAT ASAR images. ASAR has several 'modes' that can operated; the two modes applicable to glaciology are the *image mode* and the *wide swath mode*. The image mode provides data at the finer pixel size (30 m), however coverage of this was inadequate over Folgefonna and only the *wide swath mode* images were available. These cover a larger area and have a short revisit time, but at a pixel size of 75 m (ESA Earthnet Online, 2012, Lillesand et al., 2004).

The Nansen Environmental Remote Sensing Centre (NERSC) keeps an archive of ENVISAT ASAR images on their servers; it was possible to download thirty winter images from November, December, January and February dating back from 2005.

The ASAR images that were in the used in this study are shown in Table 4.

4.1.4 SPOT Imagery

One pre-processed natural look SPOT 5 image of Folgefonna from 03/09/2002 with a finer pixel size (2.5 m) was acquired on a DVD. Unprocessed SPOT 5 data is stereoscopic like ASTER data and can be used to generate DEMs, so it would be a great benefit to be able to use such data in this investigation. However as this image was pre-processed the spectral bands could not be configured, and the natural look band combination included was of a poor image contrast over the glacier. The stereoscopic bands were also not included. This restricted the image's use in analysis and as the image coincided with two Landsat images a month apart either side, this image was not used in analysis. It was however used as an aid for both geo-referencing and for error checking (*4.1.5, 4.3.1.3.*).

Table 2: Landsat images used in this investigation, the percentage of the glacier outline in cloud and shadow is also shown.

Date	Sensor	Pixel size/ m)	Percentage of Glacier Outline in Cloud (%)	Percentage of Glacier Outline in Shadow (%)
13/08/2011	Landsat 7ETM+	15	0.00	4.94
28/09/2010	Landsat 7ETM+	15	0.88	7.69
03/09/2010	Landsat 7 ETM+	15	0.00	9.60
14/09/2008	Landsat 7ETM+	15	0.00	15.43
27/09/2007	Landsat 7ETM+	15	0.00	13.40
08/08/2006	Landsat 7ETM	30	0.00	3.83
15/07/2006	Landsat 7ETM+	15	0.00	3.72
16/10/2005	Landsat 7ETM+	15	0.00	19.02
11/08/2004	Landsat 7ETM+	15	0.00	4.09
01/09/2003	Landsat 7ETM+	15	0.00	8.07
31/08/2003	Landsat 7ETM+	15	2.64	5.36
07/08/2003	Landsat 7ETM	30	0.00	6.91
15/07/2003	Landsat 7ETM	30	16.54	12.61
22/09/2002	Landsat 7ETM+	15	0.00	11.45
05/08/2002	Landsat 7ETM+	15	15.10	4.27
20/07/2002	Landsat 7ETM+	15	31.26	9.73
28/09/2001	Landsat 7ETM+	15	0.00	9.85
26/09/2000	Landsat 7ETM+	15	0.00	2.51
21/09/2000	Landsat 7ETM	30	0.22	1.90
06/08/1999	Landsat 7ETM+	15	0.00	2.90
31/07/1994	Landsat 5 MSS	30	0.00	5.83
31/08/1991	Landsat 5 MSS	30	18.85	9.18
07/09/1988	Landsat 5 MSS	30	9.39	4.18
04/08/1987	Landsat 5 MSS	30	22.74	2.42
21/08/1984	Landsat 5 MSS	30	0.00	4.94
31/07/1976	Landsat 1	80	0.00	3.75

Table 3: ASTER images downloaded for use in this investigation, however due to adverse cloud conditions only three images were used.

Date	Sensor	Pixel size/ (m)	Used
01/07/2010	ASTER L1B	15	Yes
14/07/2009	ASTER L1B	15	No
12/06/2009	ASTER L1B	15	No
12/07/2005	ASTER L1B	15	No
10/08/2004	ASTER L1B	15	No
10/08/2004	ASTER L1B	15	No
01/8/2004	ASTER L1B	15	No
07/07/2003	ASTER L1B	15	No
21/08/2002	ASTER L1B	15	No
21/08/2002	ASTER L1B	15	No
20/07/2002	ASTER L1B	15	Yes
20/07/2002	ASTER L1B	15	Yes
21/10/2001	ASTER L1B	15	No

Table 4: ENVISAT ASAR Wide swath images used in this investigation, many of the images had signs of glacier surface melting on them, for the most cases the images could still be partially used however.

Date	Pixel size (m)	Melt on images
09/02/2011	75	No
03/12/2010	75	No
19/11/2009	75	Partial melting
12/12/2009	75	Yes
06/02/2009	75	No
06/01/2009	75	Yes
05/12/2008	75	Partial melting
07/02/2008	75	No
02/12/2007	75	Partial melting
05/02/2007	75	No
08/01/2007	75	Yes
20/12/2006	75	Partial melting
05/02/2006	75	No
16/01/2006	75	Partial melting
09/12/2005	75	Partial melting

Table 5: Non-satellite data used in this investigation, data was acquired from a variety of sources. The three maps and aerial photos were used to map the glacier extent, while the two DEMs, digital contour lines and 1937 topographic map were used to measure the glacier volume.

Date	**Data type**	**Scale/ Pixel Size**	**Coverage**	**Mapped by**
1860	Map	1:50,000	Southern margin of Sørfonna not shown	Ltn. Christophersen
1864	Map	1:50,000	Entire of Folgefonna	S.A. Sexe
1937	Topographic Map	1:100,000	Southern Margin of Sørfonna not shown	Norges geografiske oppmåling
1962	Aerial Photos	1:25,000	Eastern Margin of Sørfonna not shown	Widerøe's Flyveselskap
1987	Digital contour lines	n/a (vector data)	Entire of Folgefonna	Statens kartverket
1999	DEM	90 m	Entire of Folgefonna	NASA
2007	DEM	30 m	Entire of Folgefonna	NVE

4.1.5 Digital Elevation Models (DEMs)

A very precise 2007 DEM generated from a LIDAR (Light Detection And Ranging) laser altimetry campaign was provided by the Norwegian Water and Energy Department (NVE) In addition to this a 90 m pixel size DEM from the 1999 SRTM (Shuttle Radar Topography Mission) was downloaded using *NASA REVERB*.

Five DEMs were generated; all were constructed using PCI Geomatica for the ASTER DEMs and ArcMap's *Topo to Raster* tool in the case of the contour DEMs.

4.1.5.1 ASTER DEMs

Three ASTER DEMs were generated, one from the 01/07/2010, and two from the 20/07/2002 which were combined to cover the whole glacier.

The two stereoscopic bands (3N and 3B) of each image were linked together by designating tie points, that is that the same visible features on both images were marked. This was done both using an automatic tie point collection tool as well as manual collection.

The images were then geo-referenced against the SPOT image, as well as online maps from norgeskart.no and Google Earth when coverage from the SPOT image was inadequate. A bundle adjustment model was run to link the images together before the two stereoscopic bands were transformed into an *epipolar image,* where both images are orientated together along the same horizontal axis (Kääb, 2002), as shown in Figure 10. When each DEM was generated the pixel size was set to 30 m; this was both because this was the pixel size of the precise NVE Laser DEM, but also because this pixel size has been reported to contain the least amount of errors (Raup et al., 2007, Toutin, 2011). Figure 11 shows a flow chart summary of the methods followed on PCI Geomatica in order to create an ASTER DEM.

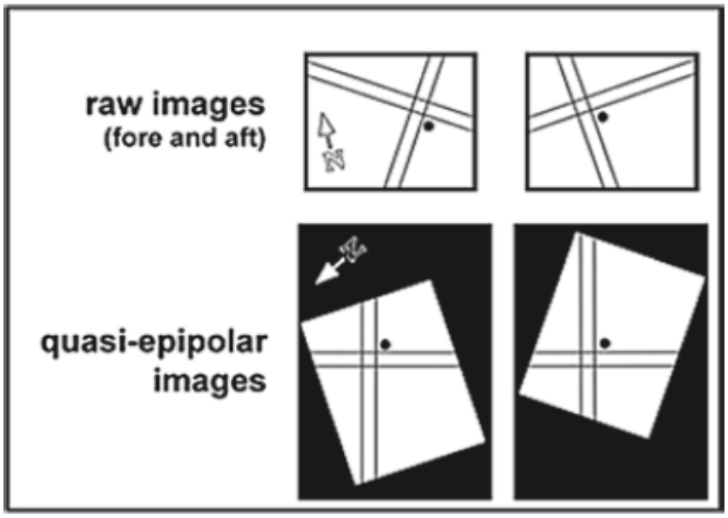

Figure 10: Creating epipolar images orientates the two stereoscopic images to share a common x-axis, and thereby eases the process of DEM extraction (Toutin, 2011).

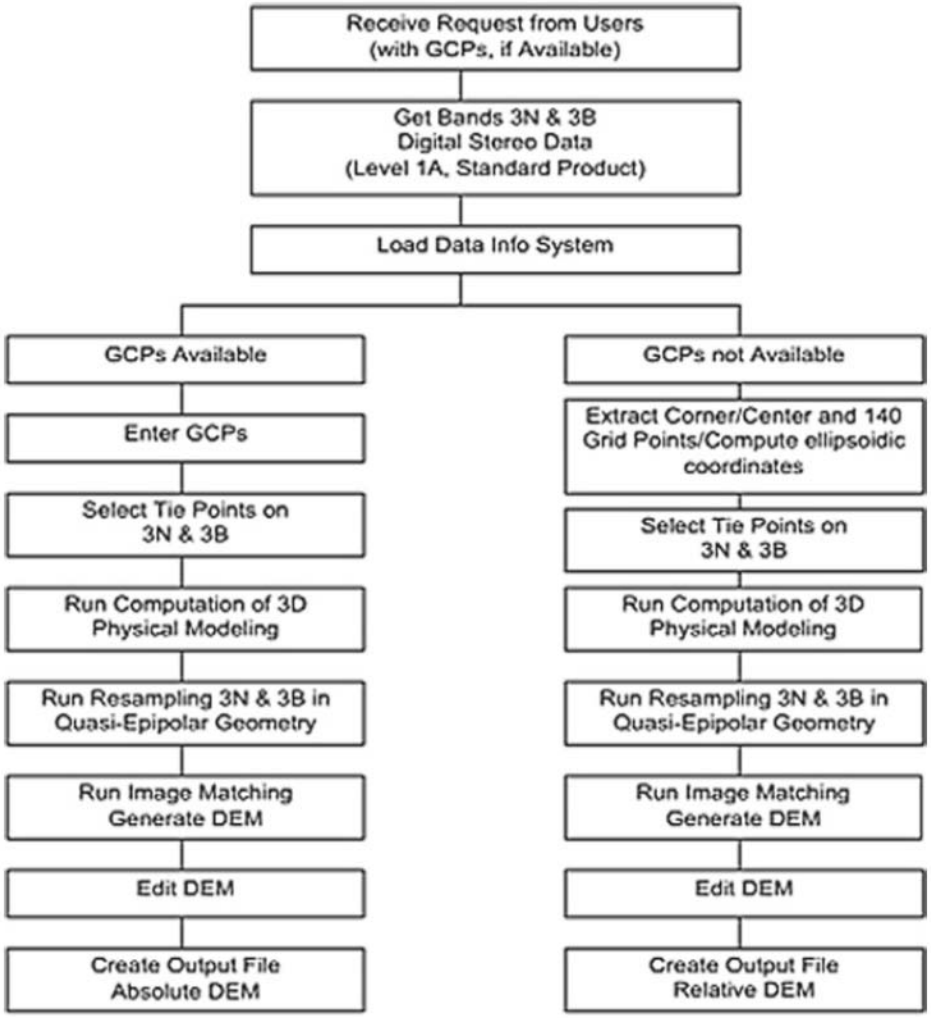

Figure 11: A flowchart showing the methodology used on PCI Geomatica to create DEMs from ASTER imagery at The Land Processes Distributed Active Archive Centre (LP DAAC) (Toutin, 2011). The left hand column shows the methods in this investigation, if no GCPs had been available then just a relative DEM could have been generated (right hand column.)

4.1.5.2 Digitised contour lines

Two sets of digitised contours were interpolated to create digital elevation models. An already digitised topography map of Etne and Kvinnherad communes from the mid-1980s with an average date of 1987 was provided by Statens Kartverk through the *Norge Digital* portal. In addition to this the contour lines of a map of the area from 1937 (*4.2.1*) were scanned in and digitised. For each dataset the shapefiles containing the digitised contour lines were input into the *Topo to Raster* model on ArcMap 10, which interpolates between the contour lines using a *discretized thin plate spline interpolation*, allowing the DEM to follow complex terrain accurately (Arc GIS Resource Center, 2011b). In accordance with the other DEMs the output pixel size was set to 30 m, and the number of iterations (which determines the smoothness of the finished product) was set to 10. This number of iterations was found to be a compromise between smooth elevations and over-simplifications of topography.

All generated DEMs were then spatially referenced to the same dataframe as the other data: the *WGS 1984 zone 32 north* projection.

4.2 Other Data

Historical maps over Folgefonna dating from 1860, 1864, and 1937 were generously provided by *Statens kartverk* and *a* set of aerial photographs from 1962 were provided by the Institute of Earth Science at the University of Bergen.

The maps and aerial photos were digitised at a resolution of 600 to 1500 DPI depending on the size of the image using an Epson GT-15000 scanner located in the Institute of Geography. This is more than a sufficiently high enough resolution as some studies have worked with topographic maps scanned in as low as 300 dpi (Surazakov and Aizen, 2006).

4.2.1 Old Maps

The maps were georeferenced using *ArcMap* against a 2002 Landsat image with optimum conditions, using the technique commonly referred to as *rubbersheeting*. Between 10 and 15 Ground Control Points (GCPs) on stable terrain were found on each scanned-in map before the same points were identified on the Landsat image. Care was taken to select points that could be assumed to have remained mostly stable over the whole investigatory timescale (Raup et al., 2007), such as prominent edges of the fjord, or corners of non-glacial lakes. The 1864 and 1937 maps did not fully cover Sørfonna, therefore changes undergone at Sørfonna were examined back to these dates all of the data was clipped to the extent of these maps.

4.2.3 Aerial Photos

The scanned aerial photos were processed using *PCI Geomatica*. Each separate image had a *fiducial* mark in the corner, and the positions of these were marked on the software to allow the images to be orientated, rotated and resized by the software. GCPs were selected between the aerial photos and a "reference image"; again the combination of the SPOT image, norgeskart.no and *Google Earth* were used. Tie-points were also designated linking the series of images together. The aerial images were then orthorectified to account for changes in elevation and terrain before all of the images were automatically mosaiced together. The finished aerial photograph mosaic had a pixel size of 1 m and covered all of Nordfonna and Midtfonna, as well as the eastern margin of Sørfonna.

Figure 12: Collecting ice thickness measurements using Georadar equipment towed behind a Snowmobile. (Photo: Åsmund Bakke). A combination of GPR and ICE-Radar measurements were used to map the subglacial drainage of Nordfonna.

4.2.4 Field Data

The bedrock topography beneath Nordfonna was mapped using a combination of GPR (Ground-Penetrating Radar) and a more deeply penetrating ICE-Radar towed behind a snowmobile, as seen

in Figure 12 (Førre, 2012). This data was provided to the author as a TIN file, which was then converted to a raster image.

4.3 Methods

4.3.1. Delineation of glacier area

The glacier areas were delineated both manually as well as using automatic band ratios. ASTER images weren't used for glacier delineation in this study as Landsat provided a more than thorough enough record for the ASTER era (post-2002) at the same pixel size. As the historical maps and aerial photos were not multispectral data they could only be analysed using manual delineation.

Note though that the visible part of Sørfonna on the 1962 aerial photo mosaic has been combined with the 1976 outline to give some indicate of Sørfonna's response in the 1960s, therefore this area measurement is most likely an underestimate. For the 1962 aerial photos only the eastern side of Sørfonna was covered, therefore only the position of the glacier margin could be examined for Sørfonna in 1962 (Figure 28).

4.3.1.1 Manual Delineation

Manual delineation of multispectral data was aided by using different spectral band combinations. Landsat band combinations 5,4,2 and 4,5,3 have proven to be useful at discrimination areas of glacier ice from rock (Paul et al., 2002). "Natural look" images (3,2,1) were also used for identifying pro-glacial lakes from ice.

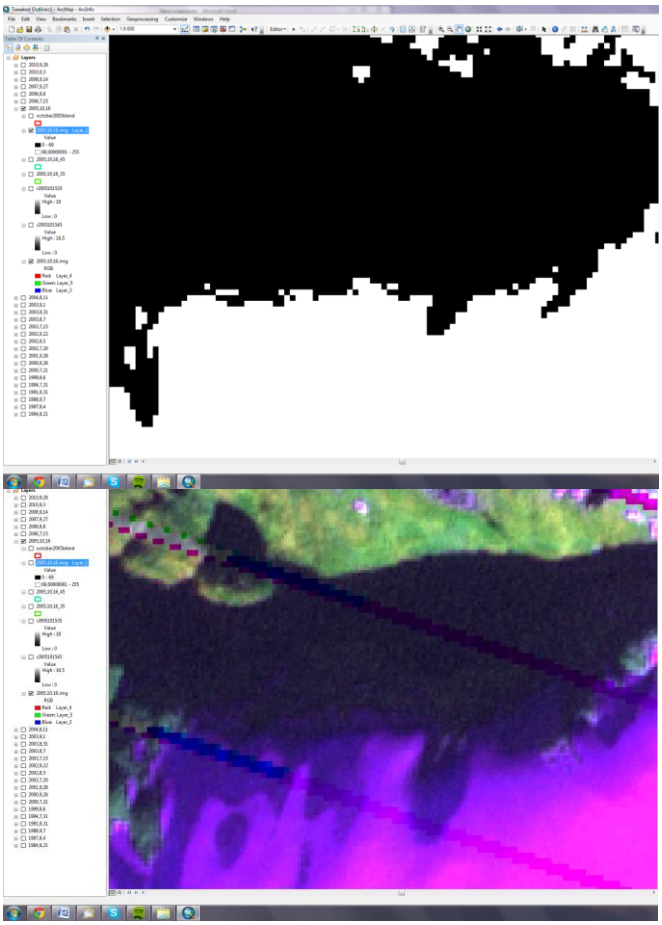

Figure 13: In areas where the glacier margin was obscured by shadow (bottom) the 1st Landsat spectral band could be used with a classification set at pixel values of 69 (top). Although not a perfect solution this certainly helped delineate Folgefonna's margin.

While manually delineating the glacier there were portions of the glacier cast into shadow or covered by cloud. In the case of areas in shadow it was possible to slightly alleviate the problem by using the first spectral band (TM band 1) and classifying the image to a threshold of pixel value 69 (Figure 13) (Konig et al., 2001). Although not always completely successful this certainly helped delineate the outline at times. When this method was of no avail or when opaque cloud masked parts of the glacier the outline was assumed to be the same as the previously delineated outline, as the images were worked on

starting with the most recent this would have caused slight underestimations of ice-covered area in some cases. This is taken into account in the errors discussion (*6.1*).

4.3.1.2 Automatic delineation – segregated band ratios

The glacier area was delineated automatically using both the TM 3/TM 5 and TM 4/TM 5 band rations using *ArcMap's Raster Calculator.* The threshold value was tweaked and the results compared with the manually delineated outlines. Optimum threshold values were found to be *3.0* for the TM 4/TM 5 ratio, and *4.5* for the TM 3/TM 5 ratio. Following this a 5x5 median filter was applied to remove small snow patches lying close to the glacier and fill in debris patches on the glacier (Andreassen et al., 2008). Lastly all the glacier outlines were separated into Western and Eastern halves using ArcMap's *split* function. This was to assess whether the stronger westerlies during positive NAO phases had an effect on the western or eastern side of Folgefonna. An average was taken of the percentages of expansion or retreat of each side to make an index showing either a predominant Western or an Eastern Folgefonna reaction

4.3.1.3 Quality checking

The quality of the results was checked by comparing the outlines against the original Landsat image as well as the SPOT image and the NVE DEM, any necessary modifications were made. For method comparison purposes both the measured areas from the automatic band ratios and the manual delineations were recorded, this shall be further discussed in *5.4.2.5.*

4.3.2. Delineation of glacier volume

As the bedrock topography had been mapped for Nordfonna total ice volumes could be calculated. For Midtfonna and Sørfonna the bedrock elevation was unknown rendering the calculation of ice volumes impossible. Instead the change in ice volume between years was worked out. Changes in volume (m^3) were converted to changes in mass by dividing by the assumed constant density of ice (917 kgm^{-3}). As the density of pure water is 1000 kgm^{-3} this means that each kg of ice would produce 1.091 litres of meltwater.

4.3.2.4. Calculating Ice Volume (When subglacial topography is known)

The volumes between the glacier surface and the underlying bedrock were calculated using the *raster calculator.* The subglacial bedrock topography was subtracted from the glacier surface elevation producing pixel values for ice thickness; this was then multiplied by the cell length and width (30 m) to convert each pixel into a volume. *Zonal* Statistics was then used to sum up the volume across all of Nordfonna. A visual explanation of the processes used in raster calculator is shown in the appendix (Figure 86).

4.3.2.5. Calculating Ice Volume Change (When subglacial topography is unknown)

To calculate the change in volume, first of all a flat, planar bedrock was assumed, an assumption which upon looking at the mapped topography beneath Nordfonna is clearly not true but is adequate enough for gauging the change in ice volume. By assuming that the ice surface elevation

is normally distributed around the mean elevation, planar elevations were calculated that were below 95% of the ice. This gave values of *1258 m* and *1188 m* for Midt- and Sørfonna respectively. A value of *1291* m was calculated for the portion of Sørfonna that was visible on the 1937 topographic map.

As the bedrock surface assumed for these two ice masses is flat the calculation is much simpler. The *ArcMap* tool *Surface Volume* was used to calculate the volume above the fixed planar surfaces. These volumes were converted to a change in mass by multiplying by the assumed density of ice (917 kgm^{-3}).

Lastly in order to assess the surface elevation change at different heights across the glacier, Folgefonna was split into zones based on the 1987 surface elevation with 25 m intervals and the surface change was measured for each zone.

4.3.3. Measuring the transient snow line (TSL)

The TSL was measured using two methods: by using the fourth spectral band on Landsat images from the end of the ablation period, and using ENVISAT ASAR images from mid-winter, where the TSL was preserved beneath the dry snow.

4.3.3.1 Mapping the Transient Snow Line using Landsat images.

Fifteen of the Landsat images that were used for the glacier area delineation were found to be suitable for mapping the TSL. The remaining images were subject to either fresh snow at high altitudes or freezing rain, which increases the surface reflectance (Williams et al., 1991).

Upon inspection it became apparent that several glacier facies were visible on each Landsat scene, the most prominent boundary visible was therefore traced on ArcMap (as shown in Figure 14). The *Add Surface Information tool* was then used to read off the mean, maximum and minimum elevations from a DEM. The NVE laser DEM was used to obtain elevations for images from 2000 onwards, while the NASA 1999 DEM was used for images older than 2000. It was decided that only these DEMs would be used because they had both undergone thorough error checking and can be said to be the most reliable.

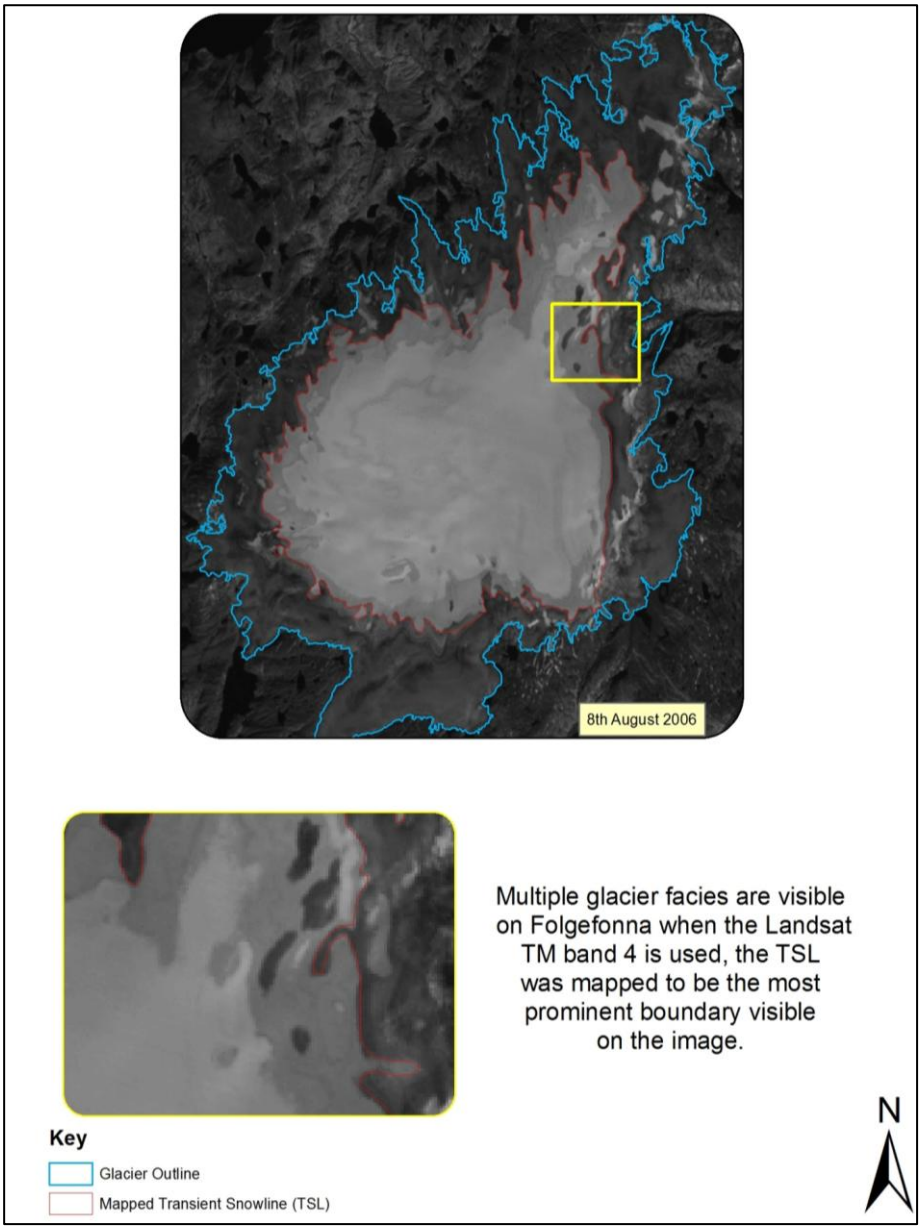

Figure 14: Mapping the TSL was done by delineating the most prominent boundary visible using both the Landsat TM band 4 (pictured) and ENVISAT ASAR images from mid-winter. The subjectivity of these measurements is a clear source of error.

4.3.3.2. Mapping the Transient Snow Line using ASAR images.

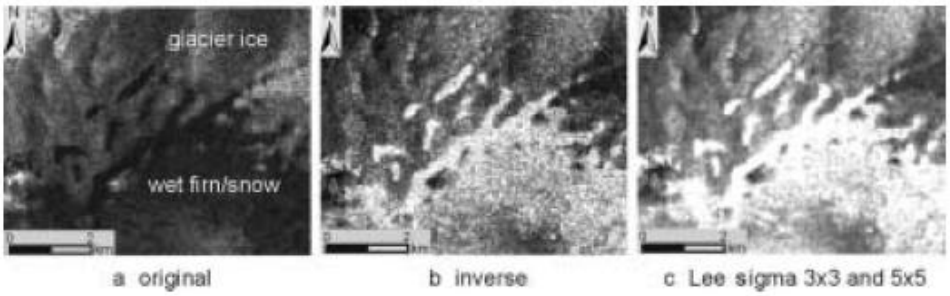

Figure 15: Example of the processing steps taken to better visualise the distinction between wet snow and glacier ice, the SAR images were inverted before two Lee sigma filters were carried out (Jaenicke et al., 2006), this was all done using NEST 4B-1.1.

The ASAR images were processed and subsetted using *NEST 4B-1.1*, a program designed to specifically handle SAR imagery. Following the advice (Figure 15) set out by Jaenicke *et. al.* (2006), *NEST 4B-1.1* was used to augment the contrast between the wet and dry snow by first inverting the image to increase the brightness in dark areas, and then applying two *Lee Sigma* filters, first a 3x3 window followed by a 5x5 window. This makes the boundaries sharper and the areas within the boundaries more homogenous.

The images were then loaded into *ArcMap*, where they were aligned together by matching up features such as the surrounding fjords to the 2002 Landsat image used previously. Upon inspection only 15 of the 30 images downloaded were suitable for mapping the TSL, many of the images captured Folgefonna during a time where temperatures must have risen above freezing; dark streaks running across the glacier could represent areas of melted wet snow. Similarly the edges of the glacier are in some cases marked by dark splodges, these could be interpreted as superimposed ice. Either way images where the glacier was undergoing some level of melting increased the reflectivity of the glacier surface hindering the usefulness of the microwaves at being able to penetrate to the end of ablation season conditions (Jaenicke et al., 2006).

Then in the same manner as with the Landsat snowlines; the most prominent boundary was traced and the mean elevation, along with the maximum and minimum elevations of the line were extracted.

The results gathered from the above mentioned methodologies are discussed in the following chapter.

5. Results

The results obtained for measurements of the glacier area, volume and the elevation of the Transient snowline (TSL) shall now be described. In addition to this the trend in the TSL is extrapolated over the next 20 years. The results from this investigation are then compared with the total winter precipitation, mean summer temperature and NAO index, along with *in-situ* mass balance and ELA data.

5.1 Change in Glacial Area from 1860 to 2011

The glacier area was calculated between 2011 and 1976 with Landsat images, additional data from aerial photos (1962) and historical maps (1937, 1864 and 1860) were also used.

The two historical maps from 1860 and 1864 roughly agree that at around that time Nordfonna, Midtfonna and Sørfonna were approximately 48.8 km^2, 28.8 km^2 and 195 km^2 in size, this date is also considered to be the approximate LIA maxima (Nussbaumer et al., 2011). No data exists between the 1860s and the 1937 topographic map; over this time span it appears a dramatic decrease in ice-covered area occurred. Nordfonna and Midtfonna shrank by 34% and 41% respectively, while Sørfonna shrank by a more modest 7% (Figure 17, Figure 16, Figure 18). All of Folgefonna then entered a period of relative stability; the 1962 aerial photography mosaic doesn't fully cover Sørfonna, however by examining the glacier margin position of Sørfonna and the areas of Nord- and Midtfonna it can be seen that between 1937 and 1962 there was a gentle decrease in glacier area of between 1 and 2% (Figure 28). This was then followed by a slight increase in area up to 1976 suggesting that during this 40 year period only minor fluctuations were experienced. All three ice masses then started a slightly stronger retreat into the 1980s, a trend which continued until 1988 when Nordfonna, Midtfonna and Sørfonna had lost a combined 24.7 km^2 over 11 years, which amounts to losses of 16%, 19% and 9% respectively.

The three ice masses then advanced rapidly throughout the 1990s. Between 1988 and 1994 Nordfonna, Midtfonna and Sørfonna all expanded by 9%, 18% and 6% respectively. On average the whole of Folgefonna expanded by 2.45 km^2yr^{-1} between 1988 and 1994. The area decrease between 1994 and 1999 is very small and it is therefore likely that many parts of Folgefonna continued to expand up to the turn of the millennium. Upon examination of the glacier outlines it can be seen that the western sides of Folgefonna began retreating between 1994 and 1999, while the eastern side remained comparatively stable. This shall be looked at later (*6.3*).

The period from 1999 onwards has the most data points in the investigation. A sharp and unprecedented glacier shrinkage up until present day can be seen over this timespan, although all three ice mass records are punctuated by a short-lived glacier advance between 2005-2008. However following this small relapse, the rate in reduction of ice-covered area all increase dramatically. By 2011 Nordfonna had shrank by 20% of its 1994 area, Midtfonna by 43% and

Sørfonna by 13% (Figure 21, Figure 22, Figure 23). In total all of Folgefonna lost on average 2.97 km^2yr^{-1} over the 17 year (1994 to 2011) period. It can be stated from observations in Figure 25, Figure 26 and Figure 27 that after 1999 it was the south-west and north-west of each ice mass underwent the greatest retreat; generally the western side of Folgefonna has retreated more than the east.

As the climate has warmed it is not surprising to find that it is the portions of the glacier with lowest elevations that have retreated. The area of retreated ice had a mean elevation of 1265 m.a.s.l. although some parts reached down to 471 m.a.s.l. It is interesting to note that the mean elevation of the glacier margins has stayed more or less on track with the glacier area record and is therefore also influenced by the same climate forcing (Figure 24). Between 1984 and 2011 the mean elevation of the glacier margin rose by 4.9%, from 1301 m to 1364 m for Nordfonna, by 4.2% from 1311 m to 1366 m for Midtfonna and by 3.3% from 1240 m to 1280 m for Sørfonna.

In 2011 Nordfonna, Midtfonna and Sørfonna measured 24.8 km^2, 9.1 km^2 and 156.7 km^2 respectively, reductions of 47%, 68% and 20% compared with the LIA maxima size in 1860.

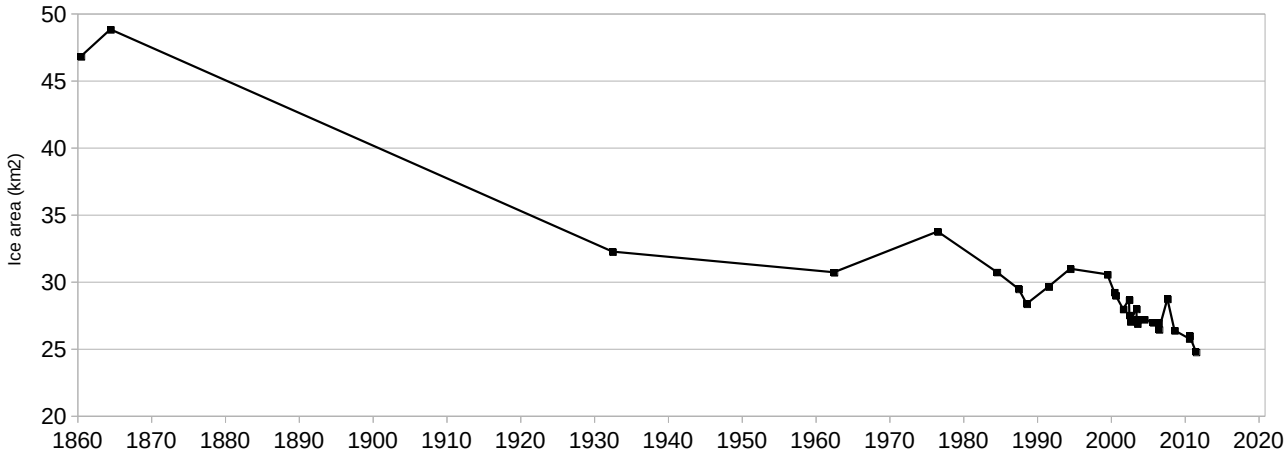

Figure 16: The ice covered area of Nordfonna from 1860 to 2011 measured using a combination of Landsat images, aerial photographs and old maps.

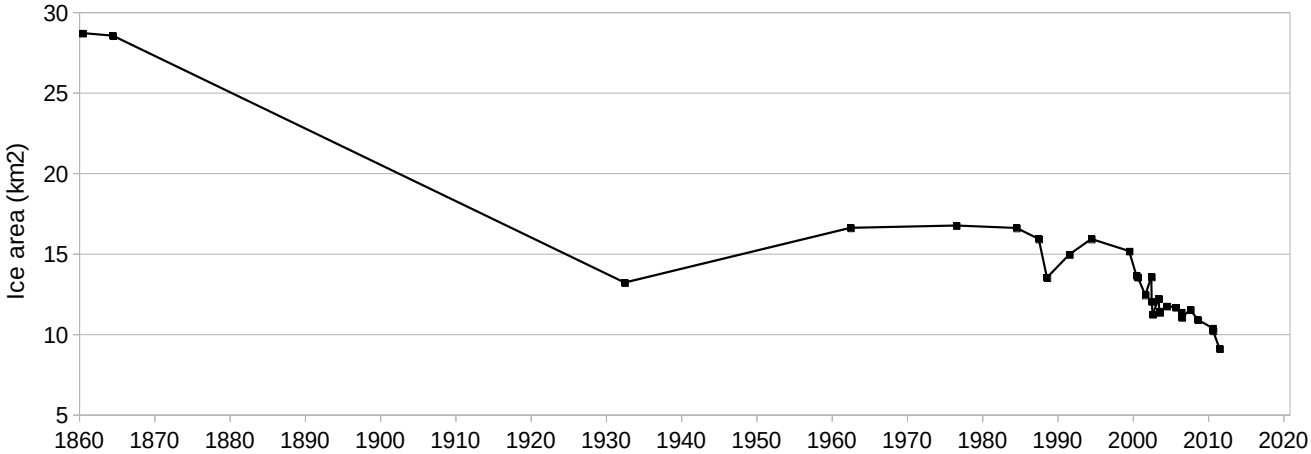

Figure 17: The ice covered area of Midtfonna from 1860 to 2011 measured using a combination of Landsat images, aerial photographs and old maps.

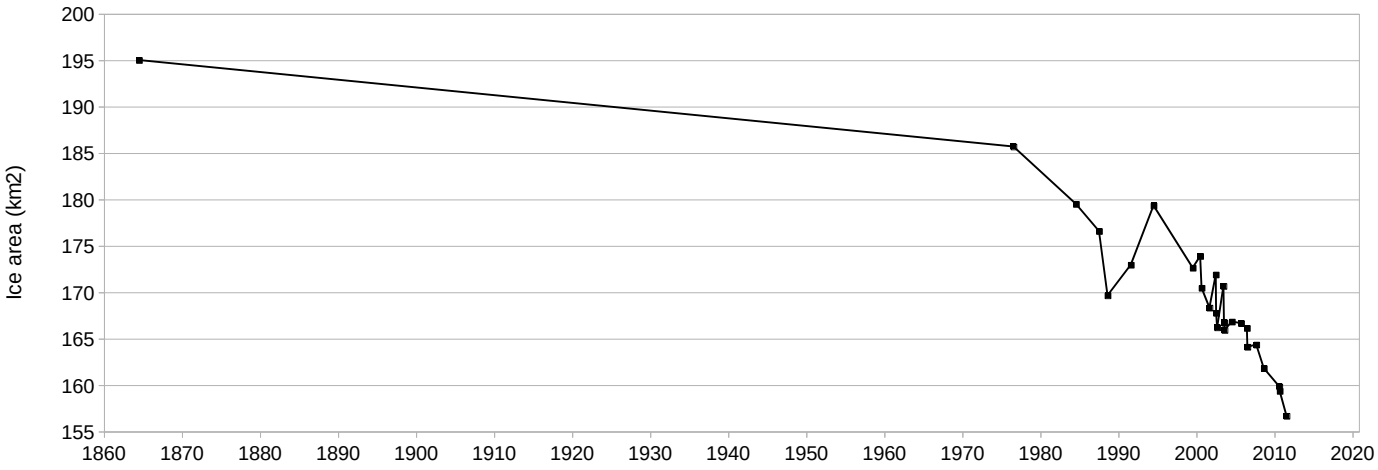

Figure 18: The ice covered area of Sørfonna from 1860 to 2011 measured using a combination of Landsat images, aerial photographs and old maps. For comparability reasons all glacier outlines are trimmed to the extent of the 1937 map.

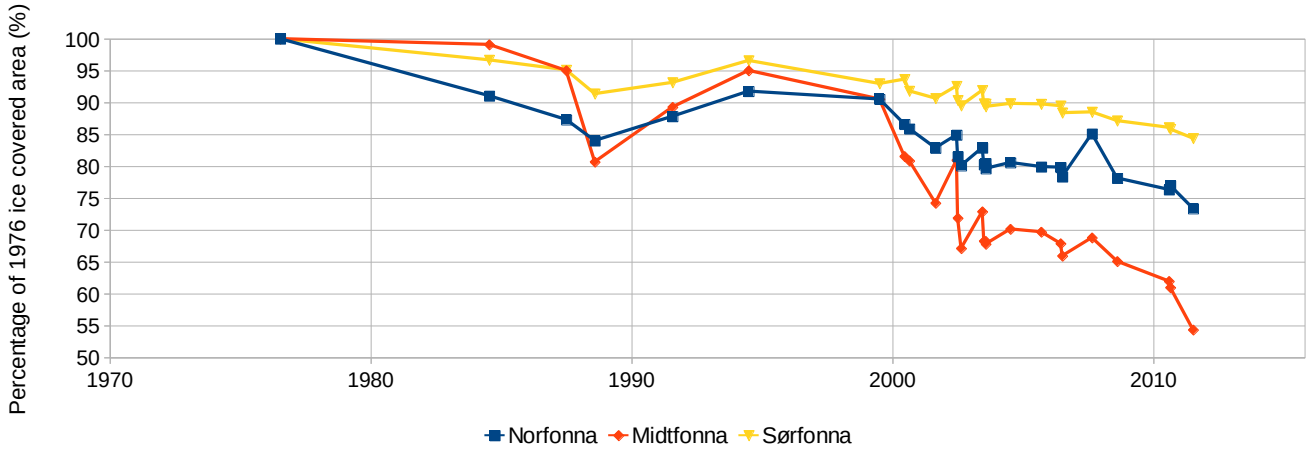

Figure 19: Total standardised glacier retreat from 1976 to 2011 of Nordfonna, Midtfonna and Sørfonna. As one would expect the larger the ice mass, the least amount of ice proportionally lost. It seems that the three ice masses were more or less in track with each other until around 2000, when Midtfonna and Nordfonna began to retreat proportionally more.

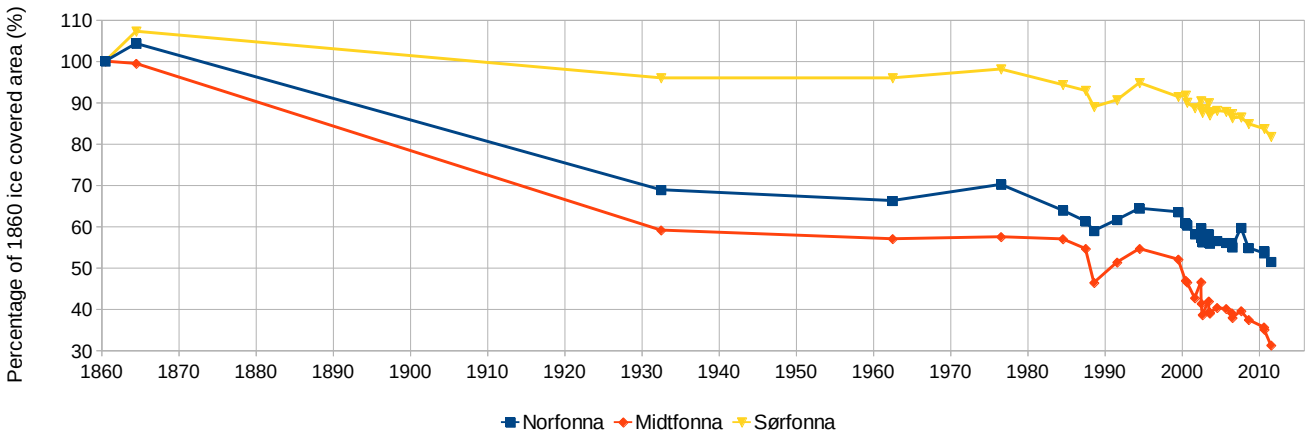

Figure 20: Total standardised glacier retreat from 1860 to 2011. of Nordfonna, Midtfonna and Sørfonna. Again as one would expect the larger the ice mass, the least amount of ice proportionally lost.

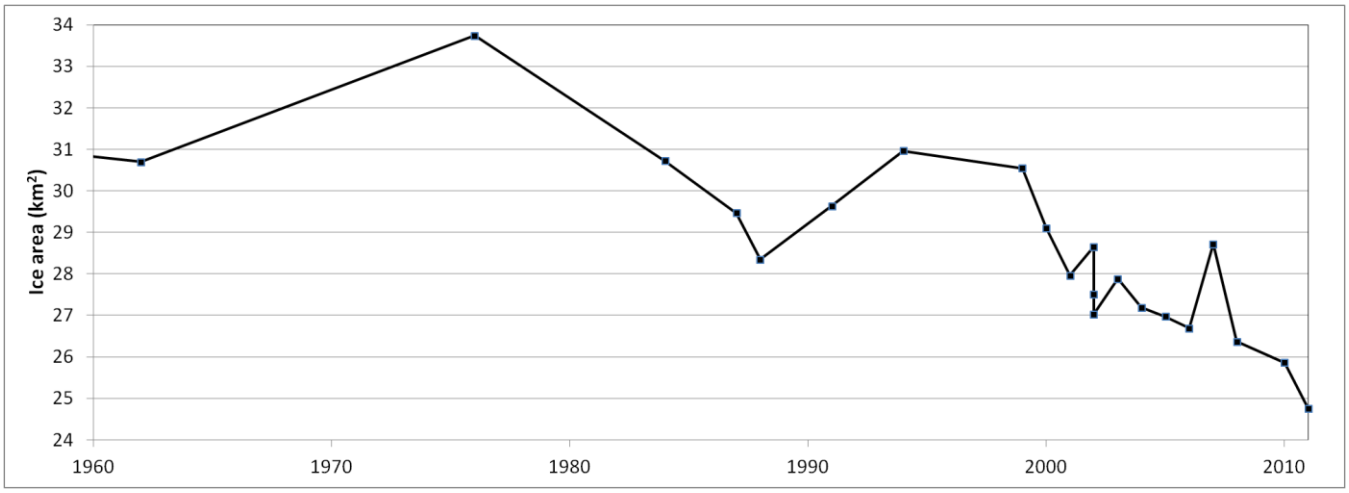

Figure 21: Ice-covered area of Nordfonna between 1960 and 2011 measured using a combination of Landsat images, aerial photographs and old maps to delineate the glacier area. Note that as some years have multiple datapoints, the mean for the years 2000, 2003, 2006 and 2010 were taken.

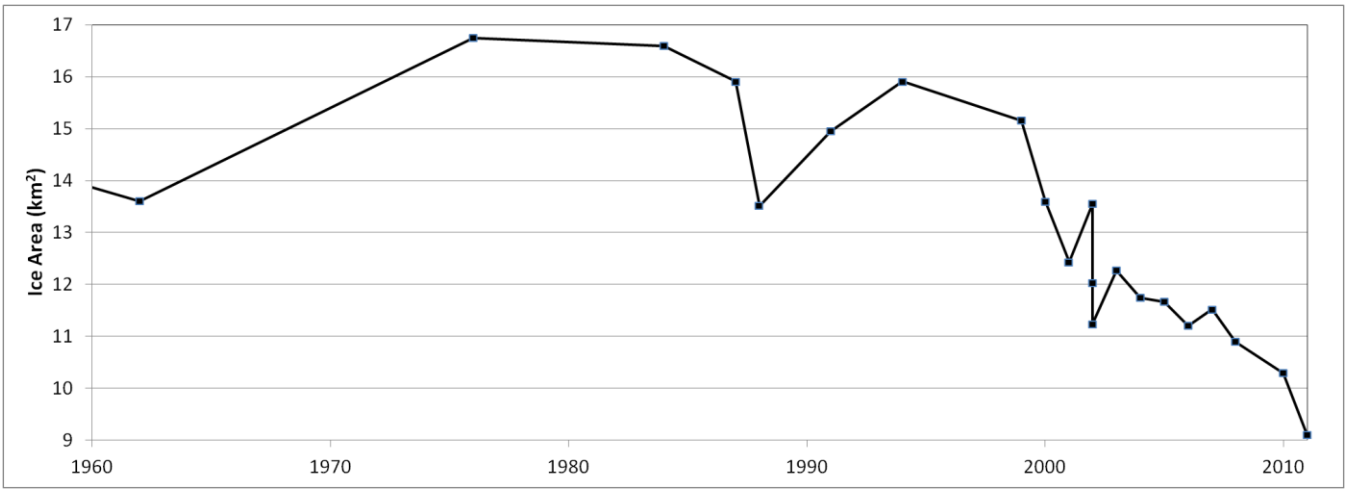

Figure 22: Ice-covered area of Midtfonna between 1960 and 2011 measured using a combination of Landsat images, aerial photographs and old maps to delineate the glacier area. Note that as some years have multiple datapoints, the mean for the years 2000, 2003, 2006 and 2010 were taken.

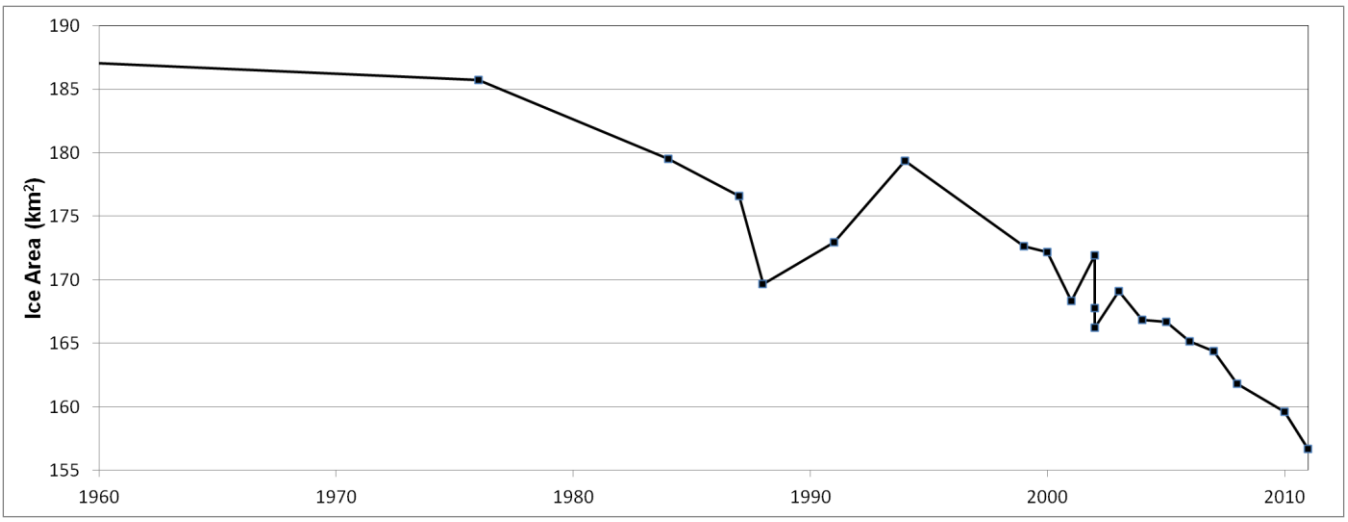

Figure 23: Ice-covered area of Sørfonna between 1960 and 2011 measured using a combination of Landsat images, aerial photographs and old maps to delineate the glacier area. Note that as some years have multiple datapoints, the mean for the years 2000, 2003, 2006 and 2010 were taken.

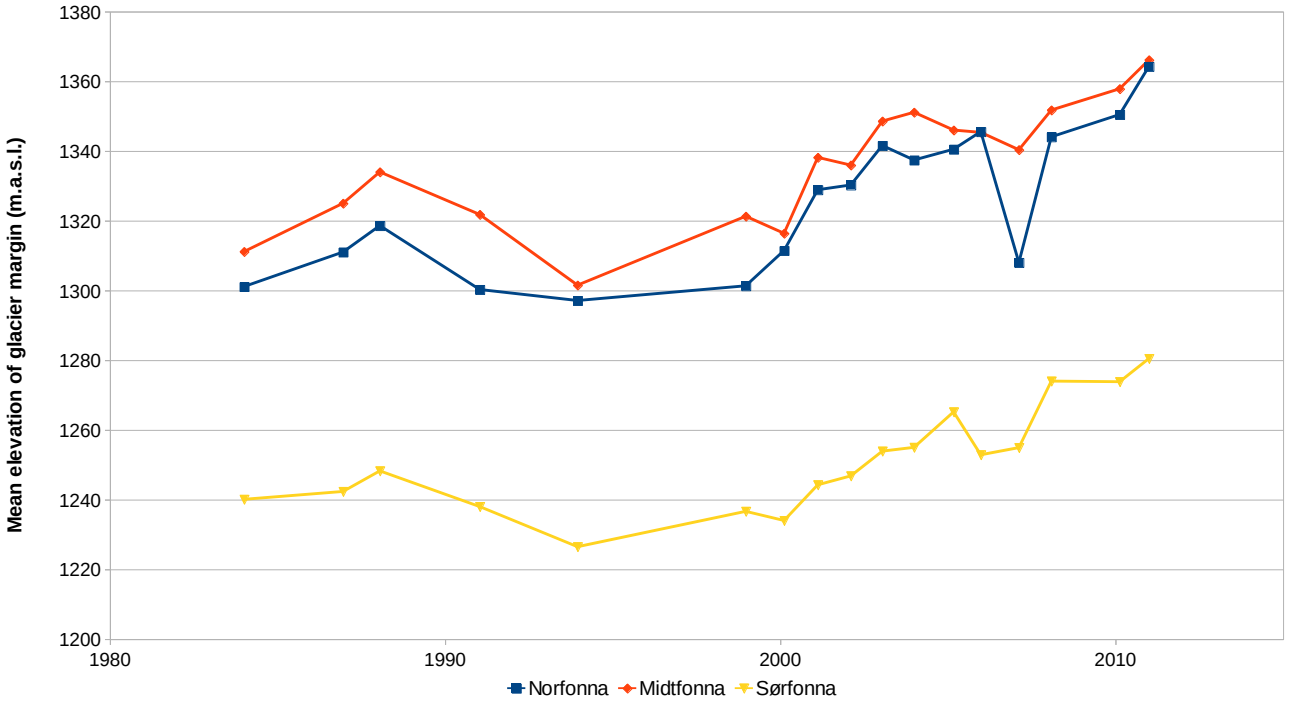

Figure 24: Mean elevation of Folgefonna's glacier margin between 1984 and 2011. Generally the height of the glacier margin kept track with the trends seen in the glacier area.

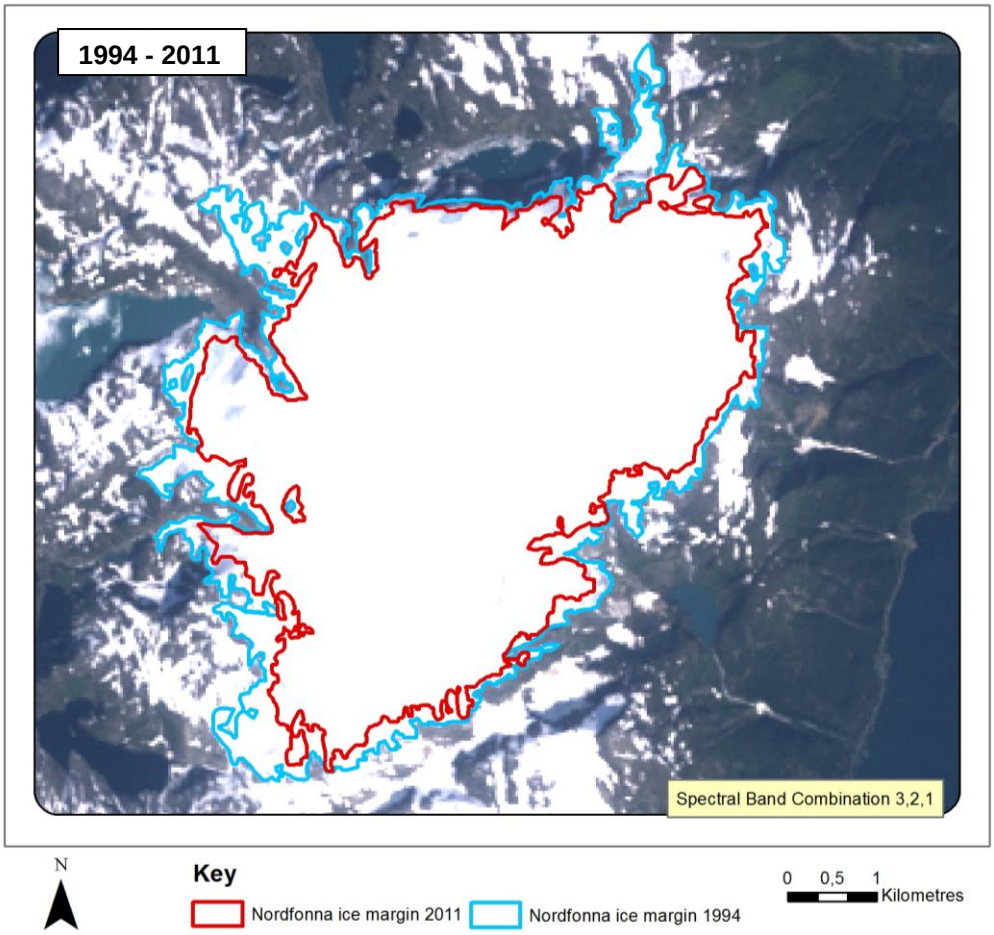

Figure 25: Change in Nordfonna's glacier covered area between 1994 and 2011, the background image is the 1994 Landsat image. The western side of Nordfonna has retreated more than the eastern side, with exposed corridors or ice especially prone to retreat.

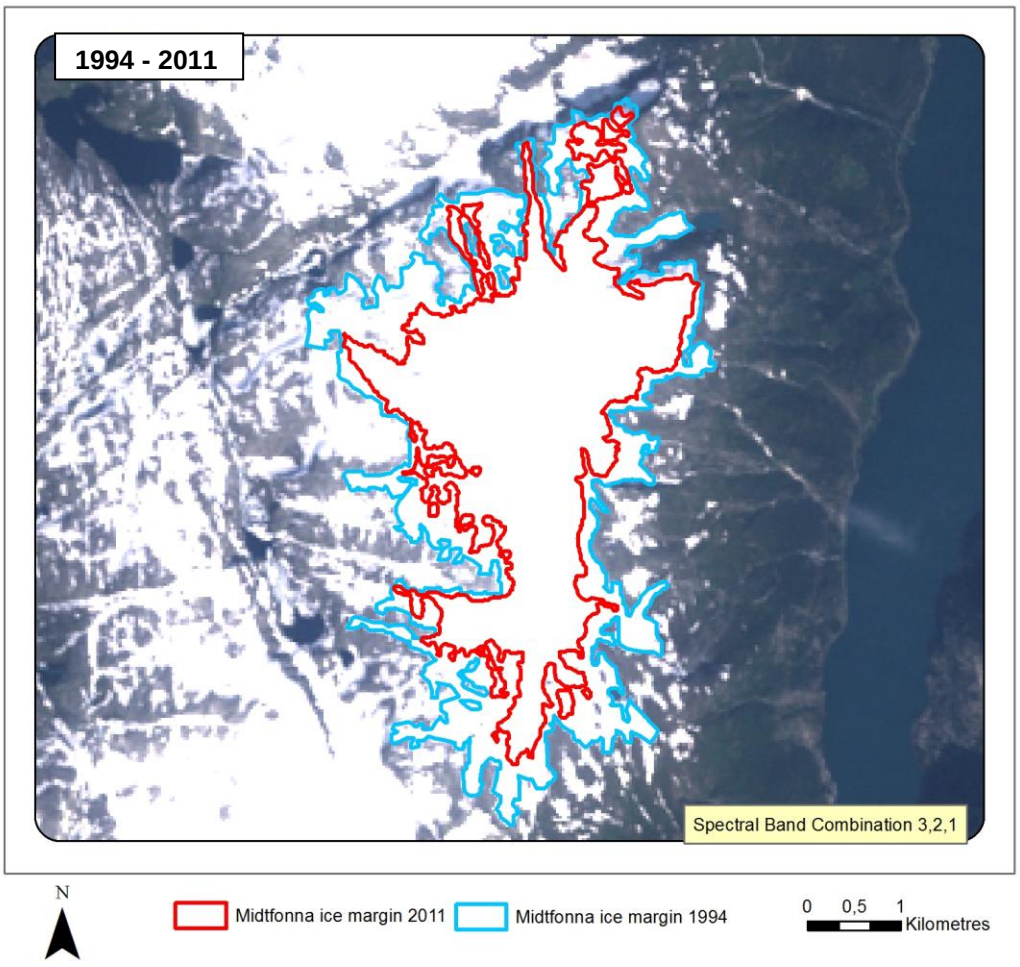

Figure 26: Change in Midtfonna's glacier covered area between 1994 and 2011 the background image is the 1994 Landsat image. Midtfonna has generally retreated from all margins, although again the western side has retreated more than the eastern side.

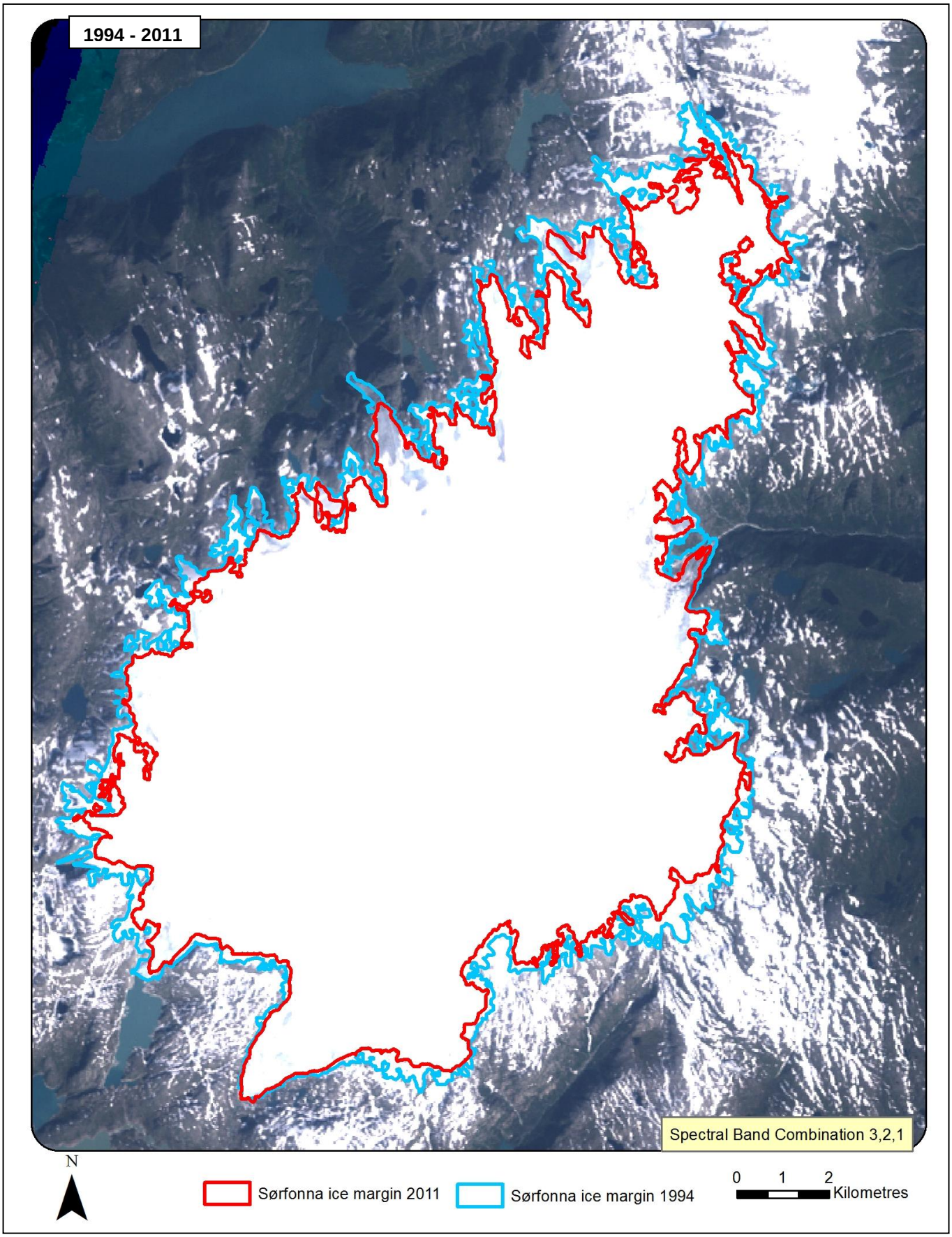

Figure 27: Change in Sørfonna's glacier covered area between 1994 and 2011 the background image is the 1994 Landsat image. The northern third of Sørfonna has lost the most ice, while the higher elevation, southern portion has retreated less. The same bias of a more stable eastern side is also evident here.

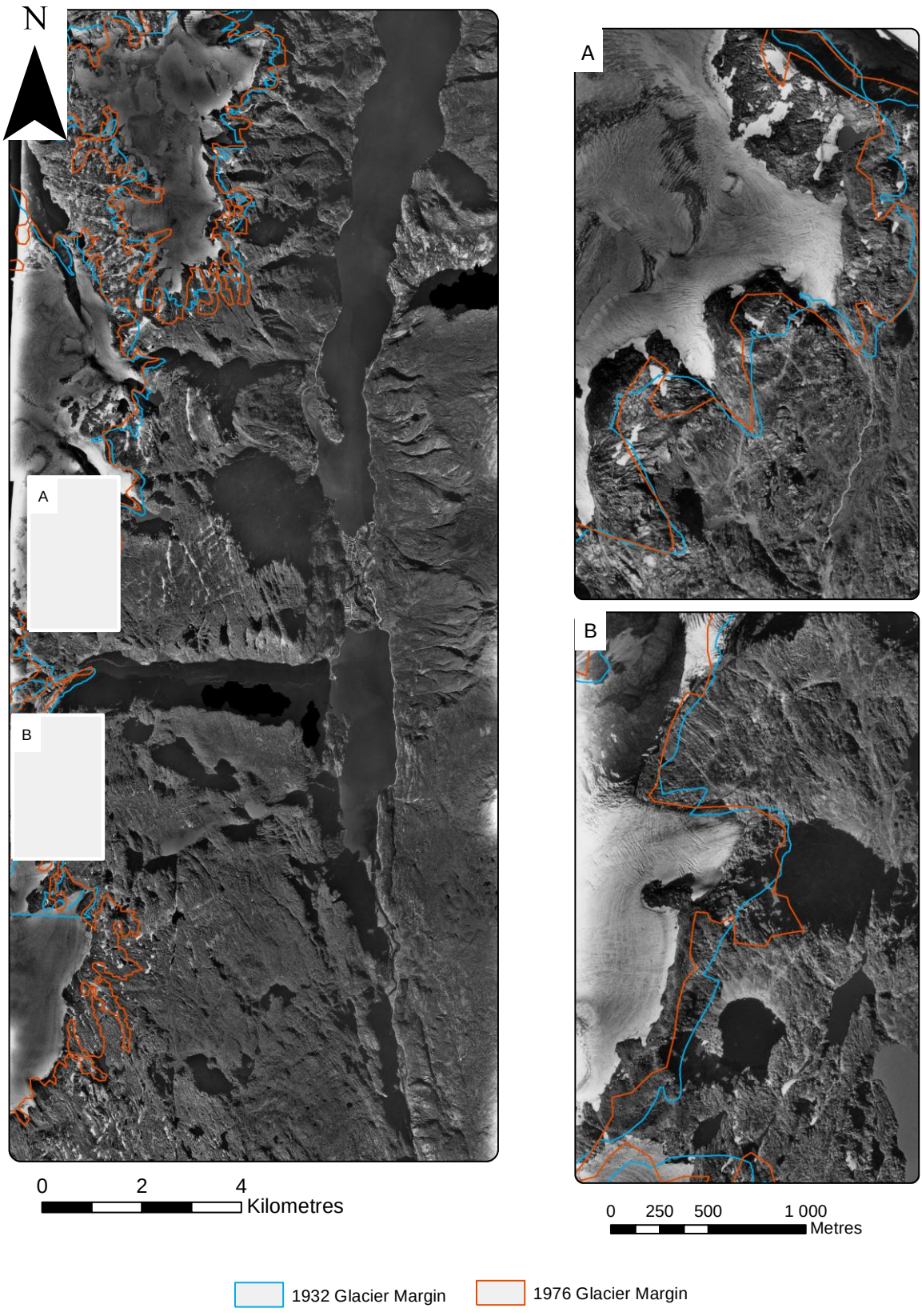

Figure 28: The 1967 aerial photography mosaic does not cover Sørfonna in its entirety, however by expecting the portion of glacier margin visible it can be seen that in a similar vein to Nordfonna and Midtfonna, the glacier margin is generally further retreated than both the 1937 and 1976 glacier extents, suggesting that all of Folegefonna shrank by a modest amount during the mid-20th century.

5.2 Change in Glacial Volume from 1937 to 2011

The surface elevation of Folgefonna was compared with different DEMs, which were either derived from ASTER stereoscopic imagery, provided pre-prepared or generated from digitised contour lines (*4.1.5*). As already mentioned the bedrock topography information was only available for Nordfonna, therefore only the *change* in volume could be determined for Midtfonna and Sørfonna.

In 1937 the volume of Nordfonna was approximately 3.23 km^3. No other DEM is available until 1987, within this time period Nordfonna reduced in volume by 454 million kg (Figure 29), a reduction of 13%. Midtfonna and the portion of Sørfonna visible on the 1937 topographic map also both shrank by similar amounts – 409 million kg (14%) and 3688 million kg (14%) respectively (Figure 30 and Figure 32). Until 1987 the losses on the different segments of Folgefonna had stayed in track with each other (Figure 20), however from then onwards Midtfonna has lost proportionally the most mass, followed by Nordfonna, while Sørfonna has lost proportionally the least mass since 1987. Between 1937-1987 and 1987-1999 the rate of loss of mass on Nordfonna and Midtfonna accelerated considerably, from 9.1 million $kgyr^{-1}$ and 8.2 million $kgyr^{-1}$ respectively to 47.6 million $kgyr^{-1}$ and 48.3 million $kgyr^{-1}$. As the 1937 topographic map used to generate the DEM does not fully cover Sørfonna it is not possible to determine a true rate of ice loss before 1987, however Sørfonna also continued to lose mass.

Nordfonna had an ice volume of 2.29 km^3 of ice in 1999, a reduction of 571 million kg or 19% from its 1987 volume, while Midtfonna and Sørfonna shrank by 579 million kg and 4188 million kg, or 24% and 8.4% of their 1987 volumes (Figure 34). Between 1999 and 2002 Nordfonna increased in volume by an incredibly dubious 29% up to 2.95 km^3 of ice. Midtfonna's volume increased by a more believable 58 million kg or 3.1% while Sørfonna experienced a slight decrease in volume of 862 million kg or 1.9% of the 1999 volume. The increases in volume are evident in Figure 38. Between 2002 and 2007 Nordfonna and Midtfonna reduced in volume; Nordfonna shrank to 2.62 km^3 of ice, a reduction of 11%; a value perhaps a little inflated due to the overestimate of growth between 1999 and 2002. Midtfonna lost 162 million kg of mass (8.4% of its 2002 volume). Sørfonna on the other hand grew by 2.3% over the 5 years, a gain of 1015 million kg.

In the years following 2007 all of Folgefonna has lost mass at an increasing rate, Nordfonna and Midtfonna's rates of glacial downwasting increased by 390% and 360% respectively compared with between 2002 and 2007. Nord-, Midt- and Sørfonna lost 29.9%, 19.6% and 9.4% respectively of their mass between 2007 and 2010, although again the value for Nordfonna seems exaggerated.

In August 2010 Nordfonna had an ice volume of approximately 1.84 km^3 and had lost in total 1.40 km^3 of ice compared with its 1937 ice volume, equivalent to 1521 million kg or 43.2%. Midtfonna lost 1.32km^3 of ice between 1937 and 2010, equivalent to 1441 million kg or 50.3%. Sørfonna shrank by 7.58 km^3 or 8268 million kg (18.3%) between 1987 and 2010, and the area visible on the 1937 topographic map shrank by 21.1% (5.19 km^3 or 5658 million kg) between 1937 and 2010

(Figure 33). It is interesting to note the highest point (1651 m.a.s.l.) of Sørfonna did not change between 1937 and 2007 suggesting that ablation hardly affects the highest reaches of Folgefonna. Generally more mass was lost from the Western Margins of Folgefonna than the East, although low-lying ice such as Buerbreen on Eastern Folgefonna significantly downwasted. (Figure 36, Figure 37, Figure 39). The last decades have seen a more pronounced Western Folgefonna ablation (Figure 38). Additionally it appears that the northern third of Sørfonna has undergone more downwasting than the higher elevation southern portion. As the south of Sørfonna is excluded on the 1937 map it is not possible to see if this was the case previously, however from Figure 36 it appears if ablation was more evenly distributed.

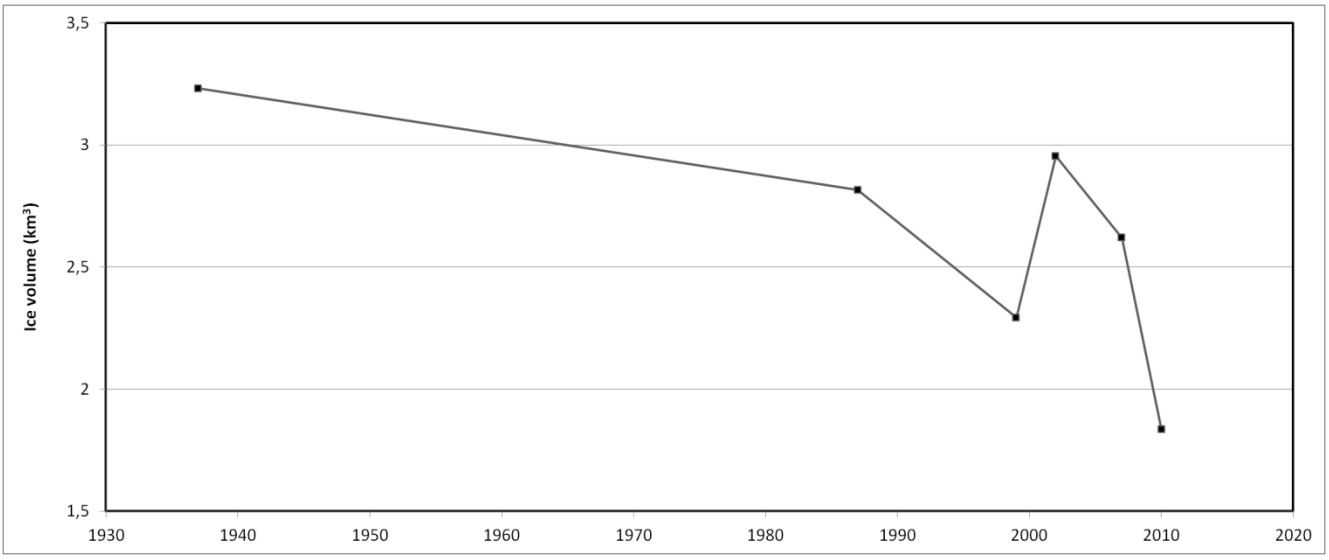

Figure 29: Volume of Nordfonna between 1937 and 2010 measured by comparing DEMs generated from digitised contour lines, ASTER images and provided pre-prepared. The volume trend shows the same trend as glacier area albeit not at the same resolution. Nordfonna is depicted having shrunk since 1937, a noticeable gain in mass occurred between 1999 and 2002.

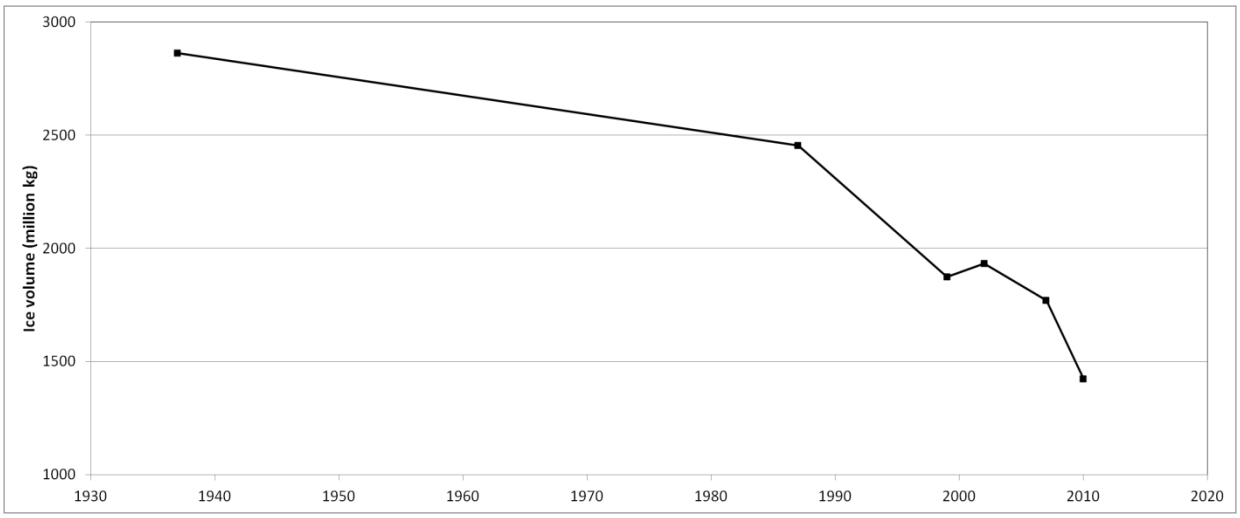

Figure 30: Change in volume of Midtfonna between 1937 and 2010 measured by comparing DEMS generated from digitised contour lines, ASTER images and provided pre-prepared. The volume trend shows the same trend as glacier area albeit not at the same resolution. Midtfonna is depicted having shrunk since 1937, a noticeable gain in mass occurred between 1999 and 2002. As the bedrock topography is unknown the volume cannot be calculated, only the change in volume.

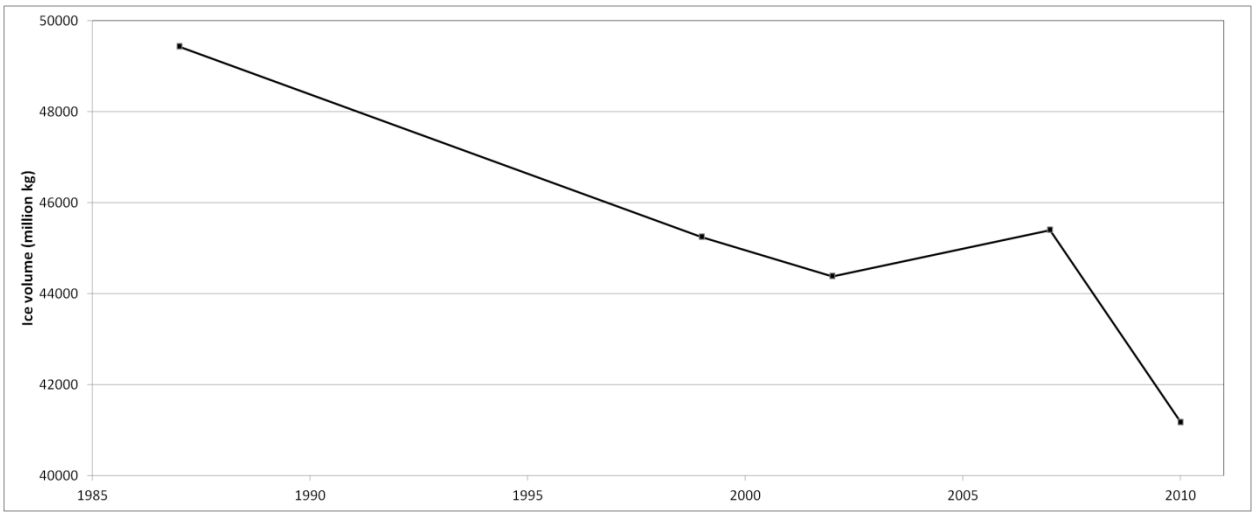

Figure 31: Change in volume of Sørfonna between 1987 and 2010, measured by comparing DEMS generated from digitised contour lines, ASTER images and provided pre-prepared. The volume trend shows the same trend as glacier area albeit not at the same resolution. Sørfonna is depicted having shrunk since 1987, a noticeable gain in mass occurred between 2002 and 2007. As the bedrock topography is unknown the volume cannot be calculated, only the change in volume. As the bedrock topography is unknown the volume cannot be calculated, only the change in volume.

Figure 32: Change in volume of Sørfonna measured by comparing DEMS generated from digitised contour lines, ASTER images and provided pre-prepared. The volume trend shows the same trend as glacier area albeit not at the same resolution. Sørfonna is depicted having shrunk since 1937, a noticeable gains in mass occurred between 1987 and 1999 and 2002 and 2007. As the bedrock topography is unknown the volume cannot be calculated, only the change in volume. As the bedrock topography is unknown the volume cannot be calculated, only the change in volume. The data was trimmed to the extent of the 1937 topographic map extent between 1937 and 2010, as the bedrock topography is unknown the volume cannot be calculated, only the change in volume.

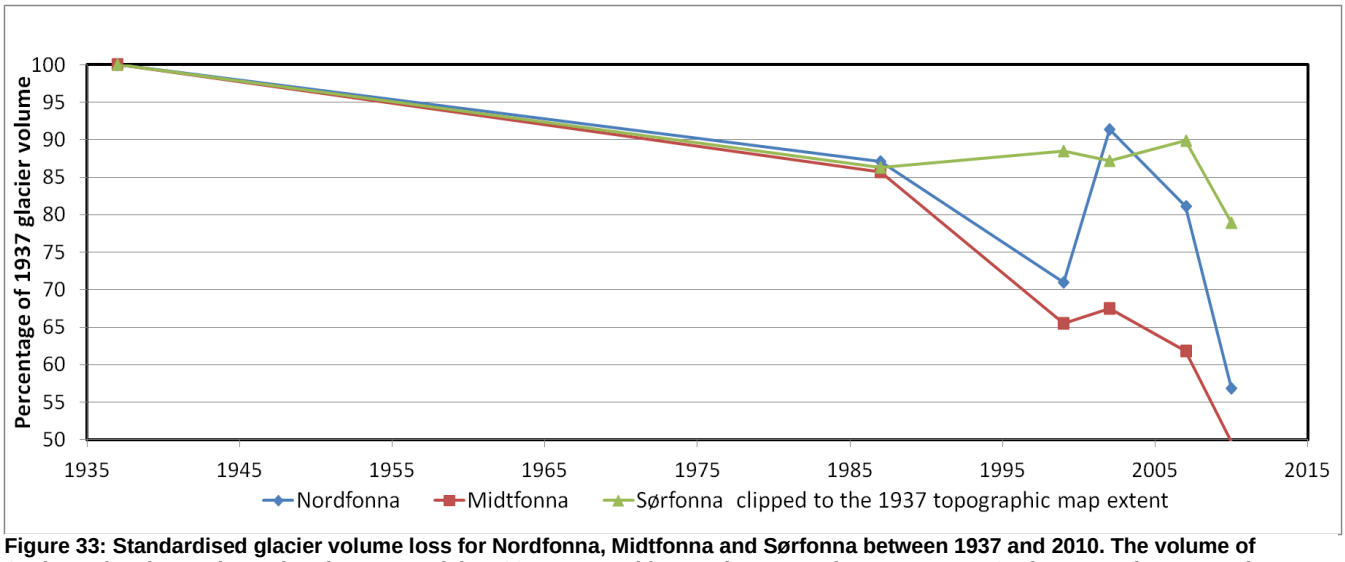

Figure 33: Standardised glacier volume loss for Nordfonna, Midtfonna and Sørfonna between 1937 and 2010. The volume of Sørfonna has been trimmed to the extent of the 1937 topographic map for comparison purposes. Sørfonna can be seen to have grown gradually while Nordfonna and Midtfonna shrank between 1987 and 1999 and 2002 and 2007, this could be due to the sheer size of Sørfonna.

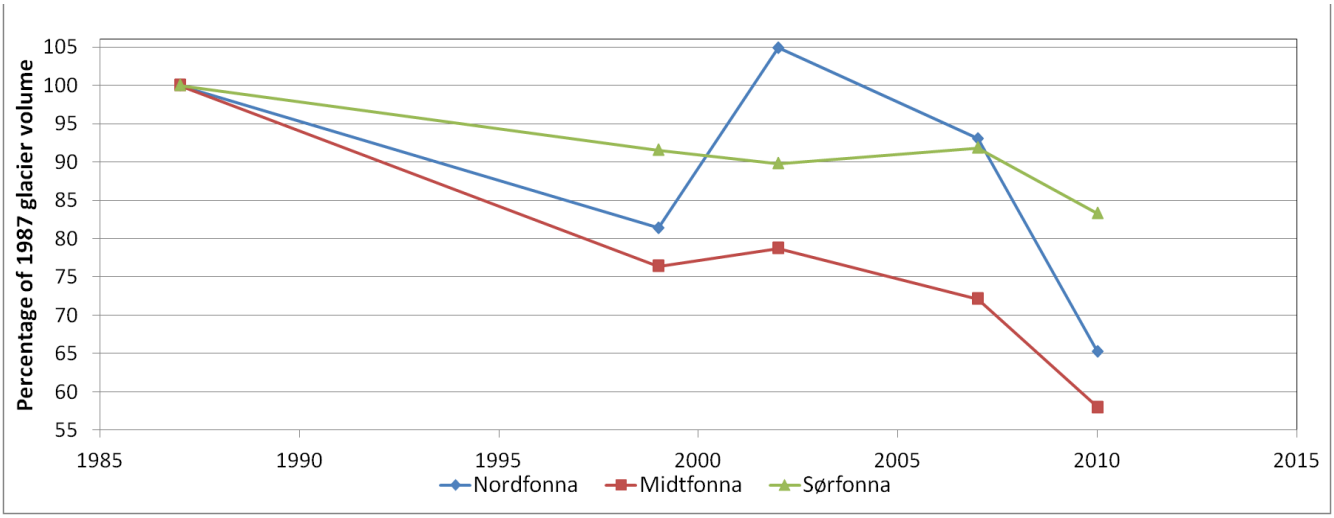

Figure 34: Standardised glacier volume loss for Nordfonna, Midtfonna and Sørfonna between 1987 and 2010. The expansion of Nordfonna between 1999 and 2002 seems exaggerated, as both before and after this event Nordfonna and Midtfonna proportionally lost the same amount of mass.

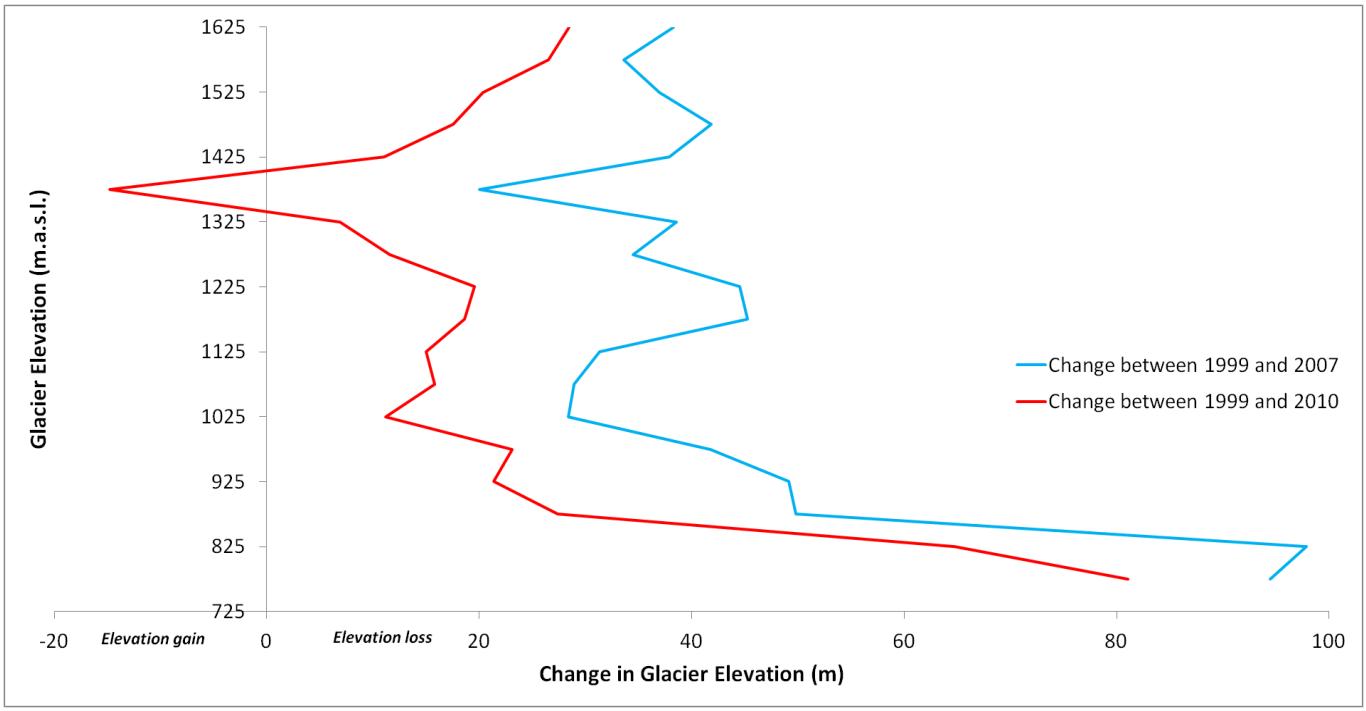

Figure 35: The change in glacier surface elevation at different elevations on Folgefonna between 1999 and 2007. As would be expected the lower margins of Folgefonna have lost the most elevation, while the higher reaches of the glacier ablated less. It seems unlikely that Folgefonna would have gained mass at ~1400 m.a.s.l. This graph is discussed in *6.6*.

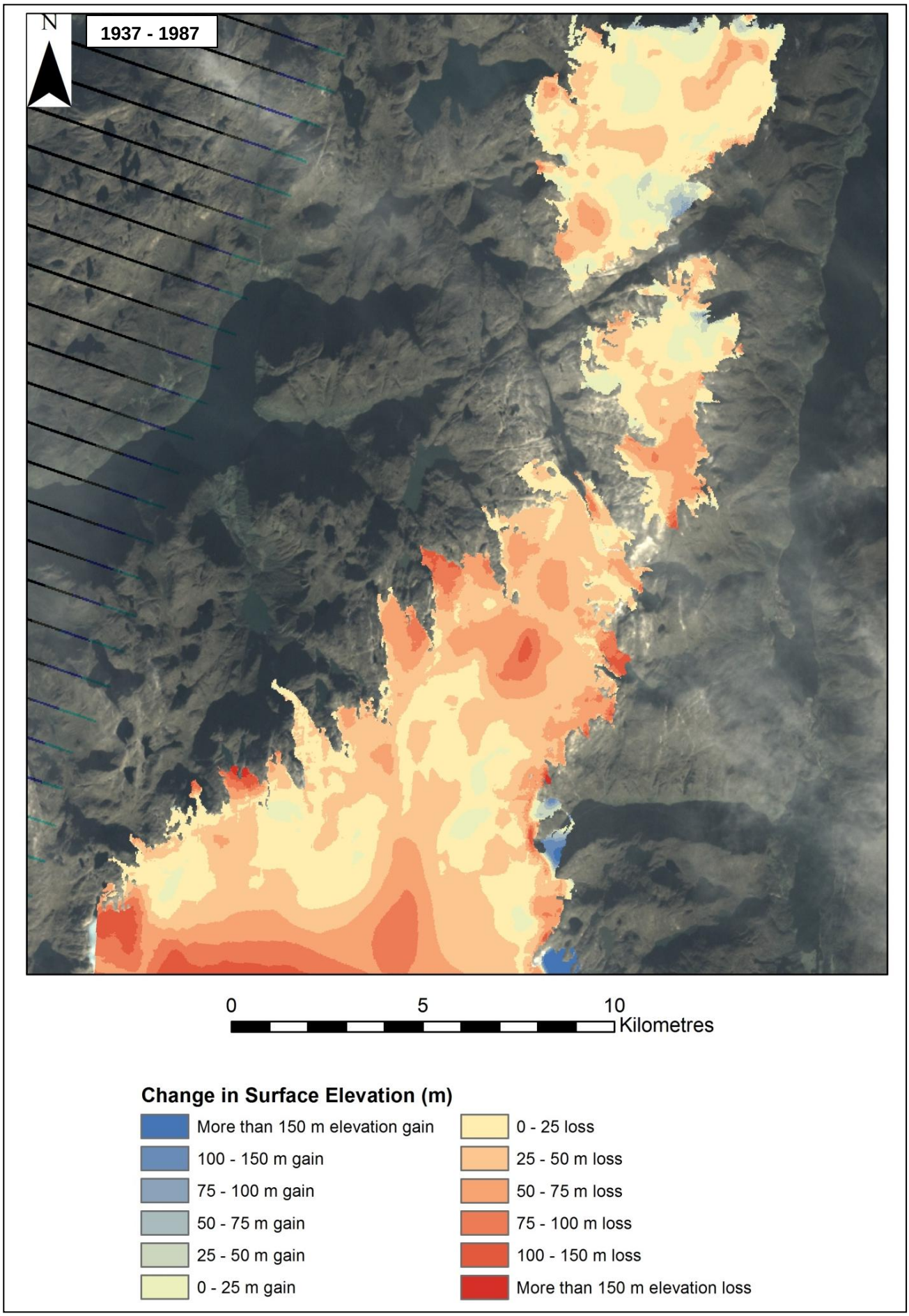

Figure 36: Change in surface elevation of Folgefonna between 1937 and 1987. The display has been clipped to the extent of the 1937 topographic map. The northern third of Sørfonna can be seen to have lost more mass than the lower portions, although some large losses are depicted at the very south of the ice mass. Losses over Nordfonna and Midtfonna don't show any strong west/east bias. Midtfonna is depicted losing the most mass from the low lying plateau in its south.

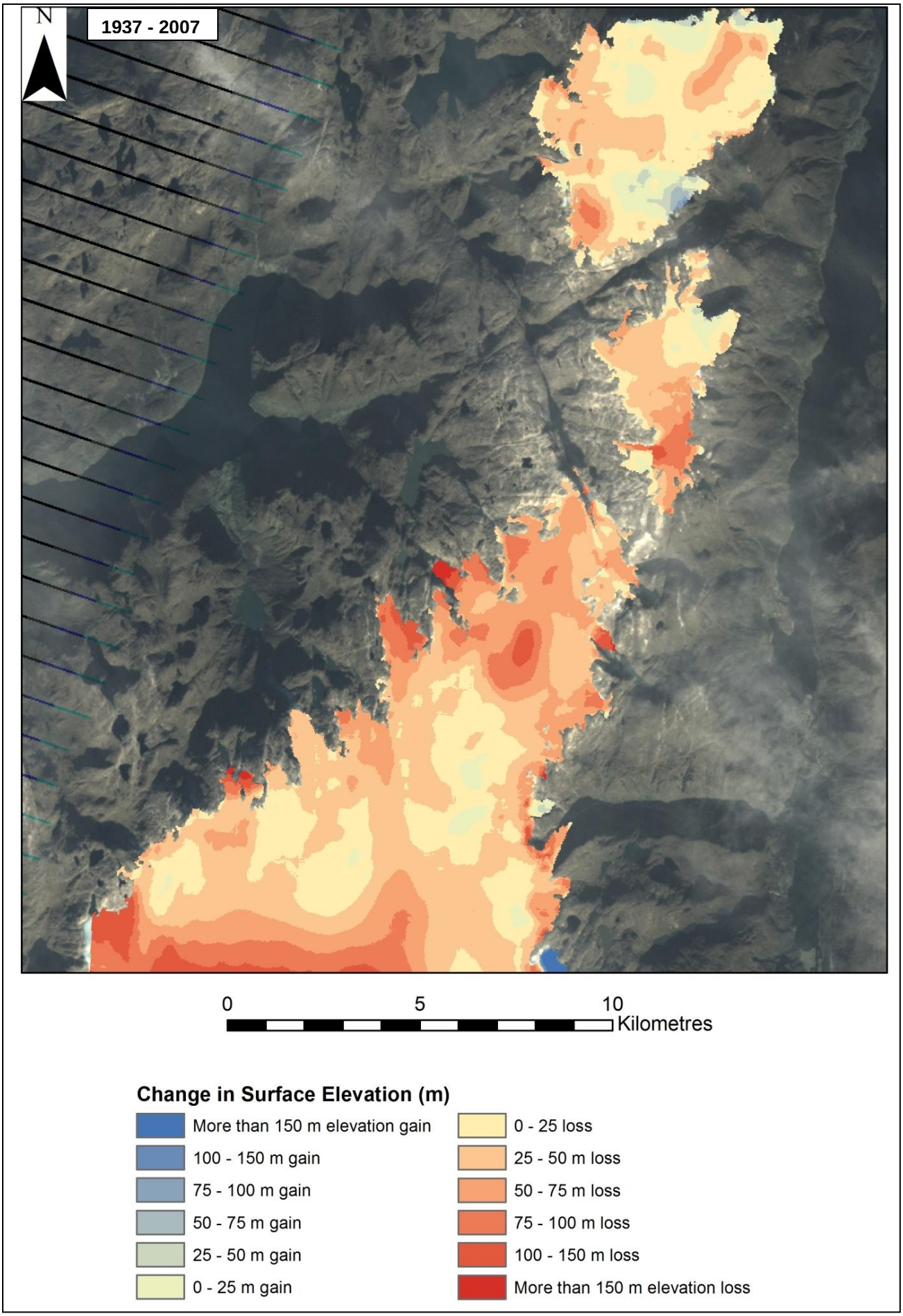

Figure 37: Change in surface elevation of Folgefonna between 1937 and 2007. The display has been clipped to the extent of the 1937 topographic map. As well as northern Sørfonna losing more mass than the southern part, a general bias of western mass loss can be seen across all three ice masses.

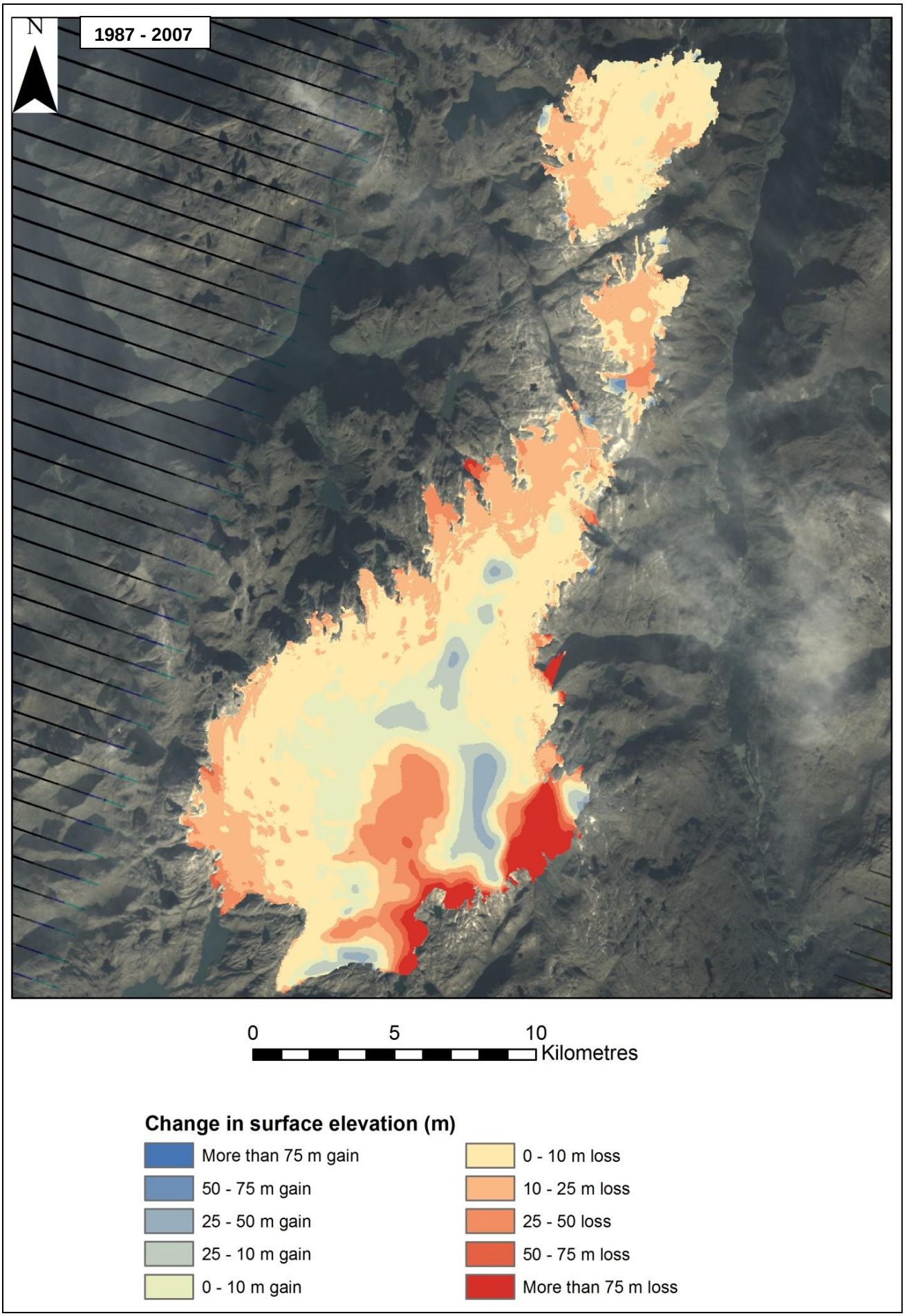

Figure 38: Change in surface elevation of Folgefonna between 1987 and 2007. Other than some extreme losses on parts of eastern Sørfonna which are most likely errors (*6.1.2.3*), a general predominant western loss of mass can be seen, small gains in elevation occurred in the interiors of Nordfonna and Sørfonna.

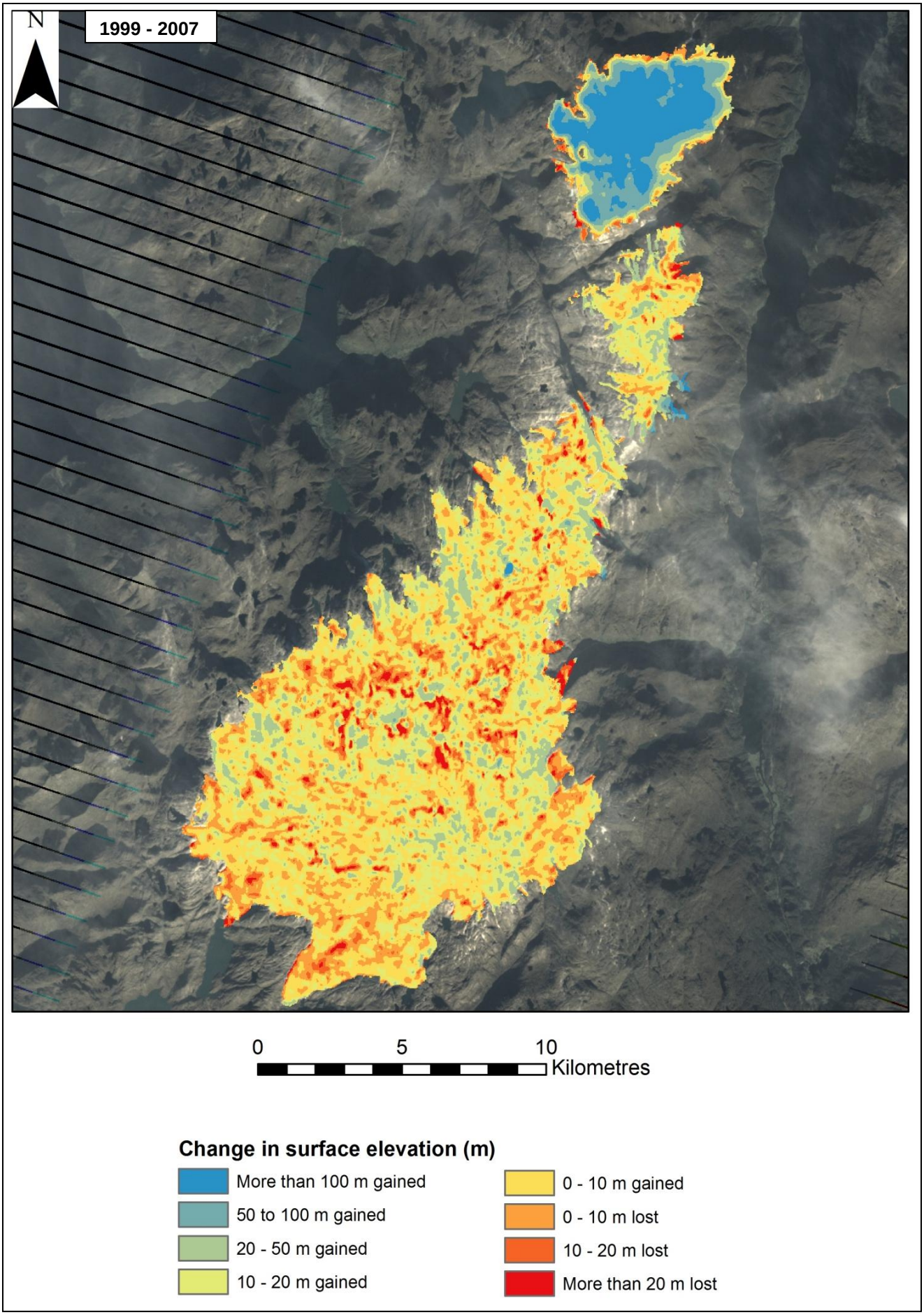

Figure 39: Change in surface elevation of Folgefonna between 1999 and 2007. No real intelligent trend can be seen, the huge gain in mass over Nordfonna seems very unlikely (*6.6*).

5.3 Change in Elevation of the Transient Snowline (TSL) on Sørfonna

The transient snowline (TSL) was mapped using both the fourth spectral band on Landsat TM images between 1986 and 2010, and with ENVISAT ASAR winter images between 2005 and 2011.

5.3.1 Results from Landsat TM band 4

The results show that from August 1984 to August 1991 the TSL descended from 1448 m to 1408 m. From 1991 onwards the TSL elevation steadily rose by 5.1 myr^{-1} on average to 1449 m in 1999, this rate increased to 7.8myr^{-1} in the period from 1999 to 2010. By the start of September 2010 the TSL lay at an altitude of 1535 m.a.s.l., a total rise of 86 m since 1984 (Figure 40, Figure 42).

5.3.2 Results from winter ENVISAT ASAR images

The series starts in the winter of 2005/06. The measured TSLs for December, January and February were 1453 m, 1441 m and 1468 m. Bearing in mind that the resolution of the ASAR images is 75 m per pixel this is quite an astounding accuracy to be within 27 m of each other. After 2005/06 the three measurements diverge, and later converge again in the winter of 2008/09, when the elevations stood at 1509 m, 1494 and 1503 m. The December and February ASAR measurements show the short-lived glacier advance in the mid-2000s as a levelling out of the TSL trend, this event however is not visible on the Landsat or January ASAR measurements. The three TSL measurements then continued to rise more or less in step with each other to reach elevations in December 2010 and February 2011 of 1527 m and 1531 m; the image from January 2011 was unusable due to surface melt, however the January 2010 TSL elevation was 1505. m (Figure 40 and Figure 43). Over the whole time period the TSL ASAR measurements were found to rise at a rate of 14.8 myr^{-1},16 myr^{-1} and 12.6 myr^{-1}, a rate approximately double that as determined with the Landsat method.

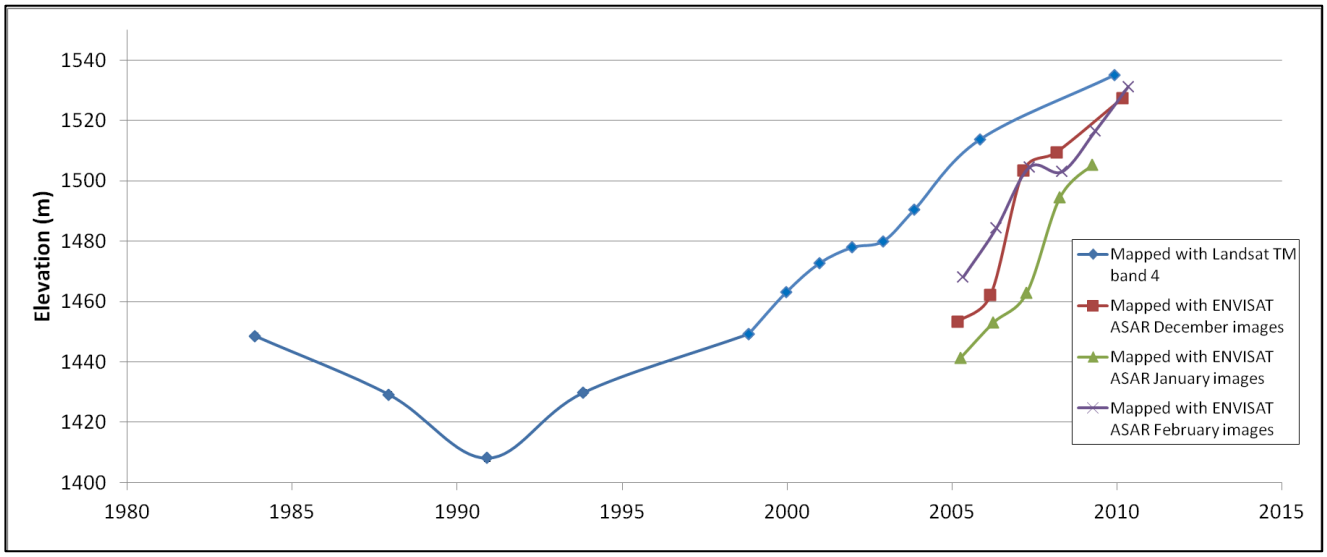

Figure 40: Change in the elevation of the Transient Snowline (TSL) on Sørfonna, mapped using both Landsat TM band 4 and ENVISAT ASAR winter images. Despite the ENVISAT ASAR images having a pixel size that is nearly three times that of the Landsat TM band 4 images, the ASAR images show more fluctuations in the trend. All the data agree that the 2010 ablation season TSL was between 1527 and 1535 m.a.s.l.

5.3.3 Expected future trends in the TSL

From Figure 40 it is evident that the TSL (and therefore the assumed ELA) generally shows two distinct phases. Prior to 1991 the TSL shows a trend of decreasing elevation. After this the TSL experiences an uninterrupted increase in TSL elevation albeit with a levelling out of the ASAR December and February images. Given that temperatures are predicted to continue to rise in Western Norway (*6.13)* it can be assumed that the TSL of Folgefonna will continue to rise in elevation reflecting an increasingly negative mass balance.

Linear relationships were assumed for the ENVISAT ASAR December images which mirror the mass balance record the most closely, and the Landsat TM band 4 images which has the most data points compared with the other datasets. These relationships were then extrapolated (Figure 41). When the Landsat dataset is extrapolated linearly it becomes apparent that if the TSL continues to rise in elevation at its current rate then it will reach an elevation above Sørfonna (1661 m) sometime around ~2030. This means that the ELA would be completely above Folgefonna causing severe downwasting and melting over the entire glacier during the ablation season. Very little accumulated snow would therefore survive until the winter, causing Folgefonna to be thrown into a severely negative state of glacier mass balance. The ASAR measurements paint an even darker picture, predicting that the TSL will be in a position above Folgefonna at around 2020.

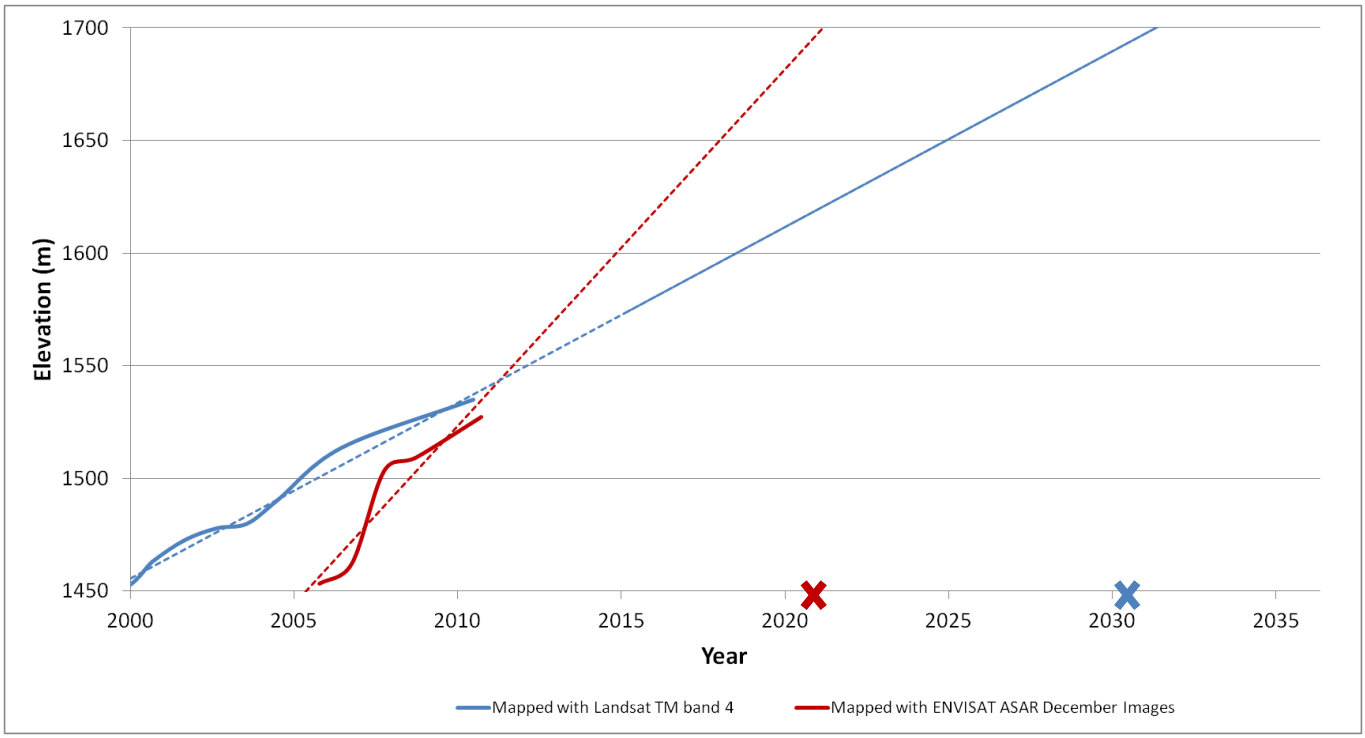

Figure 41: By assuming a linear increase in the TSL elevation from 1999 and onwards, both the Landsat TM band 4 dataset results, and the ENVISAT ASAR December dataset were extrapolated. As the highest point on Folgefonna was approximately 1660 m.a.s.l. in 2007 the extrapolation is continued until the TSL elevation surpassed 1700 m.a.sl. The ENVISAT ASAR data shows that the TSL will be above Sørfonna about 10 years before the Landsat data do. The red and blue crosses indicate the times when the linear extrapolation exceeds 1700 m.

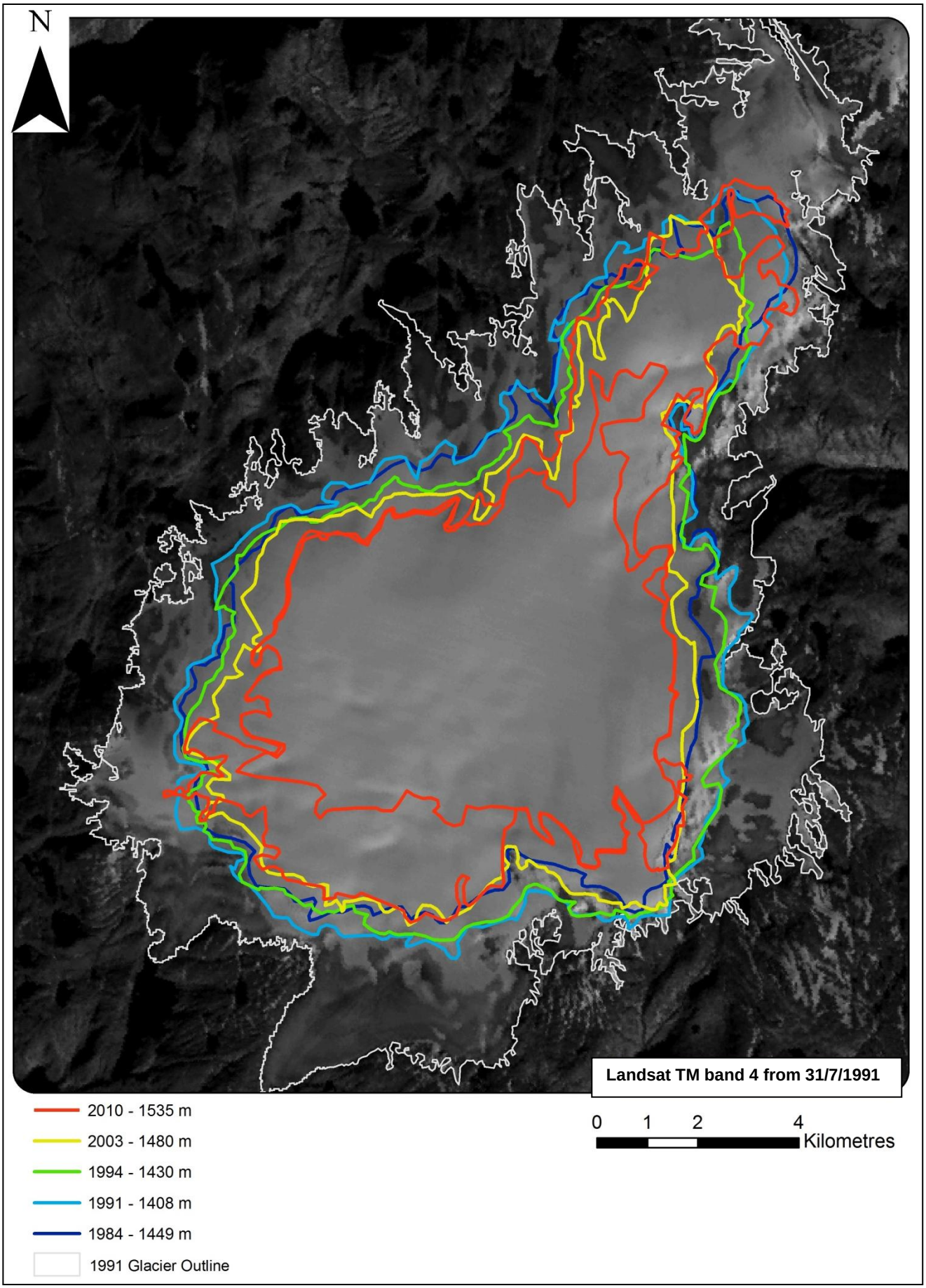

Figure 42: Transient snowlines and their corresponding mean elevations above sea level, as mapped with Landsat TM band 4 on Sørfonna. TSLs are shown from 2010, 2003, 1994, 1991 and 1984.

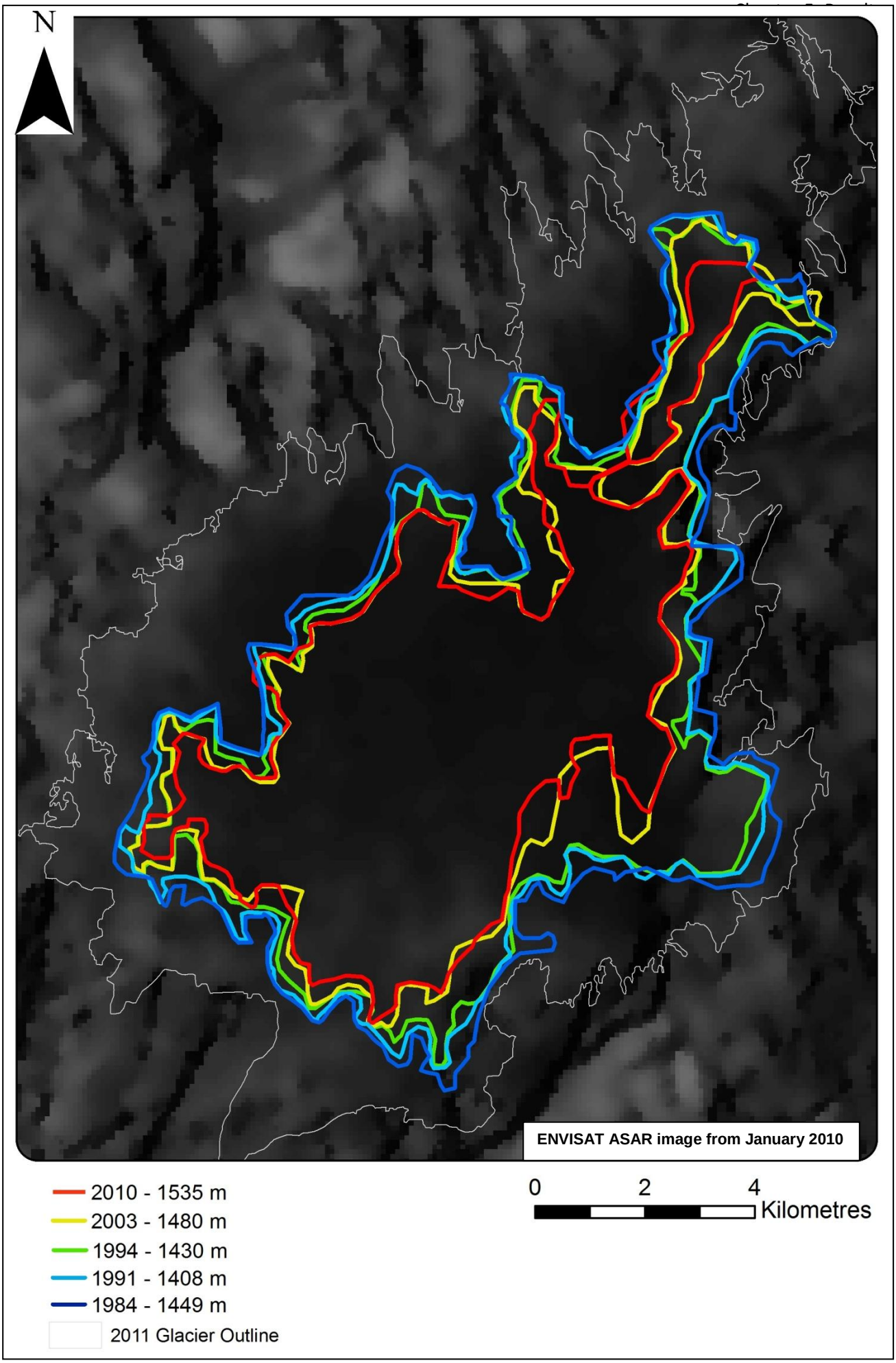

Figure 43: Transient snowlines and their corresponding mean elevations above sea level, as mapped ENVISAT ASAR Winter Images on Sørfonna. TSLs are shown each January between 2006 and 2010.

5.4 Correlation with climatic data and in-situ data

In this section the results obtained of glacier area, volume and TSL elevation are compared with climatic and *in-situ* mass balance data to assess the usefulness of remote sensing as a glaciology method.

5.4.1. Correlation with climatic data

Meteorological data was downloaded from the Norwegian Meteorological Institute's *eKlima* service. Precipitation data was available from 1930 from Rosendal, to the West of Folgefonna. Temperature records from the region are considerably more sporadic and irregular. Data exists between 1962 and 1977 and from 2009 onwards from Ullensvang Forsøksgard, located on the western side of Hardangerfjord just across from Folgefonna. When this data was plotted against corresponding temperature data from Florida, Bergen a correlation of 0.99 was found (Figure 44). This therefore allows changes in the ice-covered area of Folgefonna to be compared with the long-term temperature record of Bergen, which goes back to 1870.

Data about the *North Atlantic Oscillation* index was acquired from the University of East Anglia Climatic Research Unit (Osborn, 2012, Salmon, 2004); the DJFM (December, January, Febuary, March) averages between 1860 and 2011 were examined.

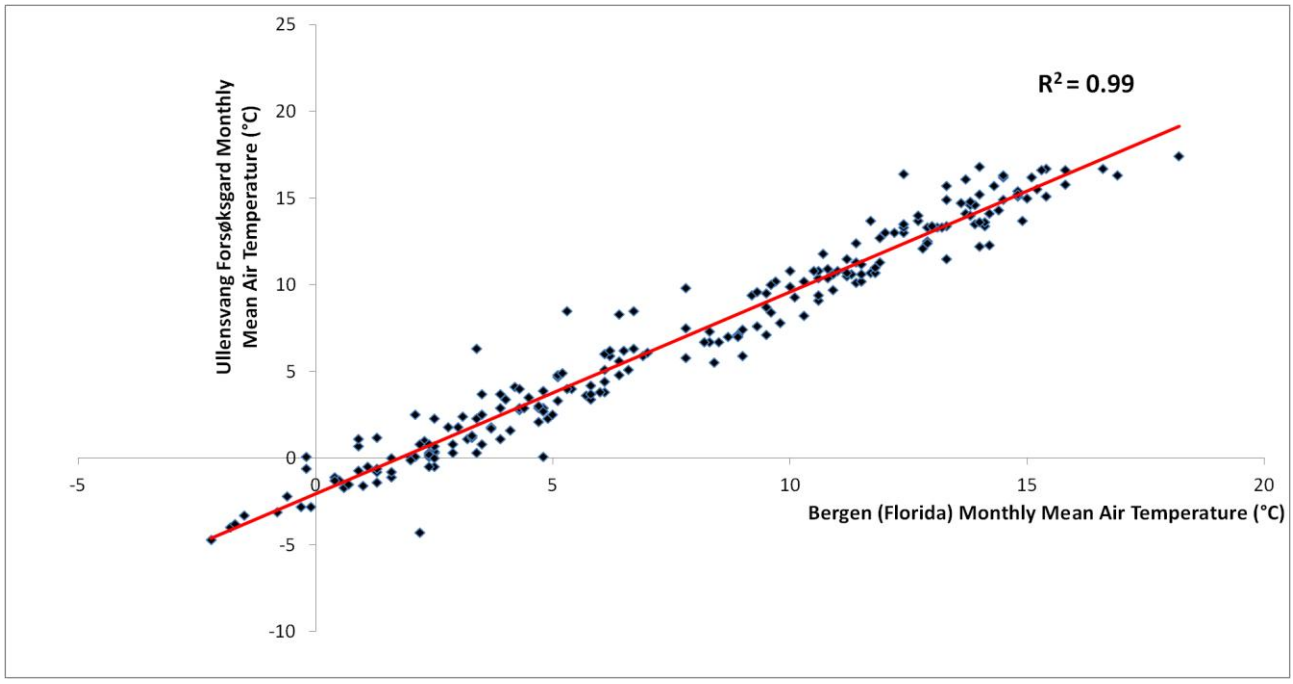

Figure 44: A very strong, positive correlation (R^2 = 0.99) exists between the monthly mean temperature of Florida, Bergen and of Ullensvang Forsøksgard, Hardangerfjord. Therefore the temperature record of Bergen can be taken to be reprehensive of the Folgefonna area.

5.4.1.1. Correlation between ice-covered area and winter precipitation

Graphs of the glacier area of Nord-, Midt- and Sørfonna between 1937 and 2011 were compared with a graph of the total accumulation season (October to April) precipitation, with 5 year and 12 year moving averages (Figure 45). If the 5 year moving average is considered it becomes evident there is a gradual fall in the precipitation between 1935 and 1950 by approximately 200 mm *(a)* that coincides with a gradual reduction in ice-covered area. Nordfonna and Midtfonna both shrink slightly over the same time period by 1.5 km^2 and 1 km^2 respectively, while Sørfonna continued to retreat until about 1960. Several spikes in winter precipitation between 1964 and 1976 cause the 5 year moving average to rise and peak around 1972 *(b)*. This same trend is very well reflected in the expansion of Nordfonna and Midtfonna, no expansion however is apparent in the glacier area record of Sørfonna.

Between 1982 and 1985 a dramatic drop in precipitation occurred from ~1500 mm to less than 900 mm *(c)*, coinciding with all three ice masses undergoing similar decreases in area. A drawn-out increase in the 12 year moving average precipitation then a slight levelling-off and eventual decrease between 1988 and 1994 *(d)* is replicated in Nordfonna and Midtfonna. Sørfonna appears to track more the 5 year moving average, showing a sharper decease in area after the initial augmentation.

From the mid-1990s onwards the glacier area correlates less well with the winter precipitation. Two precipitation spikes between 1995 and 1997 are seen as spiked increases in area during an otherwise decreasing glacier area trend *(e)*, although the magnitude of the two spikes does not seem consistent – Nordfonna and Midtfonna both appear to expand more during the smaller first spike than the larger second. A significant increase in winter precipitation between 2004 and 2007 *(f)* is seen to correspond to a short-lived glacier advance on all three ice-masses which terminated in 2008, the role of precipitation can be seen too from a sudden drop in the amount of precipitation in 2010 accompanies a steepening of the rate of area loss on all ice masses (g).

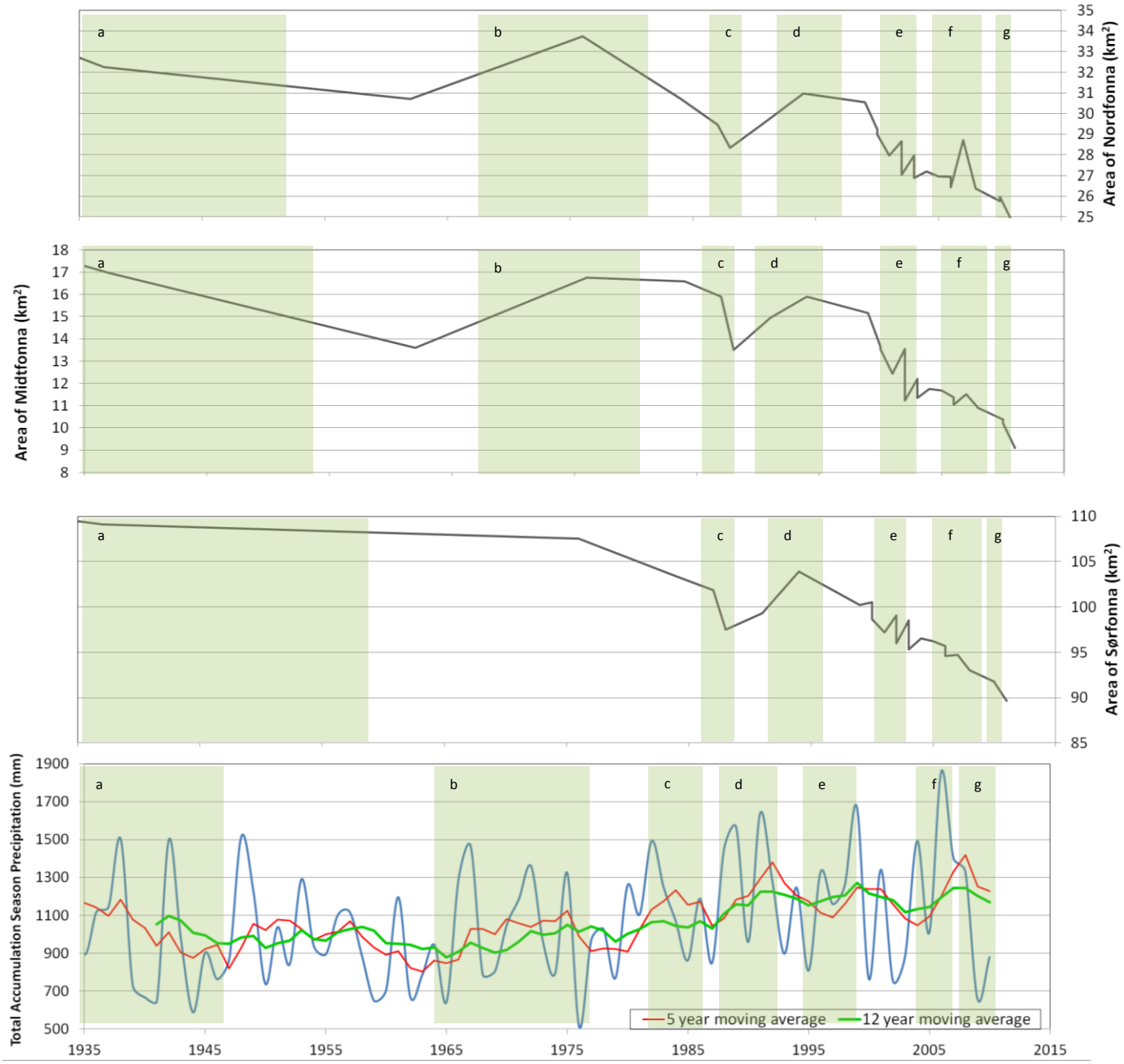

Figure 45: A comparison between the accumulation season (October to April) precipitation and the ice covered areas of Nord-, Midt- and Sørfonna between 1935 and 2011. The highlighted corresponding time periods (a - g) indicate assumed corresponding trends between the datasets. Note that as there are multiple data points for the years 2000, 2002, 2006 and 2010 there is some noise for these years.

5.4.1.2. Correlation between ice-covered area and summer temperature

The relationship between the ice-covered areas of Folgefonna and the mean ablation season (1st May - 31st September) temperature for the most part of the time-span studied appears insignificant. As Figure 46 shows there is essentially no correspondence between the temperature and the glacier area between 1870 and 1985, although the sparse number of data points could possibly mask some levels of correlation. As can be seen in Figure 47(*a*) a slight drop in temperature from the mid-1980s until 1989 and subsequent rise until ~1993 is accompanied by the expansion and later retreat of all three ice masses.

Between 1995 and 2004 summer temperatures increased steadily by approximately 1°C, this was accompanied by a consistent glacier retreat which was punctuated by the two rapid oscillations depicted in Figure 47(*b*). The general trend of increasing summer temperatures continued to lag behind the decrease in glacier area (c).

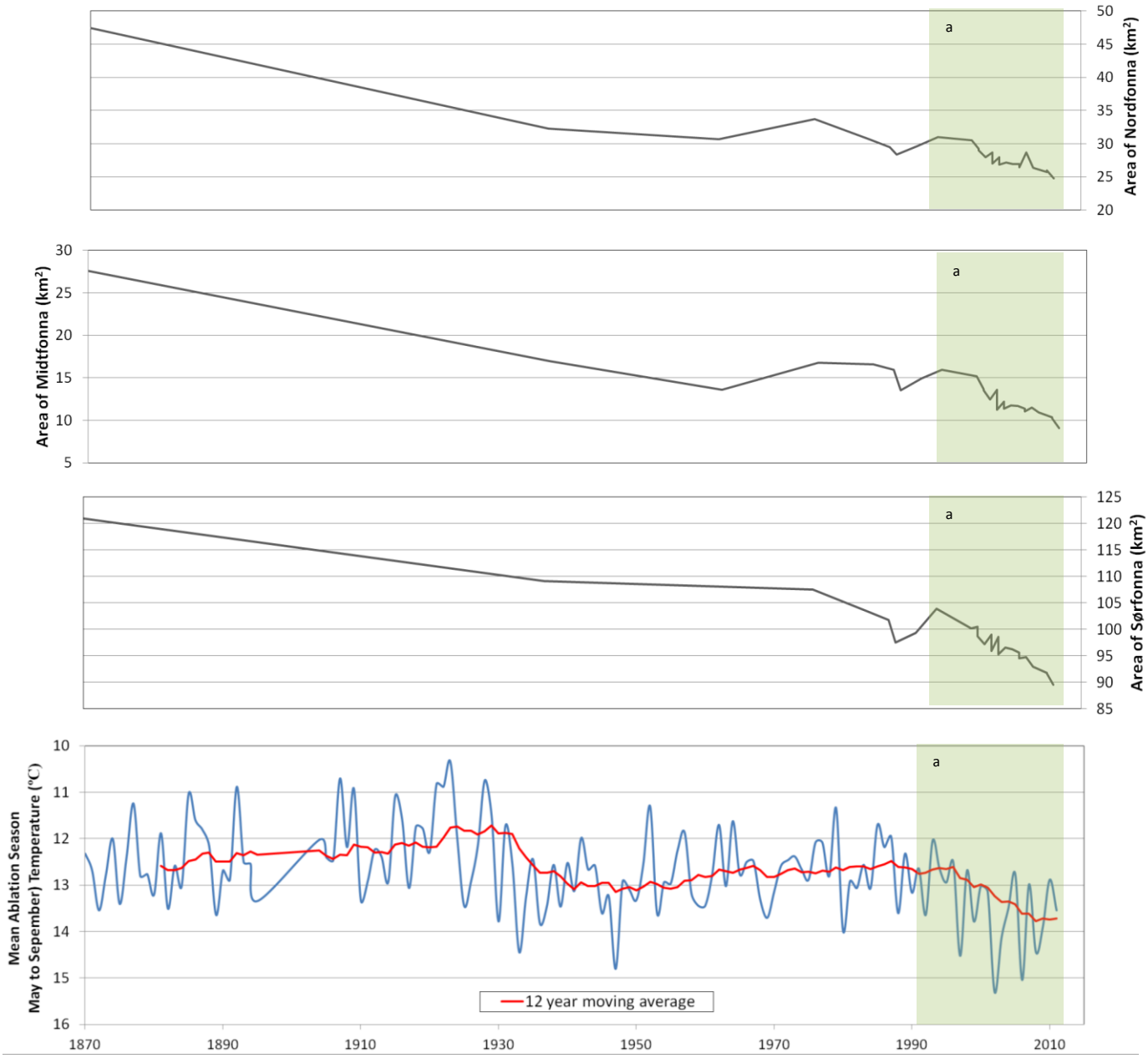

Figure 46: A comparison between the ablation season (May to September) mean temperature (note the axis has been inversed) and the ice covered areas of Nord-, Midt- and Sørfonna between 1870 and 2011. The highlighted area (a) indicates assumed corresponding trends between the datasets. Note that temperature axis has been inversed to make relationships easier to clarify. Note that as there are multiple data points for the years 2000, 2002, 2006 and 2010 there is some noise for these years.

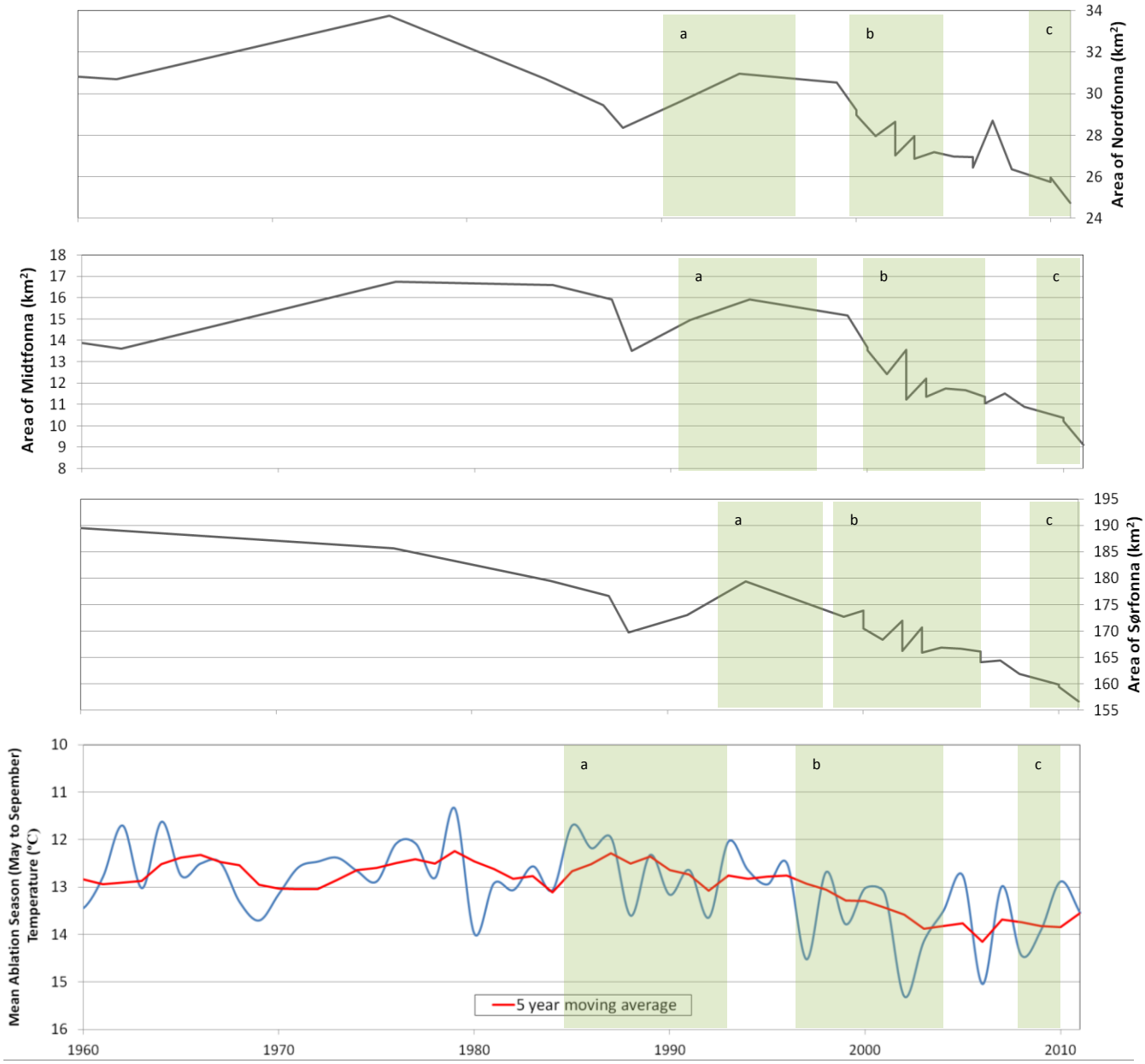

Figure 47: A comparison between the ablation season (May to September) mean temperature (note the axis has been inversed) and the ice covered areas of Nord-, Midt- and Sørfonna between 1960 and 2011. The highlighted areas (a-c) indicate assumed corresponding trends between the datasets. Note that as there are multiple data points for the years 2000, 2002, 2006 and 2010 there is some noise for these years.

5.4.1.3. Correlation between ice-covered area and the North Atlantic Oscillation (NAO)

It is impossible to assess the extent that the glacier area reflects the NAO between 1864 and 1937 due to lack of data points. However when the 12 year moving average is considered it can be seen quite clearly from Figure 48*a* that between 1915 and 1967 the long-term reduction in glacier area of Nord-, Midt and Sørfonna follows a steady decline in the NAO index to more negative values. The small expansion observable in both Nordfonna and Midtfonna also correlate nicely with a brief episode of more positive NAO values during the 1970s *(b)*, as does the episode of glacier expansion in the 1990s *(c)*.

When the time series is looked at in more detail (Figure 49) it can be seen that the periodic shifts to more positive NAO values from the mid-1980s to the late-1990s *(a, b)* generally mirror the trends of glacier area expansion and retreat. After 1997 however the correlation does not hold up so strongly, although three peaks of positive values *(c)* between 1997 and 2004 seem to correspond with a brief notch of glacier expansion on Sørfonna, as well as the two peaks of advance visible on all three ice-masses already mentioned (Figure 45*e*). A fairly rapid episode of positive NAO values between 2005 and 2009 *(d)* is clearly identifiable as an advance in the trend of otherwise continuous glacier retreat for all parts of Folgefonna, however even after this period there is a level of agreement between the datasets. The 5 year moving average gradual shift towards more negative NAO values matches the continued glacier shrinkage albeit nowhere as near as strongly as it had previously.

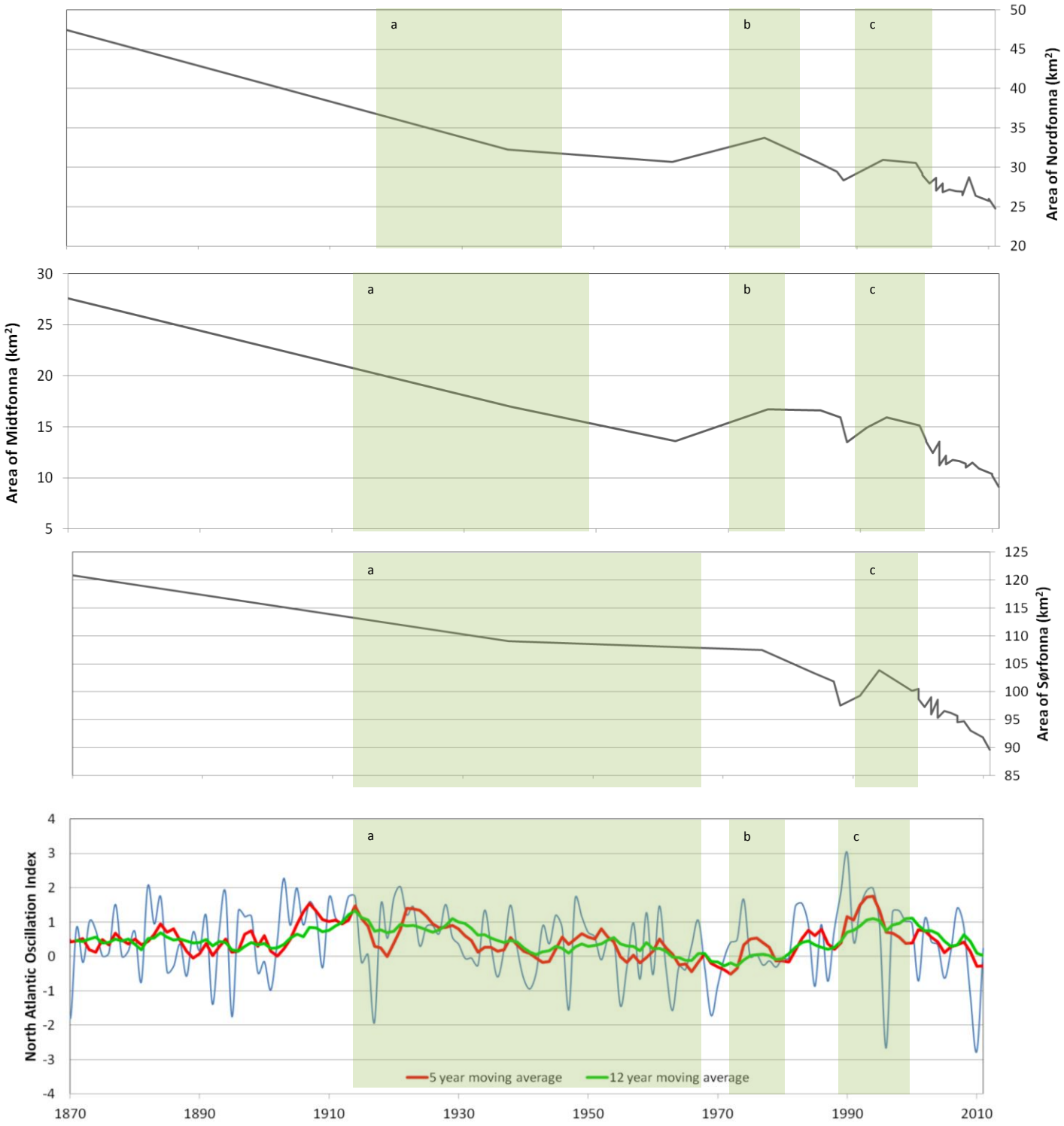

Figure 48: A comparison between North Atlantic Oscillation Index (winter DJFM averages) and the ice covered areas of Nord-, Midt- and Sørfonna between 1870 and 2011. The highlighted areas (a-c) indicate assumed corresponding trends between the datasets. Note that as there are multiple data points for the years 2000, 2002, 2006 and 2010 there is some noise for these years.

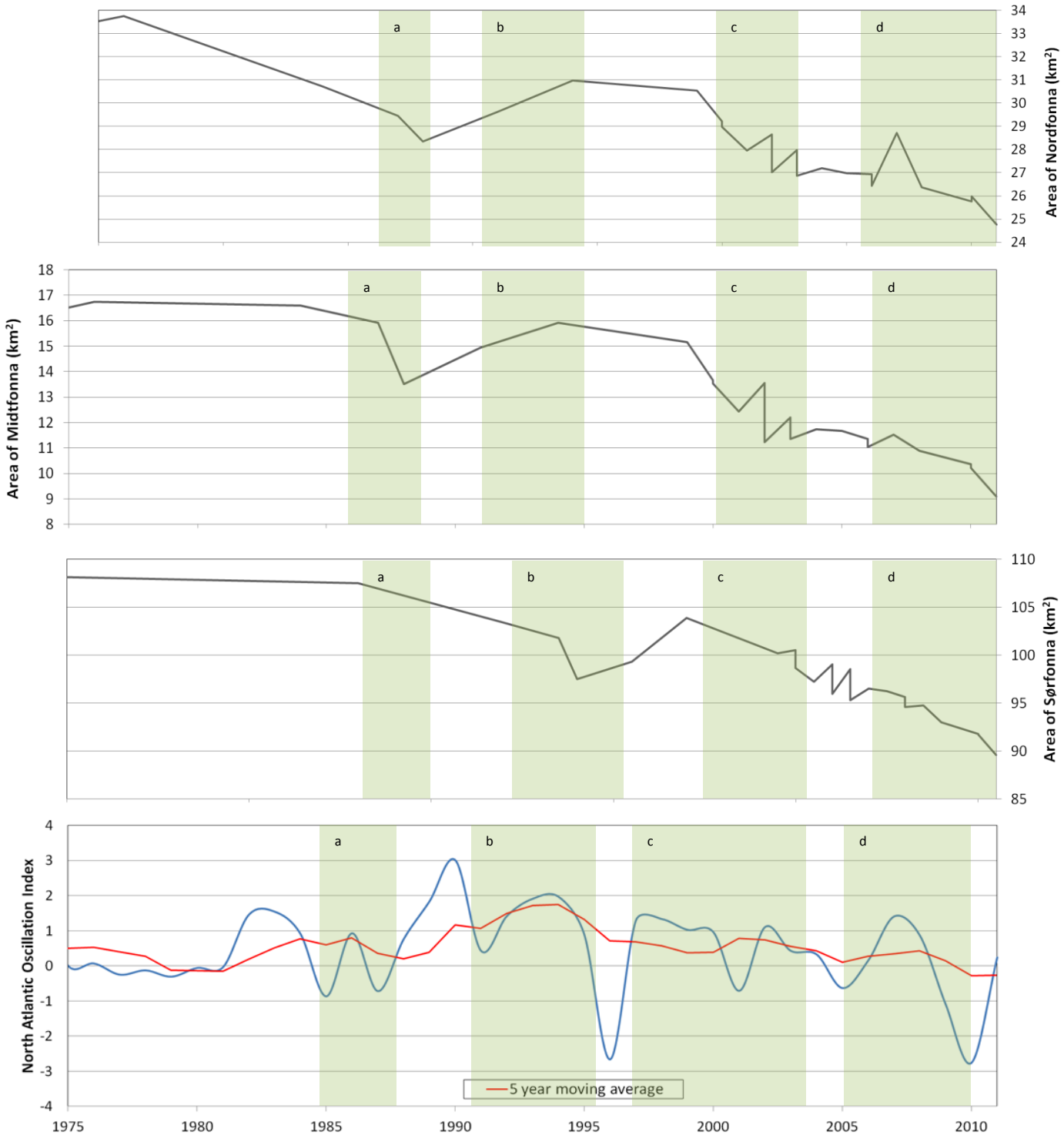

Figure 49: A comparison between North Atlantic Oscillation Index (winter DJFM averages) and the ice covered areas of Nord-, Midt- and Sørfonna between 1975 and 2011. The highlighted areas (a-d) indicate assumed corresponding trends between the datasets. Note that as there are multiple data points for the years 2000, 2002, 2006 and 2010 there is some noise for these years.

5.4.1.4. Correlation between the direction of glacier expansion area and the NAO

The index created showing whether Western or Eastern Folgefonna responded more (*4.3.1.2*) was compared to the NAO index.

As can be seen in Figure 50(a) and Figure 51(a) the positive NAO phase between 1987 and 1991 corresponds almost perfectly with a greater reaction of western Nordfonna and Midtfonna. Other areas of the graphs show a correlation, but the strength of the relationship varies *(*Figure 50*b,c,d,* Figure 51b,c,d*)*. Conversely when the NAO is negative, both sides of the glacier react in unison. No intelligent trend can be seen with Sørfonna's direction of reaction, it is possible that a large amount of seasonal snow in 1992 on the western side is responsible for the unrealistically large western orientated response, which distortes the remainder of the graph. However even when this event is removed there are still only two noticeable reactions (Figure 52.*a,b*) which lag behind the NAO by approximately 3 to 5 years.

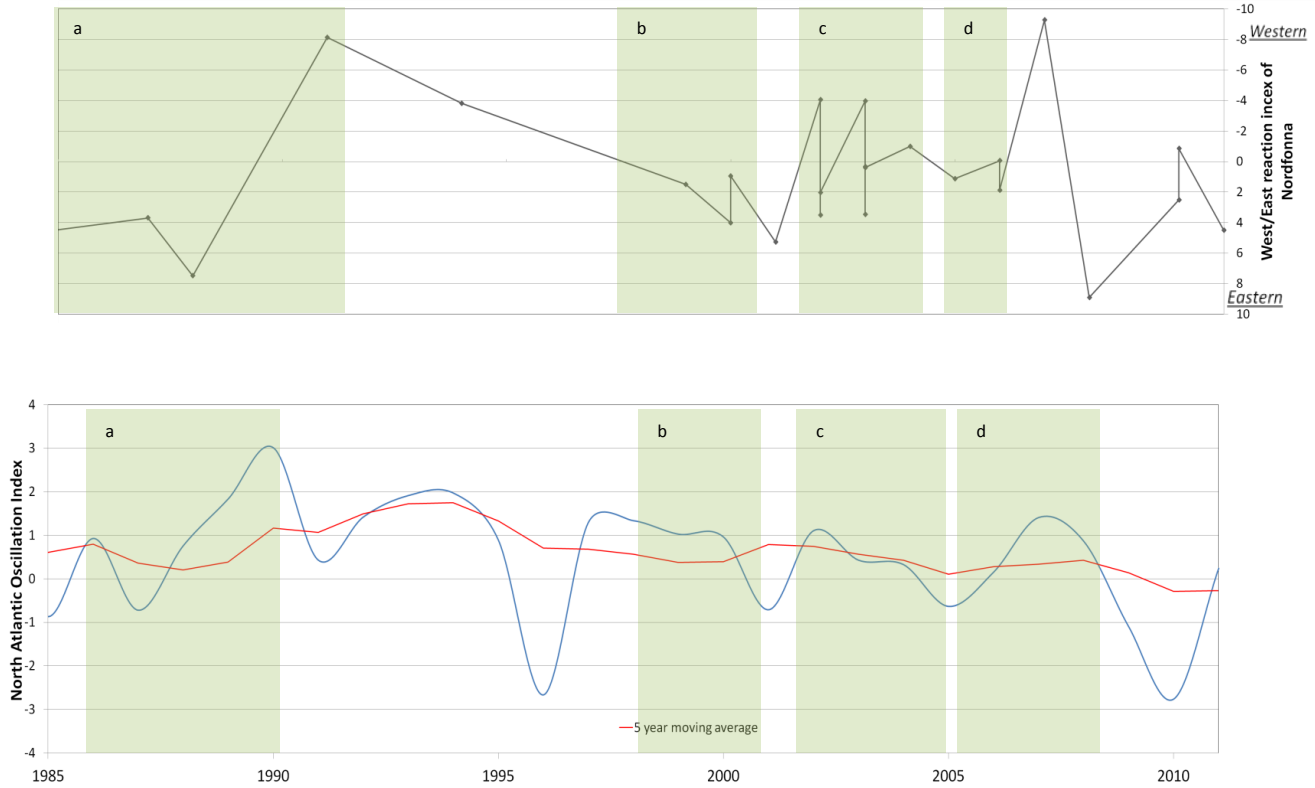

Figure 50: A comparison between North Atlantic Oscillation Index (winter DJFM averages) and the dominant direction (west/east) of glacier advance and retreat of Nordfonna between 1985 and 2011. The highlighted areas (a-d) indicate assumed corresponding trends between the datasets. Note that as there are multiple data points for the years 2000, 2002, 2006 and 2010 there is some noise for these years.

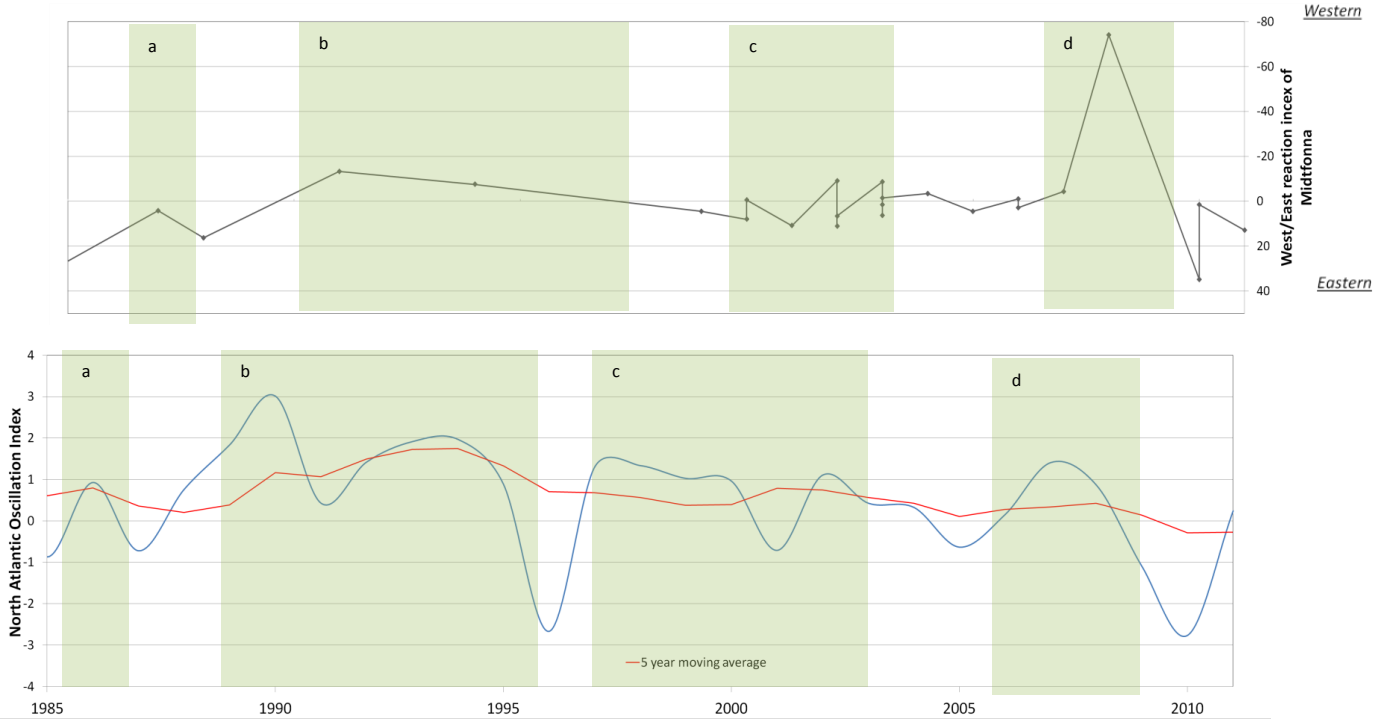

Figure 51: A comparison between North Atlantic Oscillation Index (winter DJFM averages) and the dominant direction (west/east) of glacier advance and retreat of Midtfonna between 1985 and 2011. The highlighted areas (a-d) indicate assumed corresponding trends between the datasets. Note that as there are multiple data points for the years 2000, 2002, 2006 and 2010 there is some noise for these years.

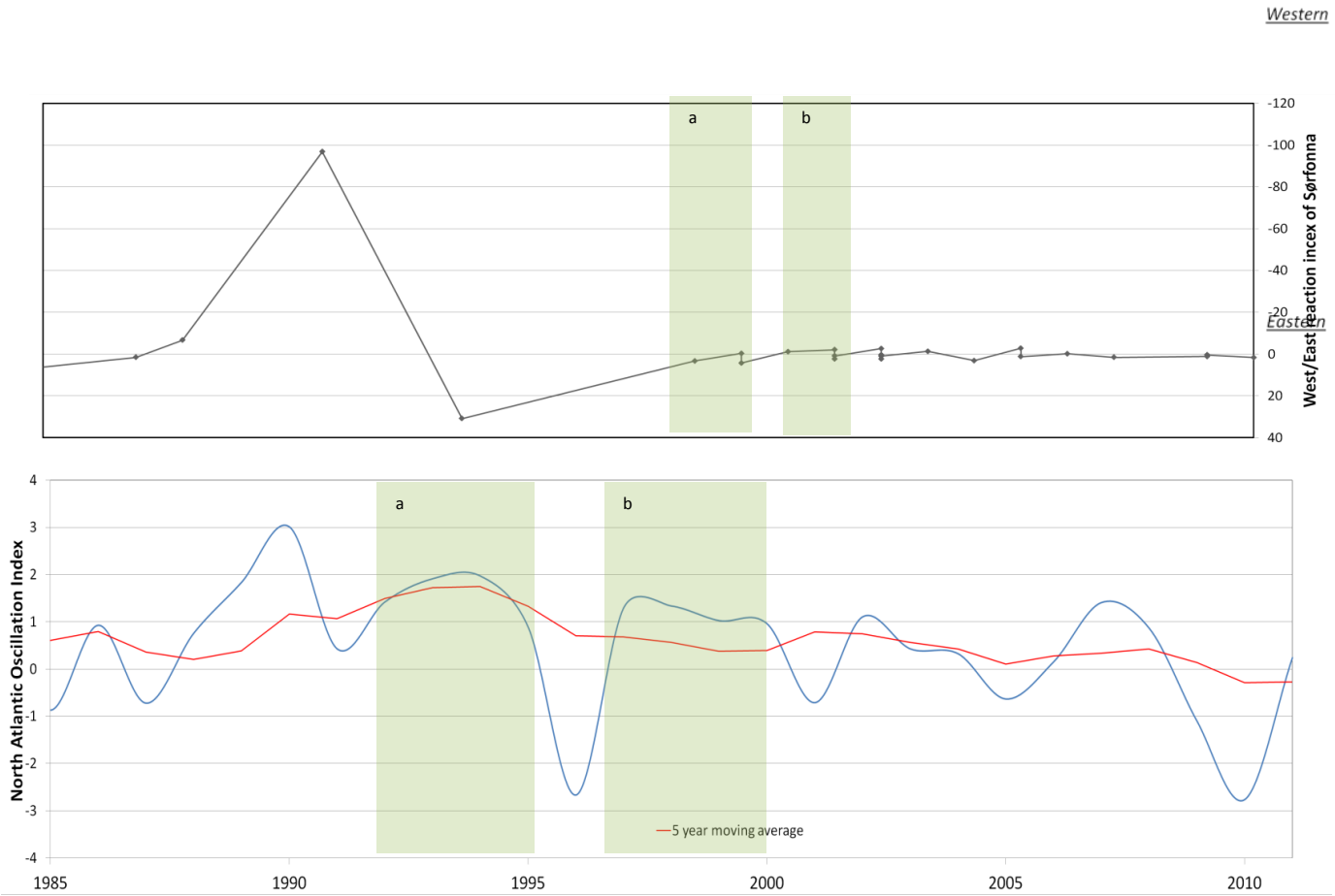

Figure 52: A comparison between North Atlantic Oscillation Index (winter DJFM averages) and the dominant direction (west/east) of glacier advance and retreat of Sørfonna between 1985 and 2011. The highlighted areas (a-b) indicate assumed corresponding trends between the datasets. Note that as there are multiple data points for the years 2000, 2002, 2006 and 2010 there is some noise for these years.

5.4.1.5. Calculating the lag times between the climate and the area, volume and transient snowline response

Three noticeable points were taken in the 5 year moving averages of the winter precipitation and the NAO and the same points were found in the other datasets. It was found that the area of Nordfonna lagged behind the winter precipitation forcing by 3-6 years (Figure 53), Midtfonna lagged by between 3-4 years and Sørfonna by 3-4 years. The volume of Nordfonna was also examined and was found to respond slightly quicker than the area (3-4 years) but the low amount of volume data points only facilitated two corresponding events to be matched up. The transient snowline of Sørfonna has a lag time behind the change in precipitation by one to two years.

Similarly the glacier area was found to lag behind the NAO by 3-5 years for Nordfonna, 4-5 years for Midtfonna and 4-5 years for Sørfonna. Nordfonna's glacier volume and Sørfonna's TSL elevation lagged by ~2 years (Figure 56).

A spiked increase in winter precipitation noticeable in 2005 appears to precede the reactions of all three ice-masses by 2 years (yellow line), the same event is also noticeable on the summer temperature trend in 2007. It seems that the lag time behind the summer temperature is incredibly short, no real corresponding events can be seen until the final part of the time series, where the two events noted lag by between one year and less than one year (Figure 55).

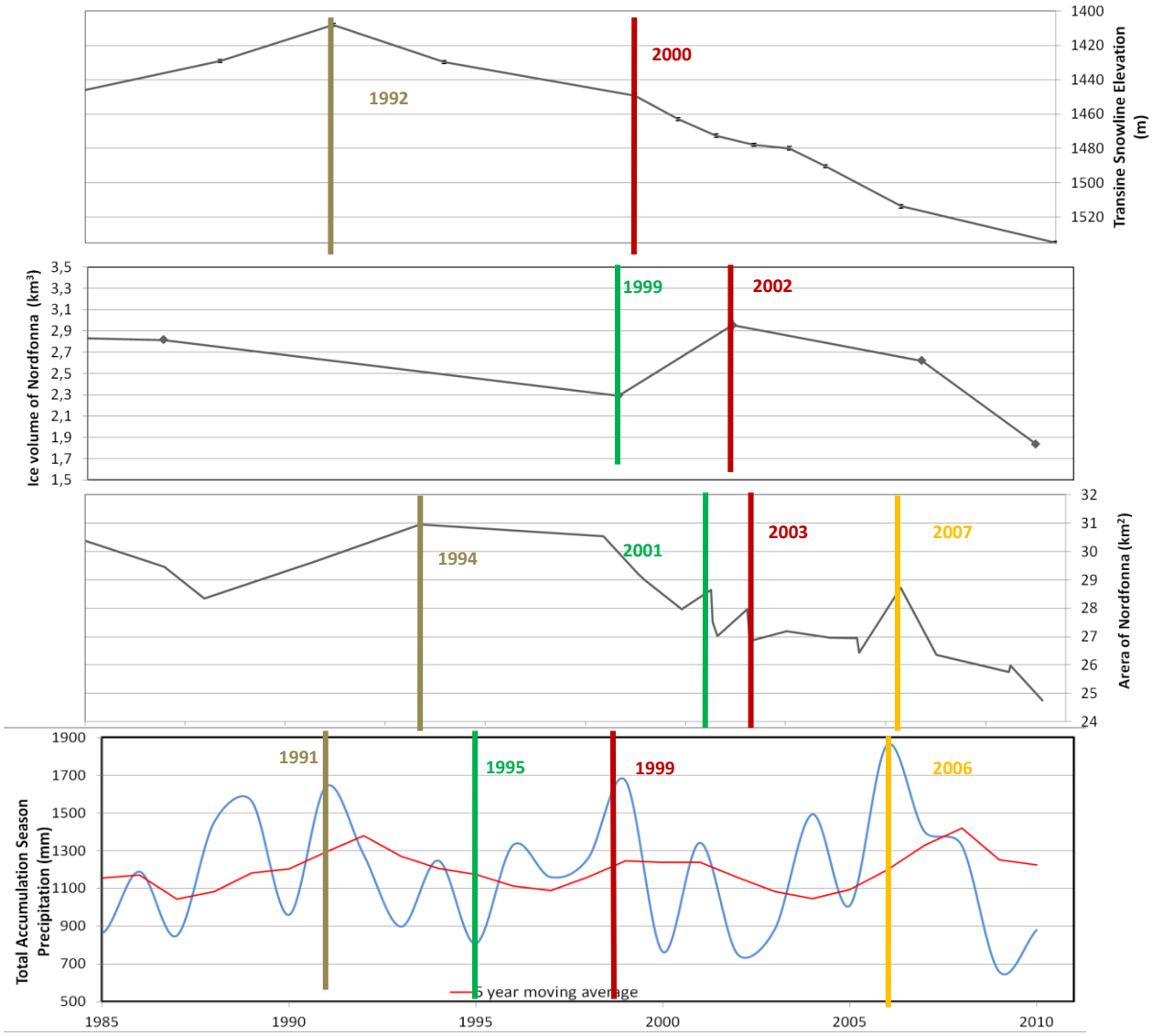

Figure 53: The lag times between the forcing of the total winter precipitation and the glacier area and volume of Nordfonna, and elevation of the Transient Snowline (TSL) measured on Sørfonna. Note that as there are multiple data points for the years 2000, 2002, 2006 and 2010 there is some noise for these years.

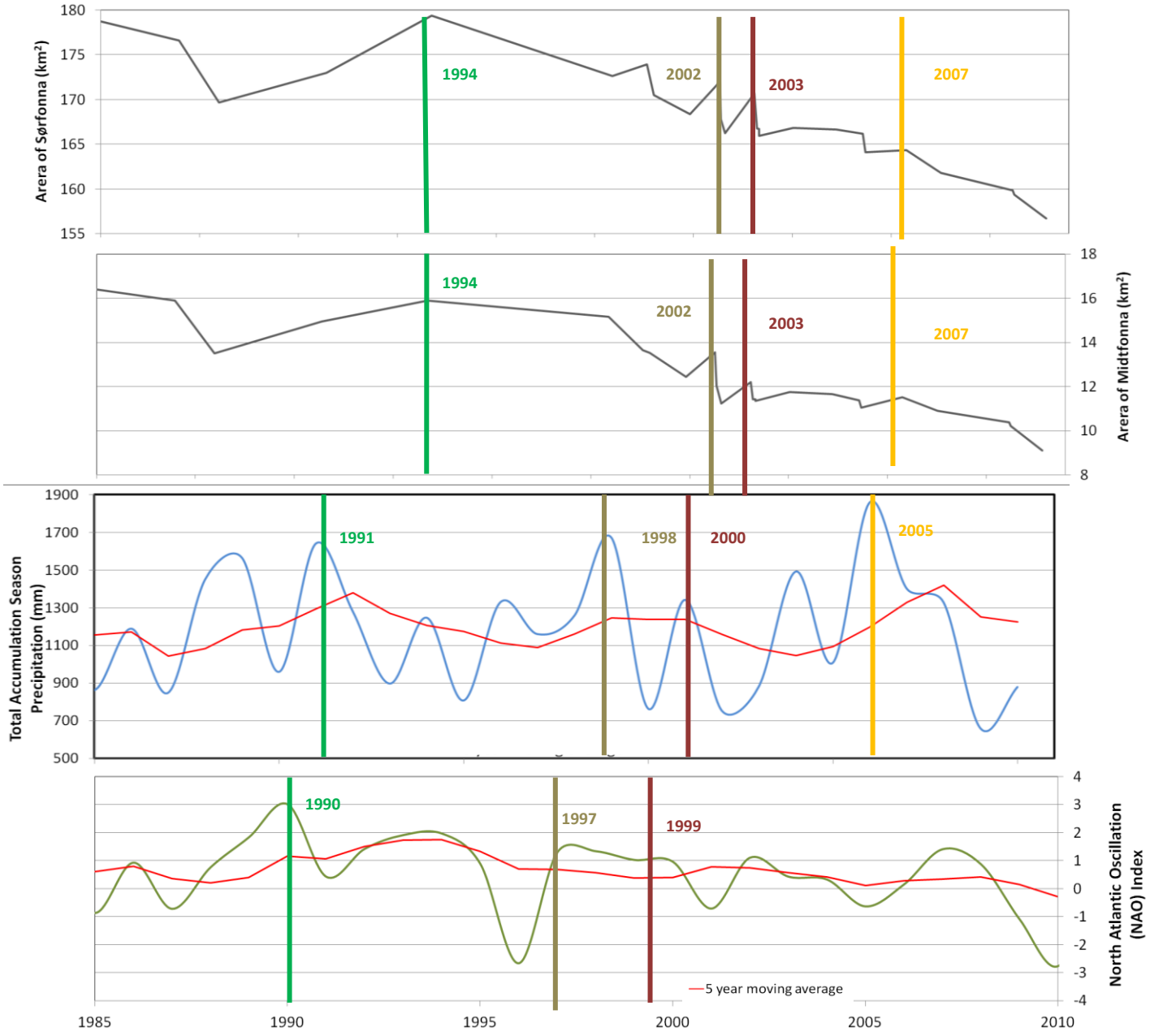

Figure 54: The lag times between the forcing of the total winter precipitation and the North Atlantic Oscillation (NAO) , and the glacier areas of Nordfonna and Midtfonna. Note that as there are multiple data points for the years 2000, 2002, 2006 and 2010 there is some noise for these years.

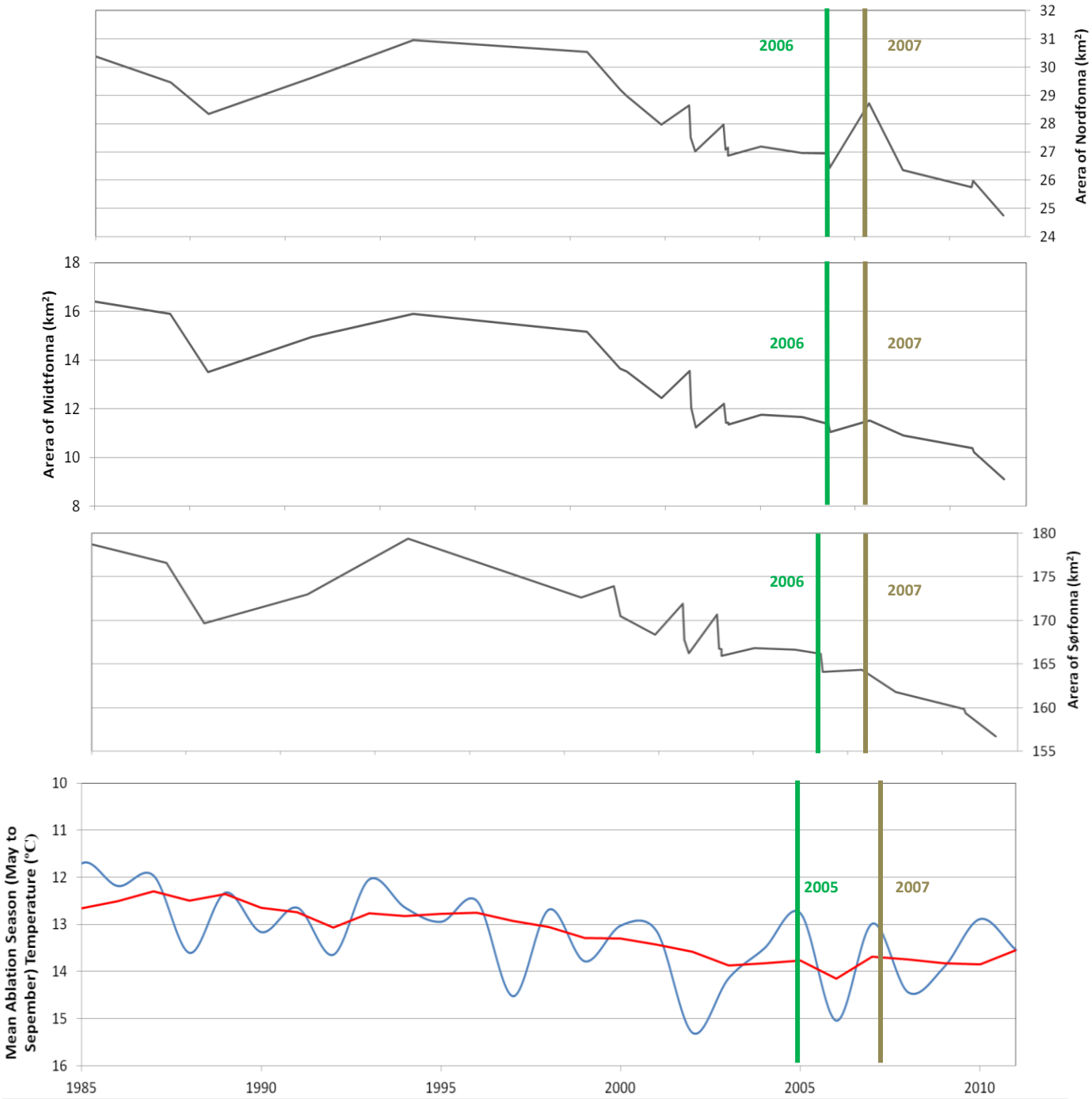

Figure 55: The lag times between the forcing of the ablation season average temperature (note axis has been reversed) and the glacier areas of Nordfonna, Midtfonna and Sørfonna.. Note also that as there are multiple data points for the years 2000, 2002, 2006 and 2010 there is some noise for these years.

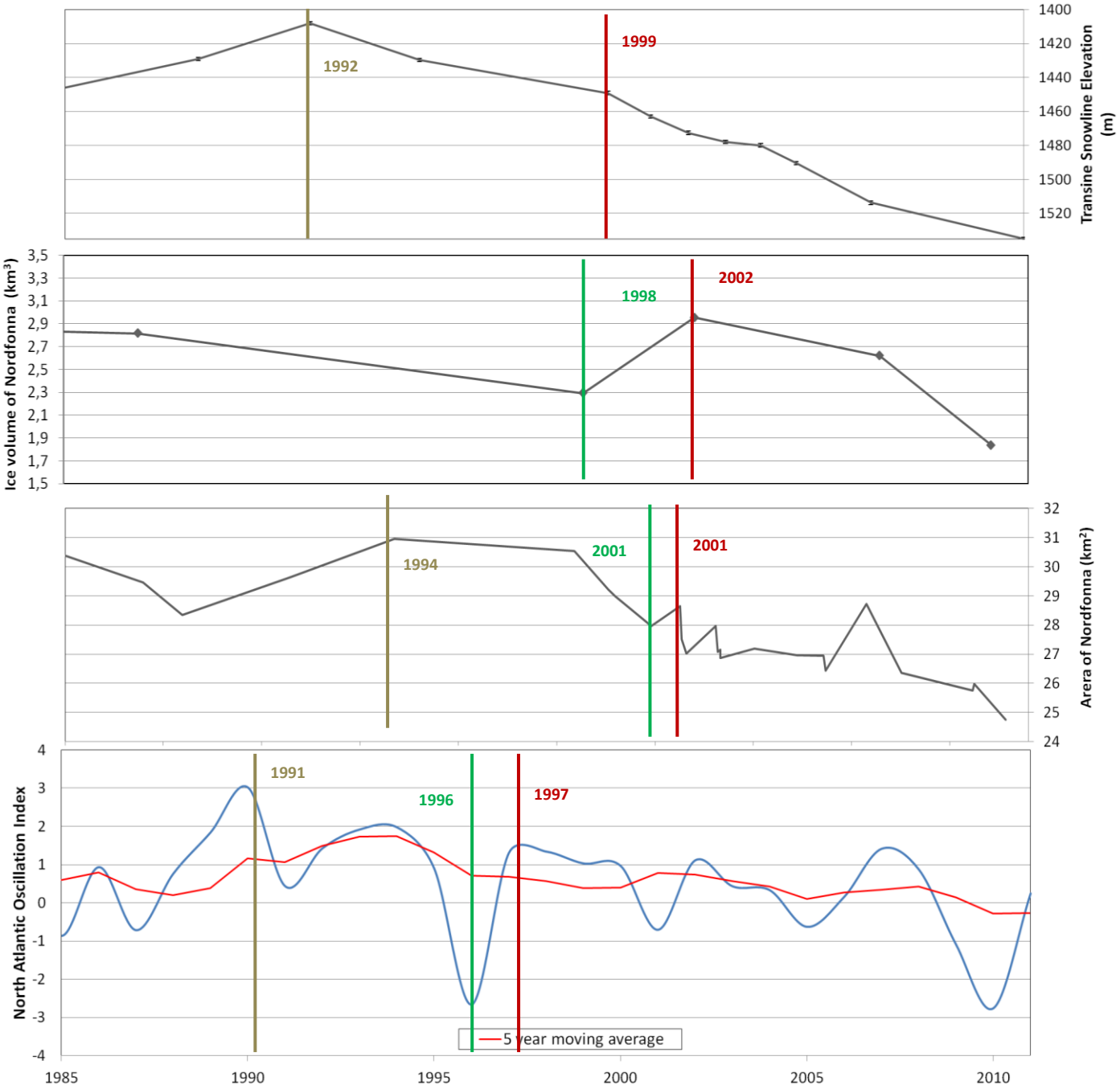

Figure 56: The lag times between the forcing of the North Atlantic Oscillation (NAO) index and the glacier area and volume of Nordfonna, and elevation of the Transient Snowline (TSL) measured on Sørfonna. Note that as there are multiple data points for the years 2000, 2002, 2006 and 2010 there is some noise for these years.

5.4.2. Correlation with *in-situ* data

5.4.2.1. Correlation between the ice-covered area and in-situ mass balance data

In-situ mass balance and ELA data has been collected by *NVE* from four catchments on Sørfonna – Svelgjabreen, Blomstølskardsbreen, Breidablikkbrea and Gråfjellsbrea, as shown in Figure 57. Data collected here however is sparse. The records from Breidablikkbrea and Gråfjellsbrea contain sporadic data from the 1960s (and in the case of Gråfjellsbrea the mid-1970s also) as well as from 2003 onwards. Data from Svelgjabreen and Blomstølskardsbreen dates back only to 2007. This makes it difficult to ground-truth the data collected using remote sensing in an accurate manner, however a continuous mass balance record from Rembesdalskåka, an outlet glacier of nearby Hardangerjøkulen extends back to 1963 (Figure 59). When the recorded mass balances of Hardangerjøkulen are compared with those taken on Sørfonna (Figure 58) very strong positive correlations are found, as was also reported by Elvehøy (1998). For this reason, as well as comparing the remotely sensed dataset with the *in-situ* data from Sørfonna, the relationship between Sørfonna and Hardangerjøkulen was used to reconstruct a mass balance record for Sørfonna back to 1963.

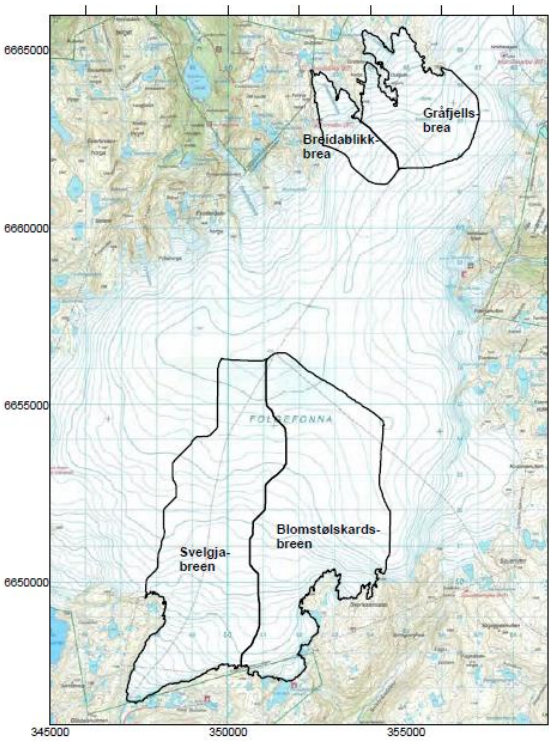

Figure 57: Sørfonna with the four catchments in which in-situ mass balance measurements are taken by NVE (Kjøllmoen, 2011).

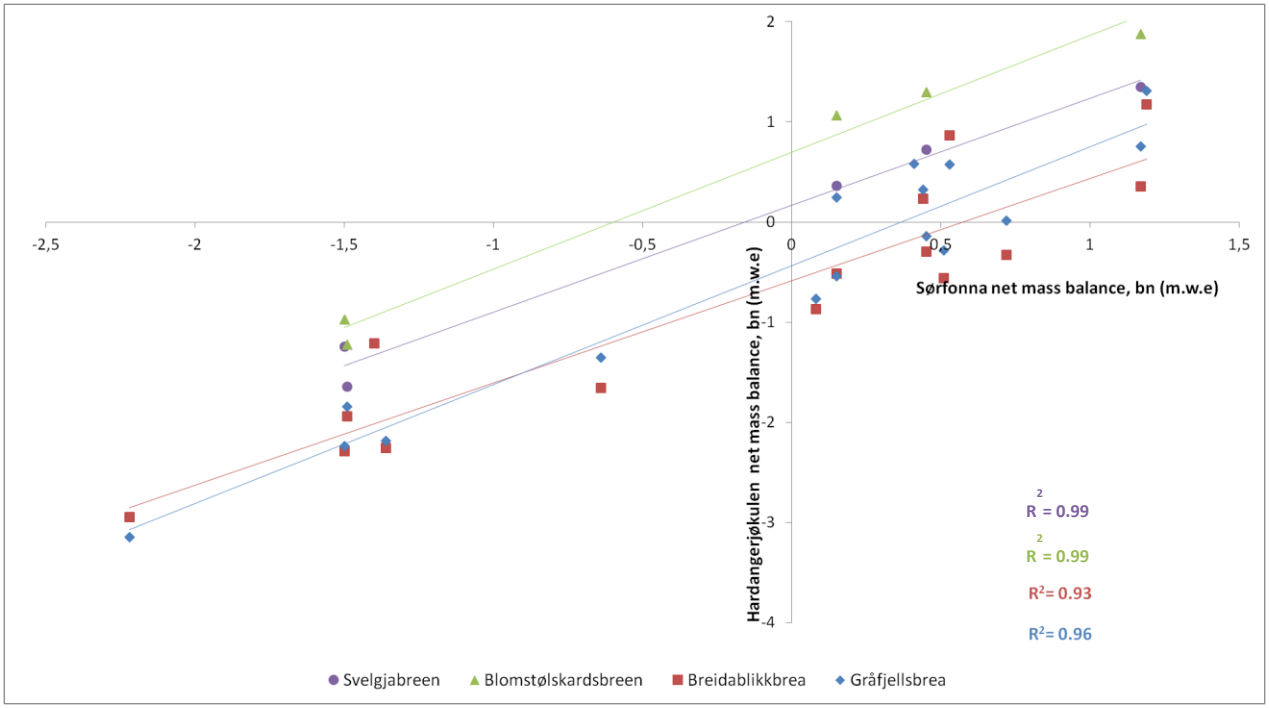

Figure 58: A comparison between the mass balances measured on Sørfonna (Svelgjabreen, Blomstølskardsbreen, Bridablikkbrea and Gråfjellsbrea) with the mass balance of Hardangerjøkulen. The strong relationships mean that the Hardangerjøkulen mass balance can be used to reconstruct the mass balance at Gråfjellsbrea, Sørfonna back to 1963.

Figure 59: As the mass balance record for Folgefonna (lower left) is sporadic and infrequent, a regression relationship from Hardangerjøkulen (upper right) which has a continuous mass balance record that extends back to 1963 allowed Folegefonna's mass balance to be interpolated (Map: Kartverket (2012)).

When the Folgefonna mass balance data are compared with the remote sensing data over its entire timespan (Figure 60) it can be noted that the data from Breidalblikkbrea and Gråfjellsbrea in the 1960s shows an increase in mass balance values from a trough in the mid-1960s *(a)*. The 1962 aerial photographs did not cover Sørfonna in its entirety so this event cannot be seen in Sørfonna's glacial area trend, however it can be seen clearly in the glacier area of Nordfonna, albeit not nearly to the same magnitude.

The very limited data from Gråfjellsbrea in the mid-1970s corresponds well to the general trend of decreasing glacier area of Sørfonna *(b)* while all the mass balance data from 2003 onwards agrees with the remotely sensed area trend, although again large shifts in mass balance are accompanied by only modest changes in the glacier area.

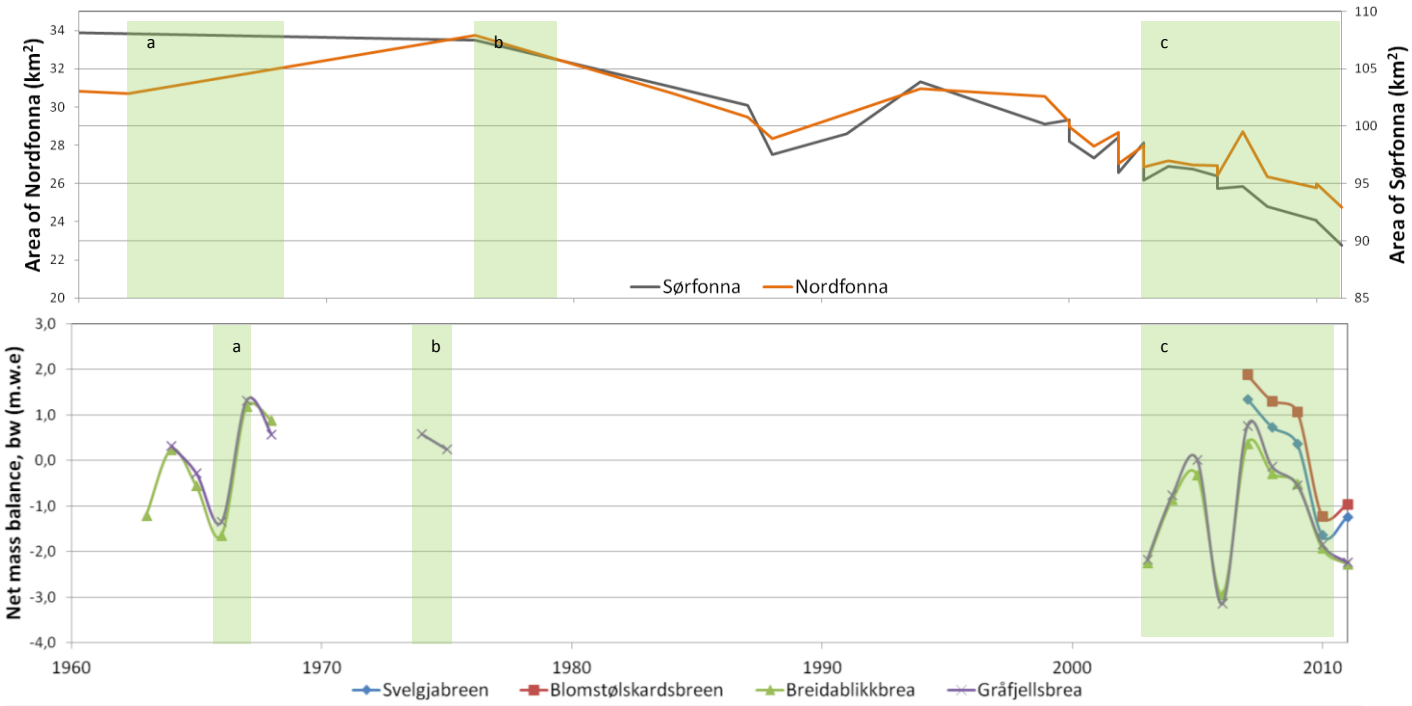

Figure 60: A comparison between the remotely sensed record of ice-covered area of Sørfonna with the *in-situ* mass balance data from Sørfonna (Svelgabreen, Blomstølskardsbreen, Breidablikkbrea and Gråfjellsbrea) between 1963 and 2011. The visible part of Sørfonna on the 1962 aerial photo mosaic has been combined with the 1976 outline to give some indicate of Sørfonna's response in the 1960s. The highlighted areas (a-c) indicate periods of assumed corresponding trends. Note that as there are multiple data points for the years 2000, 2002, 2006 and 2010 there is some noise for these years.

When the period of 2003 and after is examined in more detail (Figure 61) it becomes apparent that there is a lag of about one year between the traditionally measured mass balance data and the remote sensing data. Nevertheless there is a high level of correspondence between the two trends. Two noticeable peaks of positive mass balance values between 2004 - 2006, and 2005 - 2008 are both visible as slight areal expansions of Sørfonna *(a,b).* The increase in the rate of mass lost in 2009 is also detectable as an accelerated glacier retreat from 2010 *(c)*.

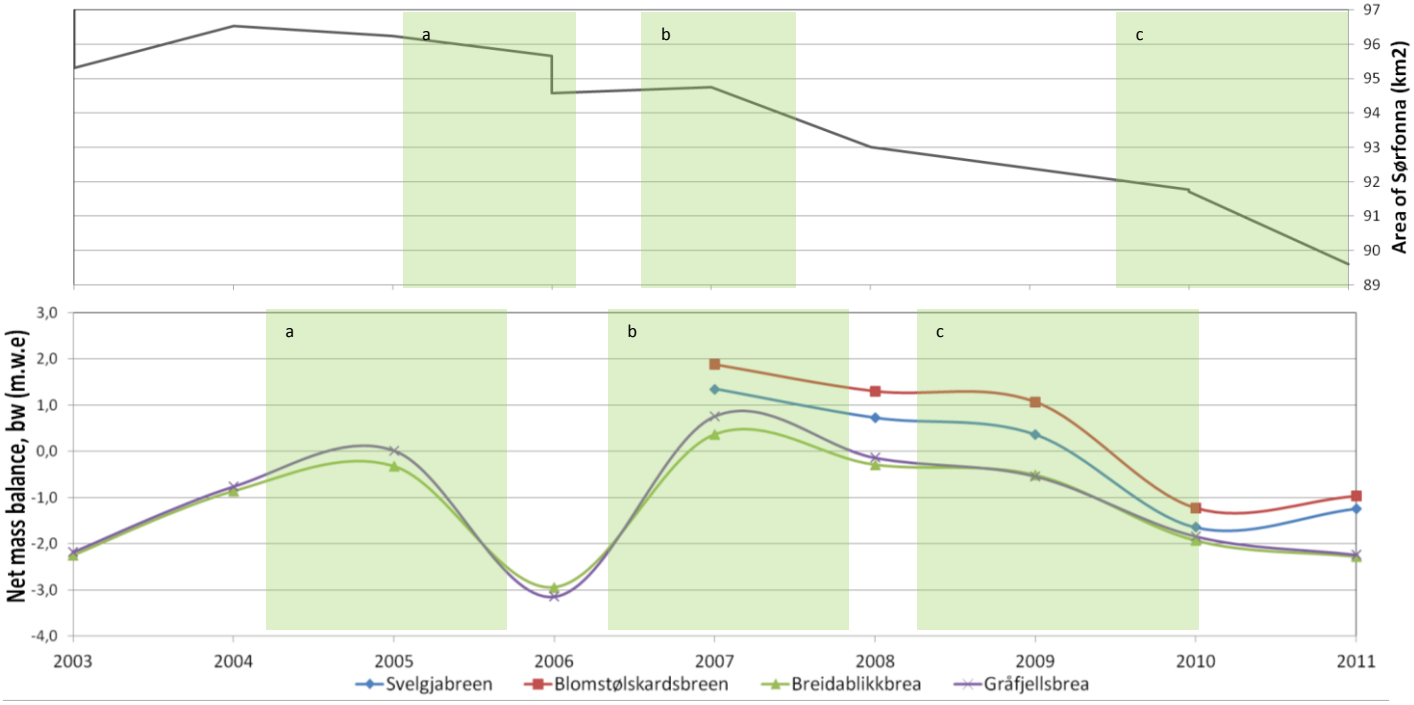

Figure 61: A comparison between the remotely sensed record of ice-covered area of Sørfonna with the *in-situ* mass balance data from Sørfonna (Svelgabreen, Blomstølskardsbreen, Breidablikkbrea and Gråfjellsbrea) between 2003 and 2011. The highlighted areas (a-c) indicate periods of assumed corresponding trends. Note that as there are multiple data points for the years 2006 and 2010 there is some noise for these years.

5.4.2.2. Correlation between the remotely sensed transient snowline elevation (TSL) and the in-situ measurements of the equilibrium line altitude (ELA)

When the remotely sensed data is compared with *in-situ* ELA data there is a satisfactory level of coherence (Figure 62), especially with the December and February ASAR datasets. The drop and subsequential rise by as much as 100 m in the ELA between 2004 and 2006 *(a)* recorded at Breidablikkbrea and Gråfjellsbrea is also evident in the December ASAR data, and to a much less extent in the February ASAR data as well, although both respond an order of magnitude less than the in-situ data. The rise in ELA out of this trough is reflected to some degree on all the ASAR data. Both the December and February datasets also depict the drop in the ELA between 2007 and 2008 *(b)*. The remotely sensed data all shows a general rise in the TSL from 2008 onwards, which fails to depict the accelerated rate of ELA rise between 2009 and 2010 and the following flattening out of the trend at Breidablikkbrea while the ELAs of Blomstølskardsbreen and Gråfjellsbrea dropped by 50-100 m *(c)*.

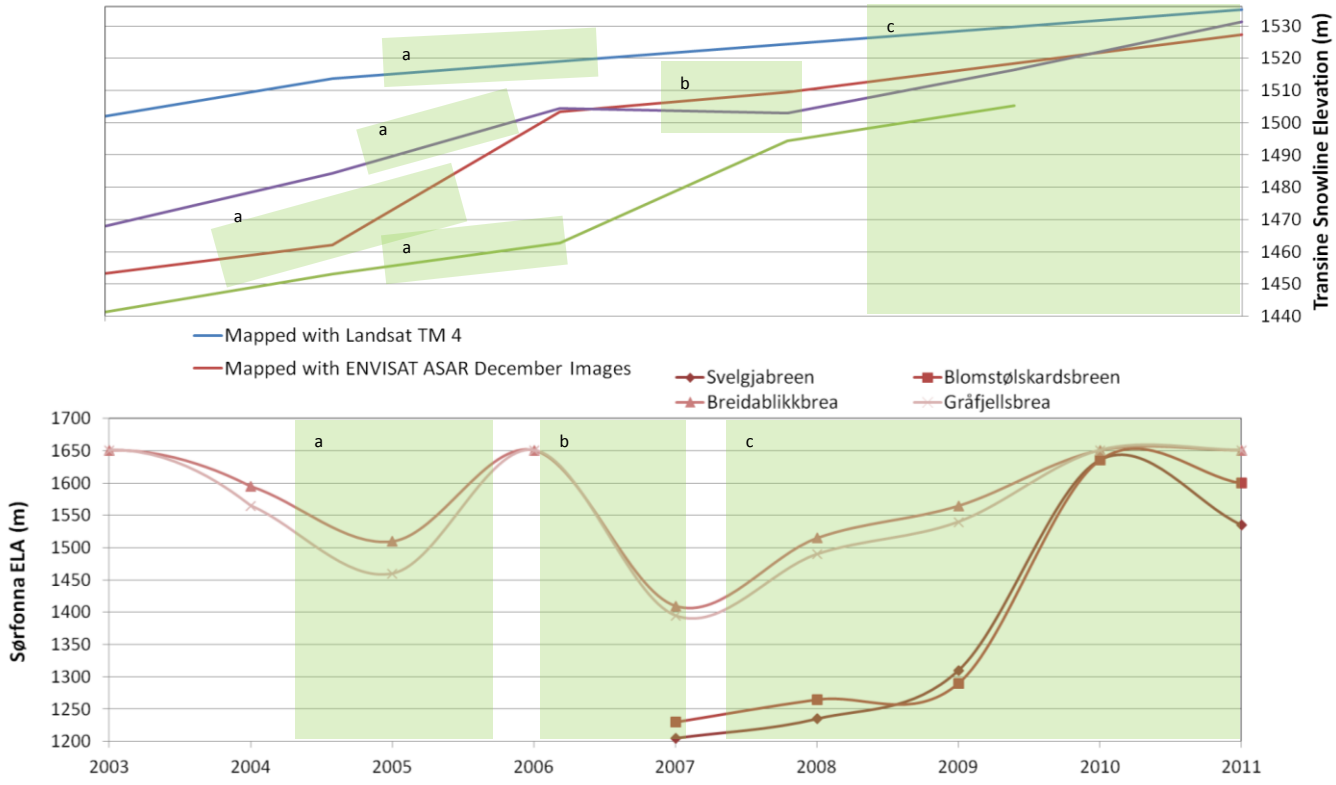

Figure 62: A comparison between the remotely sensed record of the transient snowline elevation on Sørfonna with the *in-situ* ELA data from Sørfonna (Svelgabreen, Blomstølskardsbreen, Breidablikkbrea and Gråfjellsbrea) between 2003 and 2011. The highlighted areas (a-c) indicate periods of assumed corresponding trends.

5.4.2.3. Correlation between the ice-covered area and constructed mass balance data based on the record of Hardangerjøkulen

By assuming a linear relationship between the mass balance records of Grafjellsbrea and Hardangerjøkulen (r^2=0.96) mass balance variations were reconstructed for Gråfjellsbrea between 1962 and 2011. These reconstructed data were compared with the glacier area record (Figure 63).

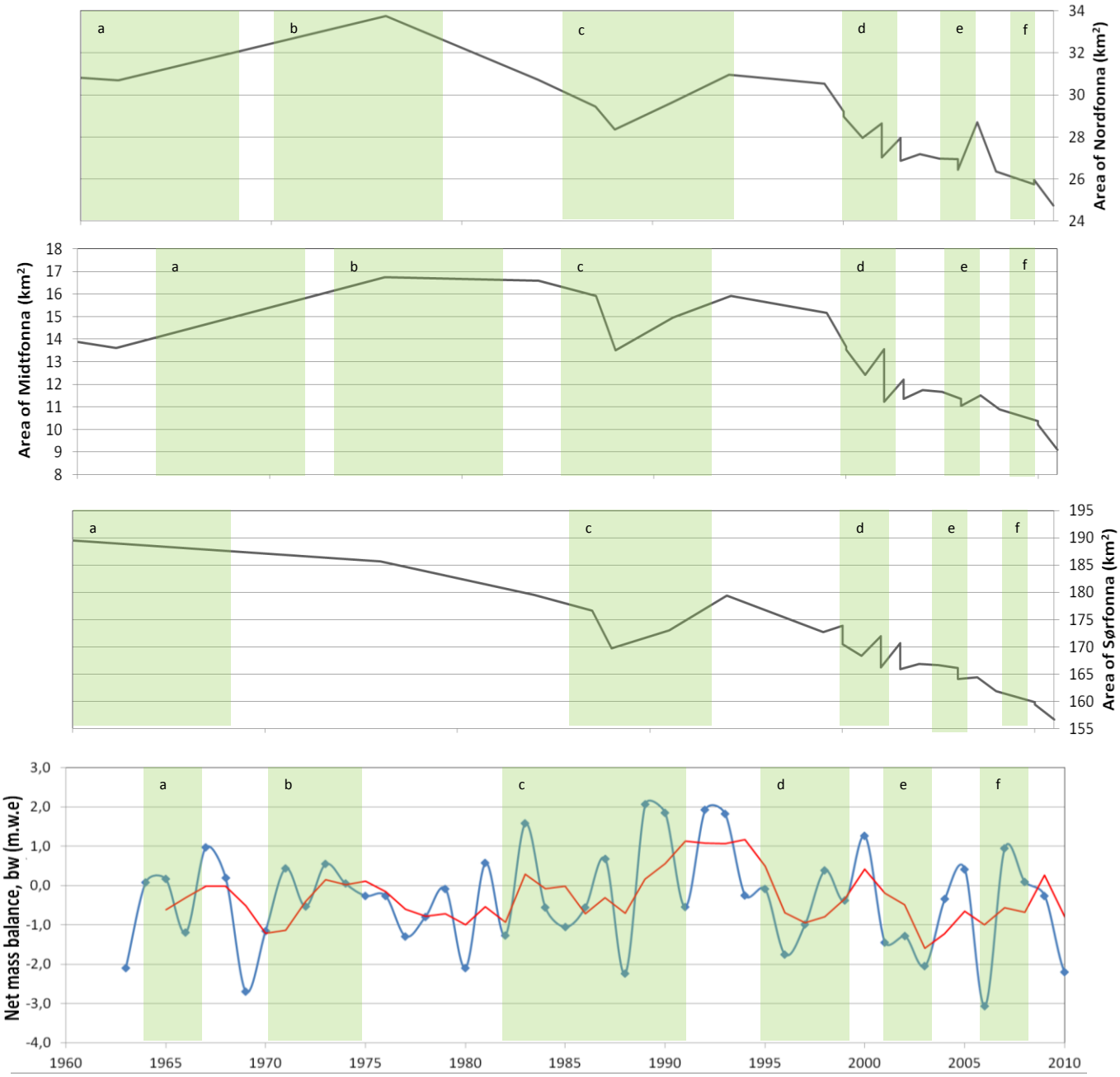

Figure 63: A comparison between the remotely sensed record of glacier area of Nordfonna, Midtfonna and Sørfonna, with a reconstructed mass balance series from Gråfjellsbrea based on a regression co-efficient with the mass balance series of Hardangerjøkulen between 1964 and 2011. The highlighted areas (a-f) indicate periods of assumed corresponding trends. Note that as there are multiple data points for the years 2000, 2002, 2006 and 2010 there is some noise for these years.

All the glacier area records show a slight dip around 1965 – 1967 *(a)* and peak at around 1973 – 1975 *(b)* that correspond to similar trends in the reconstructed mass balance. The 3 year moving average of mass balance replicates the sharp decrease and following gradual increase and levelling off of glacier area between 1983 and 1993 *(c)*. The two dramatic ice advance peaks between 1998 and 2001 that have been mentioned previously are also present in the mass balance record *(d)* as is the brief advance and retreat between 2005 and 2008 *(e)*, while the increased rate of glacier retreat since 2009 also correlated neatly with a sudden swing of mass balance to more negative values *(f)*.

5.4.2.4. Correlation between the remotely sensed Transient Snowline (TSL) and constructed mass balance data based on the record of Hardangerjøkulen

The Landsat TSL record shows a gradual decrease in TSL elevation climaxing around 1990, this corresponds neatly to the observed increase and decrease in glacier mass balance on the 3 year moving average (Figure 64a). Similarly an accelerated increase in the TSL elevation between 1999 and 2003 and following fall in values resembles the in-situ data well, although again with less magnitude (b). The ASAR December and January images both show a slight increase and then decease in the TSL elevation around 2006/2007 (c) which is followed by another small peak in the December and February images (d). Both of these seem to match a brief peak of increased glacier mass balance between 2004 and 2006 and again between 2007 and 2009.

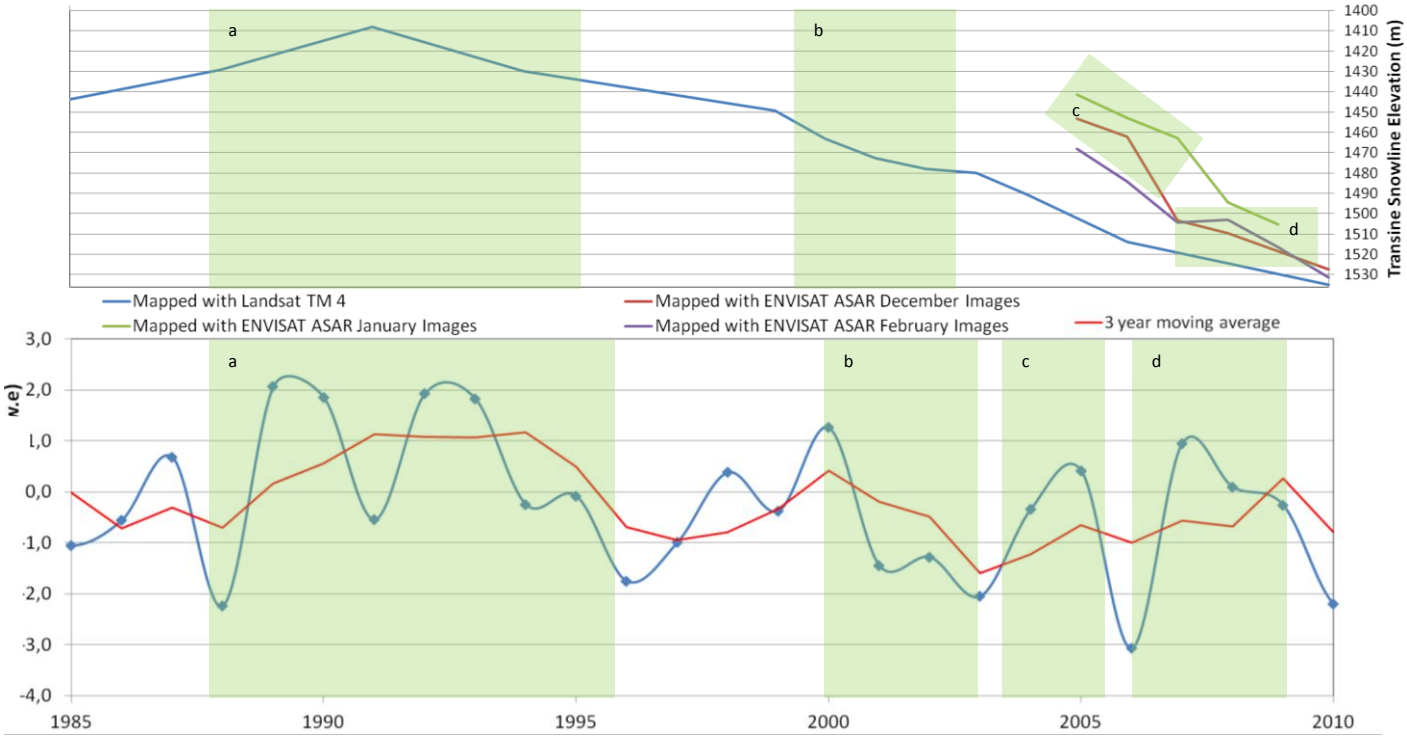

Figure 64: A comparison between the transient snowline (TSL) measured with both Landsat TM band 4 images, and ASAR winter images (note the y-axis has been reversed) with the reconstructed mass balance of Gråfjellbrea based on the Hardangerjøkulen record. The highlighted areas (a-d) indicate periods of assumed corresponding trends. Note that the vertical axis for the TSL has been inverted.

5.4.2.5. Comparison of manual delineation and automatic band ratio extraction.

In total the TM3/TM5 areas for Nordfonna, Midtfonna and Sørfonna varied by 14%, 23% and 7% compared with the manually delineated areas, while the TM4/TM5 areas varied by 34%, 74% and 13% respectively. For the most part these are underestimations with the results from 2001, 2002 and 2003 being severe underestimations for both methods. The TM4/TM5 method seems more prone to exaggerations than the TM3/TM5 method, as evident in 1994, 1999 and 2008. The reasons behind these variations shall be discussed in *6.8*.

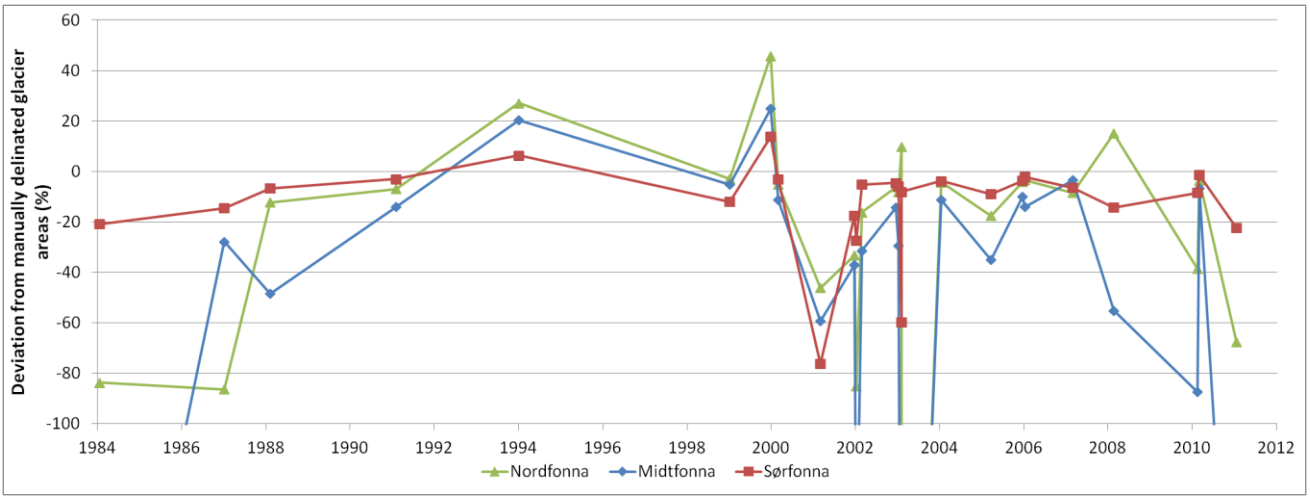

Figure 65: The percentage deviation of the Landsat TM3/TM5 automatic band ratio method compared with manually delineated glacier outlines for Nord-, Midt- and Sørfonna between 1984 and 2011. This proved to be the lesser accurate of the two automatic methods trialled.

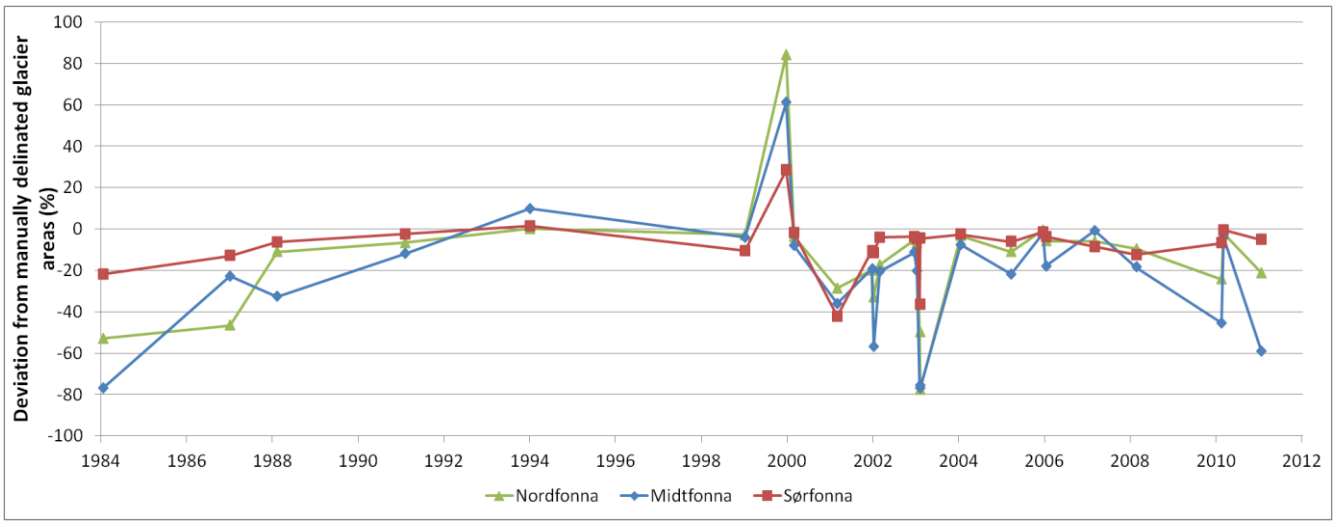

Figure 66: The percentage deviation of the Landsat TM4/TM5 automatic band ratio method compared with manually delineated glacier outlines for Nord-, Midt- and Sørfonna between 1984 and 2011. This proved to be the more accurate of the two automatic methods trialled.

6.0 Discussion

In this chapter the errors and uncertainties that are present in the data used in this investigation including the amount of time that each parameter lags behind the climatic forcing shall be discussed. The results obtained in this investigation are then compared with other work on Folgefonna for each parameter. Noticeable features and trends are discussed and accounted for as well as possible before the trends recorded from Folgefonna are put in a local, regional and global context.

6.1. Errors and uncertainty in the data used in this investigation

There are different types of error in a remote sensing investigation: spectral errors and systematic errors (Kääb et al., 2005a).

6.1.1. Spectral Errors

Spectral errors are erroneous results that arise due to the satellite sensor. Examples include spectral similarities between glacier ice and cloud or snow, elevation distortion on steep slopes facing away from a photogrammetric sensor, or the assumptions used on a uniform glacier density (Kääb et al., 2005a, Haug et al., 2009). As snow and ice are not lambertian reflectors the viewing angle, angle of the sun and topography of the area all also contribute to the image recorded. Similarly the age of snow and presence of dust particles can affect the reflectance (Albert, 2002, Hall et al., 1988). Spectral errors cannot be examined without comprehensive ground-truthing fieldwork; data would have to be captured at the same time as the satellite imagery which is not always easy (Paul and Andreassen, 2009). However some authors (Andreassen et al., 2005b, Paul et al., 2011) working in Norway state that all this accounted for when working with Landsat data in areas of clean ice the accuracy is generally better than 5%, with deviations of up to 10% possible in areas of heavy cast shadow.

As mentioned in the methods chapter (*4.3.1*) when it was not possible to map the glacier outline due to cloud, shadow or excessive snow, the outline from the previous image (the next one chronologically) was assumed, this could have caused slight underestimations of glacier area in some cases. The amount of error this contributes to the investigation cannot be assessed, but as no more than 20% of any glacier outline was obscured *(6.1.1.1*) and in most cases the outline assumed was not wildly different from that being mapped the error is not expected to be especially significant.

6.1.1.1 Obstructive cloud and cast shadows

It is possible however to assess the proportion of each image that is effected by cloud cover and cast shadows, both of which can add to the spectral error. The proportion of each glacier outline obscured was assessed.

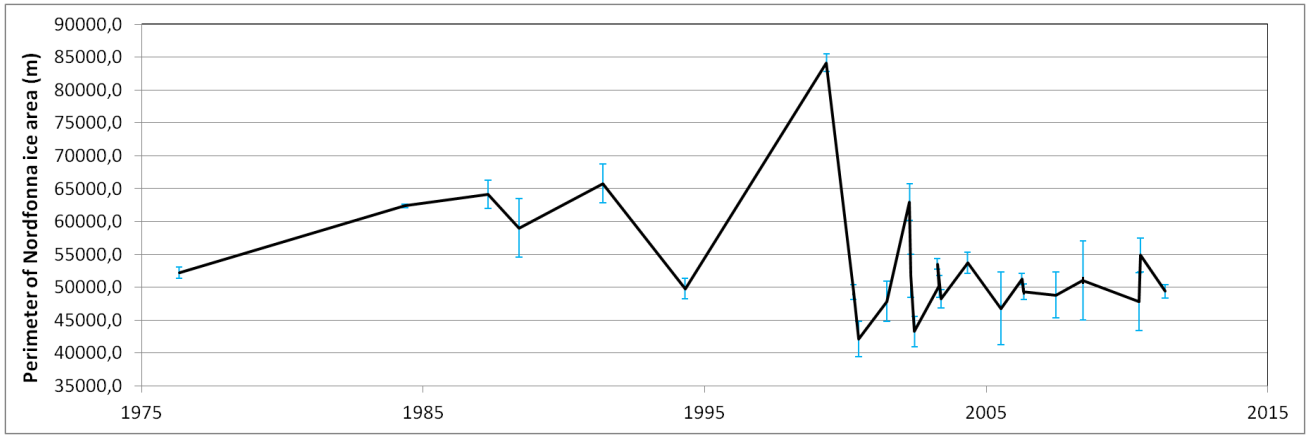

Figure 67: The total perimeter of the ice-covered area of Nordfonna and the proportion of the perimeter that was cast in shadow between 1976 and 2011. When the glacier margin was obscured the previously analysed outline was assumed which would have caused some underestimates in glacier area (*6.1*).

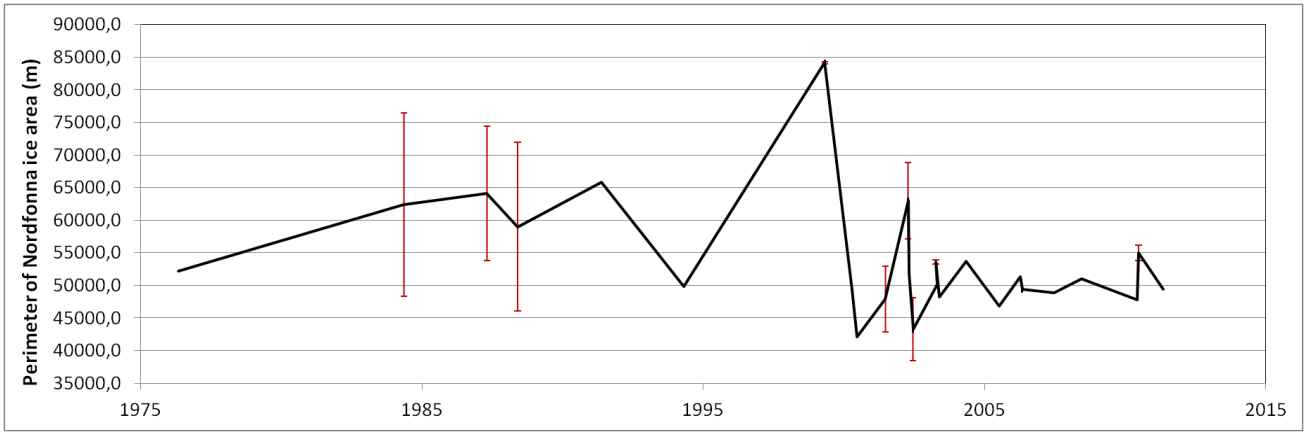

Figure 68: The total perimeter of the ice-covered area of Nordfonna and the proportion of the perimeter that was obscured by thick cloud between 1976 and 2011. When the glacier margin was obscured the previously analysed outline was assumed which would have caused some underestimates in glacier area (*6.1*).

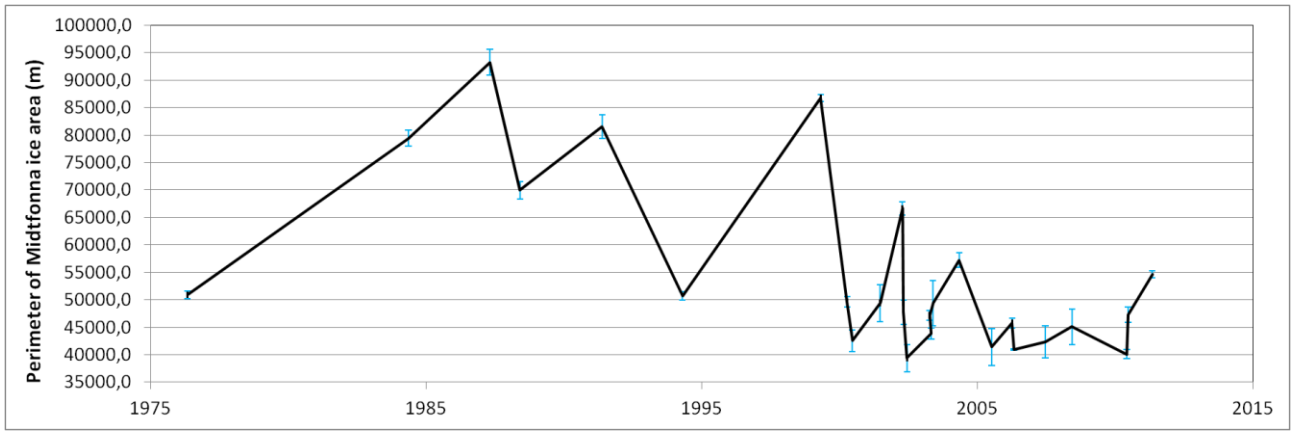

Figure 69: The total perimeter of the ice-covered area of Midtfonna and the proportion of the perimeter that was cast in shadow between 1976 and 2011. When the glacier margin was obscured the previously analysed outline was assumed which would have caused some underestimates in glacier area (*6.1*).

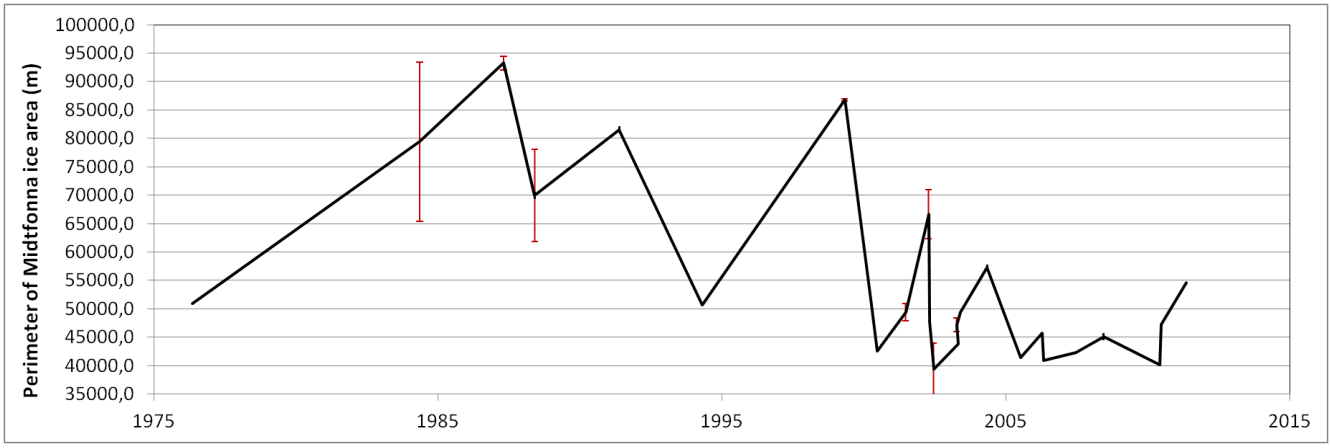

Figure 70: The total perimeter of the ice-covered area of Midtfonna and the proportion of the perimeter that obscured by thick cloud between 1976 and 2011. When the glacier margin was obscured the previously analysed outline was assumed which would have caused some underestimates in glacier area (*6.1*).

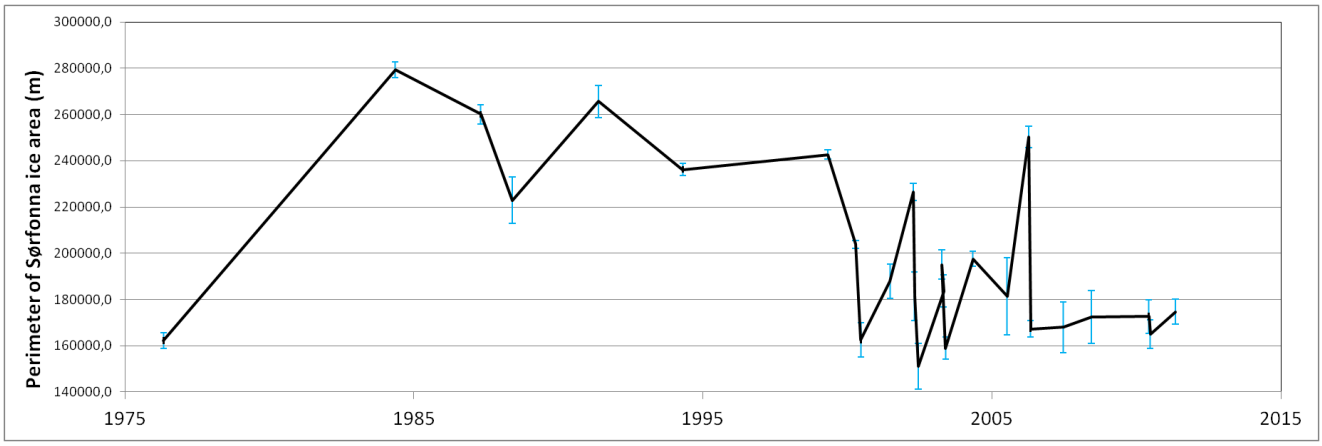

Figure 71: The total perimeter of the ice-covered area of Sørfonna and the proportion of the perimeter that is cast in shadow between 1976 and 2011. When the glacier margin was obscured the previously analysed outline was assumed which would have caused some underestimates in glacier area (*6.1*).

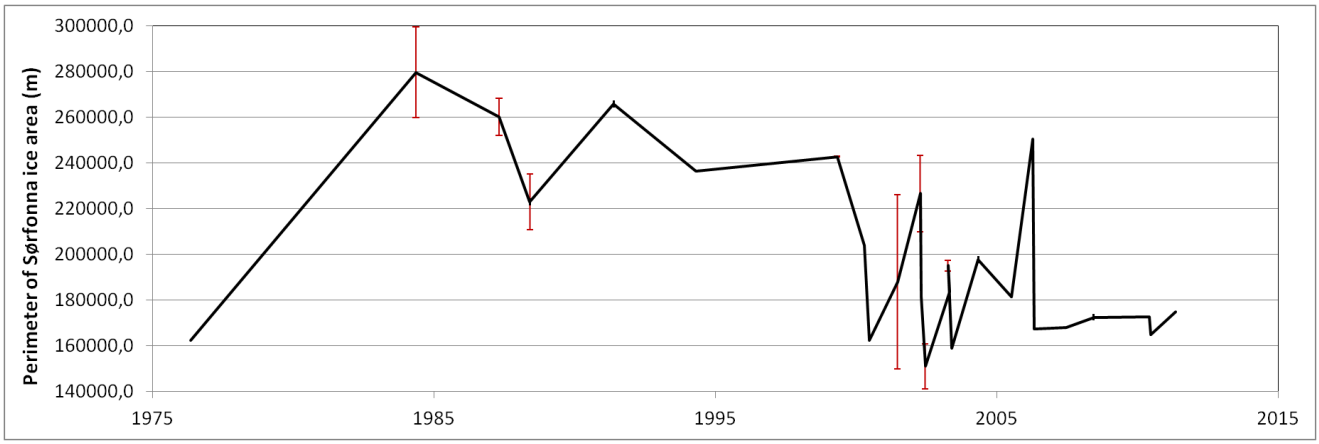

Figure 72: The total perimeter of the ice-covered area of Sørfonna and the proportion of the perimeter that is obscured by thick cloud between 1976 and 2011. When the glacier margin was obscured the previously analysed outline was assumed which would have caused some underestimates in glacier area (*6.1*).

On average Nordfonna, Midtfonna and Sørfonna had 9.2%, 6.8% and 6.9% of their perimeters obscured in shadow. As would be expected images acquired in July and August were less prone to being affected by shadows (1.9% total obscuration on 06/08/1999 3.8% on 08/08/2006) while the images with the highest proportion of the glacier outline being obscured occurred in September and October (19.0% total obscuration on 16/10/2005 15.4% on 14/09/2008), when the sun is lower in the sky, thus making long shadows more likely, as illustrated in Figure 73.

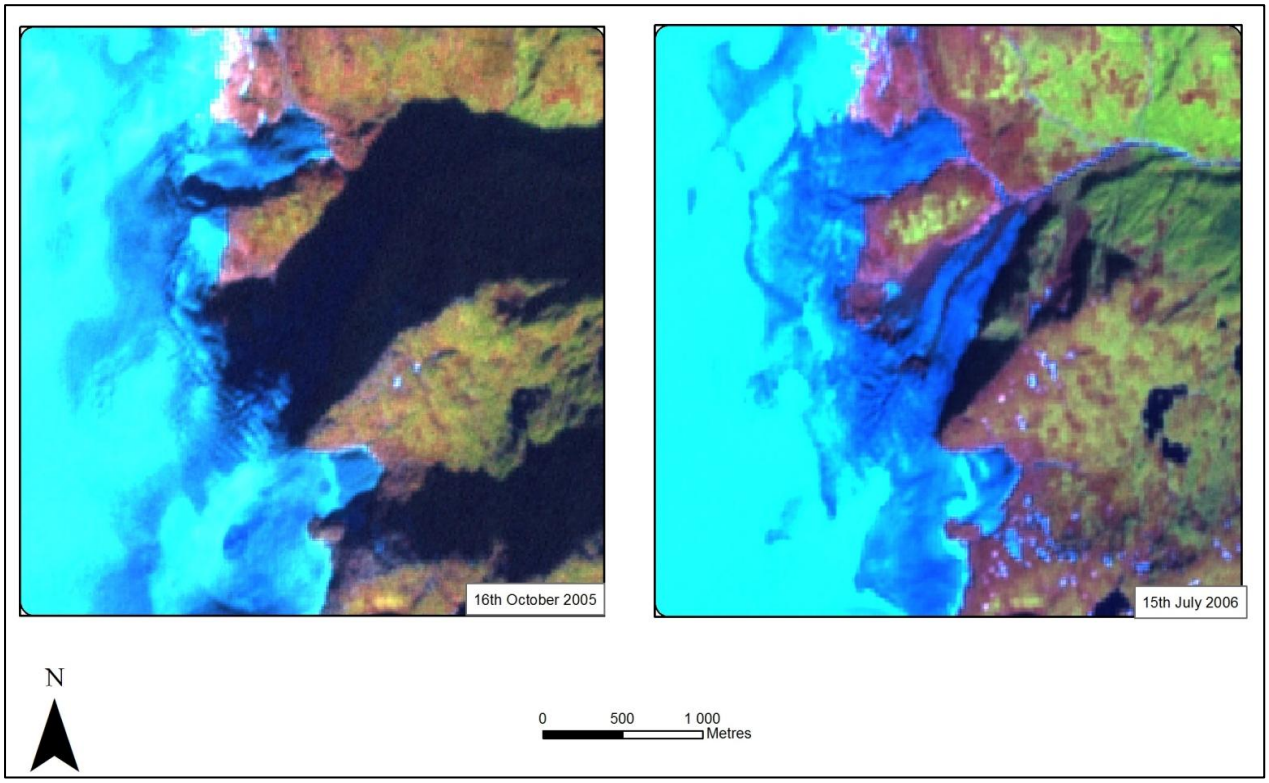

Figure 73: An illustration of the affect of cast shadow on glacier outline delineation at Buerbreen, Sørfonna with a spectral combination of 5,4,2. Generally satellite images acquired further from the summer solstice had more of the glacier outline cast in shadow.

On average all of Folgefonna had 4.7% of their perimeters obscured by opaque cloud, 18 of the images contained less than 1% cloud, while at the other extreme four images (22/09/2002, 28/09/2001, 07/09/1988 and 21/08/1984) had more than 15% of their total perimeter obscured. Cloud was especially copious in the September 2001 image with 21.1% of Nordfonna, 6.3% of Midtfonna and 40.4% of Sørfonna's outline obscured.

6.1.1.2. Seasonal Snow

Seasonal snow was troublesome on some images, especially on the images from July 2000 and from July 1994. As mentioned earlier (*4.3.1.1*) when the glacier margin was obscured, the previously worked on outline was used. This can have the effect of masking trends in the data, for example the August 1999 image shows Folgefonna slightly smaller than it was in the 1994 image, which was affected quite severely by seasonal snow. This suggests that *the Brikdalsbre Event* was centred around a maximum extent in 1994, however it seems much more likely that without the

seasonal snow the period of expansion would be seen to continue to 1999 and therefore centre around 1999 instead, as suggested by the literature (Nesje and Matthews, 2012).

Seasonal snow could also be a problem with ASTER DEMs. The three ASTER images used were all from July, a month where considerate amounts of snow usually persist on Folgefonna. It is therefore possible that the DEMs from 2002 and 2010 slightly over exaggerate the glacier elevation. However the depth of accumulated snow did not exceed 4.7 m when mass balance fieldwork was conducted in May 2010 (Kjøllmoen, 2011), such amounts of snow are less than the potential error terms of the ASTER DEMs (*6.1.2.3*). In addition to this the snow depth is certainly less by July when the ASTER images were acquired. It can therefore be concluded that the error from seasonal snow on the DEMs is not of high importance.

6.1.1.3. Time of image acquisition

Like the ASTER images not all of the Landsat images are from the ideal end of ablation season time period. Images range from being acquired between July and October. While for the most part seasonal snow is at a minimum; it is likely however, that a considerable amount of melt will occur between an image taken at the start of the ablation season (mid – late July) and an image taken towards the end of the ablation season (late September/early October). Measured ice areas between the 15/07/2003 and the 01/09/2003 varied by 3.9%, 7.0% and 2.8% for Nord-, Midt- and Sørfonna, while variations of 5.7%, 17.1% and 3.3% existed between the 20th 20/07/2002 and the 22/09/2002.

In addition even if seasonal snows were not present at the glacier margin, at higher elevations measurements of the TSL are extremely susceptible to surviving snows in the early ablation season, or the first snows towards the end of the season (Mathieu et al., 2009).

6.1.2. Systematic Errors

It is possible to gauge the systematic errors, that is to say errors due to the resolution of the data source

6.1.2.1. Systematic Errors of the glacier area time series

The *spatial-resolution-related uncertainty*, or U_{res} depends on the pixel size (r) of all datasets:

$$U_{res} = \sqrt{{r_a}^2 + {r_b}^2 + {r_c}^2 + \cdots +} \qquad \text{(Li et al., 2006),}$$

Given that the glacier area time series included one aerial photography mosaic with a pixel size of 1 m, 15 Landsat ETM+ images of 15 m pixel size, 9 Landsat ETM or MSS images with 30 m pixel size and the Landsat 1 image with 80 m pixel size can be said to be:

$$U_{res} = \sqrt{1^2 + (15 \times 15^2) + (9 \times 30^2) + 80^2}$$

$$U_{res} = \pm \mathbf{133.7\ metres}$$

Therefore the values given for the change in ice covered area between 2011 and 1962 are accurate to approximately ±135 m. This accuracy rises to ~83 m if the changes are examined only back to 1999 and approximately ±107 m if back to 1984. By using the glacier outline from 07/08/2003 as an example, these pixel uncertainties can be converted into percentage uncertainties. The total uncertainty for Nord-, Midt and Sørfonna if the changes are examined between 2011 and 1999 are **±16%, ±38%** and **±3%** respectively, if the changes are back until 1962 but excluding the 1976 image this error increases to **±20%, ±49%** and **±3%**, and if the 1976 Landsat image is considered this rises further to **±27%, ±64%** and **±6%** respectively. These error terms may sound extremely large, but they are over the entire time series and include 26 images. If two images are compared, such as in the maps produced in this investigation the errors are considerably less (Table 6).

Table 6: The uncertainty from when comparing different Landsat images together.

Comparison	Pixel Size comparison	Error for Nordfonna	Error for Midtfonna	Error for Sørfonna
Landsat 7 ETM+ to Landsat ETM+	15 m:15 m	±4%	±10%	±2%
Landsat 7 ETM+ to Landsat 5	15 m: 30 m	±6%	±15%	±4%
Landsat 5 to Landsat 5	30 m: 30 m	±10%	±23%	±6%
Landsat 7 ETM+ to Landsat 1	15 m: 90 m	±17%	±41%	±11%
Landsat 5 to Landsat 1	30 m: 90 m	±18%	±43%	±11%

It is impossible to know the accuracy of historical maps (Hall et al., 2003). The 1937 map is based on aerial photography yet the map was clearly not designed for glaciological purposes as the actual glacier outline is not marked, just whether a contour line overlies snow and ice or over rock. The contour lines are spaced only every 30 m causing the DEM that was generated to contain three times less detail than the DEM based on the 1987 contours. The glacier margin on this map was assumed to be up to the first rock contour line, there is obviously some uncertainty in doing this, but generally around the glacier the contour lines are quite closely spaced, and the total accuracy is assumed to definitely be no greater than the ±135 m mentioned above.

The accuracy for the two nineteenth century maps is significantly lower. These maps are much more rudimentary and due to the technology and methods available at the time most likely contain large spatial error. They also seem to display significant exaggerations of the ice cover, showing areas of very high topography as being beneath the glacier, such results are unlikely (Bakke, 2012b). They also almost certainly subjective and influenced by the personal experiences of the

cartographer (Salerno et al., 2008). The results from the 1860s should therefore be taken a little sceptically

6.1.2.2. Errors in the 1962 aerial photography mosaic

Upon inspection of the 1962 aerial photography mosaic, the edges of the surrounding fjords, prominent road intersections and identifiable features such as lakes near to the glacier appear to be georeferenced perfectly with other data. Although errors in aerial photography can arise when the photographs are taken at a very high elevation, (in this case the flying altitude is reasonable at ~4500 m.a.s.l.) the error is assumed to be minimal in the mosaic.

6.1.2.3. Systematic Errors of the glacier volume time series

The error and uncertainty of the glacier volume calculations depends on the accuracy vertical accuracy of the DEMs and on the uncertainty of the corresponding glacier area outlines. By using the equation given in *6.1.2.1* this outline accuracy would be ±40m. The later error is not considered here and just the error when volumes are considered by themselves is evaluated.

Maximum error estimations in the volume calculations were only possible for Nordfonna as the absolute ice volumes of Midtfonna and Sørfonna are unknown. However if the same relationship for glacier area exists then the error for Sørfonna could be expected to be approximately 7 times less than Nordfonna, while the error for Midtfonna could be around double Nordfonna's error.

Following the methodology of Ye et al. (2006), DEMs generated in this investigation were compared with the SRTM DEM at 50 stable bedrock locations to obtain the vertical error per pixel. These values were compared with the 2007 DEM, these values were then used in calculating the maximum error per volume measurement for Nordfonna (Table 7). For these measurements the 30/08/2003 glacier outline was assumed.

Table 7: The vertical error per pixel for the 6 DEMs used in this investigation, and the maximum error for Nordfonna's volume measurements in 2007. The vertical error and the glacier area were used to calculate the potential largest and smallest volumes of Nordfonna which was then used to calculate the maximum percentage error.

DEM	Vertical error per pixel	Maximum error for 2007 Nordfonna Volume
ASTER 2010	±26 m	±54%
NVE LiDAR 2007	±0.15 m (Arnold et al., 2006)	±0.3%
ASTER 2002	±35 m	±72%
SRTM 1999	±12.5 m (Schiefer et al., 2007, Surazakov and Aizen, 2006)	±26%
Contours 1987	±50m	±103%
Contours 1937	±102m	±211%

Other than for the LiDAR DEM these errors are quite substantial (Figure 74), however in the author's opinion the error for the two contour DEMs is considerably less than reported. This is because the quality check points can only take place around the glacier margin on the stable bedrock, there is therefore no guarantee that these areas are representative of the glacier itself (Rolstad et al., 2009). For the two contour DEMs only contour lines on the glacier and not the surrounding bedrock were used for the DEM generation, indeed it can be seen that the DEM distorts considerably the further away from the glacier you are.

It is therefore impossible to fully gauge the error of these two DEMs without re-generating them with all contour data included, for the 1937 DEM this would involve an arduous process of manual digitising. Vignon et al. (2003) generated a DEM from a topographic map of the same scale (1:100,000) over Peru and found the finished product to be accurate to ±10 m. If the same level of accuracy is assumed for the contour DEMs used here then the accuracy is in line with the SRTM DEM. It can be observed however that despite the sizable errors the trend from 1987 onwards is still significant (Figure 74).

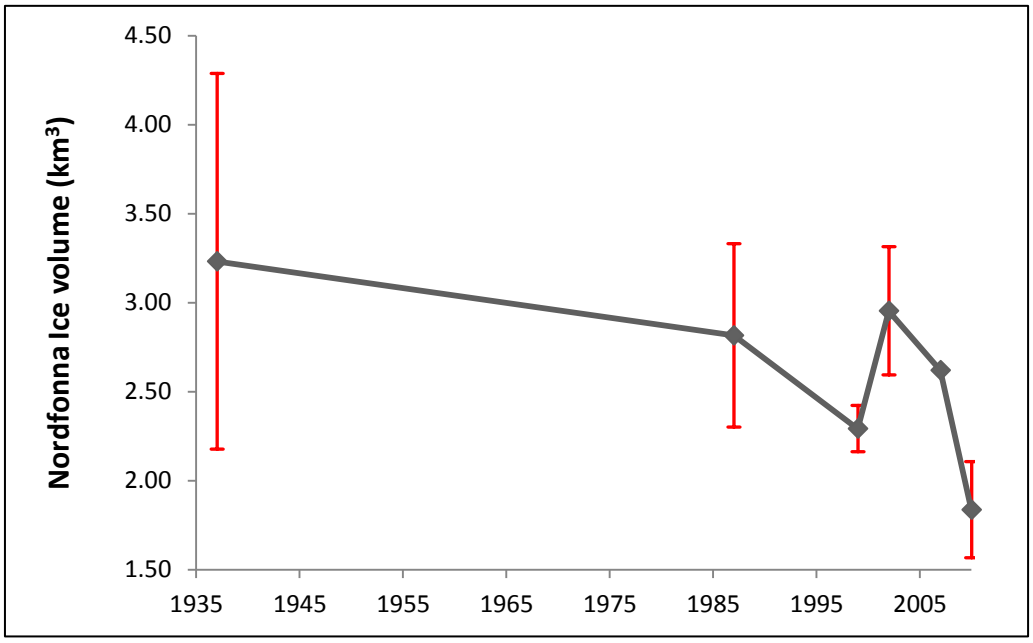

Figure 74: The error for each glacier volume measurement, the error for 2007 is so small it cannot be seen. It is however thought that the error for the 1937 and 1987 DEMs are gross exaggerations as the points in which the accuracy was determined were all in areas where contour lines had not been digitised. It can be remarked however that even with the substantial error terms the trend from 1987 onwards is still observable.

Despite the claimed high accuracy of the LiDAR DEM (Arnold et al., 2006), it seems that the precision and accuracy of the measurements fall significantly over complicated terrain. For example Rolstad et al. (2009) reported errors of 15 m on complicated terrain over Svartisen glacier. As the horizontal accuracy is ~1.2 m on steep terrain this can cause significant elevation errors (Figure 75). Given the high accuracy of the LiDAR DEM one would assume any errors would not surpass those present in the other DEMs. However without ground-truthing fieldwork this cannot be confirmed.

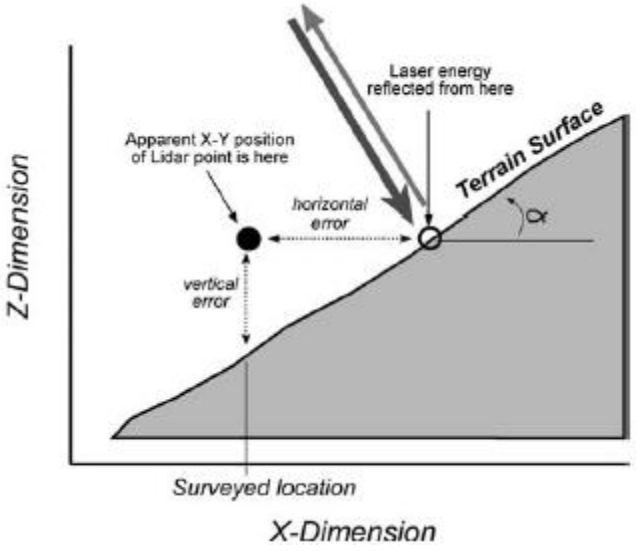

Figure 75: An illustration of how the steepness of the terrain being measured can impact the error in elevation values with LiDAR measurements (Goulden, 2009).

All of the glacier volume maps display a prominent area running up the eastern side of the glacier, which apparently has seen large elevation gains. Due to the distinct shape this area is probably a result of an error towards the edges of the 2007 DEM, and indeed this portion of Folgefonna has been excluded from the Statkraft volume change investigation (Kjøllmoen et al., 2008).

Despite these errors the 2007 and 1999 DEM are still expected to contain the least error, therefore it is mostly these two DEMs that are used for generating figures of volume change.

6.1.2.4. Systematic Errors of the transient snowline elevation time series

The uncertainty of the TSL calculations depends on both the pixel size of the sensor (15 m or 30 m for Landsat images, and 75 m for EVISAT ASAR Wide-swath images) and the vertical DEM accuracy used when reading the snowline elevations. The DEMs used for this were the NVE 2007 Laser DEM and the NASA 1999 SRTM DEM, which as already reported have relatively high vertical accuracies of ±10-15 cm and ±12.5 m per pixel respectively. In addition to this there is a portion of human error to be considered, with many glacier facies visible plus areas that could be superimposed ice. It was therefore up to the analyst to consistently plot the same boundary on each image.

The maximum and minimum elevations of each TSL measurement were recorded in an attempt to gauge the certainty of each measurement. For the Landsat TM band 4 dataset on average each measurement varied by between 15% and 25% around the mean elevation. The ENVISAT ASAR measurements have a pixel size nearly three times as coarse as the Landsat method yet the range of values is proportionally less. The December measurements have an average range of 26% around the TSL mean elevation. The January measurements have a smaller range of 27% while the February measurements are the most precise with a range of 24% around the mean TSL elevation.

These ranges of values obviously reflect quite a substantial error term. It is possible that the afore mentioned areas of surface melt and superimposed ice could have led the analyst astray and caused another glacier facies boundary to be partially digitised. It is also possible that a proportion of this range is due to geography and local climate of the area. This shall be discussed further later (*6.3*).

6.2. Lag time between the forcing climate and the glacier response

As has been shown in the results section (*5.4.1.5*) all of the parameters measured remotely lag behind the driving force. It is interesting when assessing the potential of remote sensing as a tool in glaciological investigations to determine this lag time, of course the same lag will exist when using the traditional methods but remote sensing allows multiple glacier parameters to be monitored, all with of which lag by different times behind the climate.

The lag times were reported in *5.4.1.5*. It would be assumed that the larger ice masses take the longest to responds, and generally this is the case although it seems unrealistic that Nordfonna would take longer to respond to than Sørfonna. A possible explanation can be offered for this - the 2001 event in which the 6 year lag time was calculated from, has already been shown to contain a high amount of seasonal snow. This means that the 'trough' that the lag period was established for could have occurred in 2000 or 1999, therefore increasing the lag time. The lag time when the NAO is considered is longer for Sørfonna (4-5 years) than both Nordfonna and Midtfonna (3-5 years) to respond, suggesting that the given explanation is true. These with the findings of Nesje (2005) and Imhof et al., (2011) who state that Bondhusbreen and Buerbreen lag behind the climate by between 2 and 4.5 years, while similar glaciers in Jotunheimen were found to lag behind a change in mass balance by 3-4 years (Winkler et al, 2009). It should be noted that glacier lag times are dynamic in nature and vary throughout time as the glacier geometry, aspect and topography all change (Nesje, 2005).

When the temperature trend is considered it can be noted how the lag times are dramatically shorter than those with the winter precipitation or the NAO. For the portion of the time series where summer temperature drives the glacier area the lag time was found to be one year or less. Nesje (2005) explains how higher summer temperatures and hence ablation rates cause an instantaneous augmentation in glacier downwasting and retreat, temperatures of the ice in the ablation zone are typically close to the melting point already so any excess heat is used solely to augment ablation. Therefore the lag times during periods of glacier retreat are considerably less than during times of glacier advance. A change in precipitation on the other hand occurs in the accumulation zone of a glacier must be worked through the glacier before a change in glacier area occurs.

It appears that the volume lag time (3-4 years) is less than the maximum glacier area lag time. This is to be expected, as changes in volume react in synchronisation with accumulation and ablation rates, and do not have to be transported through the ice-mass before being manifested as a change in glacier area.

The TSL was found to lag behind the climate by between 1-2 years. This is considerably quicker than the glacier area or volume, yet one would have expected that the snowline would react without a delay to a change in temperature or precipitation. As shall be discussed in *6.5* this is

further evidence that the phenomena being measured is actually the firn line instead of the snowline. The glacier parameters also lag behind the in-situ mass balance data, for the case of glacier are and volume this is to be expected, as a change in the health of a glacier would have to be sustained for several years before any change in area or volume can occur.

Now that the errors and lag times for the results have been discussed, the findings from this investigation can be used to determine the changing influence of different forcings on Folgefonna, as well as comparing the findings to other work on Folgefonna and further afield.

6.3. Driving forces responsible for changes undergone on Folgefonna

Throughout Folgefonna's history it is evident that the glacier has been driven by different forces at different times. It can be seen that between 1860 and the late-1980s the glacier area was driven primarily by the winter season precipitation (Figure 45). The mean summer temperature seems to have very little control on the glacier area during this time. Fealy and Sweeney (2005) state that during the 1960s and 1970s it was lower summer temperatures that caused an increase in glacier mass balance rather than the modest precipitation rise. The lack of data-points from this investigation during this period means that no such correlation was observed.

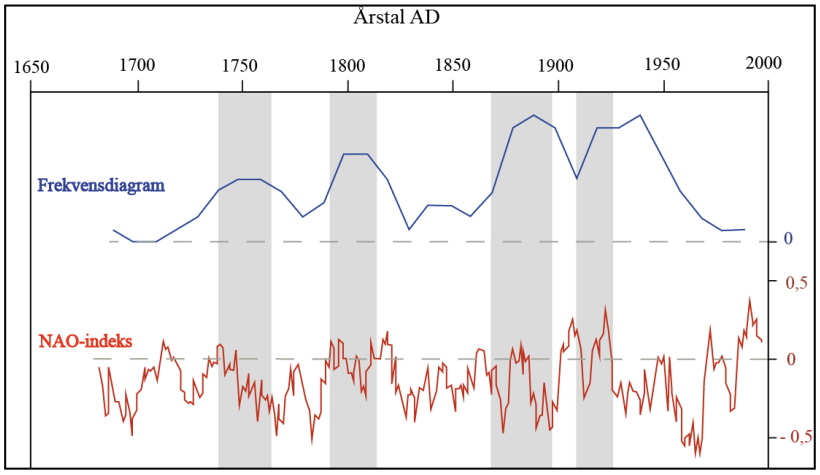

Figure 76: A comparison between the size of Folgefonna reconstructed with lichen chronology (blue line) and the NAO index (red line). Figure from Furdal (2010).

A weak level of correspondence appears between the temperature and the glacier size from the 1980s onwards but the lengthy lag time suggests that perhaps in this case the temperature is not the principal glacier driving force. This is in broad agreement with the findings of others (Winkler and Nesje, 2009, Nesje et al., 2000, Nesje et al., 2008b, Nesje, 2005).

Folgefonna's glacial area appears to follow the trends in the NAO for the majority of the examined time span; again complimenting the work of others (Nesje et al., 2000, Imhof et al., 2011). The lack of data in the early part of the time series makes it impossible to fully assess how the glacier area record corresponded to the NAO between 1860 and 1915. However when lichen reconstructions are examined (Figure 76) it can be seen that in-between the data points of 1864 and 1937 Folgefonna indeed expanded until ~1890 before entering a period of retreat that lasted until ~1910, mirroring the NAO index. The glacier began retreating once more around 1940, at around the time of a drop in NAO values (Furdal, 2010), as no remote sensing data points are available until 1962 a general glacier retreat is the only trend seen in this investigation's data (Figure 16, Figure 17, Figure 18.)

A shift towards more positive NAO values began in 1984, peaking around 1993. The subsequent increase in accumulation season precipitation from 1986 to 1997 are thought to be the cause of the well documented period of glacier advance (the Brikdalsbre event) across Western Norway (Nesje and Matthews, 2012, Nesje, 2005, Imhof et al., 2011) that is clearly identifiable in the glacier record (Figure 22, Figure 23, Figure 21). Fealy and Sweeney (2005) find that 1988 was the pivot year that signified the start of a trend of increasing precipitation in Western Norway.

The NAO also correlated well with the direction of Folgefonna's reaction, with positive phases of the NAO seeing western Folgefonna advance, while negative phases saw it retreat. Eastern Folgefonna has generally remained more stable. This is most likely as the increase in the strength of the westerlies associated with a positive NAO phase brings more precipitation off of the ocean, which due to the orographic effect is precipitated on the western portion of Folgefonna. The milder summer temperatures also brought about by the NAO reduce the amount of ablation at lower elevations allowing western Folgefonna to expand. During negative NAO phases the western flank of Folgefonna retreats more, this can be explained by the eastern side being cast in shadow due to the topography of the area during the afternoons, causing a diurnal hysteresis in heating. Melting is more effective in the afternoon owing to higher temperatures, which causes asymmetrical glacier ablation. This is more evident in Scandinavia than anywhere else in the world (Evans, 2006). Evans (2011) notes that in Norway the prevailing westerly winds can also help feed the eastern sides of glaciers, therefore adding to the relative stability.

The rate the NAO has been changing appears to be outpaced by the recent increase in summer temperatures over the last two decades. This accelerated warming seems to have brought about a shift in the primary driver of the glacier from winter accumulation rates to summer ablation rates. From 1990 onwards it appears that Folgefonna is becoming increasingly sensitive to changes in the summer temperature, this is in alignment with the findings of Winkler et al. (2009). The summers of 2002 and 2006 were especially warm with average ablation season temperatures in Rosendal of 15.3°C and 15.1°C; this is 2.3°C and 2.0°C warmer than the 1960 to 2010 average. From this it can be inferred that the additional warming in the summer has become sufficient to ablate away any surplus accumulation resulting from positive phases of the NAO. The winter precipitation still affects Folgefonna, as evident from the 2005-2008 glacier advance and the sharp 2010 glacier retreat. Nesje (2005) states how the balance year of 2002/03 saw glaciers in western Norway receive 156% of their normal ablation yet only 66% of their normal accumulation, resulting in the feature noticeable in Figure 45e and Figure 47b and the associated glacier retreat. It seems that that since 2000 while temperature is the main driver of Folgefonna, the precipitation acts to dampen or amplify changes.

6.4 Comparison with other records and findings on Folgefonna's glacial area

6.4.1. Comparison with reconstructions and in-situ data

There are a bountiful amount of historical and proxy sources that can be compared to the record of glacier area measured in this investigation. Nussbaumer et al. (2011) compiled maps, artwork and written documents to reconstruct the historical glacier fluctuations at Buerbreen and Bondhusbreen. Although the number of data points during the early part of the remotely sensed record are sparse, the record agrees with the general consensus of a period of glacier retreat, although Sørfonna's retreat is depicted as being less severe after 1937, which is in contrast to the findings of Oerlemans (2005), who describes Norwegian glaciers entering a period of substantial retreat in the 1930s.

Furdal (2010) reconstructed the relative size of many of Folgefonna's outlet glaciers using lichen chronology, in some cases back to the late 1600s. The end portion of the reconstruction can therefore be compared with the early part of this investigation's glacier area record (Figure 76). Furdal's reconstructions between 1860 and 1937 are much more detailed than this investigation's record and depict a glacier advance until 1890 which was then followed by a retreat until 1910 and subsequent glacier advance until 1940. As no remote sensing data sources exist between 1864 and 1937 this investigation's trend shows a gradual glacier decline over this entire period. Furdal's reconstruction however claim that the glacier advance during the early twentieth century caused Folegfonna to reach a size comparable to that of the LIA peak of the 1870s (Figure 76). This is disputed by length variations from Bondbusbreen and Buerbeen which show a re-advance but to a smaller size (Nussbaumer et al., 2011, Imhof et al., 2011).

Furdal's reconstructions show a rapid glacier retreat from 1940 which slows down in the 1970s. This is at odds to the remotely sensed data and the reconstructed Folgefonna mass balance data (*5.4.2.3*) which depict a slight advance in the 1970s. However the 1976 Landsat image is slightly blighted with seasonal snow so it is possible that the actual glacier area could have remained stationary between the 1960s and the late 1980s, as depicted in the glacier length variations. The lichen reconstructions, outlet glacier length variations, literature and the remotely sensed data however all agree that the glacier underwent a rapid re-advance in the 1990s followed by a new period of accelerated glacier retreat after the turn of the millennium (Nesje and Matthews, 2012, Nesje, 2005, Winkler and Nesje, 2009).

Sporadic in-situ mass balance data exists from Sørfonna from parts of the 1960s, 1970s and post-2003. This data reflects the remotely sensed glacier area record almost perfectly (Figure 60) as does the reconstructed mass balance record based on a regression correlation with nearby glacier Hardangerjøkulen (Figure 63). It is noted that the mass balance data shows greater fluctuations than the glacier area record. This is to be expected, as a swing in mass balance would have to be sustained for multiple balance years before the glacier area responds.

Between 2005 and 2009 all three components of Folgefonna underwent a short-lived glacier advance as evident in the remotely sensed glacier area record (Figure 21, Figure 22, Figure 23). This event was well documented on other Norwegian glaciers (NRK, 2008), although it is possible that seasonal snow in 2007 may have exaggerated the scale of this advance somewhat. In the last few years Folgefonna along with other Norwegian glaciers have continued to retreat (Kjøllmoen, 2011).

6.4.2. Comparison with other remote sensing work

Baumann (2010) mapped the LIA moraines of glaciers in Jotunheimen with the aid of Landsat images and aerial photos. Between the LIA maximum and 2003 the glaciers of Jotunheimen lost on average 35% of their area, only slightly less than the 42% Nordfonna lost between 1860 and 31/08/2003, Midtfonna lost a greater amount at 60% while Sørfonna lost 15% between 1864 and 2003.

Kjøllmoen (2009) compared glacier outlines from a 2006 satellite image and a 1981 map with additional area information from 1972, 1962 and 1969. All but the 1969 data (as there is no corresponding data point in this investigation) are compared below:

Table 8: A comparison between the areas of Nordfonna, Midtfonna and Sørfonna from an investigation conducted by NVE (Kjøllmoen, 2009) and the areas measured in this investigation. Generally the level of agreement is high, especially for dates that coincide with each other.

	Area, km^2 (Kjøllmoen, 2009)				**Area, km^2 (Robson, 2012)**		
	Nordfonna	Midtfonna	Sørfonna		Nordfonna	Midtfonna	Sørfonna
2006	26.5	11.4	166.5	**2006**	26.4	11.5	164.4
1981	27.3	12.0	167.8	**1984**	30.7	16.6	179.5
1972	35.4	19.8	189.2	**1976**	33.7	16.7	185.7
1962	31.1	13.5	180.6	**1962**	30.7	13.2	n/a

The only two dates that match up are 2006 and 1962. The data for 2006 is incredibly similar, Nordfonna and Midtfonna vary by only 0.1 km^2 while the two area sources for Sørfonna; despite being over 6 times the size of Nordfonna varied by only 2 km^2. The 1984 Landsat areas are slightly larger than the 1981 NVE outlines; this can most likely be explained by snow still being present on portions of this image while cloud was prevalent over the entire glacier but especially over Midtfonna. As explained in *4.3.1.1* this would have caused the 1987 outline to be used. The 1976 Landsat measurements are all slightly smaller than the 1972 NVE areas by between 2 and 5 km^2, given that four years separate these two measurements this disparity is reasonable if a little on the high side. However as mentioned in the errors chapter (*6.1*) the 1976 Landsat image was of an extremely course (90 m) pixel size, and also contained some snow along the margins. The 1962

aerial photo mosaic didn't cover Sørfonna in its entirety; however the areas measured for Nordfonna and Midtfonna only differ by 0.4 and 0.3 km^2 respectively.

A map showing the area lost between 1981 and 2006 is also given by Kjøllmoen (2009) which agrees with the maps created in this investigation. They show that western Folgefonna has retreated a lot more than eastern Folgefonna, with the north west of Nordfonna, central western Midtfonna and the upper third of Sørfonna seeing the most glacial area lost.

Kjøllmoen et al. (2008) collected glacier outlines from the 2007 LiDAR campaign. These outlines were compared with the Landsat outlines from this investigation. As the 2007 Landsat outlines were from late September they were slightly disrupted by seasonal snow as well as the SLC malfunction the 2006 Landsat outlines were also compared (Table 9).

Other than the 2006 Midtfonna measurement the NVE outlines gave areas slightly smaller than those measured with Landsat. The 2006 outline was especially similar to the NVE results, the only differences arose from including what the author deems to be seasonal snow patches that are not present in the surrounding images, and areas that were hidden in shadow in the Landsat image. The high level of coherence between the NVE LiDAR measurements and those measured in this investigation provide an illustration of the accuracy of the remote sensing method. Given that the 2006 image was a Landsat 5 scene and therefore possessed a 30 m pixel size, glacier areas varying by between 0.08 and 1.09% is an astonishing level of accuracy.

Table 9: A comparison between the remotely sensed NVE LiDAR glacier outlines and the Landsat glacier outlines measured in this investigation. As the 2007 Landsat images was effected by snow, the 2006 Landsat image is also compared.

	Nordfonna Area (km^2)	**Midtfonna Area (km^2)**	**Sørfonna Area (km^2)**
NVE 2007 LiDAR outlines	26.42	11.05	162.35
Landsat 8th August 2006 outline	26.44	11.04	164.13
Difference (%)	*0.08*	*0.12*	*1.09*
Landsat 27th September 2007 outline	28.72	11.52	164.37
Difference (%)	*8.0*	*4.03*	*1.23*

6.5. Transient Snowline (TSL) measurements

It was noted that there were some potentially significant errors in the TSL measurements as evident from the range of TSL values for each measurement (*6.1.2.4*). Different answers can be offered for the source of this range of values. Folgefonna has a very high precipitation gradient between the more maritime western side of the glacier and the more continental eastern side. Therefore it is not surprising that when the TSLs were split into segments for the western and eastern sides of the glacier, it became apparent that the western portions of the TSL were up to 3.2% higher than the TSL on the eastern side (Table 10). This occurred for all the years other than the initial two 1980s which were during the early Briksdalsbre event when Western Folgefonna would have received more accumulation. Initially this is not as one would expect, it would be assumed that the higher rates of precipitation on the western sides would allow the TSL to persist to a lower elevation; however as discussed in (*6.3*) Scandinavian glaciers often exhibit an eastern bias (Evans, 2006). Nevertheless even with a maximum deviation of 3.2%, this only explains a small amount of the range in values present.

Table 10: Difference in metres and percentage of the transient snowline (TSL) mean elevation between the Eastern and Western portions of Folgefonna. This disparity can be explained by a general eastern bias of Scandinavian glaciers during times of retreat, while the western side was more responsive during times of glacier advance. The reasons for this are given in *6.3*.

Date	Difference (m)	Difference (%)
08 August 2006	6,4	0,4
11 August 2004	0,0	0,0
01 September 2003	24,3	1,6
22 September 2002	24,6	1,7
28 September 2001	42,4	2,9
25 September 2000	30,0	2,0
06 August 1999	32,9	2,3
31 July 1994	46,8	3,2
31 August 1991	30,4	2,1
07 September 1988	-10,6	-0,8
21 August 1984	-11,4	-0,8

When the remotely sensed TSL was compared with climatic data it was found that there was a high level of correspondence. Both the Briksdalsbre Event in the 1990s and the mid-2000s glacier advance are visible as periods where the TSL either levelled out, or slightly decreased. The steepening rise in TSL reflects the increased warming since 2000.

It was noted in *5.4.2.4* that when compared with the *in-situ* mass balance and ELA data, the remotely sensed TSL responded at a lessened magnitude. A similar outcome was found by Rabatel et al. (2008) when using Landsat images to monitor the TSL on Glacier Blanc in the French Alps. A reduced inter-annual variability was explained in this case by the fact the annual

mass balance varies much more in the lower elevations. However in this investigation the TSL was also shown to vary less than the *in-situ* ELA data suggesting this answer does not apply to Folgefonna.

It is instead inferred that the phenomenon being measured is in actual fact the *firn line* (FL). The FL is still a valid approximation for the ELA over longer timescales as long as superimposed ice is not present (Storvold et al., 2004). However as Folgefonna is a temperate maritime glacier such conditions are not certain. Unlike the snowline the FL is not related to the annual mass balance of an ice mass and instead responds to changes over several balance years, this is why the assumed TSL was found to lag behind changes in the climate by 1-2 years (Figure 53). The FL therefore still responds to a changing climate, a prominent shift in the ELA will cause it to also change, although the relationship between the two parameters contains a lag (König et al., 2001, De Wildt and Oerlemans, 2003). The FL is also influenced by ice flowing (König et al., 2000) which could also explain some of the range of values. Storvold et al. (2004) however claim that due to a reduced variance the firn-line may be preferable to changes in the snowline or ELA as an indicator of climate change.

There is not so much comparable work on the TSL for Norway, perhaps because of the difficulty in finding images with optimum conditions very few investigations use Landsat images to map the TSL. A small amount of work has been done on Svartisen in Northern Norway (Heiskanen and Pellikka, 2003, Braun et al., 2007), where despite good results being obtained it is noted that it is hard to obtain images from the optimum time period and that some years no suitable data was found. The degree of subjectivity is also pointed out.

More work has been carried out on Norwegian glaciers using SAR images, although as was found in this investigation this method is not ideally suited to temperate glaciers where temperatures above freezing can cause problems. Most studies opt not to use winter SAR images to map the TSL beneath the accumulated snow and use summer imagery instead (König et al., 2000, König et al., 2001, Storvold et al., 2004). Brown et al. (2005) conclude that as the snow grain-size and density primarily control the backscatter on SAR images over temperate glaciers this can mask changes due to the glacier mass balance, and as such some of the variance of the change in SAR backscatter are caused by the metamorphism of snow and not a change in mass balance. The TSL measured on SAR images can therefore not be used to determine the mass balance of a temperate glacier, but as a proxy that can be correlated well with the net- or total mass balance (Brown et al., 2005).

It is difficult to recommend one method of mapping the TSL over another, for although the Landsat and February ASAR measurements contained the smallest range of values (22% and 24%) they also reflected the fluctuations in the glacier mass balance the least (Figure 64). It seems that Landsat is advantageous due to the longer time series, and while the error is less than the ASAR

measurements it is proportionally higher when the pixel size is considered. It would seem that ideally SAR imagery of a higher resolution should be used to map the TSL, both ENVISAT ASAR in image mode or data from ERS 1/ERS 2 are potentially good options, with spatial pixel sizes comparable to that of Landsat (Celentano, 2006).

6.6. Glacier Volume measurements

As with the glacier area (*5.1*) between 1937 and 2007 the greatest losses in glacier surface elevation and hence glacier volume were on the western sides of Nordfonna. Midtfonna lost the most mass from the south and the west while Sørfonna lost mass generally from all its margins, although the western side appears to have lost slightly more elevation than the eastern, this is especially prominent over the last two decades where western Folgefonna has melted away more. It is possible that the differences between the western and eastern sides (*6.3*) of the glacier are partially responsible for the irregular change at difference elevations seen in Figure 35. The higher elevated southern portion of Sørfonna seems to be more stable than the northern third. This is in agreement with Elvehøy (1998).

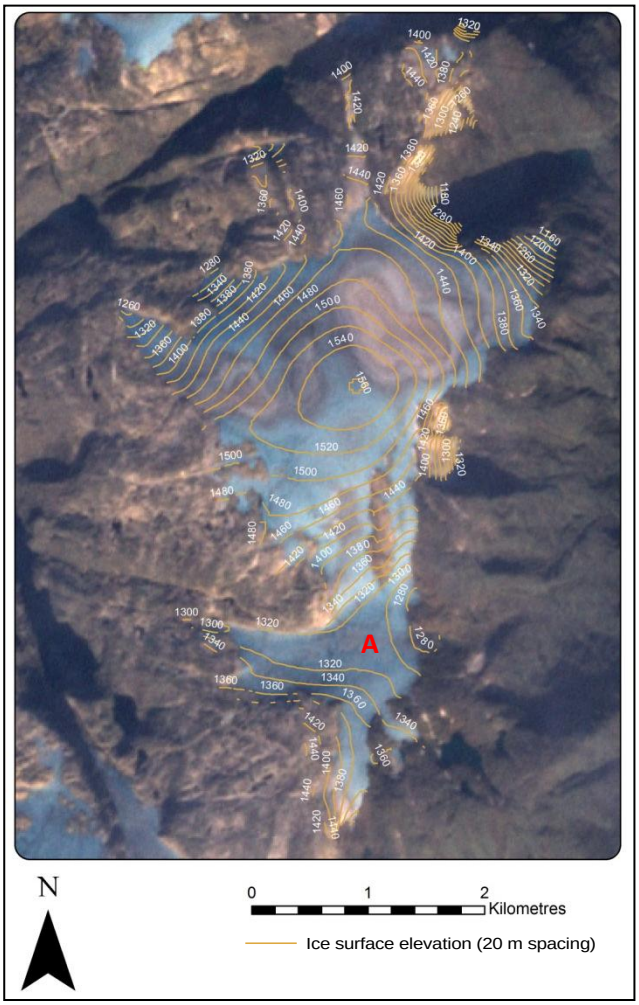

Figure 77: Elevation of Midtfonna in 2007 (Landsat image is from 2011). The majority of ice lost on Midtfonna was from around a plateau feature, marked A on the map.

Figure 35 shows how the surface elevation of Folgefonna varied with height between 1999 and 2007 and 1999 and 2010. Some errors must be present as the 2010 data depicts the ice at a height of ~1400 m having gained in elevation, while in both cases surface downwasting of over 80 m at ~700 m.a.s.l. over such a short time period seems a little extreme baring in mind that Kjøllmoen et al. (2008) found the elevation to have not changed more than 50 m between 1997 and 2007. Nevertheless despite some noise for both years the trend is similar; generally Folgefonna lost the most elevation at lower heights, while the higher interiors of the glacier were more stable. This is what would be expected, with warmer temperatures at lower elevations increasing the rate of ablation.

Between 1987 and 2007 the greatest mass lost on Midtfonna occurred around a flat plateau feature at the south of the ice mass (Figure 77). The ice surface elevation in this area is the lowest

on the glacier, and the area is surrounded by short steep ice margins that are likely to respond quickly to a change in the climate (Nesje, 2005, Raper and Braithwaite, 2009).

An erroneous result arises between 1999 and 2007; much of Nordfonna appears to have gained large amounts of mass, increasing in elevation by at least 20 m (Figure 39). Such an expansion is extremely unlikely in the glacier interior. From Figure 34 this increase in volume in Nordfonna can be seen to be clearly proportionally larger than the increases in both Midtfonna and Sørfonna. It is strange that firstly the overestimation would be so acute on Nordfonna, yet neither of the other ice masses, and secondly both of these DEMs compared (1999 SRTM DEM and 2007 LiDAR DEM) were generated by NASA and NVE respectively and both have supposed high levels of accuracy.

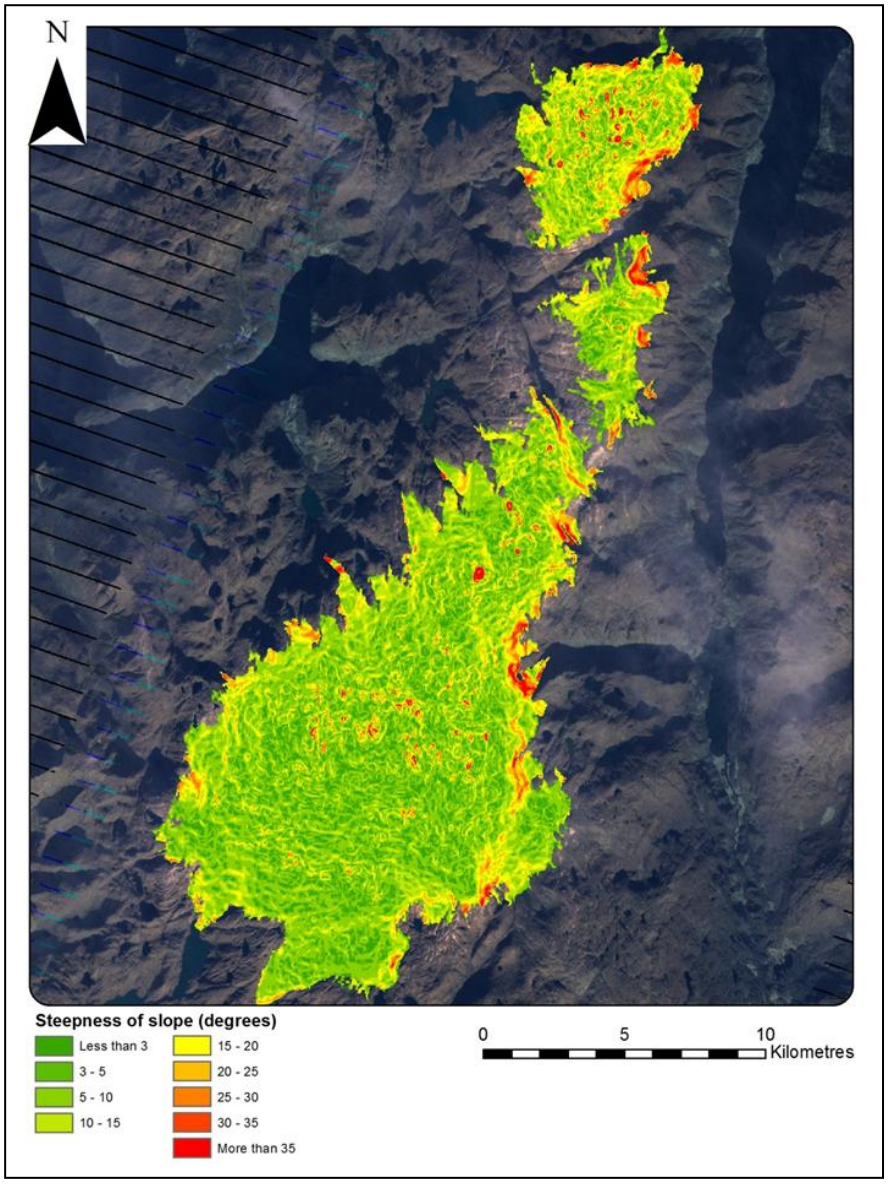

Figure 78: The steepness of the ice surface in 1999 on Folgefonna. The areas of steep topography coincide with the areas that unreasonale elevation results arise in the LiDAR measurements. This is taken to be an additional source of error.

The error must arise therefore from either the 1999 NASA DEM, the 2007 NVE DEM or the methodology used in this investigation. Førre (2012) used identical methods in determining the glacier volume of Nordfonna using the same 2007 LiDAR DEM and the same bed topography data and found a very similar glacier volume, therefore the error must lie in one of the DEMs. Each downloadable segment of the NASA SRTM 1999 DEM covers a very broad area and indeed all three ice masses were covered in one segment. Therefore one would assume the error would lie in the 2007 DEM, however the remaining volume comparison on Nordfonna uses the 2007 DEM and the results seem perfectly reasonable so it is not obvious where the error derives from.

Western Sørfonna can be quite clearly seen to have lost the most mass, when compared between 1987 and 2007 (Figure 38), while small ice mass gains have been made in the very interior of Sørfonna. A striking loss in glacier mass appears to occur in the south-east of Sørfonna and on Buerbreen, these losses occur in areas of steep and complicated topography (Figure 78) where the InSAR sensor used in generating the 1999 SRTM DEM copes well but as mentioned earlier (*6.1.2.3*) the 2007 LiDAR DEM struggles. Similar areas of steep topography (more than ~25°) on Nordfonna and Midtfonna can also be seen to correspond to areas of an apparent rapid ice mass, the proportion of this mass loss that is due to steeper glaciers having shorter lag times or due to the 2007 DEM underestimating the ice surface elevation cannot be speculated upon.

6.7. Comparison with the glacier volume findings of others

As part of a Statkraft investigation Kjøllmoen et al. (2008) compared a DEM derived from a set of aerial photo acquired in 1997 with the 2007 LiDAR DEM. When the distribution of glacier ablation between 1937 and 2010 are compared with Statkraft's data the same patterns are evident. The south-west of Nordfonna as well as Jordalsbreen in the north-west, and the area around Dettebreen in the south-east have lost the most volume.

Similarly the Statkraft investigation is in agreement with this investigation that Midtfonna lost the most ice volume from the flat plateau in the south (Figure 37), as well as pockets of ablation just to the south of the ice peak, and to the north east and north west. In contrast the Statkraft data shows a large decrease in surface elevation along most of western Midtfonna which is only shown in patches in this investigation; however such discrepancies can be explained by the 2 year gap between the 1997 aerial photographs used by Statfraft and the 1999 SRTM DEM used in this investigation. Glacier area has been shown to have shrunk after 1994 and as glacier volume is more responsive than area it can be assumed that the surface elevation in 1999 was lower than in 1997.

Both the Statkraft investigation and this investigations' data are also in agreement that as one would expect the lower lying margins of Sørfonna lost the most mass. However the Statkraft results do not agree with this investigation that the central parts of Sørfonna gained a small amount of mass. This could perhaps be explained by Figure 38 depicting changes from 1987, while the Statkraft data is calculated from 1997. Given that we know that Folgefonna gained mass between the late 1980s and ~2000 it would be expected that the central parts of the glacier would be higher in 2007 than in 1987.

Smith-Mayer and Trede (1996) showed that the Blomsterkarbreen, at the very south of Sørfonna (location shown in Figure 1) gained a considerable amount of mass between 1959 and 1995; rising 20 m in elevation, while Møsevassbreen, to the immediate west of Blomsterkarbreen lowered by 70 m in some places. Sauabreen to the immediate east of Blomsterkarbreen only marginally gained mass. Unfortunately the very south of Sørfonna is not included on the 1937 topographic

map so this investigation's results cannot be directly compared, although it can be seen that between 1987 and 2007, the west (Møsevassbreen) lost considerably more mass than the higher elevated Blomsterkarbreen (Figure 38). Similarly Elvehøy (1998) claims how the southern portion of Sørfonna has a higher winter mass balance than the northern part of Sørfonna, Midtfonna and Nordfonna while the summer balance is similar across all of Folgefonna. This is not completely straightforward to assess with this investigation's data, however there is a clear area along the north of Sørfonna which was a higher rate of elevation loss than southern Sørfonna.

6.8 Accuracy of Automatic Glacier Area Techniques

The outlines used in the results of this investigation were manually delineated although the automatic band ratio outlines were examined as part of quality checking in an attempt to remove any subjectivity. Several authors however claim automatic band ratio outlines alone are up to 96% accurate in tested areas (Albert, 2002, Paul, 2001). It is interesting to assess their capability in a more maritime setting where seasonal snows and overcast weather are fairly common.

The accuracies of these automatic spectral band ratio methods (TM3/TM5 and TM4/TM5) compared with the manually delineated areas were evaluated in *5.4.2.5*. Both methods were found to underestimate the volume by significant amounts because of spectral difficulties such as cloud, seasonal snow and areas cast in shadow. Such spectral similarities can be overcome by a human analyst but the band ratio methods can only "see" pixels in terms of their pixel value.

The initial Landsat images from 1984 to 1988 were plagued by partial cloud cover explaining the sizable underestimations made by the automated methods. In 1984 the TM4/TM5 and TM3/TM5 methods underestimated the area of Nordfonna by 53% and 84% respectively; this disparity was reduced to 7% for each technique in

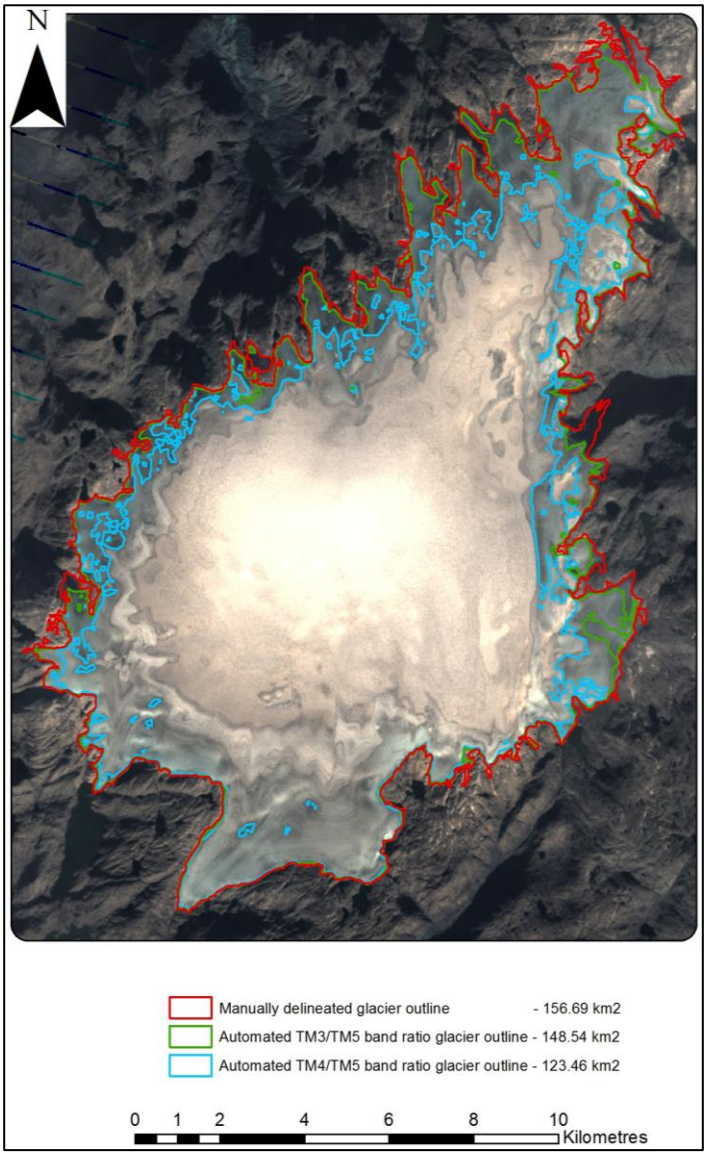

Figure 79: Comparison between the manually delineated glacier outline of Sørfonna, with the automated TM3/TM5 and TM4/TM5 band ratioing method for the 13th August 2011. Spectral combination 3,2,1. Even under optimum conditions a slight haze is enough to disrupt the automatic delineation methods.

1991. Seasonal snow in 1994 then inflated all the ice area estimates; the TM4/TM5 method seems especially susceptible to this giving overestimates in the range of 6% to 27%, while TM3/TM5 overestimated by only 0.2% - 10%. The three methods are roughly in agreement in 1999, although the image edge cuts through the very south-west of Sørfonna causing colour irregularities that cause the automatic methods to falter somewhat. Seasonal snows were very much still rife in the July 2000 image explaining the profuse overestimations, again the TM3/TM5 method responded to this better, showing a mean exaggeration of all ice masses of 28%, compared with 58% from TM4/TM5. Between 2000 and 2003 errors were considerably less, even allowing three serious underestimates due to thick cloud in 2001, 2002 and 2003 the mean deviation during this time for TM3/TM5 and TM4/TM5 was 17% and 33%, although if the three especially prominent errors are excluded this falls to 9% and 12%.

The two automated methods also perform more accurately between 2004 and 2008 with mean deviations of 8% for TM3/5 and 11% for TM4/TM5. The deviation widened post-2008 due to both some cloud on parts of the images, and also some images badly affected by the SLC malfunction mentioned earlier (*3.2.1*). A thin hazy cloud in 2011 distorted the automatic delineation over Nordfonna and especially Midtfonna, yet this didn't hamper manual delineation in the slightest. Figure 79 shows how even under optical conditions the TM4/TM5 method frequently underestimates the glacier area, the TM3/TM5 method on the other hand is considerably more accurate.

From this analysis it is clear that out of the two automatic band ratios the TM3/TM5 is more preferable having on average 2. 5X less error. However neither of the methods matched the accuracies claimed by other authors. As both methods for the most part underestimated the glacier areas, it is possible that the threshold values selected needed to be adjusted to incorporate a wider range of pixels into each area, but with such a wide range of over- and underestimations changing the pixel threshold value can only help so far. It seems that other than under optimal conditions these methods cannot be relied upon for accurate results for maritime glaciers.

6.9. Applicability of remote sensing in long term glacier change investigations in maritime environments

From this investigation it has become clear that there are clear advantages and disadvantages to the use of remote sensing in glaciological investigations in a maritime setting such as Western Norway. A large amount of the satellite images available were completely unusable due to excessive cloud cover, dramatically reducing the amount of data available. In addition to this the time window that images can be useful for analysis is quite limited (late July to the end of September/start of October) with persisting or fresh snows possible for much of this time span. However 26 Landsat images with good conditions were available over a time span of 35 years, 19 of which were from 2000 onwards. This is a more than adequate dataset, even with some images tainted with small amounts of cloud, cast shadow and seasonal snows.

The number of glacier volume estimates is however not so satisfactory. This is mainly because of a lack of DEMs available. One of the main advantages of remote sensing over traditional methods is that the surface elevation and therefore loss of mass over the entire ice mass can be visualised. This has certainly been achieved but it would have been interesting with more data points to see how the glacier volume had varied in relation to the glacier area on an annual basis. It could have been especially worthwhile to analyse how glacier volume changed in relation to glacier area during the *Briksdalsbre event*.

6.10. Implications for the economy of Western Norway

Folgefonna's runoff is utilised to generate electricity at different locations around the glacier. Given Folgefonna's recent rate of glacier retreat a major concern is that due to the subglacial topography the meltwater could be re-routed and re-distributed away from the areas currently harnessing the water (Bakke et al., 2011). Folgefonna is also important for tourism in western Norway, with summer skiing, glacier hiking and climbing popular. Between the 1930s and 1960s glaciers throughout Norway were retreating, during this time the interest for glacier tourism on Jostedalsbreen dramatically fell (Aall et al., 2005). Given the current state of Folgefonna it is likely that both the hydro-power production and the glacier tourism industry will be adversely affected in the future.

6.11. Wider context considerations

The trends observed in Folgefonna shall now be compared with regional trends across Scandinavia, a wider comparison with glaciers in Iceland and in the European Alps, as well with trends occurring further afield in the northern hemisphere in Canada and Alaska to assess how Folgefonna compared with a wider perspective of ice masses.

These locations were considered for a number of reasons. On a practical note these regions have a good amount of in-situ mass balance and length variation data (Zemp et al., 2008). A comparison with glaciers in tropical or polar areas would not be meaningful, due to differences in the drivers of such glaciers and in the magnitude of the regional climate. It was therefore decided that the largest mid-latitude Northern Hemisphere glaciated areas would be compared, these glaciers are known to respond to some of the same drivers as Folgefonna. Coastal Canadian glaciers for example, as in Scandinavia, known to be traditionally driven primarily by the winter precipitation.

6.11.1. Scandinavian glacier trends

In general Scandinavian glaciers underwent a mild retreat towards the end of the nineteenth century, which then accelerated with intermittent phases of glacier advance around 1910, 1930, the mid to late 1970s and the 1990s. More maritime glaciers gained mass after the 1960s while continental glaciers have maintained a sustained retreat (Figure 80).

Since 2001 all Scandinavian glaciers have been losing mass (Zemp, 2008, Andreassen et al., 2004, Orlove et al., 2008). In particular glaciers across Norway underwent a large retreat in 2006 (Andreassen et al., 2007), although higher winter accumulations actually caused some of the coastal glaciers to between 2005 and 2008 (NRK, 2008).

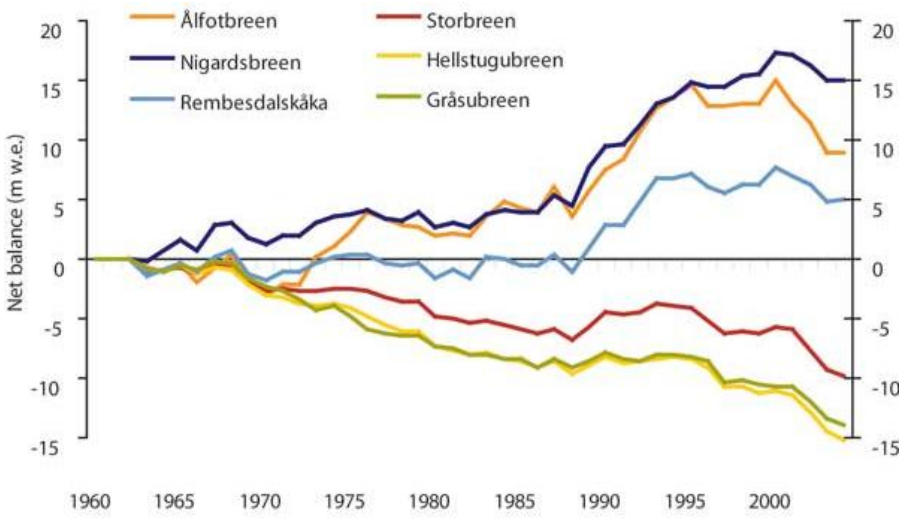

Figure 80: Cumulative mass balance measurements for six Norwegian glaciers, the continental glaciers (Storbreen, Hellstugubreen and Gråsubreen) have undergone a near continuous retreat since the 1960s, while the continental glaciers have had periods of glacier advance, especially during the 1990s (Andreassen et al., 2005a). Folgefonna can therefore be assumed to be a typical maritime Scandinavian glacier

The remote sensing data on Folgefonna is sparse and the advance centred around 1910 is undetectable, although it is recognisable on the lichen reconstructions conducted by Furdal (2010) (Figure 76).The 1930 advance is perhaps recognisable as a reduction in the rate of retreat on Nordfonna and Midtfonna and again is evident in the lichen reconstructions. The 1970s and 1990s advances, the subsequent rapid retreat and the short-lived advance between 2005 and 2008 however are clearly evident on all three segments of Folgefonna with the remotely sensed data. From this comparison it has become clear that there is a large contrast between maritime and continental glaciers in Scandinavia (Figure 80), and that Folgefonna is a typical maritime Scandinavian glacier.

6.11.2. Broader European trends

6.11.2.1. Icelandic glacier trends

Icelandic glaciers started retreating after their LIA peak around the end of the 1800s (Aðalgeirsdóttir et al., 2011, McKinzey et al., 2005), approximately the same time that Folgefonna has been reported to (Nussbaumer et al., 2011). Generally throughout the twentieth century Icelandic glaciers have undergone a steady retreat (Zemp, 2008, Hall et al., 1992), which was punctuated by a period of advance between 1970 and the late-1980s/early 1990s (Sigurðsson et al., 2007), followed by an accelerating rate of mass loss. Changes in Icelandic glaciers have also been found to relate to the NAO index (Bradwell et al., 2006). Since 2000 all Icelandic non-surging glaciers have been retreating (Magnússon et al., 2010). This corresponds broadly to the trends of gentle retreat, subsequent advances in the 1970s and 1980s and more recent rapid shrinkage seen on Folgefonna.

6.11.2.2. European Alps glacier trends

Similar to the other glaciated regions of Europe and to Folgefonna, the glaciers in the European Alps reached their LIA maxima towards the end of the nineteenth century and subsequently began to retreat (Zemp, 2008). Since the LIA the majority of the Alp's glaciers have continuously retreated, although some smaller mountain glaciers have shown small advances in the 1890s, 1920s and 1970-80s (Zemp et al., 2008). The first two of these events correspond roughly with the lichen reconstructions of Folgefonna by Furdal (2010), while the 1970-1980s advance is evident in the remotely sensed area trend of all three Folgefonna ice masses (Figure 16, Figure 17, Figure 18). Wanner et al. (2005) (in Zemp et al. (2008)) states how these periods of advance corresponded to periods of negative NAO index values, bringing a more maritime climate of less sunshine and more precipitation to the Alps (Schöner et al., 2000). This is the complete opposite to what has been reported for Folgefonna and maritime Scandinavian glaciers (Nesje et al., 2000, Nesje et al., 2008b).

Since 1850 the Alps have lost approximately 50% of their ice mass (Zemp et al., 2008), this is comparable to the 45% volume loss of Midtfonna, but much more than the 37% and 10% lost from Nordfonna and Sørfonna. Perhaps this reflects the size of glaciers in the Alps compared with Scandinavian plateau glaciers such as Folgefonna. The summer of 2003 saw a considerable ice loss of nearly seven times the 1967 – 2000 average in the Alps (Zemp et al., 2008), while Folgefonna also saw a drop in glacial area in this year the reduction was not nearly as severe.

6.11.2.3. Summary of trends in Folgefonna in a European Context

In summary Folgefonna exhibits some levels of coherence with other glaciated regions in Europe, Folgefonna attained its LIA maxima at approximately the same time as glaciers in the rest of Scandinavia, Iceland and the European Alps. Since then Folgefonna, Scandinavian glaciers and to an extent Icelandic glaciers have undergone periods of gentle retreat, while gaining significant amounts of mass in the 1970s, 1970s and 1980s/1990s. Glaciers in the European Alps on the other hand have been retreating rapidly with some smaller ice also advancing in the 1920s and 1970s. Within the last two decades Scandinavian glaciers have deviated from the wider trend of glacier retreat with substantial glacier advances during the 1990s and again in the mid-2000s. However since the start of the twenty-first century glaciers across Europe have been retreating and shrinking at an accelerated rate.

6.11.3. Broader Global trends

Given that atmospheric and oceanic circulations link Europe with other glaciated regions in the Northern Hemisphere and indeed worldwide it is interesting to place the trends seen in Folgefonna in an even wider context. Folgefonna shall now be compared with the trends of glaciers seen in Alaska and in the Canadian Rocky Mountains.

6.11.3.1. Alaskan glacier trends

As a region Alaska has seen some of the largest changes in climate on the planet so far. Mean temperatures have risen by 2°C (Molnia, 2007), while minimum winter temperatures in the interior of the Juneau Icefield have increased from -30°C to -10°C over the last 30 years (Miller, 2008). This has caused the ablation season to be extended by a month between 1988 and 1998 (Criscitiello et al., 2010).

Alaskan glaciers attained their LIA maxima at different times. The majority reached their maximum size in the 1700s and 1800s although in the northeast Brooks Range the maxima was reached as early as the late 1400s (Zemp, 2008). In either case this was much earlier than Folgefonna and maritime Scandinavia.

There is a range of responses to climate for Alaskan glaciers. The majority of Alaskan ice masses have generally retreated since the late 1800s or the LIA maxima (Molnia, 2007, Motyka et al., 2003). During the 1970s and 1980s some maritime glaciers such as Wolverine Glacier gained mass which has been put down to fluctuations in the Pacific Decadal Oscillation (PDO), a decadal scale climate shift similar to the NAO (Josberger et al., 2009) which brought increased winter precipitation to the region. This expansion is a parallel to the Scandinavian glacier advances such as Folgefonna in the 1990s caused by the NAO.

In recent decades however those glaciers retreating have had their rate of mass loss accelerate, which Josberger et al. (2007) have linked to warmer and drier summers. Molnia (2007) states that nearly all Alaskan glaciers that extend below ~1500 m are currently retreating or thinning, while less than 2% of Alaskan glaciers continue to expand; and those that do are mainly tidewater glaciers or have high elevation accumulation areas. One example of these is Taku glacier, which due to its size, height and incredible depth (over 1400 m in places (Nolan and Motkya, 1995)) has continuously advanced since measurements began in 1946 (Pelto et al., 2008). Although Taku glacier continues to advance, its mass balance between 1988 and 2005 was slightly negative, and the glacier has thinned. It is expected that this state will have to be sustained for another 20 years before the changes are manifested in the glacier terminus (Pelto et al., 2008).

6.11.3.2. Canadian Rocky glaciers trend

Luckman (2000) states that for much of the Canadian Rockies the greatest ice cover was around the mid-1800s which roughly synchronises with the LIA maxima for Folgefonna and Europe as a whole, although some regions reached their LIA maxima earlier between the 1690s–1720s (Koch et al., 2009). It is estimated that between the LIA maxima and 1987/88 the glaciers of Garibaldi Park, Southern British Columbia lost 41% of their volume, which is comparable to the 37% Nordfonna lost over the same period, while the proportions lost from Midtfonna (45%) and Sørfonna (10%) diverge from this result. Between 1987/88 and 2005 the Garibaldi Park lost 18% of

its ice area (Koch et al., 2009), much more than the 8% total reduction across all of Folgefonna during this time.

Following the LIA, glaciers in Western Canada underwent a steady retreat interrupted by advances in the 1920s 1960s and 1980s and then an accelerated and uninterrupted retreat since the 1990s. Similar to Scandinavian maritime glaciers, maritime Canadian glaciers are controlled by changes in winter precipitation during periods of glacier advance, while increased summer temperatures can force glacier retreats (Koch et al., 2009, Josberger et al., 2007).

6.11. 3.3. Summary of trends in Folgefonna in a Global Context

There is a high level of similarity between the driving forces of Scandinavian maritime glaciers such as Folgefonna and glaciers in the Canadian Rockies, especially those nearer the coast. Some level of synchronicity also exists with Alaskan glaciers. Scandinavian, Canadian Rocky and some maritime Alaskan glaciers have shown to be controlled by changes in the winter precipitation brought on by a shift in the values of the NAO index and the PDO index respectively. However many periods of glacier retreat in Europe and North America also correspond to periods of growth in the Andes, New Zealand, the Himalayas, the Pyrenees and the Antarctic Peninsula. This suggests that a global forcing may be responsible (Kaser, 1999, Koch et al., 2009). Indeed the times of most rapid glacier retreat (1920 – 1940 and after 1975) have corresponded to higher global temperatures (Figure 81), while periods of glacier advance worldwide occur in-between these warmer decades, especially around the 1960s and 1970s (Koch et al., 2009).

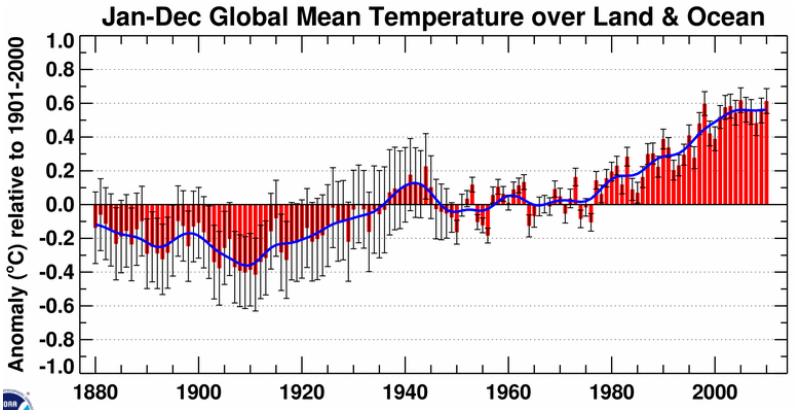

Figure 81: Global combined land and ocean temperature anomalies between 1880 and 2010 (National Oceanic and Atmospheric Administration, 2011). Global glacier fluctuations correspond to the air temperature trend. Glaciers retreated in the 1930s and 1940s at a time of higher global temperatures, while the 1960s and 1970s saw many glaciers worldwide advance, when global temperatures were cooler.

Due to the sheer size and depth of some Alaskan glaciers it is not surprising that the glacier trends do not align with the relatively fast responding ice-masses of Scandinavia and that some glaciers continue to advance. The last decade however has broadly seen a trend of accelerated glacier retreat globally, including the regions of Scandinavia, Alaska and the Canadian Rockies.

6.11.4. Comparison with global sea level trends

Given that more than a quarter of the projected rise in sea level by 2050 is estimated to be from the melting of small, temperature mountain glaciers (Raper and Braithwaite, 2006), it is interesting to assess whether the rates of glacier melting on Folgefonna have been keeping pace with the rate of change of global sea level.

Brest, France, has one of the longest records for sea level anywhere in the world. Data from 1950 to 2010 were downloaded from the *Permanent Service for Mean Sea Level* (PSMSL) website. Ideally numerous records would be combined to avoid local tectonic biases such as done by Jevrejeva et al. (2008), however for simplicity reasons the Brest record was used by itself and compared with the glacier area record. As Midtfonna has been shown to react far more than Nordfonna, and Sørfonna cannot be fully analysed back to 1860 due to the limitations of the topographic maps (4.2.1), the sea level record was compared with the glacier area of Nordfonna (Figure 82).

For the portion of the glacier record that has a suitably dense enough number of data points it is clear that in general during times that Folgefonna was advancing (*b,d,*), sea levels either fell, or the rate of increase was reduced. Conversely during times of glacier retreat (*a,d*) the rate of sea level rise increased. A noticeable drop and subsequent rise is sea level also corresponds to the mid-2000s short-lived glacier advance and subsequent retreat. Obviously Folgefonna's contribution to sea level rise is microscopic, given that for every 361 km^3 of water added to the oceans results in a 1 mm rise in global sea level (Dyurgerov et al., 2002); all of Nordfonna (1.84 km^3 of ice in 2010) would contribute less than half a hundredth of a millimetre. However as much of the planets glaciers seem to react in rough synchronisation (*6.1.2*) it can be said that when Folgefonna is contributing meltwater to the oceans, so are a large number of other ice masses globally.

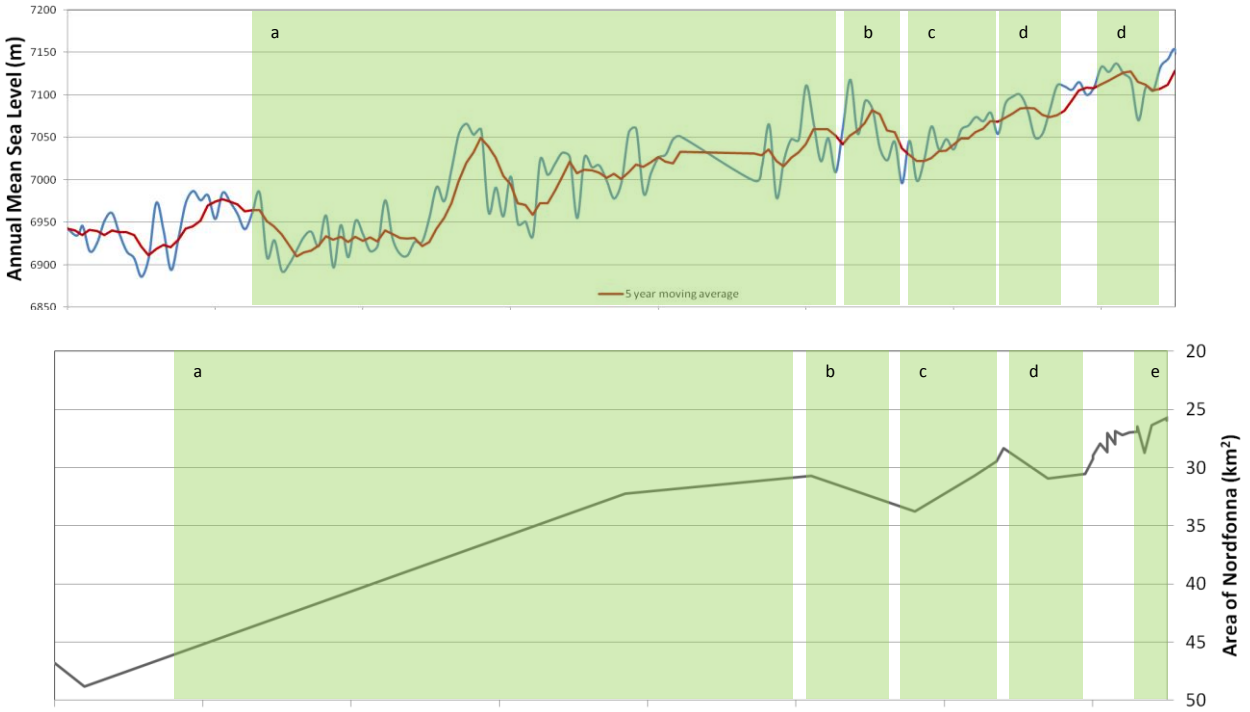

Figure 82: A comparison between the annual mean sea level measured in Brest, France, and the ice covered area of Nordfonna between 1850 and 2010. Note that for comparability reasons the vertical axis of the glacier area has been inversed. Periods of assumed correlation (a-e) are highlighted. Note also that as there are multiple data points for the years 2000, 2002, 2006 and 2010 there is some noise for these years.

6.11.5. Summary: Changes of Folgefonna in a wider context

To summarise, Folgefonna can be considered a typical Scandinavian glacier, showing a high correspondence to other glaciers located in Western Norway. Generally Folgefonna reacted in phase with glaciers throughout Europe, while glaciers in the Canadian Rockies and to an extent Alaska were analogous to this trend too. Glaciers in other regions worldwide also exhibit a level of parallelism with these trends, mostly showing a general reduction in area following the LIA with advances in the 1960s and 1970s and noticeably sharp retreats in the 1920s, 1940s and the last two decades. Scandinavia and New Zealand glaciers are the most prominent deviations from these trends, both showing strong glacier advances in the 1990s caused by increased westerly atmospheric circulation supplying abundant winter precipitation (Chinn et al., 2005). Evidence of this worldwide cohesion can be found in the sea level record (*6.12.4*). Folgefonna could obviously make no noticeable difference to sea level on its own, however as many glaciers worldwide have reacted in synchronisation a relationship appears between the times Folgefonna was advancing or retreating, and the fall and rise of global sea level.

98% of glaciers worldwide are now retreating (Hambrey et al., 2010), with a minority of glaciers with high-elevation accumulation zones still advancing in Alaska, New Zealand and Patagonia (Zemp, 2008, NSF, 2009). In Norway as of 2011 Bøyabreen in Jostendalbreen and Steindalsbreen in Lyngen were the only glaciers to advance compared with their 2010 positions, while Koppangsbreen in Lyngen and Austerdalsbreen in Jotunheimen were stationary (NVE, 2011b). This compared with 3 advancing (Briksdalsbreen, Svelgjabreen (Sørfonna) and

Corneliussenbreen near Svartisen) and one stationary glacier in 2010 (Kjøllmoen, 2011) . Other than a small scale advance in the mid-2000s Folgefonna's glacial history over the last 20 years has mirrored that of the majority of the planet's ice masses of an accelerated glacier retreat.

6.12. Predictions for the future

In terms of the immediate future it has already been shown that the different glacier parameters lag behind the forcing climate and also slightly behind the *in-situ* measurements (*5.4.1.5*). The very end of the summer season temperature trends shows how after a period of warmer than usual summers (especially 2002, 2006 and 2008) the previous three summers (2009, 2010 and 2011) have not been as warm; with 2010 being colder than the 1960 – 2010 average (Figure 83). The *in-situ* mass balance data from Sørfonna similarly shows the rate of mass loss decreasing from 2010 to 2011; it can therefore be assumed that after the approximate 3-6 year lag time Folgefonna's rate of area shrinkage will also undergo a brief reduction.

From Figure 83 it can be seen how in-between the two warmest summers on record (2006 and 2008), the summer of 2007 was also markedly colder than average, while a similar dip happened with colder summers in 2000 and 2001. It is therefore extremely likely that after an interlude of one or two milder summers the temperature will continue to steadily rise.

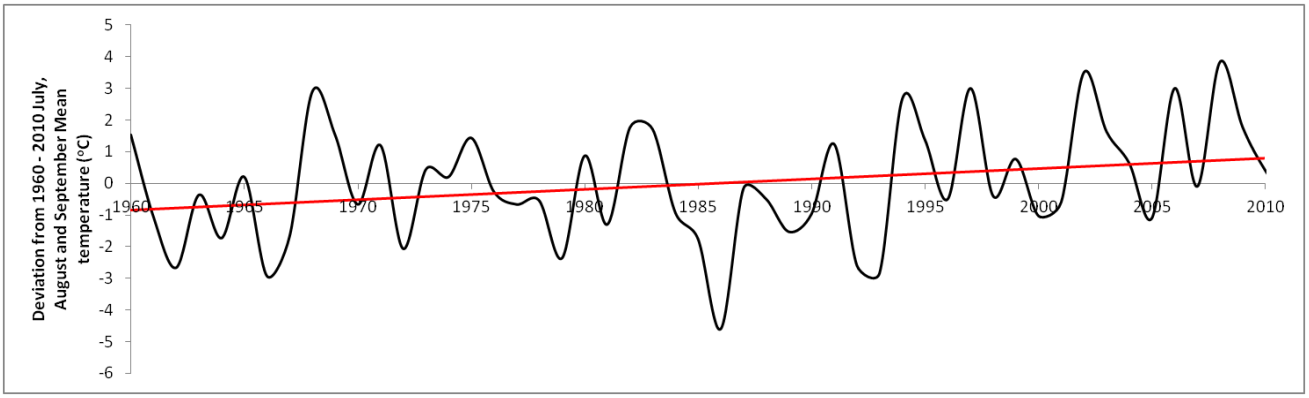

Figure 83: Deviation from the 1960 - 2010 average temperature from Bergen Flesland. The linear trendline (red) shows a clear increase in temperatures over this time period. Data downloaded from eklima.met.no.

Western Norway is expected to warm less than the rest of the country, with the Folgefonna area potentially warming by up to 3.5°C by 2100 (Figure 84). Much of this warming is predicted to occur in the winter, therefore shortening the ablation season. For example the number of days with temperatures below freezing in Voss, to the north of Folgefonna, is expected to decrease from 108 (mean 1981 - 2000) to 82 (2021 – 2050) (Sygna et al., 2009).

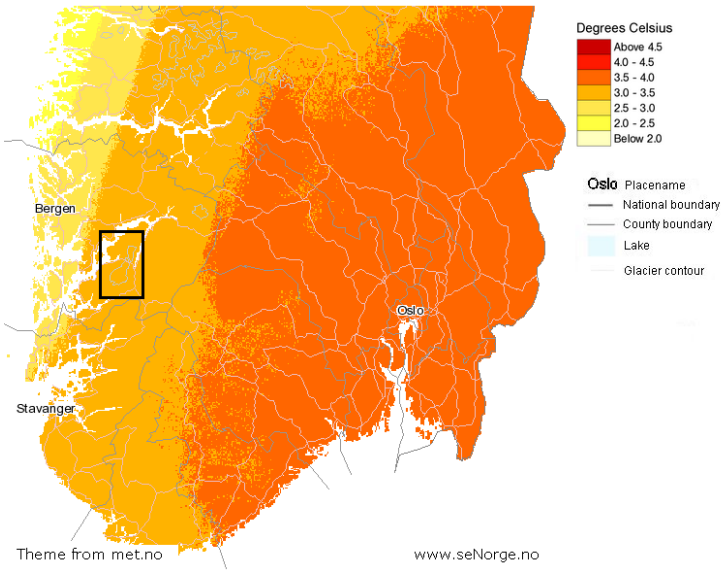

Figure 84: The predicted change in annual temperature across Southern Norway from the 1961 - 1990 average to the 2021-2100 average. These predictions assume the IPCC A2 prediction scenario, assumed by some to be the realistic emissions scenario (Select Committee on Economic Affairs Minutes of Evidence, 2005) Folgefonna is highlighted in the black rectangle (senorge.no, 2012).

The amount of winter precipitation is predicted to also increase, but not enough to compensate for this warming (Nesje et al., 2008a). This is expected to raise the ELA of Norwegian glaciers by 260 ± 50 m on average and cause a reduction in total glacier area across Norway by 34%. Based on current trends the TSL is expected to be above Folgefonna by between 2020 and 2030 (Figure 41). This will cause Folgefonna to enter a phase of accelerated ablation. Similarly Laumann and Nesje (2009) predict that the warming climate could see outlet glaciers such as Brikdalsbreen retreat up to 5 km by 2085. While the sheer size of Folgefonna means that it is not going to completely disappear anytime soon, the glacier is likely to enter a phase where the entire glacier surface ablates each summer which would dramatically increase the net balance of the glacier, and possible put in into a regime that is hard to recover from.

7. Conclusion

This study used a variety of remotely sensed sources to assess the evolution of Folgefonna glacier from 1860 to present day.

Based on the research questions originally set out in *1.5*, the following conclusions can be drawn:

1. Since the LIA maxima Folgefonna has been retreating with noticeable advances in the 1890s, 1920, 1960s/1970s and 1990s. A small scale advance also occurred between 2005 and 2008. The three latest advances, along with the accelerated glacier retreat from 2000 are all clearly visible in the remotely sensed data. In 2011 Nord-, Midt- and Sørfonna measured 24.8 km^2, 9.1 km^2 and 156.7 km^2 respectively, a reduction of 47%, 68% and 20% compared with the LIA maxima size in 1860.

2. A similar trend can be seen in the glacier volume record. All of Folgefonna downwasted from 1937, Nordfonna and Midtfonna grew between 1999 and 2002, while Sørfonna grew between 2002 and 2007. Since 2007 the rate of downwasting has dramatically accelerated. In 2010 Nordfonna measured 1.84 km^3 a reduction by 43.2% since 1937. If planar bedrock surfaces are assumed beneath Midtfonna and Sørfonna it can be estimated Midtfonna lost 1.3km^3 (50.3%) over this time-period, while Sørfonna lost 7.6 km^3 (18.3%) between 1987 and 2010. The portion of Sørfonna visible on the 1937 map lost 21.1% of its volume between 1937 and 2010.

3. Folgefonna has traditionally been driven by the amount of winter precipitation, with the ablation season temperature acting only to amplify or dampen changes due to the precipitation. In particular the advances in the 1990s and mid-2000s were caused predominantly by an abundance of winter precipitation. However since 2000 the rising summer temperature has become sufficient to melt any surplus accumulation making the temperature become the dominant driving force. Winter precipitation still is influential – for example both the mid-2000s advance and the dramatic decrease in area in 2009 correlate with changes in precipitation. The NAO still appears to correlate fairly well still with the glacier area record up until present day. There is a scarcity of volume data points, however generally the same trend is scene in both the glacier area and volume records so it is assumed the driving forces are equally significant to both parameters.

4. The TSL was measured to fall from 1986 to 1991, thereafter it rose consistently, the rate of rise increased from 1999 onwards. According to Landsat by the start of September 2010 the TSL lay at an altitude of 1535 m.a.sl., a total rise of 86.6 m since 1984. The coarser ENVISAT ASAR images detected a steeper rise in TSL by between 1.5X and 2.2X between 2005 and 2010 than depicted on the Landsat images, however all the data agrees that at the end of the 2010 ablation season the TSL lay at between 1527 and 1535 m. Despite sizable uncertainties in the measurements the TSL measurements have been found to correlate well with *in-situ* measurements of both ELA and

glacier mass balance, although fluctuations are not as noticeable. It is therefore inferred that the phenomenon measured is the firnline and not the TSL.

5. The glacier area measurements lag behind the winter precipitation by 3-6 years for Nordfonna, 2-3 years for Midtfonna and 2-3 years for Sørfonna. When the NAO is considered Nord-,Midt- and Sørfonna lagged behind by 3-5 years, 3-5 years and 4-5 years. Seasonal snow is blamed for making this lag time appear smaller than would be expected behind the winter precipitation. The TSL measurements can be seen to be much more direct at between 1-2 years, the scarcity of glacier volume makes it challenging to attain a lag time, however from the two lagtime measurements possible it appears that glacier volume responds quicker to the climatic forcing than the glacier area, but slower than the TSL. As would be expected the larger ice masses take a longer time to respond to the climate.

6. Despite a scarcity of data during the early part of the investigatory time period, the remotely sensed glacier area record can be said to correlate excellently with historical sources, in-situ mass balance data, and other work on Folgefonna glaciers conducted. A lack of data means that the 1920s advance and 1940s retreat observed in the lichen records and historical records are not resolvable in the remote sensing data, however there is a very high level of correspondence with in-situ mass balance data from 1962 onwards.

In reference therefore to the original research question (*1.5*) it can be deducted from this investigation that remote sensing is incredibly well suited for glaciological work. Remote sensing has permitted fluctuations in Folgefonna glacier to be observed over both short-term (annual) and long-term time scales (decadal).

In-situ mass balance data is very sparse both temporally and spatially over Folgefonna. Remote sensing has allowed data to be collected at a scale that would not have been possible using traditional glaciology methodologies, and allowed the entire glacial system to be assessed at a fraction of the cost. It is imperative that such glacier changes are analysed and quantified, as glaciers such as Folgefonna are important to local economies due to hydro-electric power, tourism and water resources.

The author is confident that given more time it would be possible to acquire more data to fill in the data gaps that exist. Additional aerial photographs and old maps could be used to assess the glacier area in the mid-20th century, while DEMs could be generated from SAR inferograms from ERS and ASAR data to visualise the volume change in Folgefonna over the last 20 years. Remote sensing would therefore be recommended as a principle method to be used in future glaciological studies, for use in regional or larger scale analyses, extracting records for glaciers where none exist, or for validating and error checking existing glacier records.

8. Future directions

Over a relatively short time-span remote sensing as a method in all kinds of scientific fields has grown exponentially to the level it is at now (Figure 85). It is likely that the near-future will see an increased availability of data as well as more powerful satellite sensors. The next Landsat sensor (*the Landsat Data Continuity Mission*) is expected to be launched in December 2012 while efforts to authorise the development of the next two satellites – Landsat 8 and 9 are in progress (Loveland and Dwyer, Wulder et al., 2012). However even without considering future developments in the technology of remote sensing there are still many ways that future investigations can be expanded upon, these shall now be discussed.

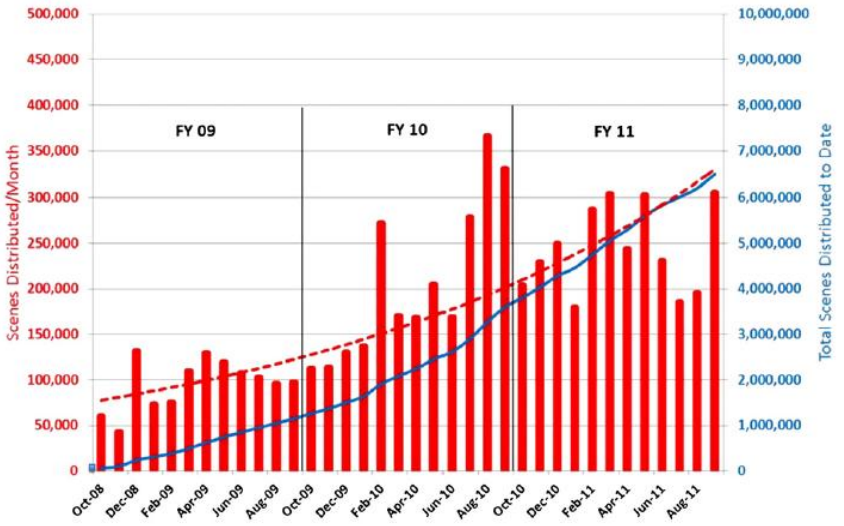

Figure 85: Landsat images are one of the most important remote sensing glaciology sources, since October 2008 the number of Landsat scenes downloaded has grown significantly (Wulder et al., 2012).

8.1. Assumptions about glacier density

As mentioned earlier; *Sorge's Law* - that the density of the glacier is a constant value of 917 kgm^{-3} throughout the glacier, was assumed for the glacier volume measurements. This is clearly not fully accurate and one minor improvement that could be made is assuming a different density for the accumulation and ablation areas. Some studies have assumed a density of 600 kgm^{-3} above the equilibrium line (Berthier et al., 2007, Gardelle et al., 2012). It would certainly be interesting to see what difference this alteration makes given that mass lost generally occurs in the ablation area, while any increase in mass occurs above the equilibrium line.

8.2. Development of glacier volume analysis

The glacier volume time series in this investigation to be visualised, but not with the resolution of the glacial area calculations. It would be beneficial for the understanding of Folgefonna's evolution to assess the change in volume using more DEMs. The 1962 aerial photographs could most likely be used to generate a DEM, similarly aerial photographs of Folgefonna exist from the 1937, 1951 and 1981 that could be utilised. Time constraints meant that only the 1962 aerial photos were chosen as they contained the most complete coverage of Folgefonna compared with the other images, and had an excellent image contrast over the glacier. In addition to this DEMs had already been generated from 1937 and 1987 so the additional aerial photography DEMs would not serve to fill in the data gaps. Also the 1937 images didn't contain any fiducial markers making orientation more complex (PCI-Geomatica, 2010). Although not free of charge, SPOT 5 data dates back to

2002 and are of a high resolution and can be used to generate DEMs with its stereoscopic bands. Although such data coincides with ASTER images it could certainly be beneficial to have more DEMs within the last decade to assess the downwasting Folgefonna has experienced.

An additional source of DEMs from the 1990s and onwards would be SAR microwave images. ERS1, ERS2 and ENVISAT ASAR images can be used to generate accurate DEMs using interferometry (Abdelfattah and Nicolas, 2002). Free access to such imagery is only available back to 2005, however if ERS1 and ERS2 data from the 1990s could be acquired it would allow Folgefonna's evolution during the Briksdalsbre event on an annual basis. Lastly, Cryosat II, a high-accuracy radar altimetry satellite has recently started transmitting data (Amos, 2012), which means that incredibly accurate (centimetre scale) DEMs can be generated in the near future.

8.3. Glacier velocity measurements

Unfortunately velocity measurements were not possible in this investigation due to both the data sources available, and the effects of cloud on the few suitable images. SPOT images are a definite solution to this problem, providing high resolution and frequent imagery (Debella-Gilo and Kääb, 2011), as is SAR Interferometry from ERS or ENVISAT ASAR images (Shiyong et al., 2011). If the rate of velocity change over time could be measured then it could give an idea of glacier area response times, given the speed that mass is transported from the accumulation area to the ablation area.

8.4. Closer integration between traditional glaciology methods and fieldwork with remote sensing

There are calls from some authors (Braithwaite, 2002, Andreassen, 1999) for a greater integration between the traditional glaciological methods and the remote sensing/geodetic methods of glaciology. This could make error analysis easier as well as being able to weigh the effects of certain assumptions used by each method. Cox and March (2004) for example found a disagreement of up to 6% between long term records of direct mass balance measurements and remotely sensed measurements based on the elevation change of Gulkana Glacier, Alaska.

However using both methods simultaneously is clearly not fully in alignment with the initiatives of GLIMS, nor does it make sense financially. It would seem more logical that once remote sensing has proven itself as a reliable and accurate methodology for glaciological investigations it can be used to help fill the large geographic lap in which little or no glacier records exist (Nesje and Matthews, 2012).

Instead it has been suggested that photographs are taken depicting the typical in-situ snow conditions from around the time of satellite image acquisition (Paul and Andreassen, 2009), this would allow more sound error estimations and make discrimination between glacier ice and seasonal snow more precise.

8.5. Mapping of LIA moraines using satellite images

Another possible expansion of the investigation would be to use a Landsat image draped over a DEM to delineate the LIA maximum extent moraines, such work was carried out in Jotunheimen (Baumann, 2010) and for South Tyrol, Italy (Knoll et al., 2009). Such maximum extents would not be able to be put into a time series without field based dating techniques, but the maximum extents of glaciers could nevertheless be a useful thing to know.

8.6. Mapping of Midtfonna and Sørfonna's subglacial topography

It would be intriguing to map the sub-glacial topography beneath Midtfonna and Sørfonna. Not only would this enable absolute volumes of ice to be calculated, it would allow the catchments of each outlet glacier to be mapped and the response times to therefore be estimated. The subglacial topography could also give an understanding of the stability of Folgefonna, and provide an insight into whether the topography is aiding or dampening the ice retreat. As far as the author knows to date only Nordfonna, as well as Kjerringbotnbreen Blomsterskarsbreen and Sauabreen on Sørfonna have had their subglacial topography mapped (Elvehøy, 1998, Kennett and Sætrang, 1987, Førre, 2012).

8.7. Appliance of remote sensing to widen global cryospheric knowledge

Globally there is a deficit in data from large mountain and piedmont glaciers, as well as from glaciers in the Himalayas, Siberia, ice caps around the Antarctic and Greenland ice sheets and the Andes. There is also a strong bias in measurements from maritime glaciers in Europe, Scandinavia, Svalbard and North America (Dyurgerov et al., 2002). Remote sensing can, and is being used to rectify these data gaps (Bolch, 2007, Berthier et al., 2007, Johannessen et al., 2011).

When it comes to ice sheets Quincey and Luckman (2009) argue that remote sensing data not only complements field investigations but through such techniques as DEM generation (SAR interferometry, altimetry and photogrammetry), feature tracking and gravimetry provide new understandings of ice sheets. Indeed many of the methodologies found in this investigation have also been used successfully on the planet's ice sheets: the area of local ice caps and outlet glaciers have been measured both using manual and automatic band ratio methods (Johannessen et al., 2011, Yu et al., 2011), ASTER DEMs have been used to work out surface lowering on glaciers formerly buffered by the Larsen Ice Shelf (Shuman et al., 2011), while the TSL has been mapped on the Antarctic Peninsula using ENVISAT ASAR images (Arigony-Neto et al., 2009), and optical imagery over outlet glaciers in North-West Greenland (Decker, 2010). There is therefore a huge potential for remote sensing to provide new scientific knowledge and insights about ice masses across the entire planet.

9. References

AALL, C., HOYER, K., HALL, C. & HIGHAM, J. 2005. Tourism and climate change adaptation: The Norwegian case. *Tourism, recreation and climate change*, 209-221.

ABDELFATTAH, R. & NICOLAS, J. M. 2002. Topographic SAR interferometry formulation for high-precision DEM generation. *Geoscience and Remote Sensing, IEEE Transactions on,* 40, 2415-2426.

AÐALGEIRSDÓTTIR, G., GUÐMUNDSSON, S., BJÖRNSSON, H., PÁLSSON, F., JÓHANNESSON, T., HANNESDÓTTIR, H., SIGURDSSON, S. & BERTHIER, E. 2011. Modelling the 20th and 21st century evolution of Hoffellsjökull glacier, SE-Vatnajökull, Iceland. *The Cryosphere,* 5, 961-975.

AGRAWALA, S., RAKSAKULTHAI, V., VAN AALST, M., LARSEN, P., SMITH, J. & REYNOLDS, J. 2003. Development and climate change in Nepal: Focus on water resources and hydropower. *Environment Directorate and Development Cooperation Directorate, Organisation for Economic Cooperation and Development (OECD), Paris*.

ALBERT, T. H. 2002. Evaluation of remote sensing techniques for ice-area classification applied to the tropical Quelccaya ice cap, Peru. *Polar Geography,* 26, 210-226.

AMOS, J. 2012. *Cryosat mission's new views of polar ice* [Online]. Vienna. Available: http://www.bbc.co.uk/news/science-environment-17803691 29/04/2012].

ANDREASSEN, L. M. 1999. Comparing Traditional Mass Balance Measurements with Long-term Volume Change Extracted from Topographical Maps: A Case Study of Storbreen Glacier in Jotunheimen, Norway, for the Period 1940–1997. *Geografiska Annaler: Series A, Physical Geography,* 81, 467-476.

ANDREASSEN, L. M., ELVEH, Y, H., KJ & LLMOEN, B. 2002. Using aerial photography to study glacier changes in Norway. *Annals of Glaciology,* 34, 343-348.

ANDREASSEN, L. M., ELVEHØY, H. & B, K. 2004. Massebalansemålinger i Norge- en oppsummering. NVE.

ANDREASSEN, L. M., ELVEHØY, H. & B, K. 2005a. Store endringer i Norges isbreer. *Cicerone 2 2005*.

ANDREASSEN, L. M., ELVEHØY, H. & B, K. 2007. Norges isbreer minket kraftig i 2006. *Cirerone 2-2007*.

ANDREASSEN, L. M., ELVEHOY, H., KJOLLMOEN, B., ENGESET, R. V. & HAAKENSEN, N. 2005b. Glacier mass-balance and length variation in Norway. *Annals of Glaciology, Vol 42, 2005,* 42, 317-325.

ANDREASSEN, L. M., PAUL, F., KAAB, A. & HAUSBERG, J. E. 2008. Landsat-derived glacier inventory for Jotunheimen, Norway, and deduced glacier changes since the 1930s. *Cryosphere,* 2, 131-145.

ARC GIS RESOURCE CENTER. 2011a. *About the pan-sharpen process* [Online]. Available: http://help.arcgis.com/en/arcgisdesktop/10.0/help/index.html#//009s0000006n000000.htm [Accessed 19/01/12.

ARC GIS RESOURCE CENTER. 2011b. *How Topo to Raster works* [Online]. Available: http://help.arcgis.com/en/arcgisdesktop/10.0/help/index.html#//009z0000007m000000.htm [Accessed 1/5/2012.

ARIGONY-NETO, J., SAURER, H., SIMOES, J. C., RAU, F., JANA, R., VOGT, S. & GOSSMANN, H. 2009. Spatial and temporal changes in dry-snow line altitude on the Antarctic Peninsula. *Climatic Change,* 94, 19-33.

ARNOLD, N. S., REES, W. G., DEVEREUX, B. J. & AMABLE, G. S. 2006. Evaluating the potential of high-resolution airborne LiDAR data in glaciology. *International Journal of Remote Sensing,* 27, 1233-1251.

ARORA, M. & PATEL, V. 2002. *SAR Interferometry for DEM Generation* [Online]. Available: http://www.gisdevelopment.net/technology/rs/techrs0021b.htm [Accessed 19/04/2012.

BAKKE, J. 2010. *RE: Email correspondence* Type to ROBSON, B. A.

BAKKE, J. 2012a. *RE: Discussion about hydro-electric power around Folgefonna.* Type to ROBSON, B. A.

BAKKE, J. 2012b. *RE: Discussion about the accuracy of the maps from the 1800s.* Type to ROBSON, B. A.

BAKKE, J., MESQUITA, M. D. S., RASMUSSEN, R., NESJE, A., LAUMANN, T., MELVOLD, K., KOLBERG, S., FLOWERS, G., HARESTAD, S., JANSEN, E. & SYLTE, G. 2011. Project Description: GLACIERMELT (Melting glaciers and hydroelectric power production towards 2040). BCCR.

BAKKE, J., NESJE, A. & DAHL, S. O. 2005. Utilizing physical sediment variability in glacier-fed lakes for continuous glacier reconstructions during the Holocene, northern Folgefonna, western Norway. *The Holocene,* 15, 161-176.

BAMBER, J. L. & RIVERA, A. 2007. A review of remote sensing methods for glacier mass balance determination. *Global and Planetary Change,* 59, 138-148.

BARRY, R. G. 2006. The status of research on glaciers and global glacier recession: a review. *Progress in Physical Geography,* 30, 285-306.

BAUDER, A., FUNK, M. & HUSS, M. 2007. Ice-volume changes of selected glaciers in the Swiss Alps since the end of the 19th century. *Annals of Glaciology,* 46, 145-149.

BAUMANN, S. C. 2010. *Mapping, analysis, and interpretation of the glacier inventory data from Jotunheimen, South Norway, since the maximum of the 'Little Ice Age'.* Universitätsbibliothek der Universität Würzburg.

BENISTON, M., DIAZ, H. F. & BRADLEY, R. S. 1997. Climatic change at high elevation sites: An overview. *Climatic Change,* 36**,** 233-251.

BENN, D. I. & EVANS, D. J. A. 2010. *Glaciers and glaciation*, Hodder Education.

BERTHIER, E., ARNAUD, Y., KUMAR, R., AHMAD, S., WAGNON, P. & CHEVALLIER, P. 2007. Remote sensing estimates of glacier mass balances in the Himachal Pradesh (Western Himalaya, India). *Remote Sensing of Environment,* 108**,** 327-338.

BERTHIER, E., VADON, H., BARATOUX, D., ARNAUD, Y., VINCENT, C., FEIGL, K. L., REMY, F. & LEGRESY, B. 2005. Surface motion of mountain glaciers derived from satellite optical imagery. *Remote Sensing of Environment,* 95**,** 14-28.

BHAMBRI, R., BOLCH, T. & CHAUJAR, R. 2011. Mapping of debris-covered glaciers in the Garhwal Himalayas using ASTER DEMs and thermal data. *International Journal of Remote Sensing,* 32**,** 8095-8119.

BINDSCHADLER, R., DOWDESWELL, J., HALL, D. & WINTHER, J. G. 2001. Glaciological applications with Landsat-7 imagery: early assessments. *Remote Sensing of Environment,* 78**,** 163-179.

BISHOP, M. P., OLSENHOLLER, J. A., SHRODER, J. F., BARRY, R. G., RAUP, B. H., BUSH, A. B. G., COPLAND, L., DWYER, J. L., FOUNTAIN, A. G. & HAEBERLI, W. 2004. Global Land Ice Measurements from Space (GLIMS): remote sensing and GIS investigations of the Earth's cryosphere. *Geocarto International,* 19**,** 57-84.

BLACK, R. 2012. *Some Asian glaciers 'putting on mass'* [Online]. Available: http://www.bbc.co.uk/news/science-environment-17701677 [Accessed 23/04/2012.

BØGGILD, C. E., OLESEN, O. B., AHLSTROM, A. P. & JØRGENSEN, P. 2004. Automatic glacier ablation measurements using pressure transducers. *Journal of Glaciology,* 50**,** 303-304.

BOLCH, T. 2007. Climate change and glacier retreat in northern Tien Shan (Kazakhstan/Kyrgyzstan) using remote sensing data. *Global and Planetary Change,* 56**,** 1-12.

BOLCH, T., BUCHROITHNER, M., PIECZONKA, T. & KUNERT, A. 2008. Planimetric and volumetric glacier changes in the Khumbu Himal, Nepal, since 1962 using Corona, Landsat TM and ASTER data. *Journal of Glaciology,* 54**,** 592-600.

BOLCH, T., PIECZONKA, T. & BENN, D. I. 2011. Multi-decadal mass loss of glaciers in the Everest area (Nepal Himalaya) derived from stereo imagery. *Cryosphere,* 5**,** 349-358.

BRADWELL, T. O. M., DUGMORE, A. J. & SUGDEN, D. E. 2006. The Little Ice Age glacier maximum in Iceland and the North Atlantic Oscillation: evidence from Lambatungnajökull, southeast Iceland. *Boreas,* 35**,** 61-80.

BRAITHWAITE, R. J. 2002. Glacier mass balance: the first 50 years of international monitoring. *Progress in Physical Geography,* 26**,** 76-95.

BRAUN, M., SCHULER, T. V., HOCK, R., BROWN, I. & JACKSON, M. 2007. Comparison of remote sensing derived glacier facies maps with distributed mass balance modelling at Engabreen, northern Norway. *IAHS Publications-Series of Proceedings and Reports,* 318**,** 126-134.

BROWN, I. A., KLINGBJER, P. & DEAN, A. 2005. Problems with the retrieval of glacier net surface balance from SAR imagery. *Annals of Glaciology, Vol 42, 2005,* 42**,** 209-216.

CANADA CENTRE FOR REMOTE SENSING 2008. *Fundamentals of Remote Sensing: 2.3. Spatial Resolution, Pixel Size, and Scale*, Natural Resources Canada,.

CASASSA, G., SMITH, K., RIVERA, A., ARAOS, J., SCHNIRCH, M. & SCHNEIDER, C. 2002. Inventory of glaciers in isla Riesco, Patagonia, Chile, based on aerial photography and satellite imagery. *Annals of Glaciology, Vol 34, 2002,* 34**,** 373-378.

CELENTANO, A. 2006. ERS/ENVISAT ASAR Data Products and Services (Powerpoint presentation). Rome: Eurimage.

CHINN, T., WINKLER, S., SALINGER, M. & HAAKENSEN, N. 2005. Recent glacier advances in Norway and New Zealand: a comparison of their glaciological and meteorological causes. *Geografiska Annaler: Series A, Physical Geography,* 87**,** 141-157.

COPLAND, L., POPE, S., BISHOP, M. P., SHRODER, J. F., CLENDON, P., BUSH, A., KAMP, U., SEONG, Y. B. & OWEN, L. A. 2009. Glacier velocities across the central Karakoram. *Annals of Glaciology,* 50**,** 41-49.

COX, L. H. & MARCH, R. S. 2004. Comparison of geodetic and glaciological mass-balance techniques, Gulkana Glacier, Alaska, USA. *Journal of Glaciology,* 50**,** 363-370.

CRISCITIELLO, A. S., KELLY, M. A. & TREMBLAY, B. 2010. The Response of Taku and Lemon Creek Glaciers to Climate. *Arctic, Antarctic, and Alpine Research,* 42**,** 34-44.

DE WILDT, M. S. D. & OERLEMANS, J. 2003. Satellite retrieval of mass balance: comparing SAR images with albedo images and in situ mass-balance observations. *Journal of Glaciology,* 49**,** 437-448.

DEBELLA-GILO, M. & KÄÄB, A. 2011. Sub-pixel precision image matching for measuring surface displacements on mass movements using normalized cross-correlation. *Remote Sensing of Environment,* 115**,** 130-142.

DECKER, D. T. 2010. *Remote Sensing of the Climate and Cryosphere of Nares Strait, Northwest Greenland.* Master Degree, Ohio State University.

DYURGEROV, M., MEIER, M. & ARMSTRONG, R. L. 2002. *Glacier mass balance and regime: data of measurements and analysis*, Institute of Arctic and Alpine Research, University of Colorado Boulder,, USA.

ELVEHØY, H. 1998. Samanlikning av massebalance på Hardangerjøkullen og Folgefonna. Oslo: NVE.

ESA EARTHNET ONLINE. 2012. *ENVISAT ASAR - ASAR Wide Swath Medium Resolution Image (ENVISAT.ASA.WSM_1P)* [Online]. [Accessed 11/02/12.

EVANS, A. N. 2000. Glacier surface motion computation from digital image sequences. *Ieee Transactions on Geoscience and Remote Sensing,* 38**,** 1064-1072.

EVANS, I. 2011. Glacier distribution and direction in Svalbard, Axel Heiberg Island and throughout the Arctic: General northward tendencies. *Polish Polar Research,* 32**,** 199-238.

EVANS, I. S. 2006. Local aspect asymmetry of mountain glaciation: A global survey of consistency of favoured directions for glacier numbers and altitudes. *Geomorphology,* 73**,** 166-184.

FEALY, R. & SWEENEY, J. 2005. Detection of a possible change point in atmospheric variability in the North Atlantic and its effect on Scandinavian glacier mass balance. *International Journal of Climatology,* 25**,** 1819-1833.

FJELLANGER WIDERØE. (date unknown). *Velkommen til Fjellanger Widerøe AS* [Online]. Available: http://www.fw.no/ [Accessed 1/02/12.

FØRRE, E. 2012. *Topografi og dreneringsretninger under Nordfonna, Folgefonna.* Masteroppgave i geovitenskap, Universitet i Bergen.

FOY, N., COPLAND, L., ZDANOWICZ, C., DEMUTH, M. & HOPKINSON, C. 2011. Recent volume and area changes of Kaskawulsh Glacier, Yukon, Canada. *Journal of Glaciology,* 57**,** 515-525.

FURDAL, H. 2010. *Brefluktuasjonar og Klimendringar under "Den Vesle Istid" Kring Folgefonna.* Masteroppgåve i naturgeografi, Universitetet i Bergen.

GAO, J. & LIU, Y. S. 2001. Applications of remote sensing, GIS and GPS in glaciology: a review. *Progress in Physical Geography,* 25**,** 520-540.

GARDELLE, J., BERTHIER, E. & ARNAUD, Y. 2012. Slight mass gain of Karakoram glaciers in the early twenty-first century. *Nature Geosci,* advance online publication.

GOLDSTEIN, R. M., ENGELHARDT, H., KAMB, B. & FROLICH, R. M. 1993. Satellite Radar Interferometry for Monitoring Ice Sheet Motion: Application to an Antarctic Ice Stream. *Science,* 262**,** 1525-1530.

GOULDEN, T. 2009. Prediction of Error due to Terrain Slope in LiDAR Observatiobs. *Geodesy and Geomatics Engineering* Fredericton: University of New Brunswick.

GUDMUNDSSON, S., BJÖRNSSON, H., MAGNUSSON, E., BERTHIER, E., PALSSON, F., GUDMUNDSSON, M. T., HÖGNADÓTTIR, T. & DALL, J. 2011. Response of Eyjafjallajökull, Torfajökull and Tindfjallajökull ice caps in Iceland to regional warming, deduced by remote sensing. *Polar Research,* 30.

HAGG, W. J., BRAUN, L. N., UVAROV, V. N. & MAKAREVICH, K. G. 2004. A comparison of three methods of mass-balance determination in the Tuyuksu glacier region, Tien Shan, Central Asia. *Journal of Glaciology,* 50**,** 505-510.

HALL, D. K., BAYR, K. J., SCHONER, W., BINDSCHADLER, R. A. & CHIEN, J. Y. L. 2003. Consideration of the errors inherent in mapping historical glacier positions in Austria from the ground and space (1893-2001). *Remote Sensing of Environment,* 86**,** 566-577.

HALL, D. K., CHANG, A. T. C. & SIDDALINGAIAH, H. 1988. Reflectances of Glaciers as Calculated Using Landsat-5 Thematic Mapper Data. *Remote Sensing of Environment,* 25**,** 311-321.

HALL, D. K., WILLIAMS, R. S., JR. & BAYR, K. J. 1992. Glacier recession in Iceland and Austria. *Eos Trans. AGU,* 73**,** 129-141.

HAMBREY, M. J., BAMBER, J., CHRISTOFFERSEN, P., GLASSER, N. F., HUBBARD, A., HUBBARD, B. & LARTER, R. 2010. Glaciers - no nonsence science. *Geoscientist Online.*

HAUG, T., ROLSTAD, C., ELVEHOY, H., JACKSON, M. & MAALEN-JOHANSEN, I. 2009. Geodetic mass balance of the western Svartisen ice cap, Norway, in the periods 1968-1985 and 1985-2002. *Annals of Glaciology,* 50**,** 119-125.

HEISKANEN, J. & PELLIKKA, P. Mapping glacier changes, snowline altitude and AAR using Landsat data in Svartisen, Northern Norway. 2003. 10328.

HERMAN, F., ANDERSON, B. & LEPRINCE, S. 2011. Mountain glacier velocity variation during a retreat/advance cycle quantified using sub-pixel analysis of ASTER images. *Journal of Glaciology,* 57**,** 197-207.

HEYWOOD, I., CORNELIUS, S. & CARVER, S. 2006. *Geographical information systems*, Pearson Education Limited.

HOOKER, B. L. & FITZHARRIS, B. B. 1999. The correlation between climatic parameters and the retreat and advance of Franz Josef Glacier, New Zealand. *Global and Planetary Change,* 22**,** 39-48.
HUANG, L., LI, Z., TIAN, B. S., CHEN, Q., LIU, J. L. & ZHANG, R. 2011. Classification and snow line detection for glacial areas using the polarimetric SAR image. *Remote Sensing of Environment,* 115**,** 1721-1732.
IMHOF, P., NESJE, A. & NUSSBAUMER, S. U. 2011. Climate and glacier fluctuations at Jostedalsbreen and Folgefonna, southwestern Norway and in the western Alps from the 'Little Ice Age'until the present: The influence of the North Atlantic Oscillation. *The Holocene*.
JACKSON, M., BROWN, I. A. & ELVEHOY, H. 2005. Velocity measurements on Engabreen, Norway. *Annals of Glaciology, Vol 42, 2005,* 42**,** 29-34.
JAENICKE, J., MAYER, C., SCHARRER, K., MUNZER, U. & GUDMUNDSSON, A. 2006. The use of remote-sensing data for mass-balance studies at Myrdalsjokull ice cap, Iceland. *Journal of Glaciology,* 52**,** 565-573.
JEVREJEVA, S., MOORE, J., GRINSTED, A. & WOODWORTH, P. 2008. Recent global sea level acceleration started over 200 years ago? *Geophysical Research Letters,* 35**,** L08715.
JOHANNESSEN, O. M., BABIKER, M. & MILES, M. W. 2011. Petermann Glacier, North Greenland: massive calving in 2010 and the past half century. *The Cryosphere Discuss.,* 5**,** 169-181.
JOSBERGER, E., MARCH, R. & O'NEEL, S. 2009. Fifty-Year Record of Glacier Change Reveals Shifting Climate in the Pacific Northwest and Alaska, USA. *In:* USGS (ed.).
JOSBERGER, E. G., BIDLAKE, W. R., MARCH, R. S. & KENNEDY, B. W. 2007. Glacier mass-balance fluctuations in the Pacific Northwest and Alaska, USA. *Annals of Glaciology,* 46**,** 291-296.
KÄÄB, A. 2002. Monitoring high-mountain terrain deformation from repeated air- and spaceborne optical data: examples using digital aerial imagery and ASTER data. *Isprs Journal of Photogrammetry and Remote Sensing,* 57**,** 39-52.
KÄÄB, A. Glacier volume changes using ASTER optical stereo. A test study in Eastern Svalbard. 2007. IEEE, 3994-3996.
KÄÄB, A., HUGGEL, C., FISCHER, L., GUEX, S., PAUL, F., ROER, I., SALZMANN, N., SCHLAEFLI, S., SCHMUTZ, K. & SCHNEIDER, D. 2005a. Remote sensing of glacier- and permafrost-related hazards in high mountains: an overview. *Natural Hazards and Earth System Sciences,* 5**,** 527-554.
KÄÄB, A., LEFAUCONNIER, B. & MELVOLD, K. 2005b. Flow field of Kronebreen, Svalbard, using repeated Landsat 7 and ASTER data. *Annals of Glaciology, Vol 42, 2005,* 42**,** 7-13.
KÄÄB, A., PAUL, F., MAISCH, M., HOELZLE, M. & HAEBERLI, W. 2002. The new remote-sensing-derived Swiss glacier inventory: II. First results. *Annals of Glaciology, Vol 34, 2002,* 34**,** 362-366.
KAMNIANSKY, G. & PERTZIGER, F. 1996. Optimization of mountain glacier mass balance measurements. *Zeitschrift für Gletscherkunde und Glazialgeologie,* 32**,** 167-75.
KARTVERKET. 2012. *Norgeskart.no* [Online]. Available: http://kart.statkart.no/adaptive2/default.aspx?gui=1&lang=2 [Accessed 23/03/12.
KASER, G. 1999. A review of the modern fluctuations of tropical glaciers. *Global and Planetary Change,* 22**,** 93-103.
KELLY, R. E. J. 2002. Estimation of the ELA on Hardangerjokulen, Norway, during the 1995/96 winter season using repeat-pass SAR coherence. *Annals of Glaciology,* 34**,** 349-354.
KENNETT, M. & EIKEN, T. 1997. Airborne measurement of glacier surface elevation by scanning laser altimeter. *Annals of Glaciology,* 24**,** 293-296.
KENNETT, M. & SÆTRANG, A. C. 1987. Istykkelsesmålinger på Folgefonna. NVE.
KJØLLMOEN, B. 2009. Glaciological investigations in Norway 2008. *In:* KJØLLMOEN, B., ANDREASSEN, L. M., ELVEHØY, H., JACKSON, M., RIANNE, H. G. & ARVE M, T. (eds.). Oslo: NVE.
KJØLLMOEN, B. 2011. Glaciological investigations in Norway 2010. *In:* KJØLLMOEN, B., ANDREASSEN, L. M., ELVEHØY, H., JACKSON, M. & RIANNE, H. G. (eds.). Oslo: NVE.
KJØLLMOEN, B., ANDREASSEN, L. M., ELVEHØY, H., JACKSON, M. & GIESEN, R. H. 2012. Mass Balance data from Sørfonna (Svelgjabreen, Blomstølskardsbreen, Breidablikkbrea and Gråfjellsbrea). *In:* NVE (ed.).
KJØLLMOEN, B., BØNSNES T & KVAMBEKK Å 2008. Hydrologiske undersøkelser ved Maurangervassdraget; . *In:* B, K. (ed.). Oslo: Norges vassdrags- og energidirektorat.
KJØLLMOEN, B. & ØSTREM, G. 1997. Storsteinsfjellbreen: Variations in Mass Balance from the 1960s to the 1990s. *Geografiska Annaler: Series A, Physical Geography,* 79**,** 195-200.
KNOLL, C., KERSCHNER, H., HELLER, A. & RASTNER, P. 2009. A GIS-based Reconstruction of Little Ice Age Glacier Maximum Extents for South Tyrol, Italy. *Transactions in Gis,* 13**,** 449-463.
KOCH, J., MENOUNOS, B. & CLAGUE, J. J. 2009. Glacier change in Garibaldi Provincial Park, southern Coast Mountains, British Columbia, since the Little Ice Age. *Global and Planetary Change,* 66**,** 161-178.
KÖNIG, M., WINTHER, J.-G., KNUDSEN, N. T. & GUNERIUSSEN, T. 2001. Firn-line detection on Austre Okstindbreen, Norway, with airborne multipolarization SAR. *Journal of Glaciology,* 47**,** 251-257.

KONIG, M., WINTHER, J. G. & ISAKSSON, E. 2001. Measuring snow and glacier ice properties from satellite. *Reviews of Geophysics,* 39**,** 1-27.

KÖNIG, M., WINTHER, J. G., KNUDSEN, N. T. & GUNERIUSSEN, T. Equilibrium-and firnline detection with multipolarization SAR–first results. Proceedings of EARSeL-SIG-Workshop Land Ice and Snow, 2000 Dresden.

KULKARNI, A. V., RATHORE, B. P., SINGH, S. K. & BAHUGUNA, I. M. 2011. Understanding changes in the Himalayan cryosphere using remote sensing techniques. *International Journal of Remote Sensing,* 32**,** 601-615.

LAUMANN, T. & NESJE, A. 2009. The impact of climate change on future frontal variations of Briksdalsbreen, western Norway. *Journal of Glaciology,* 55**,** 789-796.

LI, B. L., ZHU, A. X., ZHANG, Y. C., PEI, T., QIN, C. Z. & ZHOU, C. H. 2006. Glacier change over the past four decades in the middle Chinese Tien Shan. *Journal of Glaciology,* 52**,** 425-432.

LI, Z., SUN, W. & ZENG, Q. 1998. Measurements of glacier variation in the Tibetan Plateau using Landsat data. *Remote Sensing of Environment,* 63**,** 258-264.

LILLESAND, T. M., KIEFER, R. W. & CHIPMAN, J. W. 2004. *Remote sensing and image interpretation*, John Wiley & Sons Ltd.

LOVELAND, T. R. & DWYER, J. L. 2012. Landsat: Building a strong future. *Remote Sensing of Environment*.

LUCKMAN, B. H. 2000. The Little Ice Age in the Canadian Rockies. *Geomorphology,* 32**,** 357-384.

MAGNÚSSON, E., BJÖRNSSON, H., ROTT, H., GUOMUNDSSON, S., PÁLSSON, F., BERTHIER, E. & JÓHANNESSON, T. 2010. The evolution in the glacier mass balance of Hofsjökull ice cap, central Iceland, in 1986-2008, revealed by multi-source remote sensing data. *EGU General Assembly 2010, held 2-7 May, 2010 in Vienna, Austria, p. 11879,* 12**,** 11879.

MATHIEU, R., CHINN, T. & FITZHARRIS, B. 2009. Detecting the equilibrium-line altitudes of New Zealand glaciers using ASTER satellite images. *New Zealand Journal of Geology and Geophysics,* 52**,** 209-222.

MCFADDEN, E. M., RAMAGE, J. & RODBELL, D. T. 2011. Landsat TM and ETM plus derived snowline altitudes in the Cordillera Huayhuash and Cordillera Raura, Peru, 1986-2005. *Cryosphere,* 5**,** 419-430.

MCKINZEY, K. M., ORWIN, J. F. & BRADWELL, T. 2005. A revised chronology of key Vatnajokull (Iceland) outlet glaciers during the Little Ice Age. *Annals of Glaciology,* 42**,** 171-179.

MILLER, M. 2008. The implication of accelerated greenhouse effects on Alaskan glaciers, Juneau Icefield-1946-2007. *Geophysical Research Abstracts,* 10.

MOLNIA, B. F. 2007. Late nineteenth to early twenty-first century behavior of Alaskan glaciers as indicators of changing regional climate. *Global and Planetary Change,* 56**,** 23-56.

MOTYKA, R. J., O'NEEL, S., CONNOR, C. L. & ECHELMEYER, K. A. 2003. Twentieth century thinning of Mendenhall Glacier, Alaska, and its relationship to climate, lake calving, and glacier run-off. *Global and Planetary Change,* 35**,** 93-112.

MUSKETT, R. R., LINGLE, C. S., SAUBER, J. M., POST, A. S., TANGBORN, W. V., RABUS, B. T. & ECHELMEYER, K. A. 2009. Airborne and spaceborne DEM- and laser altimetry-derived surface elevation and volume changes of the Bering Glacier system, Alaska, USA, and Yukon, Canada, 19722006. *Journal of Glaciology,* 55**,** 316-326.

NAPIERALSKI, J., HARBOR, J. & LI, Y. 2007. Glacial geomorphology and geographic information systems. *Earth-Science Reviews,* 85**,** 1-22.

NARAMA, C., SHIMAMURA, Y., NAKAYAMA, D. & ABDRAKHMATOV, K. 2006. Recent changes of glacier coverage in the western Terskey-Alatoo range, Kyrgyz Republic, using Corona and Landsat. *Annals of Glaciology,* 43**,** 223-229.

NATIONAL OCEANIC AND ATMOSPHERIC ADMINISTRATION. 2011. *Global Surface Temperature Anomalies* [Online]. Available: http://www.ncdc.noaa.gov/cmb-faq/anomalies.php#anomalies [Accessed 25/04/2012.

NESJE, A. 2005. Briksdalsbreen in western Norway: AD 1900-2004 frontal fluctuations as a combined effect of variations in winter precipitation and summer temperature. *Holocene,* 15**,** 1245-1252.

NESJE, A., BAKKE, J., DAHL, S. O., LIE, O. & MATTHEWS, J. A. 2008a. Norwegian mountain glaciers in the past, present and future. *Global and Planetary Change,* 60**,** 10-27.

NESJE, A., DAHL, S. O., THUN, T. & NORDLI, O. 2008b. The 'Little Ice Age' glacial expansion in western Scandinavia: summer temperature or winter precipitation? *Climate Dynamics,* 30**,** 789-801.

NESJE, A., LIE, O. & DAHL, S. O. 2000. Is the North Atlantic Oscillation reflected in Scandinavian glacier mass balance records? *Journal of Quaternary Science,* 15**,** 587-601.

NESJE, A. & MATTHEWS, J. A. 2012. The Briksdalsbre Event: A winter precipitation-induced decadal-scale glacial advance in southern Norway in the AD 1990s and its implications. *Holocene,* 22**,** 249-261.

NOLAN, M. & MOTKYA, R. J. 1995. Ice-thickness measurements of Taku Glacier, Alaska, USA, and their relevance to its recent behavior. *Journal of Glaciology,* 41.

NRK. 2008. *Nå vokser isbreene!* [Online]. Bergen. Available: http://www.nrk.no/nyheter/distrikt/hordaland/1.6117664 [Accessed 25/04/2012.

NSF. 2009. *Glaciers in the Southern Hemisphere are growing out of step with those in the North* [Online]. National Science Foundation,. Available: http://www.nsf.gov/news/news_summ.jsp?org=NSF&cntn_id=114696&preview=false [Accessed 25/04/2012.

NUSSBAUMER, S. U., NESJE, A. & ZUMBUHL, H. J. 2011. Historical glacier fluctuations of Jostedalsbreen and Folgefonna (southern Norway) reassessed by new pictorial and written evidence. *Holocene,* 21**,** 455-471.

NVE. 2009. *De største breene i Norge* [Online]. Available: http://www.nve.no/Global/Vann%20og%20vassdrag/Hydrologi/Bre/Nedlastinger/st%C3%B8rste%20breer%20i%20Norge.pdf [Accessed 13/02/12.

NVE. 2011a. *Folgefonna - breer med frontmålinger* [Online]. Oslo. Available: http://www.nve.no/no/Vann-og-vassdrag/Hydrologi/Bre/Bremalinger/Frontposisjonmalinger/Folgefonna---breer-med-frontmalinger/ [Accessed 30/04/2012.

NVE. 2011b. *Length Change Table from 1995 to 2011* [Online]. NVE Hydrologi,. Available: http://www.nve.no/Global/Vann%20og%20vassdrag/Hydrologi/Bre/Nedlastinger/Length_Change_Table_1995-2011.pdf?epslanguage=no [Accessed 30/04/2012.

OERLEMANS, J. 2005. Extracting a climate signal from 169 glacier records. *Science,* 308**,** 675-677.

ORLOVE, B. S., WIEGANDT, E. & LUCKMAN, B. H. 2008. *Darkening peaks : glacier retreat, science, and society,* Berkeley, University of California Press.

OSBORN, T. 2012. *North Atlantic Oscillation index data* [Online]. Norwich. Available: http://www.cru.uea.ac.uk/~timo/datapages/naoi.htm [Accessed 09/01/2012.

ØSTREM, G. 1975. ERTS data in glaciology--an effort to monitor glacier mass balance from satellite imagery. *Journal of Glaciology,* 15**,** 403-415.

PASKAL, C. The Vulnerability of Energy Infrastructure to Environmental Change. 2010. 149-163.

PAUL, F. 2002. Changes in glacier area in Tyrol, Austria, between 1969 and 1992 derived from Landsat 5 thematic mapper and Austrian Glacier Inventory data. *International Journal of Remote Sensing,* 23**,** 787-799.

PAUL, F. & ANDREASSEN, L. M. 2009. A new glacier inventory for the Svartisen region, Norway, from Landsat ETM plus data: challenges and change assessment. *Journal of Glaciology,* 55**,** 607-618.

PAUL, F., ANDREASSEN, L. M. & WINSVOLD, S. H. 2011. A new glacier inventory for the Jostedalsbreen region, Norway, from Landsat TM scenes of 2006 and changes since 1966. *Annals of Glaciology,* 52**,** 153-162.

PAUL, F., HUGGEL, C. & KAAB, A. 2004. Combining satellite multispectral image data and a digital elevation model for mapping debris-covered glaciers. *Remote Sensing of Environment,* 89**,** 510-518.

PAUL, F., KAAB, A., MAISCH, M., KELLENBERGER, T. & HAEBERLI, W. 2002. The new remote-sensing-derived swiss glacier inventory: I. Methods. *Annals of Glaciology, Vol 34, 2002,* 34**,** 355-361.

PCI-GEOMATICA. 2010. *OrthEngine - Aerial Photograph: Troubleshooting Frequently asked questions* [Online]. Available: http://www.pcigeomatics.com/index.php?option=com_content&view=article&id=137&Itemid=7 [Accessed 26/04/2012.

PELTO, M. 2011. Utility of late summer transient snowline migration rate on Taku Glacier, Alaska. *Cryosphere,* 5**,** 1127-1133.

PELTO, M., MCGEE, S., ADEMA, G., BEEDLE, M., MILLER, M., SPRENKE, K. & LANG, M. 2008. The equilibrium flow and mass balance of the Taku Glacier, Alaska 1950-2006. *The Cryosphere Discussions,* 2**,** 275-298.

PONTOPPIDAN, E. 1752. *Det forste Forsorg paa Norges Naturlige Historie*.

QUINCEY, D. J. & GLASSER, N. F. 2009. Morphological and ice-dynamical changes on the Tasman Glacier, New Zealand, 1990–2007. *Global and Planetary Change,* 68**,** 185-197.

QUINCEY, D. J., LUCAS, R. M., RICHARDSON, S., GLASSER, N. F., HAMBREY, M. & REYNOLDS, J. 2005. Optical remote sensing techniques in high-mountain environments: application to glacial hazards. *Progress in Physical Geography,* 29**,** 475.

QUINCEY, D. J. & LUCKMAN, A. 2009. Progress in satellite remote sensing of ice sheets. *Progress in Physical Geography,* 33**,** 547-567.

RABATEL, A., DEDIEU, J. P., THIBERT, E., LETREGUILLY, A. & VINCENT, C. 2008. 25 years (19812005) of equilibrium-line altitude and mass-balance reconstruction on Glacier Blanc, French Alps, using remote-sensing methods and meteorological data. *Journal of Glaciology,* 54**,** 307-314.

RACOVITEANU, A. E., WILLIAMS, M. W. & BARRY, R. G. 2008. Optical remote sensing of glacier characteristics: a review with focus on the Himalaya. *Sensors,* 8**,** 3355-3383.

RAHMSTORF, S. 2010. A new view on sea level rise. 44-45.

RAPER, S. C. B. & BRAITHWAITE, R. J. 2006. Low sea level rise projections from mountain glaciers and icecaps under global warming. *Nature,* 439**,** 311-313.
RAPER, S. C. B. & BRAITHWAITE, R. J. 2009. Glacier volume response time and its links to climate and topography based on a conceptual model of glacier hypsometry. *Cryosphere,* 3**,** 183-194.
RAUP, B., KAAB, A., KARGEL, J. S., BISHOP, M. P., HAMILTON, G., LEE, E., PAUL, F., RAU, F., SOLTESZ, D. & KHALSA, S. J. S. 2007. Remote sensing and GIS technology in the Global Land Ice Measurements from Space (GLIMS) project. *Computers & geosciences,* 33**,** 104-125.
REICHERT, B. K., BENGTSSON, L. & OERLEMANS, J. 2001. Midlatitude forcing mechanisms for glacier mass balance investigated using general circulation models. *Journal of Climate,* 14**,** 3767-3784.
RIVERA, A., CASASSA, G., BAMBER, J. & KAAB, A. 2005. Ice-elevation changes of Glaciar Chico, southern Patagonia, using ASTER DEMs, aerial photographs and GPS data. *Journal of Glaciology,* 51**,** 105-112.
ROLSTAD, C., HAUG, T. & DENBY, B. 2009. Spatially integrated geodetic glacier mass balance and its uncertainty based on geostatistical analysis: application to the western Svartisen ice cap, Norway. *Journal of Glaciology,* 55**,** 666-680.
ROTT, H., NAGLER, T., MALCHER, P. & BIPPUS, G. Modelling mass balance of glaciers using satellite data. 2007.
RUDDIMAN, W. F. 2007. *Earth's climate: past and future*, W.H. Freeman.
SALERNO, F., BURASCHI, E., BRUCCOLERI, G., TARTARI, G. & SMIRAGLIA, C. 2008. Glacier surface-area changes in Sagarmatha national park, Nepal, in the second half of the 20th century, by comparison of historical maps. *Journal of Glaciology,* 54**,** 738-752.
SALMON, M. 2004. *North Atlantic Oscillation (NAO)* [Online]. University of East Anglia,. Available: http://www.cru.uea.ac.uk/cru/data/nao/ [Accessed 09/01/2012.
SALZMANN, N., KÄÄB, A., HUGGEL, C., ALLGÖWER, B. & HAEBERLI, W. 2004. Assessment of the hazard potential of ice avalanches using remote sensing and GIS-modelling. *Norsk Geografisk Tidsskrift-Norwegian Journal of Geography,* 58**,** 74-84.
SCHAEFLI, B., HINGRAY, B. & MUSY, A. 2007. Climate change and hydropower production in the Swiss Alps: quantification of potential impacts and related modelling uncertainties. *Hydrology and Earth System Sciences,* 11**,** 1191-1205.
SCHÖNER, W., AUER, I. & HM, R. 2000. Climate variability and glacier reaction in the Austrian eastern Alps. *Annals of Glaciology,* 31**,** 31-38.
SELECT COMMITTEE ON ECONOMIC AFFAIRS MINUTES OF EVIDENCE. 2005. *Memorandum by Professor Richard S J Tol, Hamburg, Vrije and Carnegie Mellon Universities. In (report): The Economics of Climate Change, the Second Report of the 2005-2006 session, produced by the UK Parliament House of Lords Economics Affairs Select Committee* [Online]. UK Parliment website,. Available: http://www.publications.parliament.uk/pa/ld200506/ldselect/ldeconaf/12/5020107.htm [Accessed 27/04/2012.
SENORGE.NO. 2012. *Changes in mean annual temperature from 1961-1990 to 2071-2100 based on a downscaled Hadley cell climate model, assuming the IPCC A2 scenario* [Online]. Available: http://www.senorge.no/mapPage.aspx [Accessed 27/04/2012.
SHI, J. & DOZIER, J. 1993. Measurements of snow-and glacier-covered areas with single-polarization SAR. *Annals of Glaciology,* 17**,** 72-76.
SHIYONG, Y., HUADONG, G., WENXUE, F., GUANG, L. & ZHIXING, R. Kekesayi glacier velocity extraction based on the offsets derived from SAR images. Geoscience and Remote Sensing Symposium (IGARSS), 2011 IEEE International, 24-29 July 2011 2011. 3179-3182.
SHUMAN, C. A., BERTHIER, E. & SCAMBOS, T. A. 2011. 2001-2009 elevation and mass losses in the Larsen A and B embayments, Antarctic Peninsula. *Journal of Glaciology,* 57**,** 737-754.
SIDJAK, R. W. & WHEATE, R. D. 1999. Glacier mapping of the Illecillewaet icefield, British Columbia, Canada, using Landsat TM and digital elevation data. *International Journal of Remote Sensing,* 20**,** 273-284.
SIGURÐSSON, O., NSSON, T., HANNESSON, T. & MAS 2007. Relation between glacier-termini variations and summer temperature in Iceland since 1930. *Annals of Glaciology,* 46**,** 170-176.
SILVERIO, W. & JAQUET, J. M. 2005. Glacial cover mapping (1987-1996) of the Cordillera Blanca (Peru) using satellite imagery. *Remote Sensing of Environment,* 95**,** 342-350.
SMITH-MAYER, S. & TREDE, A. M. 1996. Volumendringer på Søndre Folgefonna melloe 1959 og 1995. Oslo: NVE.
STATKRAFT.NO. 2008. *Kart over Folgefonn reguleringsområder* [Online]. Available: http://www.statkraft.no/energikilder/vannkraft/kart-over-reguleringsomrader/ [Accessed 26/03/2012.
STORVOLD, R., HOGDA, K. A. & MALNES, E. SAR firn line detection and correlation to glacial mass balance; Svartisen Glacier, northern Norway. Geoscience and Remote Sensing Symposium, 2004. IGARSS '04. Proceedings. 2004 IEEE International, 20-24 Sept. 2004 2004. 1124-1127.

SURAZAKOV, A. B. & AIZEN, V. B. 2006. Estimating volume change of mountain glaciers using SRTM and map-based topographic data. *Geoscience and Remote Sensing, IEEE Transactions on,* 44**,** 2991-2995.

SVOBODA, F. & PAUL, F. 2009. A new glacier inventory on southern Baffin Island, Canada, from ASTER data: I. Applied methods, challenges and solutions. *Annals of Glaciology,* 50**,** 11-21.

SYGNA, L., ERIKSEN, S., O'BRIEN, K. & NÆSS, L. O. 2009. Climate change in Norway: Analysis of economic and social impacts and adaptations. *In:* REPORT, C. (ed.). Oslo: CICERO Senter for klimaforskning.

TOUTIN, T. 2011. ASTER Stereoscopic Data and Digital Elevation Models. *Land Remote Sensing and Global Environmental Change***,** 439-461.

VIGNON, F., ARNAUD, Y. & KASER, G. Quantification of glacier volume change using topographic and ASTER DEMs. Geoscience and Remote Sensing Symposium, 2003. IGARSS '03. Proceedings. 2003 IEEE International, 21-25 July 2003 2003. 2605-2607 vol.4.

VISBECK, M. H., HURRELL, J. W., POLVANI, L. & CULLEN, H. M. 2001. The North Atlantic Oscillation: past, present, and future. *Proceedings of the National Academy of Sciences of the United States of America,* 98**,** 12876.

WANNER, H., CASTY, C., LUTERBACHER, J. & PAULING, A. 2005. 500 Jahre Klimavariabilität im europäischen Alpenraum-raumzeitliche Strukturen und dynamische Interpretationen. *Rundgespräche der Kommission für Ökologie der Bayerischen Akademie der Wissenschaften, Bd,* 28**,** 33-52.

WHILLANS, I. M. & TSENG, Y. H. 1995. Automatic Tracking of Crevasses on Satellite Images. *Cold Regions Science and Technology,* 23**,** 201-214.

WILLIAMS, R., HALL, D. K., SIGUROSSON, O. & CHIEN, J. Y. L. 1997. Comparison of satellite-derived with ground-based measurements of the fluctuations of the margins of Vatnajökull, Iceland, 1973-92. *Annals of Glaciology,* 24**,** 72-80.

WILLIAMS, R. S., HALL, D. K. & BENSON, C. S. 1991. Analysis of Glacier Facies Using Satellite Techniques. *Journal of Glaciology,* 37**,** 120-128.

WINKLER, S., ELVEHØY, H. & NESJE, A. 2009. Glacier fluctuations of Jostedalsbreen, western Norway, during the past 20 years: the sensitive response of maritime mountain glaciers. *The Holocene,* 19**,** 395.

WINKLER, S. & NESJE, A. 2009. Perturbation of Climatic Response at Maritime Glaciers? *Erdkunde,* 63**,** 229-244.

WINTHER, J., BINDSCHADLER, R., KONIG, M. & SCHERER, D. 2005. Remote sensing of glaciers and ice sheets. *GEOPHYSICAL MONOGRAPH-AMERICAN GEOPHYSICAL UNION,* 163**,** 39.

WULDER, M. A., MASEK, J. G., COHEN, W. B., LOVELAND, T. R. & WOODCOCK, C. E. 2012. Opening the archive: How free data has enabled the science and monitoring promise of Landsat. *Remote Sensing of Environment*.

YE, Q., YAO, T., KANG, S., CHEN, F. & WANG, J. 2006. Glacier variations in the Naimona'nyi region, western Himalaya, in the last three decades. *Annals of Glaciology,* 43**,** 385-389.

YU, J., LIU, H., WANG, L., JEZEK, K. C. & HEO, J. 2011. Blue ice areas and their topographical properties in the Lambert glacier, Amery Iceshelf system using Landsat ETM+, ICESat laser altimetry and ASTER GDEM data. *Antarctic Science,* 1**,** 1-16.

ZEMP, M. 2008. *Global glacier changes: facts and figures*, United Nations Envir Programme.

ZEMP, M., PAUL, F., HOELZLE, M. & HAEBERLI, W. 2008. Glacier Fluctuations in the European Alps, 1850-2000. *Darkening peaks: glacier retreat, science, and society***,** 152.

10. Appendix

The data used in this investigation is given below in tables. The shapefiles used in measuring the glacier area, volume and TSL are available to download off of https://www.dropbox.com/sh/spv8apnsl0kmzee/V7-vUXACVF.

For access to the raw Landsat, ASTER, ENVISAT ASAR or any other data please email benrobson101@gmail.com.

Glacier Area

Table 11: Results of glacier areas of Nordfonna, Midtfonna, Sørfonna and Sørfonna when clipped to the extent of the 1937 map. The areas were measured using manual delineation of Landsat images, aerial photos and old maps.

Date	Nordfonna Area (km^2)	Midtfonna Area (km^2)	Sørfonna Area (km^2)	Sørfonna Area, clipped to the extent of the 1937 map (km^2)
13/8/2011	24,75	9,10	156,69	89,61
28/9/2010	25,97	10,21	159,37	91,71
9/9/2010	25,76	10,37	159,85	91,77
14/9/2008	26,36	10,90	161,82	93,01
27/9/2007	28,72	11,52	164,37	94,74
8/8/2006	26,44	11,04	164,13	94,57
15/7/2006	26,94	11,37	166,15	95,66
16/10/2005	26,97	11,67	166,67	96,24
11/8/2004	27,19	11,74	166,84	96,52
1/9/2003	26,87	11,35	165,94	95,31
31/8/2003	27,15	11,43	166,72	96,12
7/8/2003	27,08	11,43	166,77	96,09
15/7/2003	27,97	12,20	170,68	98,55
22/9/2002	27,03	11,24	166,22	95,98
5/8/2002	27,51	12,03	167,78	96,96
20/7/2002	28,65	13,55	171,91	99,05
28/9/2001	27,96	12,43	168,35	97,22
26/9/2000	28,98	13,54	170,48	98,67
21/7/2000	29,22	13,66	173,90	100,55
6/8/1999	30,54	15,16	172,64	100,20
31/7/1994	30,96	15,91	179,35	103,89
31/8/1991	29,63	14,95	172,96	99,32
7/9/1988	28,35	13,51	169,67	97,52
4/8/1987	29,46	15,91	176,59	101,83
21/8/1984	30,72	16,59	179,52	103,38
17/8/1976	33,74	16,74	185,70	107,52
31/7/1962	31,86	16,60	181,03	105,17
1/8/1932	32,24	16,96	Not fully covered	109,09
1/8/1864	51,16	30,15	197,02	122,79
1/8/1860	46,80	28,69	Not fully covered	113,69

Glacier Area measured automatically with TM 3/ TM 5 band ratio

Table 12: Automatically measured glacier areas of Nordfonna, Midtfonna and Sørfonna, using band ratio TM 3/TM 5. The deviation from the manual delineations is also given.

Date	Nordfonna Area (km^2)	Deviation from Manually Delineated Outline (%)	Midtfonna Area (km^2)	Deviation from Manually Delineated Outline (%)	Sørfonna Area (km^2)	Deviation from Manually Delineated Outline (%)
13/08/2011	19,52	-21,13	3,73	-59,02	148,54	-5,20
28/09/2010	25,47	-1,93	9,78	-4,16	158,45	-0,58
09/09/2010	19,49	-24,32	5,66	-45,48	149,04	-6,76
14/09/2008	23,83	-9,61	8,89	-18,42	141,58	-12,51
27/09/2007	27,00	-5,96	11,43	-0,73	150,38	-8,51
08/08/2006	24,90	-5,82	9,06	-17,94	158,00	-3,74
15/07/2006	26,79	-0,55	11,12	-2,19	163,55	-1,56
16/10/2005	24,00	-10,99	9,11	-21,94	156,46	-6,13
11/08/2004	26,30	-3,28	10,85	-7,62	162,51	-2,60
01/09/2003	6,05	-77,48	2,62	-76,89	158,40	-4,54
31/08/2003	13,62	-49,84	2,79	-75,54	105,84	-36,52
07/08/2003	25,23	-6,83	9,10	-20,37	159,10	-4,60
15/07/2003	26,52	-5,17	10,82	-11,32	164,19	-3,80
22/09/2002	22,32	-17,41	8,93	-20,56	159,61	-3,98
05/08/2002	18,49	-32,80	5,19	-56,88	148,57	-11,45
20/07/2002	22,94	-19,96	10,95	-19,19	153,74	-10,57
28/09/2001	19,96	-28,62	7,94	-36,09	97,37	-42,16
26/09/2000	27,88	-3,80	12,45	-8,07	167,07	-2,00
21/07/2000	53,83	84,23	22,00	61,13	223,43	28,48
06/08/1999	29,68	-2,84	14,53	-4,13	154,46	-10,53
31/07/1994	31,02	0,19	17,48	9,89	182,04	1,50
31/08/1991	27,68	-6,60	13,16	-11,94	168,66	-2,49
07/09/1988	25,23	-10,99	9,10	-32,64	159,10	-6,23
04/08/1987	15,73	-46,62	12,27	-22,85	153,78	-12,92
21/08/1984	14,45	-52,95	3,83	-76,92	140,43	-21,77

Glacier Area measured automatically with TM 4/ TM 5 band ratio

Table 13: Table 12: Automatically measured glacier areas of Nordfonna, Midtfonna and Sørfonna, using band ratio TM 4/TM 5. The deviation from the manual delineations is also given.

Date	Nordfonna Area (km^2)	Deviation from Manually Delineated Outline (%)	Midtfonna Area (km^2)	Deviation from Manually Delineated Outline (%)	Sørfonna Area (km^2)	Deviation from Manually Delineated Outline (%)
13/08/2011	11,53	-67,75	0,02	-243,41	123,46	-22,37
28/09/2010	25,07	-3,55	9,55	-6,78	157,02	-1,49
09/09/2010	18,23	-38,62	5,43	-87,34	147,29	-8,43
14/09/2008	29,96	15,08	5,99	-55,16	141,67	-14,23
27/09/2007	26,39	-8,60	11,12	-3,49	154,68	-6,44
08/08/2006	25,60	-3,38	9,76	-14,08	160,74	-2,15
15/07/2006	25,80	-4,24	10,24	-10,09	160,23	-3,62
16/10/2005	22,76	-17,52	8,48	-35,05	152,62	-8,98
11/08/2004	26,05	-4,33	10,52	-11,33	160,64	-3,81
01/09/2003	2,13	-408,87	0,86	-399,78	153,08	-8,12
31/08/2003	28,47	9,74	2,62	-315,23	103,39	-59,84
07/08/2003	24,98	-8,33	8,75	-29,40	157,50	-5,82
15/07/2003	26,31	-6,24	10,65	-14,39	163,15	-4,59
22/09/2002	23,41	-16,21	8,44	-31,38	157,96	-5,18
05/08/2002	11,78	-85,08	3,32	-167,88	127,02	-27,44
20/07/2002	21,01	-33,32	9,50	-37,01	144,77	-17,65
28/09/2001	18,77	-46,07	7,71	-59,40	94,08	-76,27
26/09/2000	27,52	-5,24	12,14	-11,28	165,27	-3,12
21/07/2000	53,83	45,72	19,12	24,81	204,49	13,69
06/08/1999	29,65	-3,02	14,40	-5,22	154,10	-12,01
31/07/1994	39,34	27,01	19,45	20,28	190,78	6,28
31/08/1991	27,70	-6,97	13,10	-14,08	167,78	-3,07
07/09/1988	25,23	-12,35	9,10	-48,45	159,10	-6,64
04/08/1987	15,89	-86,32	12,49	-27,84	154,23	-14,54
21/08/1984	18,62	-83,71	6,43	-265,34	150,06	-20,98

Amount of Glacier Outline Obscured by Cloud and Shadow

Table 14: The percentage of Nordfonna, Midtfonna and Sørfonna's outlines obscured by cloud and shadow.

	Proportion of Glacier Perimeter obscured by cloud				Proportion of Glacier Perimeter obscured by shadow			
Date	Nordfonna (%)	Midtfonna (%)	Sørfonna (%)	Total (%)	Nordfonna (%)	Midtfonna (%)	Sørfonna (%)	Total (%)
13/8/2011	0,0		0,0	0,0	4,0	2,1	6,1	4,9
28/9/2010	4,3	0,0	0,0	0,9	9,5	5,9	7,6	7,7
9/9/2010	0,0	0,0	0,0	0,0	18,3	4,2	8,5	9,6
14/9/2008	0,0	0,0	0,0	0,0	23,6	14,3	13,3	15,4
27/9/2007	0,0	0,0	0,0	0,0	14,5	13,6	13,0	13,4
8/8/2006	0,0	0,0	0,0	0,0	4,7	0,9	4,3	3,8
15/7/2006	0,0	0,0	0,0	0,0	3,4	3,8	3,8	3,7
16/10/2005	0,0	0,0	0,0	0,0	23,5	16,3	18,5	19,0
11/8/2004	0,0	0,0	0,0	0,0	6,0	4,7	3,4	4,1
1/9/2003	0,0	0,0	0,0	0,0	5,9	16,6	6,1	8,1
7/8/2003	1,3	5,2	2,4	2,6	2,9	3,7	6,4	5,4
15/7/2003	0,0	0,0	0,0	0,0	6,6	4,5	7,6	6,9
22/9/2002	22,3	23,4	13,1	16,5	10,7	12,7	13,2	12,6
5/8/2002	0,0	0,0	0,0	0,0	12,7	9,5	11,6	11,4
20/7/2002	18,5	12,9	14,8	15,1	8,8	3,5	3,2	4,3
28/9/2001	21,1	6,3	40,4	31,3	12,8	13,5	8,0	9,7
26/9/2000	0,0	0,0	0,0	0,0	12,8	9,3	9,2	9,8
21/7/2000	0,0	0,0	0,0	0,0	4,5	4,0	1,7	2,5
6/8/1999	0,3	0,4	0,1	0,2	3,1	1,4	1,7	1,9
31/7/1994	0,0	0,0	0,0	0,0	6,4	3,0	2,1	2,9
31/8/1991	0,0	0,0	0,0	0,0	8,9	5,4	5,2	5,8
7/9/1988	43,9	23,2	10,9	18,8	15,1	4,6	9,1	9,2
4/8/1987	32,2	2,6	6,2	9,4	6,7	5,1	3,3	4,2
21/8/1984	45,0	35,4	14,2	22,7	0,8	3,6	2,4	2,4
17/8/1976	0,0	0,0	0,0	0,0	3,4	2,7	4,2	3,8

Glacier Volume

Table 15: Glacier volume of Nordfonna, Midtfonna and Sørfonna, as well as Sørfonna clipped to the 1937 map extent.

Year	Nordfonna		Midtfonna		Sørfonna		Sørfonna volume, clipped to the extent of the 1937 map	
	Volume (km^3)	Mass (million kg)	Volume (km^3)	Mass (million kg)	Volume (km^3)	Mass (million kg)	Volume (km^3)	Mass (million kg)
2010	1,84	2002,68	1,30*	1422,41*	37,75*	41170,98*	19,42*	21172,65*
2007	2,62	2857,18	1,62*	1769,47*	41,63*	45397,59*	22,12*	24122,72*
2002	2,95	3220,99	1,77*	1931,72*	40,70*	44382,44*	21,44*	23384,89*
1999	2,29	2499,55	1,72*	1874,17*	41,49*	45244,69*	21,77*	23742,82*
1987	2,82	3070,36	2,25*	2453,65*	45,33*	49433,07*	21,22*	23143,53*
1937	3,23	3524,17	2,63*	2863,08*	Not fully covered		24,60*	26831,10*

* As the subglacial topography for Midtfonna and Sørfonna is unknown these are not absolute volumes, but give an idea for the *change* in glacier volume.

Elevation Change by height

Table 16: The elevation change between 1999 and 2007, and 1999 and 2010 of different zones, based on the elevation of Folgefonna in 1987.

Elevation Zone (m.a.s.l.)	Mean Elevation 2010 (m.a.s.l.)	Mean Elevation 2007 (m.a.s.l.)	Mean Elevation 1999 (m.a.s.l.)	Change 2010 – 1999 (m)	Change per year (m)	Change 2007 – 1999 (m)	Change per year (m)
775	690,04	783,00	771,13	81,09	7,37	94,47	3,63
825	729,49	770,93	794,19	64,71	5,88	97,89	3,76
875	834,20	853,00	861,58	27,38	2,49	49,78	1,91
925	880,94	908,29	902,33	21,39	1,94	49,14	1,89
975	936,38	957,51	959,45	23,07	2,10	41,76	1,61
1025	1000,59	1015,83	1011,78	11,19	1,02	28,37	1,09
1075	1049,63	1064,25	1065,42	15,79	1,44	28,95	1,11
1125	1096,14	1115,71	1111,16	15,02	1,37	31,31	1,20
1175	1132,61	1152,74	1151,25	18,65	1,70	45,23	1,74
1225	1184,12	1205,64	1203,68	19,56	1,78	44,55	1,71
1275	1243,69	1261,49	1255,28	11,59	1,05	34,45	1,33
1325	1288,91	1306,44	1295,83	6,92	0,63	38,57	1,48
1375	1355,58	1352,12	1340,78	-14,79	-1,34	20,05	0,77
1425	1388,24	1407,39	1399,27	11,04	1,00	37,92	1,46
1475	1434,46	1460,91	1452,03	17,57	1,60	41,81	1,61
1525	1488,34	1516,93	1508,72	20,38	1,85	36,93	1,42
1575	1539,35	1571,74	1565,87	26,53	2,41	33,59	1,29
1625	1575,66	1613,57	1604,14	28,48	2,59	38,32	1,47

Transient Snowline (TSL) measured on Sørfonna (Landsat TM band 4)

Table 17: The elevation of the Transient snowline (TSL) on Sørfonna, measured using Landsat TM band 4.

Date	TSL Mean Elevation (m.a.s.l.)	Range of values (%)
03/09/2010	1535,1	15,0
08/08/2006	1513,8	20,0
11/08/2004	1490,4	22,6
01/09/2003	1480,0	22,1
22/09/2002	1477,9	21,9
28/09/2001	1472,7	23,1
25/09/2000	1463,0	25,6
06/08/1999	1449,2	23,7
31/07/1994	1429,7	22,5
31/08/1991	1408,0	23,8
07/09/1988	1429,1	24,6
21/08/1984	1448,5	19,1

Linear Extrapolation of the TSL

Table 18: Estimations of the Transient snowline (TSL) elevation from 2015 to 2050 based on the linear extrapolation of both the Landsat TM band 4, and the ENVISAT ASAR December images.

Year	TSL Elevation predicted by Landsat data	TSL Elevation predicted by ENVISAT ASAR December data
2015	1573,672	1604,817
2020	1612,221	1683,012
2025	1650,75	1761,165
2030	1689,279	1839,318
2035	1727,807	1917,471
2040	1766,357	1995,666
2045	1804,885	2073,819
2050	1843,414	2151,972

Transient Snowline (TSL) measured on Sørfonna (ENVISAT ASAR measurements)

Table 19: Table 17: The elevation of the Transient snowline (TSL) on Sørfonna, measured using mid-winter ENVISAT ASAR data from December, January and February

Ablation Season	ENVISAT ASAR December		ENVISAT ASAR January		ENVISAT ASAR February	
	TSL Mean Elevation (m.a.s.l.)	Range of values (%)	TSL Mean Elevation (m.a.s.l.)	Range of values (%)	TSL Mean Elevation (m.a.s.l.)	Range of values (%)
2005	1453,3	29,3	1441,3	35,2	1468,1	27,3
2006	1462,2	29,0	1453,0	29,2	1484,3	28,2
2007	1503,4	27,6	1462,8	27,1	1504,4	24,4
2008	1509,4	27,5	1494,4	26,7	1503,0	25,4
2009	n/a*	n/a*	1505,4	20,5	1516,5	20,5
2010	1527,3	18,3	n/a*	n/a*	1531,2	18,9

*Some images were unusable due to surface melt obscuring the glacier faces

Direction of glacier reaction

Table 20: The percentage expansion/retreat of Nordfonna, Midtfonna and Sørfonna split into western and eastern sides. The relative expansion of both sides has been used to create an index, where positive values indicate a western Folgefonna expansion, while negative values indicate an eastern reaction.

Date	Nordfonna			Midtfonna			Sørfonna		
	Western change (%)	Eastern change (%)	Index	Western change (%)	Eastern change (%)	Index	Western change (%)	Eastern change (%)	Index
13/8/2011	3.85	5.15	4.50	16.86	8.94	12.90	1.24	2.06	1.65
28/9/2010	-1.03	-0.66	-0.85	2.41	0.66	1.54	1.11	-0.34	0.39
9/9/2010	3.23	1.79	2.51	64.61	5.12	34.86	0.44	1.87	1.16
14/9/2008	11.77	6.06	8.91	-152.34	4.14	-74.10	1.82	1.32	1.57
27/9/2007	-11.54	-7.01	-9.27	-6.56	-1.94	-4.25	0.42	-0.67	-0.13
8/8/2006	2.00	1.76	1.88	3.15	2.54	2.84	1.01	1.39	1.20
15/7/2006	0.24	-0.36	-0.06	-4.09	1.98	-1.05	-0.15	-5.49	-2.82
16/10/2005	1.36	0.90	1.13	8.00	1.04	4.52	0.52	5.62	3.07
11/8/2004	-0.24	-1.73	-0.99	-4.41	-2.31	-3.36	-1.05	-1.61	-1.33
1/9/2003	-0.27	1.06	0.40	-2.46	-0.48	-1.47	0.83	1.08	0.96
31/8/2003	0.86	-0.17	0.34	2.67	0.56	1.62	0.15	0.46	0.31
7/8/2003	4.64	2.29	3.46	5.20	7.60	6.40	1.87	2.66	2.27
15/7/2003	-5.77	-2.16	-3.97	-8.38	-8.84	-8.61	-2.06	-3.21	-2.63
22/9/2002	3.06	0.99	2.03	5.97	7.30	6.64	0.66	1.15	0.91
5/8/2002	3.02	4.01	3.51	11.78	10.60	11.19	2.16	2.50	2.33
20/7/2002	-6.28	-1.81	-4.05	-8.03	-10.07	-9.05	-2.21	-1.88	-2.05
28/9/2001	8.37	2.18	5.28	8.16	13.64	10.90	-3.73	1.37	-1.18
26/9/2000	0.47	1.44	0.96	2.55	-3.75	-0.60	7.30	1.31	4.31
21/7/2000	5.43	2.59	4.01	7.65	8.45	8.05	-1.07	0.44	-0.31
6/8/1999	4.01	-1.02	1.50	1.96	7.11	4.53	3.84	2.72	3.28
31/7/1994	-3.11	-4.52	-3.81	0.45	-15.48	-7.52	65.97	-4.35	30.81
31/8/1991	-13.39	-2.90	-8.14	-25.76	-0.86	-13.31	-210.58	16.98	-96.80
7/9/1988	13.13	1.85	7.49	25.51	7.20	16.36	3.26	-16.58	-6.66
4/8/1987	1.92	5.48	3.70	2.60	5.98	4.29	1.09	2.08	1.58
21/8/1984	6.34	3.37	4.86	-0.32	76.20	37.94	20.13	-3.17	8.48
17/8/1976	70.61	-11.99	29.31	11.25	-391.52	-190.14	-83.28	-105.94	-94.61
31/7/1962	-212.21	2.51	-104.85	-10.97	17.90	3.46	1.24	2.06	1.65
1/8/1932	49.04	25.20	37.12	39.37	47.47	43.42	1.11	-0.34	0.39

Visual explanation of how volumes were calculated between the ice surface, and the bedrock topography

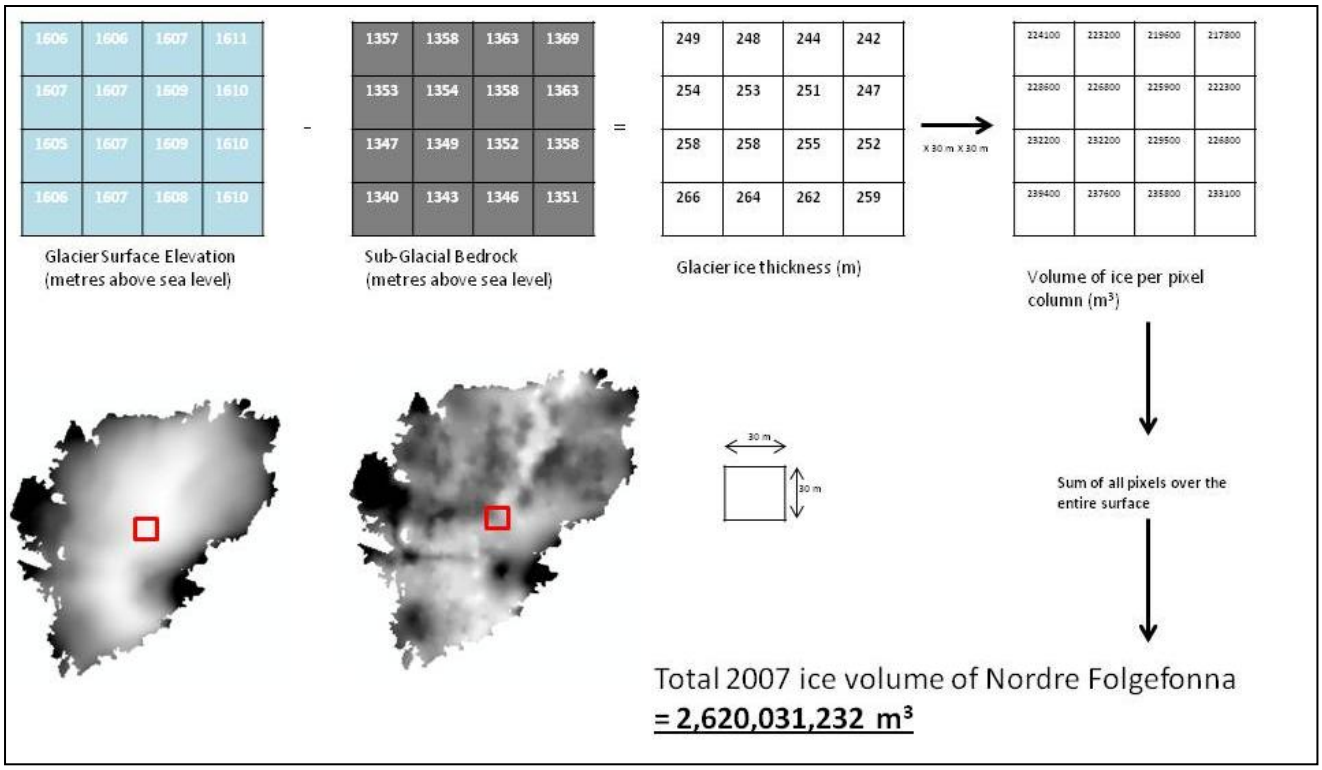

Figure 86: Visual explanation of the process conducted in ArcMap's raster calculator to measure the volume of Nordfonna.